



ISDEC
International Conference
on Intelligent Systems, Design and Energy

ULUSLARARASI AKILLI SİSTEMLER, TASARIM VE ENERJİ KONFERANSI

International Conference on Intelligent Systems, Design and Energy

BİLDİRİLER KİTABI / *Proceedings*



28-29 KASIM, SAAT: 10.00

Bitlis Eren Üniversitesi, Enstitü Konferans Salonu

28-29 NOVEMBER / 10:00 a.m.

Bitlis Eren University, Institute Conference Hall

EDİTÖRLER / Editors

Doç. Dr. Vedat TÜMEN

Arş. Gör. Gamze AKSOY





***I. ULUSLARARASI AKILLI SİTEMLER,
TASARIM VE ENERJİ KONFERANSI BİLDİRİLER KİTABI
(PROCEEDINGS OF 1st INTERNATIONAL CONFERENCE
ON INTELLIGENT SYSTEMS, DESIGN AND ENERGY)***

EDİTÖRLER / EDITORS:

Doç. Dr. Vedat TÜMEN

Arş. Gör. Gamze AKSOY

Genel Yayın Yönetmeni: Berkan Balpetek

Kapak Tasarımı: Duvar Design

Yayın Tarihi: Aralık 2025

Yayıncı Sertifika No: 49837

ISBN: 978-625-8698-77-0

© Duvar Yayınları

853 Sokak No:13 P.10 Kemeraltı-Konak/İzmir

Tel: 0 232 484 88 68

www.duvar yayinlari.com

duvar kitabevi@gmail.com

BİTLİS EREN ÜNİVERSİTESİ
MÜHENDİSLİK VE MİMARLIK FAKÜLTESİ

BİTLİS EREN UNIVERSITY
FACULTY OF ENGINEERING AND ARCHITECTURE

I. ULUSLARARASI
AKILLI SİSTEMLER, TASARIM VE ENERJİ KONFERANSI
28-29 KASIM 2025
ÖZET KİTAPÇIĞI

1st INTERNATIONAL
CONFERENCE ON SMART SYSTEMS, DESIGN AND ENERGY
NOVEMBER 28-29, 2025
PROCEEDINGS

EDİTÖRLER / EDITORS

Doç. Dr. Vedat TÜMEN

Arş. Gör. Gamze AKSOY

BİTLİS, 2025



TAKDİM

PREFACE

I. Uluslararası Akıllı Sistemler, Tasarım ve Enerji Konferansı (ISCED 2025), Bitlis Eren Üniversitesi Mühendislik ve Mimarlık Fakültesi ev sahipliğinde 28–29 Kasım 2025 tarihlerinde gerçekleştirilmiştir. Konferans; akıllı sistemler, tasarım ve enerji alanlarında çalışan araştırmacıları, kamu ve özel sektör temsilcilerini aynı çatı altında buluşturarak güncel bilimsel ve teknolojik gelişmelerin paylaşılmasını, disiplinlerarası iş birliklerinin güçlenmesini ve yeni araştırma ağlarının oluşmasını hedeflemiştir.

Bu Özet Kitapçığı'nda, konferans bilim kurulu ve hakem değerlendirmeleri sonucunda kabul edilen çalışmaların özetleri yer almaktadır. Bildirilerin, ilgili alanlarda yürütülen araştırmalara katkı sunmasını ve yeni çalışmalar için ilham vermesini temenni ederiz.

Konferansın gerçekleştirilmesinde emeği geçen Bilim Kurulu, Düzenleme Kurulu ve Sekreteryaya üyelerine; davetli konuşmacılarımıza, değerli yazarlara ve katılımcılara teşekkür ederiz. Ayrıca, konferansın hazırlık ve yürütme süreçlerine sağladıkları katkı ve destek için Bitlis Eren Üniversitesi Bilimsel Araştırma Projeleri Koordinasyon Birimi'ne (BEBAP) şükranlarımızı sunarız (Proje No: BEBAP 2025.34).

The 1st International Conference on Smart Systems, Design and Energy (ISCED 2025) was hosted by the Faculty of Engineering and Architecture, Bitlis Eren University, on November 28–29, 2025. The conference aimed to bring together researchers and practitioners working on smart systems, design, and energy to share recent scientific and technological advances, strengthen interdisciplinary collaboration, and foster new research networks.

This Book of Abstracts includes the abstracts of studies accepted after the evaluations of the scientific committee and reviewers. We hope that these contributions will support ongoing research and inspire future work.

We would like to thank the members of the Scientific Committee, the Organizing Committee, and the Secretariat; our keynote speakers; all authors and participants who contributed to the success of ISCED 2025. Also, we extend our sincere gratitude to the Bitlis Eren University Scientific Research Projects Coordination Unit (BEBAP) for their contributions and support throughout the preparation and implementation of the conference (Project No.: BEBAP 2025.34).

Prof. Dr. Hakan ÇOBAN
Kongre Başkanı / Conference Chair
Bitlis Eren Üniversitesi / Bitlis Eren University



**ULUSLARARASI
AKILLI SİSTEMLER, TASARIM
VE ENERJİ KONFERANSI**
Conference on Intelligent Systems, Design and Energy



ONURSAL BAŞKAN

HONORARY PRESIDENT



Prof. Dr. Necmettin ELMASTAŞ

Bitlis Eren Üniversitesi
Bitlis Eren University

Rektör / Rector



ULUSLARARASI AKILLI SİSTEMLER, TASARIM VE ENERJİ KONFERANSI

Conference on Intelligent Systems, Design and Energy



DÜZENLEME KURULU

ORGANIZING COMMITTEE

UNVAN AD SOYAD	ÜNİVERSİTE BİLGİSİ
PROF. DR. HAKAN ÇOBAN Kongre Başkanı (Conference Chair)	Bitlis Eren Üniversitesi Bitlis Eren University
DOÇ. DR. VEDAT TÜMEN Düzenleme Kurulu Başkanı (Organizing Committee Chair)	Bitlis Eren Üniversitesi Bitlis Eren University
DOÇ. DR. NUSRET BOZKURT	Bitlis Eren Üniversitesi Bitlis Eren University
DOÇ. DR. RIDVAN UMAZ	Bitlis Eren Üniversitesi Bitlis Eren University
DOÇ. DR. ÜMİT BUDAK	Bitlis Eren Üniversitesi Bitlis Eren University
DR. ÖĞR. ÜYESİ EMİN EL	Bitlis Eren Üniversitesi Bitlis Eren University
DR. ÖĞR. ÜYESİ İRFAN ÖKTEN	Bitlis Eren Üniversitesi Bitlis Eren University
DR. ÖĞR. ÜYESİ KERİM ÖZBEYAZ	Bitlis Eren Üniversitesi Bitlis Eren University
DR. ÖĞR. ÜYESİ MUHAMMED TANYILDIZI	Bitlis Eren Üniversitesi Bitlis Eren University
ARŞ. GÖR. CANSU AKYÜREK ANACUR	Bitlis Eren Üniversitesi Bitlis Eren University
ARŞ. GÖR. GAMZE AKSOY	Bitlis Eren Üniversitesi Bitlis Eren University
ARŞ. GÖR. NİLAY BOZKURT	Bitlis Eren Üniversitesi Bitlis Eren University
ÖĞR. GÖR. İBRAHİM AYAZ	Bitlis Eren Üniversitesi Bitlis Eren University



DANIŞMA KURULU

ADVISORY BOARD

UNVAN AD SOYAD	ÜNİVERSİTE BİLGİSİ
PROF. DR. ABDULCELİL BUĞUTEKİN	Bitlis Eren Üniversitesi <i>Bitlis Eren University</i>
PROF. DR. CENGİZ YILDIZ	Fırat Üniversitesi <i>Firat University</i>
PROF. DR. ERCAN IŞIK	Bitlis Eren Üniversitesi <i>Bitlis Eren University</i>
PROF. DR. HAKAN ÇOBAN	Bitlis Eren Üniversitesi <i>Bitlis Eren University</i>
PROF. DR. MEHMET CİHAN AYDIN	Bitlis Eren Üniversitesi <i>Bitlis Eren University</i>
PROF. DR. SABİR RÜSTEMLİ	Bitlis Eren Üniversitesi <i>Bitlis Eren University</i>
PROF. DR. SERDAR EKİNCİ	Bitlis Eren Üniversitesi <i>Bitlis Eren University</i>
PROF. DR. SERKAN ÖZEL	Bitlis Eren Üniversitesi <i>Bitlis Eren University</i>
PROF. DR. ZEKİ ARGUNHAN	Bitlis Eren Üniversitesi <i>Bitlis Eren University</i>



BİLİM KURULU

SCIENTIFIC COMMITTEE

UNVAN AD SOYAD	ÜNİVERSİTE BİLGİSİ
PROF. DR. ABDULCELİL BUĞUTEKİN	Bitlis Eren Üniversitesi <i>Bitlis Eren University</i>
PROF. DR. AHMET AKKUŞ	Cumhuriyet Üniversitesi <i>Cumhuriyet University</i>
PROF. DR. AHMET YARDIMEDEN	Dicle Üniversitesi <i>Dicle University</i>
PROF. DR. ATILLA GENCER DEVECİOĞLU	Dicle Üniversitesi <i>Dicle University</i>
PROF. DR. BAHAR DEMİREL	Fırat Üniversitesi <i>Firat University</i>
PROF. DR. BAHATTİN İŞCAN	Batman Üniversitesi <i>Batman University</i>
PROF. DR. BİLAL GÜMÜŞ	Dicle Üniversitesi <i>Dicle University</i>
PROF. DR. BORKO BULAJIC	Novi Sad Üniversitesi <i>University of Novi Sad</i>
PROF. DR. CENGİZ YILDIZ	Fırat Üniversitesi <i>Firat University</i>
PROF. DR. CİHAN ÖZEL	Fırat Üniversitesi <i>Firat University</i>
PROF. DR. DACHENG Lİ	Birmingham Üniversitesi <i>University of Birmingham</i>
PROF. DR. EMMANUEL KARLO NYARKO	Josip Juraj Strossmayer University of Osijek <i>Josip Juraj Strossmayer University of Osijek</i>
PROF. DR. EMRE ÇELİK	Düzce Üniversitesi <i>Düzce University</i>
PROF. DR. ENGİN AVCI	Fırat Üniversitesi <i>Firat University</i>

UNVAN AD SOYAD	ÜNİVERSİTE BİLGİSİ
PROF. DR. ERCAN IŞIK	Bitlis Eren Üniversitesi <i>Bitlis Eren University</i>
PROF. DR. ERDEM IŞIK	Munzur Üniversitesi <i>Munzur University</i>
PROF. DR. EROL KILIÇKAP	Dicle Üniversitesi <i>Dicle University</i>
PROF. DR. ESER SERT	Turgut Özal Üniversitesi <i>Turgut Ozal University</i>
PROF. DR. FATİH ÖZKAYNAK	Fırat Üniversitesi <i>Firat University</i>
PROF. DR. GÖKHAN DALKILIÇ	İzmir Dokuz Eylül Üniversitesi <i>Izmir Dokuz Eylul University</i>
PROF. DR. GÜLŞAH ÇAKMAK	Fırat Üniversitesi <i>Firat University</i>
DR. IEVGEN ZAITSEV	Ukrayna Ulusal Bilimler Akademisi Elektrodinamik Enstitüsü <i>The Institute of electrodynamics of the National Academy of Sciences of Ukraine</i>
PROF. DR. İBRAHİM KAYA	Dicle Üniversitesi <i>Dicle University</i>
PROF. DR. İBRAHİM TÜRKOĞLU	Fırat Üniversitesi <i>Firat University</i>
PROF. DR. KÜRŞAT ESAT ALYAMAÇ	Fırat Üniversitesi <i>Firat University</i>
PROF. DR. LAİTH ABUALİGAH	Amman Arap Üniversitesi <i>Amman Arab University</i>
PROF. DR. MARIJANA HADZİMA NYARKO	Josip Juraj Strossmayer Osijek Üniversitesi <i>Josip Juraj Strossmayer University of Osijek</i>
PROF. DR. MEHMET AKIN	Dicle Üniversitesi <i>Dicle University</i>
PROF. DR. MEHMET CİHAN AYDIN	Bitlis Eren Üniversitesi <i>Bitlis Eren University</i>
PROF. DR. MEHMET EMİROĞLU	Sakarya Üniversitesi <i>Sakarya University</i>
PROF. DR. MERAL ÖZEL	Fırat Üniversitesi <i>Firat University</i>
DOÇ. DR. MOHİT BAJAJ	Graphic Era Üniversitesi <i>Graphic Era University</i>
PROF. DR. MOHD ASHRAF AHMAD	Universiti Malaysia Pahang Al-Sultan Abdullah <i>Universiti Malaysia Pahang Al-Sultan Abdullah</i>
PROF. DR. MOHD HELMİ SUİD	Universiti Malaysia Pahang Al-Sultan Abdullah <i>Universiti Malaysia Pahang Al-Sultan Abdullah</i>

UNVAN AD SOYAD	ÜNİVERSİTE BİLGİSİ
PROF. DR. MOHD ZAİDİ MOHD TUMARİ	
PROF. DR. MUHAMMED BAHADDİN KURT	Dicle Üniversitesi <i>Dicle University</i>
PROF. DR. MURAT KAYRİ	Van Yüzüncü Yıl Üniversitesi <i>Van Yüzüncü Yıl University</i>
PROF. DR. NİCOLAY MİHAİLOV	Ruse Üniversitesi <i>University of Ruse</i>
PROF. DR. RİZK M. RİZK-ALLAH	Menoufia Üniversitesi <i>Menoufia University</i>
PROF. DR. SABİR RÜSTEMLİ	Bitlis Eren Üniversitesi <i>Bitlis Eren University</i>
PROF. DR. SALİH YAZICIOĞLU	Gazi Üniversitesi <i>Gazi University</i>
PROF. DR. SERDAR EKİNCİ	Bitlis Eren Üniversitesi <i>Bitlis Eren University</i>
PROF. DR. SERKAN ÖZEL	Bitlis Eren Üniversitesi <i>Bitlis Eren University</i>
PROF. DR. SİLVA LOZANCİC	Josip Juraj Strossmayer Osijek Üniversitesi <i>Josip Juraj Strossmayer University of Osijek</i>
PROF. DR. TÜLAY YILDIZ	Fırat Üniversitesi <i>Firat University</i>
PROF. DR. UĞUR YÜZGEÇ	Bilecik Şeyh Edebali Üniversitesi <i>Bilecik Seyh Edebali University</i>
PROF. DR. VEDAT ORUÇ	Dicle Üniversitesi <i>Dicle University</i>
PROF. DR. YÜKSEL ESEN	Fırat Üniversitesi <i>Firat University</i>
PROF. DR. ZEKİ ARGUNHAN	Bitlis Eren Üniversitesi <i>Bitlis Eren University</i>
DOÇ. DR. ABDUL HAFEEZ-BAİĞ	University of Southern Queensland <i>University of Southern Queensland</i>
DOÇ. DR. ABDULREZZAK BAKIŞ	Batman Üniversitesi <i>Batman University</i>
DOÇ. DR. ARVİND R. SİNGH	Hanjiang Normal Üniversitesi <i>Hanjiang Normal University</i>
DOÇ. DR. AYTUĞ BOYACI	Milli Savunma Üniversitesi <i>National Defence University</i>
DOÇ. DR. BEHÇET KOCAMAN	Bitlis Eren Üniversitesi <i>Bitlis Eren University</i>
DOÇ. DR. C. V. SİVA RAMA PRASAD	

UNVAN AD SOYAD	ÜNİVERSİTE BİLGİSİ
DOÇ. DR. DAVUT İZCİ	Uludağ Üniversitesi <i>Uludag University</i>
DOÇ. DR. DERYA AVCI	Fırat Üniversitesi <i>Firat University</i>
DOÇ. DR. DORİN RADU	Transilvanya Üniversitesi <i>Transilvania University</i>
DOÇ. DR. FARUK ORAL	Bitlis Eren Üniversitesi <i>Bitlis Eren University</i>
DOÇ. DR. FATİH AVCİL	Bitlis Eren Üniversitesi <i>Bitlis Eren University</i>
DOÇ. DR. İSLAM GÖKALP	Batman Üniversitesi <i>Batman University</i>
DOÇ. DR. MEHMET AKİF YERLİKAYA	Bitlis Eren Üniversitesi <i>Bitlis Eren University</i>
DOÇ. DR. MESUT TOĞAÇAR	Fırat Üniversitesi <i>Firat University</i>
DOÇ. DR. MESSAOUD SAİDANİ	Coventry Üniversitesi <i>Coventry University</i>
DOÇ. DR. MOHAMMAD SALMAN	American Middle East Üniversitesi <i>American University of the Middle East</i>
DOÇ. DR. MOSTAFA RASHDAN	American Middle East Üniversitesi <i>American University of the Middle East</i>
DOÇ. DR. MUHAMMED ALİ ARSELİM	Dicle Üniversitesi <i>Dicle University</i>
DOÇ. DR. MUHAMMED FATİH KULUÖZTÜRK	Bitlis Eren Üniversitesi <i>Bitlis Eren University</i>
DOÇ. DR. MUSA ÇIBUK	Bitlis Eren Üniversitesi <i>Bitlis Eren University</i>
DOÇ. DR. MUSTAFA İNCİ	Uludağ Üniversitesi <i>Uludag University</i>
DOÇ. DR. NAMIK YALTAY	Van Yüzüncü Yıl Üniversitesi <i>Van Yüzüncü Yıl University</i>
DOÇ. DR. NURAY ALPASLAN	Batman Üniversitesi <i>Batman University</i>
DOÇ. DR. TAHİR GÖNEN	Uşak Üniversitesi <i>Uşak University</i>
DOÇ. DR. VARUN BAJAJ	Cabalpur Bilgi Teknolojileri, Tasarım ve İmalat Hint Enstitüsü <i>Indian Institute of Information Technology Design & Manufacturing Jabalpur</i>
UNVAN AD SOYAD	ÜNİVERSİTE BİLGİSİ

DOÇ. DR. YAKUP ŞAHİN	Bitlis Eren Üniversitesi <i>Bitlis Eren University</i>
DOÇ. DR. YURDAGÜL BENTEŞEN YAKUT	Dicle Üniversitesi <i>Dicle University</i>
DOÇ. DR. ZEYNAL ABİDİN OĞUZ	Adıyaman Üniversitesi <i>Adıyaman University</i>
DR. ÖĞR. ÜYESİ AHMET NUR	Bitlis Eren Üniversitesi <i>Bitlis Eren University</i>
DR. ÖĞR. ÜYESİ ALEV AKILLI EL	Bitlis Eren Üniversitesi <i>Bitlis Eren University</i>
DR. ÖĞR. ÜYESİ ALİ EMRE ULU	Bitlis Eren Üniversitesi <i>Bitlis Eren University</i>
DR. ÖĞR. ÜYESİ ANA MAFALDA MATOS	Porto Üniversitesi <i>University of Porto</i>
DR. ÖĞR. ÜYESİ AYŞE SUNAR	University of Warwick <i>University of Warwick</i>
DR. ÖĞR. ÜYESİ BURCU BEKTAŞ GÜNEŞ	İstanbul Gedik Üniversitesi <i>Istanbul Gedik University</i>
DR. ÖĞR. ÜYESİ DAVUT ARI	Bitlis Eren Üniversitesi <i>Bitlis Eren University</i>
DR. ÖĞR. ÜYESİ EMİNE AYAZ	Bitlis Eren Üniversitesi <i>Bitlis Eren University</i>
DR. ÖĞR. ÜYESİ ERDAL EKER	Muş Alparslan Üniversitesi <i>Mus Alparslan University</i>
DR. ÖĞR. ÜYESİ ERTUĞRUL ÇAMBAY	Bitlis Eren Üniversitesi <i>Bitlis Eren University</i>
DR. ÖĞR. ÜYESİ FERİDE TUĞRUL	Munzur Üniversitesi <i>Munzur University</i>
DR. ÖĞR. ÜYESİ FİKRİYE ATAMAN	Van Yüzüncü Yıl Üniversitesi <i>Van Yüzüncü Yıl University</i>
DR. ÖĞR. ÜYESİ HALİL YETGİN	Middlesex University <i>Middlesex University</i>
DR. ÖĞR. ÜYESİ MEHTAP ÜLKER	Bitlis Eren Üniversitesi <i>Bitlis Eren University</i>
DR. ÖĞR. ÜYESİ MELTEM YAVUZ ÇELİKDEMİR	Bitlis Eren Üniversitesi <i>Bitlis Eren University</i>
DR. ÖĞR. ÜYESİ MOSTAFA JABARİ	Roma Sapienza Üniversitesi <i>Sapienza University of Rome</i>
DR. ÖĞR. ÜYESİ MURAT BİNİCİ	Bitlis Eren Üniversitesi <i>Bitlis Eren University</i>
DR. ÖĞR. ÜYESİ MUSTAFA CANER	Cumhuriyet Üniversitesi <i>Cumhuriyet University</i>
UNVAN AD SOYAD	ÜNİVERSİTE BİLGİSİ

DR. ÖĞR. ÜYESİ MUSTAFA GÜR	Fırat Üniversitesi <i>Firat University</i>
DR. ÖĞR. ÜYESİ ORHAN ARPA	Dicle Üniversitesi <i>Dicle University</i>
DR. ÖĞR. ÜYESİ OSMAN YİĞİD	Bitlis Eren Üniversitesi <i>Bitlis Eren University</i>
DR. ÖĞR. ÜYESİ ÖMER KARABEY	Bitlis Eren Üniversitesi <i>Bitlis Eren University</i>
DR. ÖĞR. ÜYESİ ÖZLEM ŞEKER	Bitlis Eren Üniversitesi <i>Bitlis Eren University</i>
DR. ÖĞR. ÜYESİ RIDVAN FIRAT ÇINAR	Batman Üniversitesi <i>Batman University</i>
DR. ÖĞR. ÜYESİ SACHİN TARAN	Delhi Teknoloji Üniversitesi <i>Delhi Technological University</i>
DR. ÖĞR. ÜYESİ SİNEM KILIÇKAP IŞIK	Bingöl Üniversitesi <i>Bingol University</i>
DR. ÖĞR. ÜYESİ SMİTH K. KHARE	Syddansk Universitet <i>University of Southern Denmark</i>
DR. ÖĞR. ÜYESİ SONER ÇELİKDEMİR	Bitlis Eren Üniversitesi <i>Bitlis Eren University</i>
DR. ÖĞR. ÜYESİ SONGÜL KARAKUŞ	Bitlis Eren Üniversitesi <i>Bitlis Eren University</i>
DR. ÖĞR. ÜYESİ ÜMİT CAN	Munzur Üniversitesi <i>Munzur University</i>
DR. ÖĞR. ÜYESİ YUNUS SAYAN	Bitlis Eren Üniversitesi <i>Bitlis Eren University</i>
DR. ÖĞR. ÜYESİ YUSUF ÇELİK	Munzur Üniversitesi <i>Munzur University</i>
ARŞ. GÖR. DR. HÜSEYİN BEYTÜT	Bitlis Eren Üniversitesi <i>Bitlis Eren University</i>



SEKRETERYA

SECRETARIAT

UNVAN AD SOYAD	ÜNİVERSİTE BİLGİSİ
ARŞ. GÖR. CANSU AKYÜREK ANACUR	Bitlis Eren Üniversitesi <i>Bitlis Eren University</i>
ARŞ. GÖR. GAMZE AKSOY	Bitlis Eren Üniversitesi <i>Bitlis Eren University</i>
ARŞ. GÖR. NİLAY BOZKURT	Bitlis Eren Üniversitesi <i>Bitlis Eren University</i>
ÖĞR. GÖR. İBRAHİM AYAZ	Bitlis Eren Üniversitesi <i>Bitlis Eren University</i>



AÇILIŞ KONUŞMACILARI

KEYNOTE SPEAKERS

METAHEURISTIC INTELLIGENCE: BRIDGING NATURE- INSPIRED OPTIMISATION AND REAL-WORLD ENGINEERING

Doç. Dr. Davut İZCİ
Bursa Uludağ Üniversitesi
Elektrik Elektronik Mühendisliği Bölümü
Assoc. Prof. Dr. Davut İZCİ
Bursa Uludağ University
Department of Electrical and Electronics Engineering

A COMPARATIVE ASSESSMENT OF RC STRUCTURES PRIOR TO AND FOLLOWING TH 2023 KAHRAMANMARAŞ EARTQUAKES

Prof. Dr. Ercan IŞIK
Bitlis Eren Üniversitesi
İnşaat Mühendisliği Bölümü
Prof. Dr. Ercan IŞIK
Bitlis Eren University
Department of Civil Engineering

1st INTERNATIONAL CONFERENCE ON SMART SYSTEMS, DESIGN AND ENERGY

November 28-29, 2025 | Hybrid | Bitlis

CONGRESS PROGRAM

IMPORTANT

- To be able to make a meeting online, login via <https://zoom.us/join> site, enter ID instead of “Meeting ID or Personal link Name” and solidify the session.
 - The presentation will have 15 minutes (including questions and answers).
 - The Zoom application is free and no need to create an account.
 - The Zoom application can be used without registration.
 - The application works on tablets, phones and PCs.
 - Speakers must be connected to the session 15 minutes before the presentation time.
 - All congress participants can connect live and listen to all sessions.
 - During the session, your camera should be turned on at least %70 of session period
 - Moderator is responsible for the presentation and scientific discussion (question-answer) section of the session.
 - Make sure your computer has a microphone and is working.
 - You should be able to use screen sharing feature in Zoom.
 - Attendance certificates will be sent to you as pdf at the end of the congress.
 - Moderator is responsible for the presentation and scientific discussion (question-answer) section of the session.
 - Before you login to Zoom, indicate hall number and your surname (Hall-1, Gamze AKSOY)
-

Meetings ID: 309 258 4587

Passcode: 12345

OPENING PROGRAM OF THE 1ST INTERNATIONAL CONFERENCE ON SMART SYSTEMS, DESIGN AND ENERGY ISDEC 2025

BITLIS EREN UNIVERSITY
CENTRAL CONFERENCE HALL
28.11.2025 | 10:00

Opening and Welcome

Introduction of the event and overview of the program.

Associate Professor Vedat TÜMEN

Conference Chair

Professor Dr. Hakan ÇOBAN

Dean of Engineering and Architecture Faculty

Professor Dr. Necmettin ELMASTAŞ

Rector of Bitlis Eren University

Associate Professor Dr. Davut İZCİ

Keynote Speaker

“Metaheuristic Intelligence: Bridging Nature-Inspired Optimization and Real-World Engineering”

Professor Dr. Ercan IŞIK

Keynote Speaker

“A Comparative Assessment of RC Structures Prior to and Following the 2023 Kahramanmaraş Earthquakes ”

Professor Dr. Ercan IŞIK

Erasmus+ project introduction

“Strengthening green and digital capacities in higher education through collaboration in integrating historical buildings into a sustainable and digital future”

FACE TO FACE PRESENTATIONS

28.11.2025 / Class 1

BITLIS EREN UNIVERSITY

GRADUATE EDUCATION INSTITUTE

HEAD OF SESSION: Prof. Dr. Serdar EKİNCİ

13:30-14:30

AUTHORS	AFFILIATION	TOPIC TITLE
Rıdvan UMAZ	Bitlis Eren University	Analysis Of 5-Level Buck Converter With Steady-State Model
Mehmet Akif Yerlikaya Yunus SAYAN	Bitlis Eren University	An Integrated Energy–Routing–Task Optimization Model for Fuel Cell Powered AGV Systems
Yunus SAYAN	Bitlis Eren University	A System-Level Review of Photovoltaic-Hydrogen-Proton Exchange Membrane Fuel Cell Chains

15:00-16:30

Sümeýra KAYA ARMAN Halit ÖZEN Güzin AKYILDIZ ALÇURA	Bitlis Eren University İstanbul Teknik University Yıldız Teknik University	Comparison Of Statistical And Machine Learning Methods Based On Sensitivity To The Deficiency Rate In Bluetooth-Based Traffic Data
Bülent KARA Faruk ORAL	Tatvan Vocational Training Center Bitlis Eren University	Offshore Wind Energy And The Current Situation in Türkiye
Nusret BOZKURT Ünal TUNÇ Erden Ozan KARACA	Bitlis Eren University	Evaluation of Pumice-Based Building Materials in Terms of Structural Lightness, Thermal Insulation and Energy Efficiency
Mehmet MOLU	Bitlis Eren University	The Effect of Training Data Order on Model Performance in Deep Learning: CIFAR-10 Analysis

All participants must join the conference 10 minutes before the session time. Every presentation should last not longer than 10-12 minutes. Kindly keep your cameras on till the end of the session.

FACE TO FACE PRESENTATIONS

28.11.2025 / Class 2

BITLIS EREN UNIVERSITY

GRADUATE EDUCATION INSTITUTE

HEAD OF SESSION: Prof. Dr. M. Cihan AYDIN

13:30-14:30

AUTHORS	AFFILIATION	TOPIC TITLE
Cansu AKYÜREK ANACUR Asuman GÜNAY YILMAZ Bekir DİZDAROĞLU	Karadeniz Teknik University	Multimodal Deep Learning-Based Classification of Handwriting Data: The Case of Alzheimer's Disease
Mehmet Kurnaz Celal ALAGÖZ	Sivas Science and Technology University	A Comparative Study of MiniRocket and cFIRE Against Image-Transformation Approaches on EEG Dataset
Kübra ÇETİN YILDIZ Emine AYAZ	Bitlis Eren University	Multi-Class Sentiment Analysis Of Mpox Disease In X(Twitter) Data

15:00-16:30

Cansu AKYÜREK ANACUR Özlem ŞEKER	Bitlis Eren University	Integrating Geospatial Analysis, Temporal Modeling, And Machine Learning For Seismic Hazard Assessment: A 24-Year Earthquake Study In Chile (2000–2024)
Yaren YALÇINKAYA Emine AYAZ Vedat TÜMEN	Bitlis Eren University	Land Cover Segmentation and Forest Loss Analysis from Satellite Images Using Vision Transformers
Mehtap ÜLKER	Bitlis Eren University	Adaptive Multi-Coefficient Quantization Index Modulation in DCT-Based Steganography

All participants must join the conference 10 minutes before the session time. Every presentation should last not longer than 10-12 minutes. Kindly keep your cameras on till the end of the session.

FACE TO FACE PRESENTATIONS

28.11.2025 / Class 3

BITLIS EREN UNIVERSITY

GRADUATE EDUCATION INSTITUTE

HEAD OF SESSION: Assoc. Prof. Nusret BOZKURT

13:30-14:30

AUTHORS	AFFILIATION	TOPIC TITLE
Nusret BOZKURT Orhan DURAK	Bitlis Eren University	Chronological Evolution of Structural Health Monitoring and Prediction Systems in Türkiye
Mehmet MOLU	Bitlis Eren University	Proposed Management System for Material and Technical Human Resources in Public Institutions
Nusret BOZKURT Saffet SOYUGÜZEL	Bitlis Eren University	Chronological Development Of Green Building Technologies In Türkiye And A Regional Perspective On Sustainability Criteria

15:00-16:30

Erden Ozan Karaca Nusret BOZKURT	Bitlis Eren University	Investigation Of The Applicability Of Fuzzy Logic Method In Estimating Load-Displacement Data Of Lightweight Concrete Beams
Özlem ŞEKER Cennet AKÇAKAYA Nurullah AKARSLAN	Bitlis Eren University	BLE Based IoT Application for Life Detection Under Debris
Nusret BOZKURT Nidahi SOYUGÜZEL	Bitlis Eren University	Chronological Evolution of Smart Concrete as a Special Composite Material
Farhad Pirmohammadi ALISHAH Mehdi Mohammad REZAEI	Islamic Azad University, Shabestar Branch	The Use of Artificial Intelligence in Petrology
Farhad Pirmohammadi ALISHAH Mehdi Mohammad REZAEI	Islamic Azad University, Shabestar Branch	Artificial Intelligence is revolutionizing energy consumption in Civil Engineering

All participants must join the conference 10 minutes before the session time. Every presentation should last not longer than 10-12 minutes. Kindly keep your cameras on till the end of the session.

ONLINE PRESENTATIONS

29.11.2025 / Hall-1 / Session-1

BITLIS LOCAL TIME

09:30 – 11:30

ZOOM ID: 309 258 4587

ZOOM PASSCODE: 12345

HEAD OF SESSION: Assist. Prof. Murat BİNİCİ

AUTHORS	AFFILIATION	TOPIC TITLE
Feride TUĞRUL	Munzur University	Effect on Decision Making Processes of Pythagorean Fuzzy Set
Murat Binici Nebi SUDAY	Bitlis Eren University	Short-Term Electricity Load Forecasting with Holt–Winters, XGBoost and Extended Hybrid Model
Celal ALAGÖZ Farhan AADIL	Sivas Science and Technology University	Adaptive Representation–Feature Selection for Efficient and Interpretable Time Series Classification
İlayda AKSOY	Bitlis Eren University	Hybrid Optimization-Based Deep Learning Model Design for Energy- Efficient Intelligent Systems
Yusuf UZ Zafer SERİN Uğur YÜZGEÇ	Bilecik Şeyh Edebalı University	Selfie2BFP: A Facial Image–Based Deep Learning Framework for Body Fat Percentage Estimation
Mehmet Emin BAKIR Sezer DÖYMAZ Vedat TÜMEN	İzmir Katip Çelebi University Bitlis Eren University	Insult Detection Across Multiple Social Media Platforms

All participants must join the conference 10 minutes before the session time. Every presentation should last not longer than 10-12 minutes. Kindly keep your cameras on till the end of the session.

ONLINE PRESENTATIONS

29.11.2025 / Hall-2 / Session-1

BITLIS LOCAL TIME

09:30 – 11:30

ZOOM ID: 309 258 4587

ZOOM PASSCODE: 12345

HEAD OF SESSION: Assoc. Prof. Rıdvan UMAZ

AUTHORS	AFFILIATION	TOPIC TITLE
Fikri AĞGÜN Raif SİME	Bitlis Eren University	A Study On Webassembly-Based Crypto Mining
Berat DEMİRKAN Tolga ÖZASLAN	Ankara Yıldırım Beyazıt University	Detecting Specular Surfaces With LiDAR–Sonar Sensor Fusion
Rıdvan Fırat ÇINAR	Batman University	Data-driven Scoring of a Continuous Water Quality Index Using Nonlinear Tree Based Machine Learning Models
Onur KAYA Songül KARAKUŞ	Bitlis Eren University	Recovering Deleted Data On Thermal Paper Using Uv Light And Image Processing In Digital Forensics
Eyyüp KARDEŞ İrfan ÖKTEN Uğur YÜZGEÇ	Bitlis Eren University Bilecik Şeyh Edebalı University	Facial Recognition-Based Security Verification in Mobile Banking: An Innovative AI-Based Approach
Erkan DEVECİ Burhan ERGEN	Osmaniye Korkut Ata University Fırat University	Automated Post-Earthquake Wall Damage Detection and Classification Using YOLOv8

All participants must join the conference 10 minutes before the session time. Every presentation should last not longer than 10-12 minutes. Kindly keep your cameras on till the end of the session.

ONLINE PRESENTATIONS

29.11.2025 / Hall-3 / Session-1

BITLIS LOCAL TIME

09:30 - 11:30

ZOOM ID: 309 258 4587

ZOOM PASSCODE: 12345

HEAD OF SESSION: Prof. Dr. Cengiz YILDIZ

AUTHORS	AFFILIATION	TOPIC TITLE
Fatih İLKBAHAR Şahin KARA Muhammed Zekeriya GÜNDÜZ	Düzce University Sakarya Applied Sciences University Bingöl University	Planning, Optimization, and Grid Integration of Electric Vehicle Charging Infrastructure: A Systematic Literature Review
Gökhan YÜKSEK	Batman University	Evaluating Meteorological Effects on Wind Turbine Performance: Anomaly Detection and Energy Loss Quantification
Serdar EKİNCİ Davut İZCİ Burcu BEKTAŞ GÜNEŞ İlayda AKSOY Mohit BAJAJ Laith ABUALIGAH	Bitlis Eren University Bursa Uludağ University Graphic Era (Deemed to be University) Al al-Bayt University	Stellar Oscillation Optimizer-based Parameter Identification for Photowatt PWP201 and STM6- 40/36 PV Modules
Abdullatif YILMAZ Cengiz YILDIZ	Fırat University	Numerical Investigation Of The Cooling Performance Of Photovoltaic Panels Equipped With Square Fins
Mustafa AKDAĞ Mehmet Salih MAMİŞ	Bitlis Eren University İnönü University	Single-Ended Fault Detection and Fault Location in Transmission Lines Using the Approximate Derivative
Fatih OKTAY Emin EL	Bitlis Eren University	Investigation of the Thermal Performance of Air-Cooled Lithium-Ion Battery Systems in Electric Vehicles

All participants must join the conference 10 minutes before the session time. Every presentation should last not longer than 10-12 minutes. Kindly keep your cameras on till the end of the session.

ONLINE PRESENTATIONS

29.11.2025 / Hall-1 / Session-2

BITLIS LOCAL TIME

13:30 – 15:30

ZOOM ID: 309 258 4587

ZOOM PASSCODE: 12345

HEAD OF SESSION: Assist. Prof. Ümit CAN

AUTHORS	AFFILIATION	TOPIC TITLE
Dilan ÖZEK İrfan ÖKTEN Lokman DOĞAN	Bitlis Eren University Kütahya Health Sciences University	A Deep Learning-Based Bidirectional Sign Language Translation System
Seda YETKİN YEŞİL Olca PALTA	Bitlis Eren University	ResNet-50 Based CNN Model for Grape Leaf Image Classification in MATLAB
Ümit CAN	Munzur University	Sentiment Analysis of Monkeypox Tweets Utilizing a Hybrid Deep Learning Model
Hasan ÖNDER İlknur ÇEVİK TEKİN	Selçuk University	Monitoring and Analysis of Employee Productivity with Artificial Intelligence: YOLO Algorithm Application
İSMAİL ÇALIKUŞU Kadir HALTAŞ	Nevşehir Hacı Bektaş Veli University	A Machine Learning and Clustering-Based Framework for Assessing Environmental Effects in the Textile Industry
Muhammed Zekeriya GÜNDÜZ Şahin KARA Fatih İLKBAHAR	Bingöl University Sakarya Applied Sciences University Düzce University	Enhancing Situational Awareness Against Ransomware Attacks: Analysis, Detection, and Prevention Approaches

All participants must join the conference 10 minutes before the session time. Every presentation should last not longer than 10-12 minutes. Kindly keep your cameras on till the end of the session.

ONLINE PRESENTATIONS

29.11.2025 / Hall-2 / Session-2

BITLIS LOCAL TIME

13:30 – 15:30

ZOOM ID: 309 258 4587

ZOOM PASSCODE: 12345

HEAD OF SESSION: Assist. Prof. Emine AYAZ

AUTHORS	AFFILIATION	TOPIC TITLE
Mehmet MOLU	Bitlis Eren University	A Conceptual Two-Layer Emotion Chain Model For In-Store Customer Satisfaction Analysis
Elif ERÇEL İrfan ÖKTEN	Bitlis Eren University	Smart Door Security System with Face Recognition: A Low-Cost IoT-Based Approach
Barış ASLAN Pınar ÜNVER Beytullah TÜTÜNCÜ Tuğçe DENİZ	Düzce University	Speaker Attribution in Dialogue-Heavy Texts: Comparative Analysis of Babelscape and SavasyBERT NER Models
Buğra Berk SARIOĞLU Tolga ÖZASLAN	Ankara Yıldırım Beyazıt University	An ESP32-Based Integrated Multi-Peripheral Platform for Micro Aerial Vehicles
Muhammet İsmail GÜNGÖR Davut İZCİ Serdar EKİNCİ Ehab GHITH	Bursa Uludağ University Bitlis Eren University Ain Shams University	Enhanced Transient Performance of Micro-Robotic Systems via SFOA-Based PID Tuning
Şafak SARI Faruk ORAL	Bitlis Eren University	Waste Heat Recovery Potential In Sofc Systems Operating At High Temperatures

All participants must join the conference 10 minutes before the session time. Every presentation should last not longer than 10-12 minutes. Kindly keep your cameras on till the end of the session.

ONLINE PRESENTATIONS

29.11.2025 / Hall-3 / Session-2

BITLIS LOCAL TIME

13:30 – 15:30

ZOOM ID: 309 258 4587

ZOOM PASSCODE: 12345

HEAD OF SESSION: Assist. Prof. Alev Akıllı EL

AUTHORS	AFFILIATION	TOPIC TITLE
Alev AKILLI EL	Bitlis Eren University	Conductive Asphalt Pavements for Snow and Ice Management on Roads
Aykut TUNTAŞ Namık YALTAY	Van Yüzüncü Yıl University	Geopolimer Brick Technology In Terms Of Energy And Sustainability
Farhad Pirmohammadi ALİSHAH Mehdi Mohammad REZAEI	Islamic Azad University, Shabestar Branch	The Application of Artificial Intelligence in Crystallography and Mineralogy
Fatih TAŞDELEN	Bitlis Eren University	An Examination Of The Effect Of Channel Height On Heat Transfer Within A Chip-Embedded Minichannel
Fatih TAŞDELEN	Bitlis Eren University	Evaluation Of Heat Transfer Behaviour In A Minichannel With Electronic Chips Using Different Fluids
Özge Nur ÇETKİN	Bitlis Eren University	Investigation of the Use of Waste Materials in Soil Improvement Methods
Zehra ERTOSUN KARABULUT Sabriye Banu İKİZLER	Muş Alparslan University Karadeniz Teknik Üniversitesi	Different Sand Soils Treated by MICP Method: Effect of Flow Rate Variation on Calcium Carbonate Precipitation

All participants must join the conference 10 minutes before the session time. Every presentation should last not longer than 10-12 minutes. Kindly keep your cameras on till the end of the session.

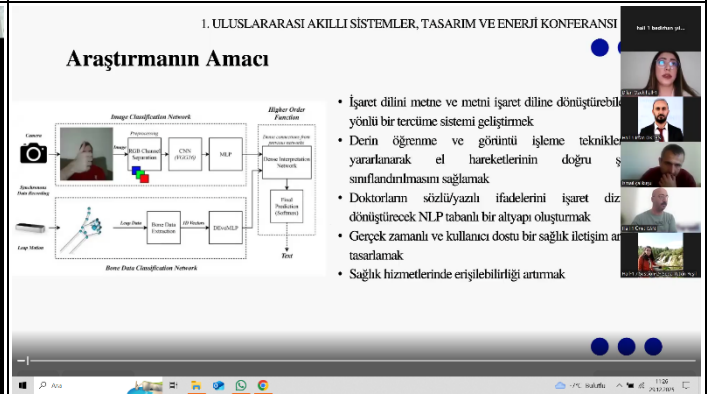
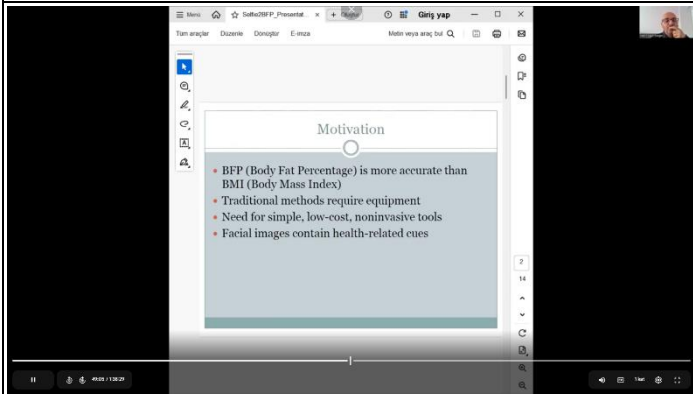
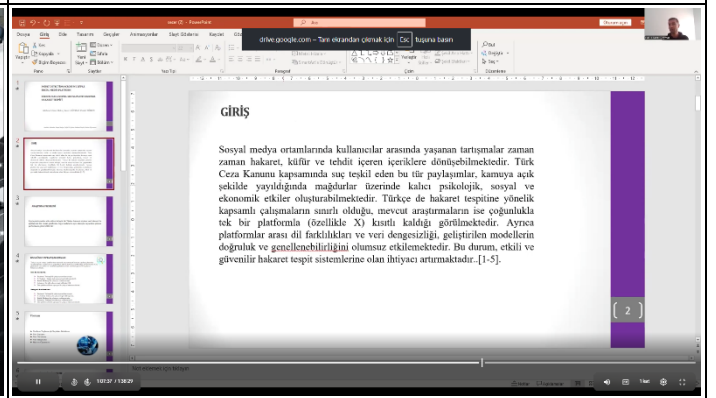
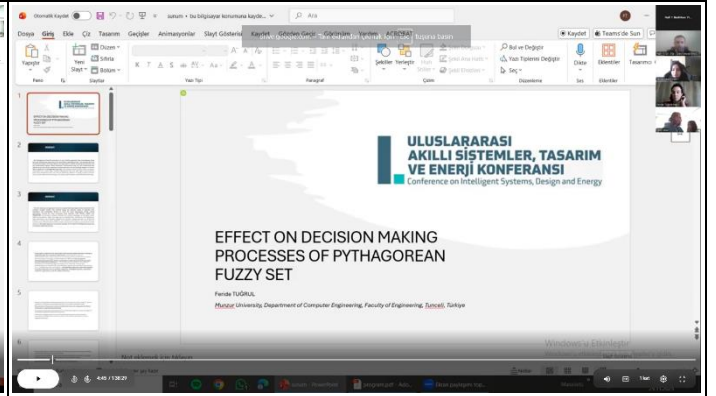
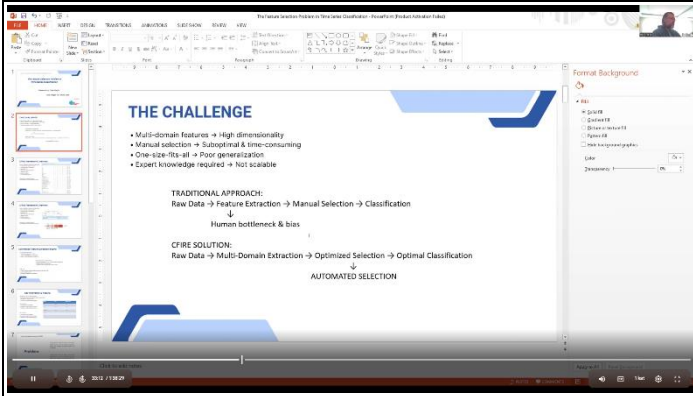
GALERİ

GALLERY



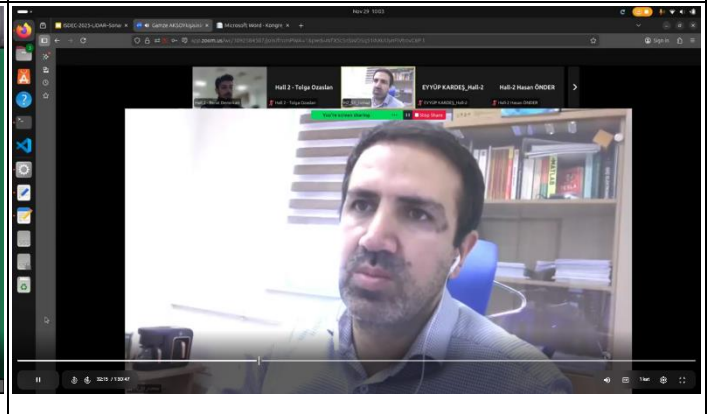
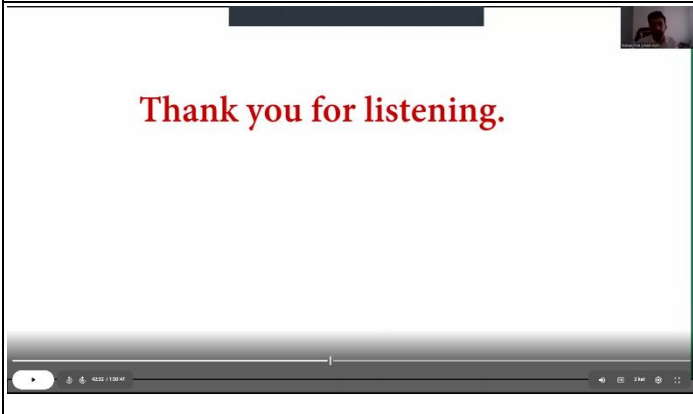
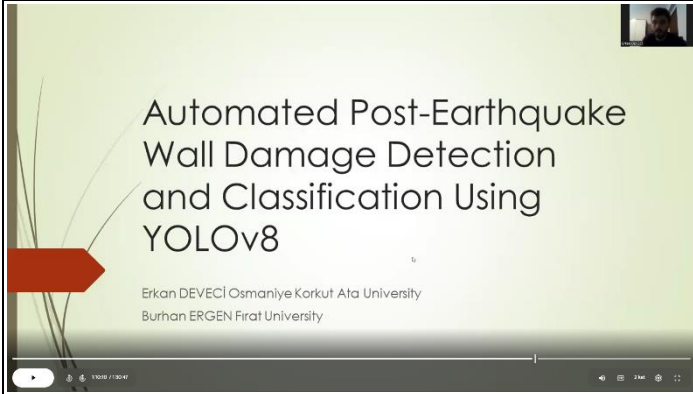
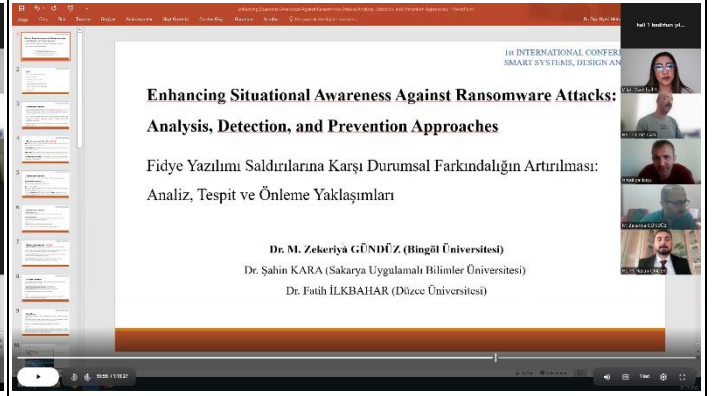
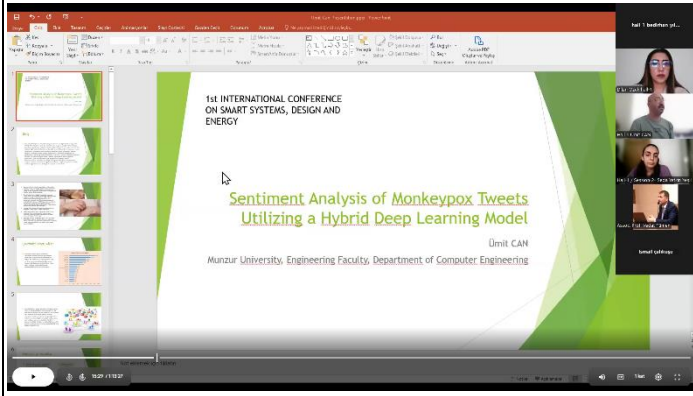
GALERİ

GALLERY



GALERİ

GALLERY




GALERİ

GALLERY


Yüzleşme: Babelscape (Evrenselci) vs. SavasyBERT (Uzman)

Babelscape (Evrenselci)



- Babelscape (Evrenselci): "Çok dilli (multilingual), geniş kapsamlı bir bilgi grafiği tabanlı model."
- "Farklı dillerde genel amaçlı bir performans sunmayı hedefler."
- "Dile özgü morfolojik ve sentaktik derinliği sınırlıdır."

SavasyBERT (Uzman)



- SavasyBERT (Uzman): "Sadece Türkçe verilerle eğitilmiş (monolingual), Transformer tabanlı bir BERT modelidir."
- "Türkçe metinlerin morfolojik ve sentaktik yapısı üzerine uzmanlaşmıştır."
- "Yerel dil yapısına duyarlılığı ve anlama kapasitesi yüksektir."

An ESP32-Based Integrated Multi-Peripheral Platform for Micro Aerial Vehicles

Buğra Berk SARIOĞLU, Dr. Tolga ÖZASLAN

ROBust Autonomous Mobility Laboratory

I. ULUSLARARASI AKILLI SİSTEMLER, TASARIM VE KONFERANSI



Yüz Tanıma Destekli Akıllı Kapı Güvenlik Sistemi: Düşük Maliyetli IoT Tabanlı Yaklaşım

Smart Door Security System with Facial Recognition: A Low-Cost IoT-Based Approach

Elif ERCEL
Dr. Öğr. Üyesi İRFAN ÖKTEN


Mağaza İçi Müşteri Memnuniyetinin İki Katmanlı Duygu Zinciri Temelli Analizi İçin Önerilen Bir Model

I. Uluslararası Akıllı Sistemler, Tasarım ve Enerji Konferansı
2025
Mehmet MOLU

ENHANCED TRANSIENT PERFORMANCE OF MICRO-ROBOTİK SYSTEMS VIA SFOA BASED PID TUNING

Muhammet İsmail GÜNGÖR
Davut İZCİ
Serdar EKİNCİ
Ehab GHITH

Analiz: Neden Derinlik Genişliği Yendi?



- Derinlik > Genişlik:** Bu görevde, dile özgü morfolojik ve sentaktik yapısı derinlemesine anlamak, çok dilli devasa bir veri kümesine yüzeysel olarak maruz kalmaktan daha etkili oldu.
- Negatif Bilgi (Negative Knowledge):** SavasyBERT, sadece neyin 'Kişi' olduğunu değil, aynı zamanda Türkçe bağlamında neyin 'Kişi' olmadığını da (örn: 'dedi' fiili) öğrenmiştir.
- Bağlamın Gücü:** Yerel model, kelimeleri sadece izole birimler olarak değil, cümle içindeki bağlamlarıyla birlikte değerlendirmede çok daha başarılıdır.
- Hipotez Doğrulandı:** Dile özgü morfolojik yeteneklerin, tespit doğruluğu için kritik öneme sahip olduğu hipotezimiz güçlü bir şekilde doğrulanmıştır.

Deneyisel Kurulum: Veri Seti ve Analiz Yöntemi

- Veri Seti:** Çeşitli dönemlere ait, diyalog yoğunluğu yüksek Türkçe edebi eserlerden oluşan bir derlem (corpus) kullanılmıştır.
- Değerlendirme Yöntemi:** Standart niceliksel metrikler (Precision, Recall) yerine, modellerin ürettiği 'Kişi' varlık listelerinin niteliksel analizine odaklanılmıştır.
- Ana Odak:** Tespitlerin sayısı (nicelik) değil, doğruluğu ve temizliği (nitelik).
- Kritik Metrik:** 'Gürültü' oranı, yani yanlış pozitif (false positive) tespitlerin sıklığı. Amacımız en 'temiz' listeyi üreten modeli bulmaktır.



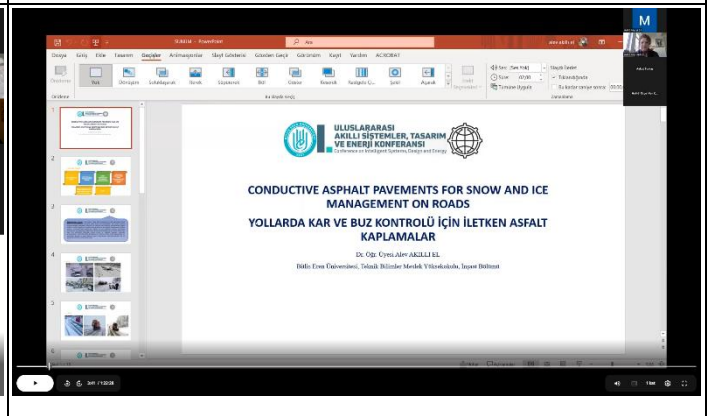
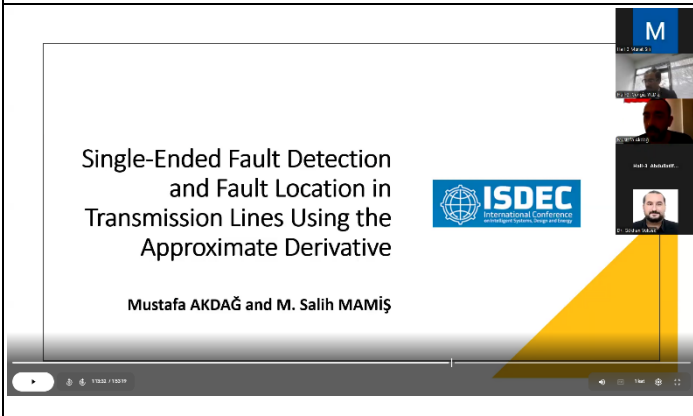
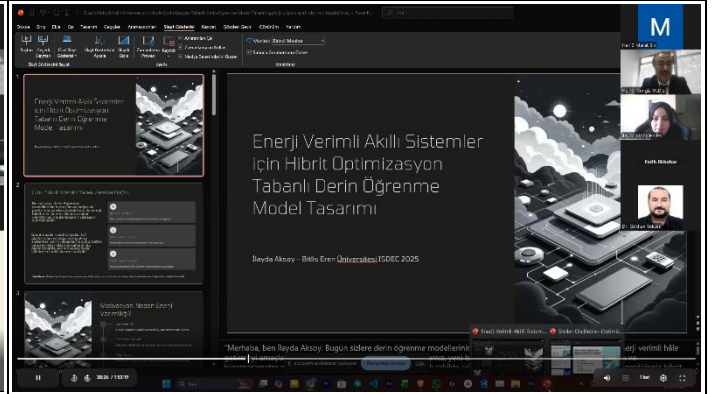
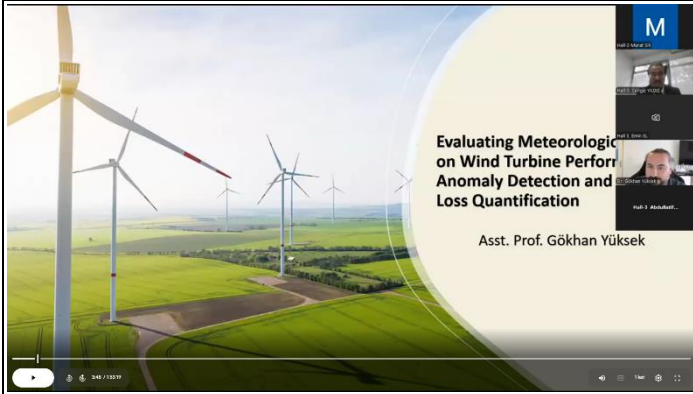
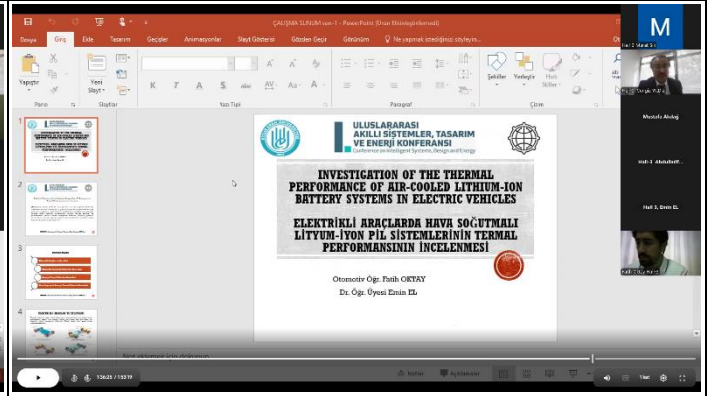
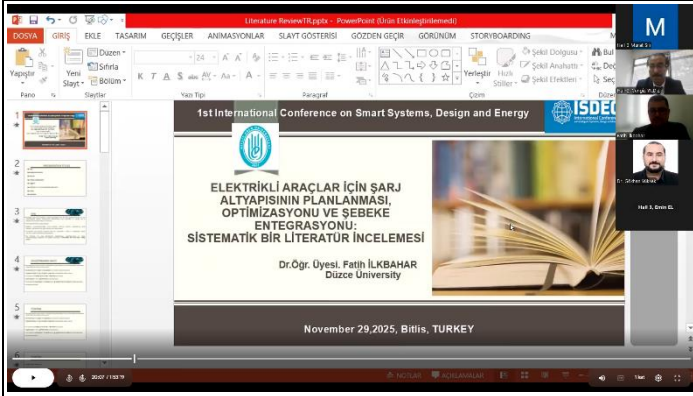
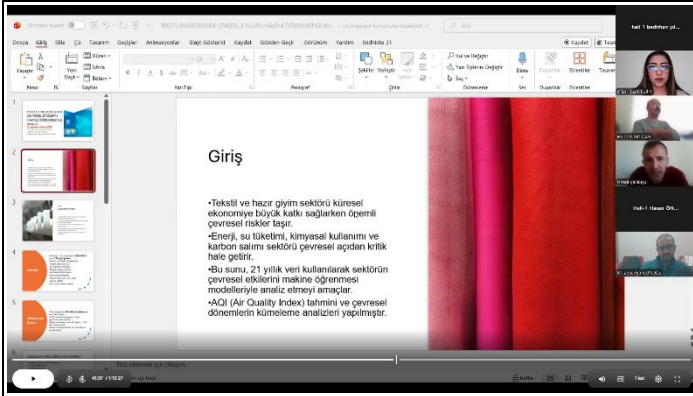
Diyalog Yoğun Edebi Korpus

Niteliksel Analiz

FOTOVOLTAİK PANELLERİN KARE KANATÇIKLARLA SOĞUTULMASININ SAYISAL OLARAK İNCELENMESİ

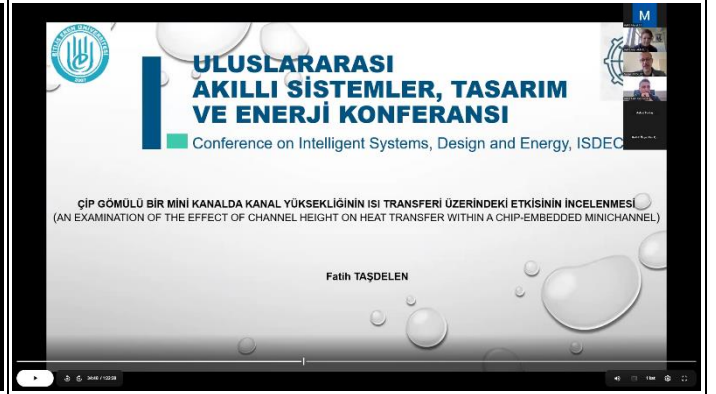
GALERİ

GALLERY



GALERİ

GALLERY





İÇİNDEKİLER

TABLE OF CONTENTS

TAKDİM.....	i
ONURSAL BAŞKAN	ii
DÜZENLEME KURULU	iii
DANIŞMA KURULU	iv
BİLİM KURULU	v
SEKRETERYA	xi
İÇİNDEKİLER.....	i
Analysls of 5-Level Buck Converter with Steady-State Model	1
An Integrated Energy–Routing–Task Optimization Model for Fuel Cell Powered AGV Systems	2
A System-Level Review of Photovoltaic-Hydrogen-Proton Exchange Membrane Fuel Cell Chains for Clean Power and Transportation	3
Comparison of Statistical and Machine Learning Methods Based on Sensitivity to the Deficiency Rate in Bluetooth-Based Traffic Data	4
Offshore Wind Energy and the Current Situation in Türkiye	6
Evaluation of Pumice-Based Building Materials in Terms of Structural Lightness, Thermal Insulation and Energy Efficiency	7
Chronological Evolution of Building Health Monitoring and Prediction Systems in Türkiye	8
Chronological Development of Green Building Technologies in Türkiye and a Regional Perspective on Sustainability Criteria	9
Chronological Evolution of Smart Concrete as a Special Composite Material: A Journey from Self-Sensing and Repair Systems to Artificial Intelligence Integration	10

The Effect of Training Data Order on Model Performance in Deep Learning: A Systematic Analysis on CIFAR-10	11
Proposed Management System to Enhance the Efficiency of Material and Technical Human Resources in Public Institutions	12
A Conceptual Two-Layer Emotion Chain Model for in-Store Customer Satisfaction Analysis.....	14
Integrating Geospatial Analysis, Temporal Modeling, and Machine Learning for Seismic Hazard Assessment: A 24-Year Earthquake Study in Chile (2000–2024)	15
Multimodal Deep Learning-Based Classification of Handwriting Data: The Case of Alzheimer’s Disease	16
Analysis of Societal Emotional Responses to Mpox Disease Based On X (Twitter) Data	17
Land Cover Segmantation and Forest Loss Analysis from Satellite Images Using Vision Transformers.....	18
Adaptive Multi-Coefficient Quantization Index Modulation in Dct-Based Steganography	19
Investigation of the Applicability of Fuzzy Logic Method in Estimating Load-Displacement Data of Lightweight Concrete Beams	20
Ble Based IOT Application for Life Detection under Debris	21
Effect on Decision Making Processes of Pythagorean Fuzzy Set	22
Short-Term Electricity Load Forecasting with Holt–Winters, XGBoost and Extended Hybrid Holt–Winters and XGBoost Model: Evidence from the AEP Hourly Dataset.....	23
Adaptive Representation–Feature Selection for Efficient and Interpretable Time Series Classification.....	24
Hybrid Optimization-Based Deep Learning Model Design for Energy-Efficient Intelligent Systems	25
SELFIE2BFP: A Deep Learning Approach for Body Fat Percentage Estimation from Facial Images	27
Cross-Platform Hate Speech Detection in Turkish.....	28
A Study on Webassembly-Based Crypto Mining.....	29
Detecting Specular Surfaces with Lidar–Sonar Sensor Fusion.....	30

Data-Driven Scoring of a Continuous Water Quality Index Using Nonlinear Tree Based Machine Learning Models	31
Recovering Deleted Data on Thermal Paper Using UV Light and Image Processing in Digital Forensics.....	32
Facial Recognition-Based Security Verification in Mobile Banking: An Innovative Artificial Intelligence-Based Approach	33
Automated Post-Earthquake Wall Damage Detection and Classification Using YOLOV8	34
Planning, Optimization, and Grid Integration of Electric Vehicle Charging Infrastructure: A Systematic Literature Review	35
Evaluating Meteorological Effects on Wind Turbine Performance: Anomaly Detection and Energy Loss Quantification.....	36
Stellar Oscillation Optimizer-Based Parameter Identification for Photowatt PWP201 And STM6-40/36 PV Modules	37
Enhanced Transient Performance of Micro-Robotic Systems Via SFOA-Based PID Tuning	38
Numerical Investigation of the Cooling Performance of Photovoltaic Panels Equipped with Square Fins.....	39
Single-Ended Fault Detection and Fault Location in Transmission Lines Using the Approximate Derivative.....	40
Investigation of the Thermal Performance of Air-Cooled Lithium-Ion Battery Systems in Electric Vehicles.....	42
A Deep Learning-Based Approach for a Two-Way Sign Language Translation System ...	43
Resnet-50 Based CNN Model for Grape Leaf Image Classification In MATLAB	44
Sentiment Analysis of Monkeypox Tweets Using A Hybrid CNN-BiGRU Based Deep Learning Model	45
Monitoring and Analysis of Employee Productivity with Artificial Intelligence: An Application Using the YOLO Algorithm	46
A Machine Learning and Clustering-Based Framework for Assessing Environmental Effects in the Textile Industry	47

Enhancing Situational Awareness Against Ransomware Attacks: Analysis, Detection, and Prevention Approaches.....	48
Smart Door Security System Whit Face Recognition: A Low-Cost IoT-Based Approach	49
Speaker Detection in Dialogue-Heavy Texts: A Comparative Analysis of Babelscape and Savasybert Ner Models	50
Conductive Asphalt Pavements for Snow and Ice Management on Roads.....	51
Geopolimer Brick Technology in Terms of Energy and Sustainability	52
Evaluation of Heat Transfer Behaviour in a Minichannel with Electronic Chips Using Different Fluids	53
An Examination of the Effect of Channel Height on Heat Transfer Within a Chip-Embedded Minichannel.....	54
Investigation of the Use of Waste Materials in Soil Improvement Methods	55
Effect of Different Flow Rate Variation on Calcium Carbonate Precipitation in Sand Soils Treated by MICP Method	56
Diyalog Ağrılıklı Metinlerde Konuşan Karakter Tespiti: Babelscape ve Savasybert Ner Modellerinin Karşılaştırmalı Analizi	138

ÖZET BİLDİRİLER



ANALYSIS OF 5-LEVEL BUCK CONVERTER WITH STEADY-STATE MODEL

Rıdvan UMAZ¹ 

¹ Bitlis Eren University, Department of Electrical and Electronics Engineering, Bitlis, Türkiye, rumaz@beu.edu.tr

ABSTRACT

Multi-level buck converters are an emerging technology for the power management systems since conventional buck converters does not operate at high frequencies (e.g., 200 MHz) and are not compatible with high technologies (e.g., 28nm CMOS). This work focuses on a 5-level buck converter that has extra three flying capacitors and extra six power FETs over conventional buck. A comprehensive theoretical analysis of the converter operating in continuous conduction mode (CCM) is covered in this study. The analysis is based on the inductor volt-second balance and the capacitor charge balance laws that allow to derive fundamental circuits for the converter. This study presents the steady-state of the 5-level converter with an equivalent circuit. Furthermore, the work addresses the conduction loss parameters of the 5-level converter which are mapped into an equivalent circuit. The RMS currents for the inductor and the filter capacitor are derived, and the overall conduction loss of the 5-level converter are formalized in the work.

Keywords :

Multi-level converter, Steady-state analysis, Conduction loss, RMS current calculation.



AN INTEGRATED ENERGY-ROUTING-TASK OPTIMIZATION MODEL FOR FUEL CELL POWERED AGV SYSTEMS

Mehmet Akif YERLİKAYA ^{1,*} , Yunus SAYAN ¹

¹ Bitlis Eren University, Mechanical Engineering Department, Bitlis, Türkiye

* Sorumlu Yazar: mayerlikaya@beu.edu.tr

ABSTRACT

This study proposes an integrated optimization framework for automated guided vehicles (AGVs) powered by hydrogen fuel cells in modern warehouse environments. The model simultaneously incorporates task assignment, routing, and scheduling decisions—typical components of industrial engineering—with the physical characteristics of proton exchange membrane (PEM) fuel cells, including hydrogen consumption, power-energy relationships, efficiency, and refueling times, which are central to mechanical engineering considerations. The energy demand of each AGV is calculated using a physics-based fuel cell power model that accounts for vehicle speed, payload, and rolling resistance. This energy model is embedded into a mixed-integer linear programming (MILP) formulation, enabling the simultaneous optimization of operational performance and energy utilization. The objective function minimizes total task completion time, hydrogen consumption, and refueling-induced delays. Computational results demonstrate that the proposed approach achieves 12–28% lower energy consumption and more balanced workload distribution compared to classical AGV planning models. The findings highlight the potential of fuel-cell-powered AGVs to improve sustainability, efficiency, and reliability in next-generation warehouse automation systems

Keywords : Fuel cell, Automated guided vehicle, Optimization, Mixed-Integer Programming, Hydrogen Consumption, Routing.



A SYSTEM-LEVEL REVIEW OF PHOTOVOLTAIC-HYDROGEN-PROTON EXCHANGE MEMBRANE FUEL CELL CHAINS FOR CLEAN POWER AND TRANSPORTATION

Yunus SAYAN¹

¹ Bitlis Eren University, Mechanical Engineering Department, Bitlis, Türkiye, ysayan@beu.edu.tr

ABSTRACT

In principle, a combined system of photovoltaic panels, water electrolysis, and polymer electrolyte membrane fuel cells has the potential to produce renewable electricity and hydrogen with water as the only byproduct. Hybrid photovoltaic–electrolyzer–fuel cell systems have been studied for over two decades and have been demonstrated in off-grid buildings, microgrids, and pilot hydrogen communities. Nevertheless, each additional energy conversion stage results in losses, thus a key design issue is why one should initially generate hydrogen from photovoltaic electricity and subsequently reconvert it to electricity in a polymer electrolyte membrane fuel cell, rather than utilizing the photovoltaic electricity directly, storing it in batteries, or sending it to the grid.

This review compares four primary photovoltaic-based clean power pathways: direct photovoltaic use, photovoltaic with batteries, photovoltaic with the grid as a virtual battery, and photovoltaic–electrolyzer–hydrogen–proton exchange membrane fuel cell systems. Using recent reviews and techno-economic studies, it provides a summary of their typical round-trip efficiencies, storage durations, and roles. Lithium-ion battery systems typically achieve 80–95% round-trip efficiency on the AC side for short-term storage. In contrast, power-to-hydrogen-to-power (P2H2P) chains generally operate at 30–50% efficiency, meaning roughly two to three times more photovoltaic electricity is required per kilowatt-hour (kWh) delivered. Even with this disadvantage, hydrogen offers unique advantages for long-duration and seasonal storage. It can also connect photovoltaic electricity to sectors where batteries or direct electrification are difficult to implement, such as heavy-duty transportation, specific industrial processes, and long-duration backup power.

The study concludes that electricity obtained from photovoltaic-derived hydrogen and polymer electrolyte membrane fuel cells should not be evaluated as a competitor to grid-connected or battery-coupled photovoltaic systems, but rather as a complementary option within a hierarchical energy system design. The design prioritizes direct use and grid integration, followed by batteries for hours to days, hydrogen for weeks to months, and multi-sector coupling. Despite its lower round-trip efficiency, this study provides practical rules of thumb for when the photovoltaic–Hydrogen–Polymer electrolyte membrane fuel cell route is justified.

Keywords : Photovoltaic, Proton exchange membrane fuel cell, Water electrolysis, Seasonal storage, Power-to-hydrogen, Round-trip efficiency.



COMPARISON OF STATISTICAL AND MACHINE LEARNING METHODS BASED ON SENSITIVITY TO THE DEFICIENCY RATE IN BLUETOOTH- BASED TRAFFIC DATA

Sümeysra KAYA ARMAN ^{1,*} , Halit ÖZEN ² , Güzin AKYILDIZ ALÇURA ²

¹ Bitlis Eren University, Civil Engineering Department, Bitlis, Türkiye

² İstanbul Teknik University, Civil Engineering Department, İstanbul, Türkiye

* Corresponding Author: skarman@beu.edu.tr

ABSTRACT

The primary objective of this study is to observe the performance of missing data imputation methods in real traffic data obtained from Bluetooth sensors at different levels of data loss and to evaluate them comparatively using statistical methods and regression-based machine learning methods. In intelligent transportation systems, traffic data may be incomplete due to data transmission problems originating from sensors, interruptions, measurement errors, or environmental factors such as weather conditions. Completing missing data is critical for data quality and subsequent analyses in areas such as travel time estimation, traffic density analysis, and traffic management. Therefore, understanding how data completion methods perform as the rate of missing data increases is an important requirement for both researchers and practitioners. The study used one week of data obtained from Bluetooth sensors in the Üsküdar Coastal Road-Beylerbeyi area of Istanbul. The dataset was divided into weekdays and weekends, and different missing data simulations were created to test the sensitivity of the methods for different missing data rates (10-20-30-40-50-60-70-80-90%), and different data completion methods were applied for each missing data level. Within the scope of statistical methods, forward/backward, median, and mean imputation approaches were evaluated; within the scope of machine learning methods, regression-based K-Nearest Neighbour, Linear Regression, Decision Trees, and Support Vector Regression methods were used. Missingness simulations were performed based on the principle of randomness and tested for each method and each missingness rate used. Data completion performance was measured using the Mean Absolute Error (MAE) and Root Mean Square Error (RMSE) metrics. The findings revealed that as the missingness rate increased, the performance of the methods diverged significantly. Among the statistical methods, the Mean and Median imputation methods achieved high error values even at low missingness rates and rapidly lost accuracy as the missingness rate increased. Forward and backward filling methods achieved successful results at low missing rate percentages (10-30%), but their performance declined rapidly as the missing rate increased, disrupting the continuity of the time series. In particular, at missing rate percentages above 70%, the error values of all statistical methods were quite high. Machine learning methods demonstrated more stable performance for each missing data rate compared to statistical methods. At low missing data rates (10-30%), KNN and SVR stood out with the lowest error values, while Decision Trees showed stable performance at medium missing data levels (40-60%). Furthermore, it was observed that the Decision Trees algorithm kept the error increase more limited as the missing rate increased. The Linear Regression algorithm showed low performance with a high error value due to the weak linear relationships in this data structure. Based on the results obtained, a decision matrix was created to facilitate method selection according to the missing rate.

Accordingly, K-Nearest Neighbour, Forward Filling, Backward Filling, and Support Vector Regression are recommended for low missing levels (10-30%); K-Nearest Neighbour and Decision Trees for medium missing levels (40-60%); and Decision Trees for high missing levels.

Keywords : Data imputation, Bluetooth data, Time series, Traffic data.



OFFSHORE WIND ENERGY AND THE CURRENT SITUATION IN TÜRKİYE

Bülent KARA ^{1,*} , Faruk ORAL ¹

¹ Bitlis Eren University, Institute of Graduate Education, Department of Mechanical Engineering, Bitlis, Türkiye

² Bitlis Eren University, Mechanical Engineering Department, Bitlis, Türkiye

*Corresponding Author: bulent_karal@msn.com

ABSTRACT

Wind energy power plants are generally divided into two main categories: onshore and offshore. Offshore wind farms consist of large-scale wind turbines installed in seas or oceans at a certain distance from the coast. These systems generate high amounts of electricity by harnessing the strong and steady wind currents found in open sea areas. Compared to onshore turbines, offshore wind turbines have larger rotor diameters and taller tower heights. The installation of offshore wind farms is typically carried out on fixed foundations in water depths ranging from 20 to 50 meters. In deeper waters, floating offshore wind technologies come into play. These systems are positioned on the sea surface without being fixed to the seabed, stabilized with anchors and mooring lines. This allows wind energy generation even at depths exceeding 100 meters. From an economic perspective, the investment cost of a wind turbine installed offshore is 25–34% higher than that of a wind turbine installed onshore. However, thanks to technological advancements, mass production, modular design, and digital twin applications, these costs are steadily decreasing. As of 2024, global wind energy installations have reached a total capacity of 1,135 GW. Approximately 93% of this capacity (1,052 GW) comes from onshore wind farms, while 7% (83 GW) is generated from offshore wind farms. Although Türkiye has not yet established a commercial-scale offshore wind farm, potential analyses indicate that the country's total offshore wind energy capacity is around 76 GW. Of this potential, 19 GW is suitable for fixed-bottom turbines in shallow waters of less than 50 meters, while 57 GW can be technically utilized with floating turbine technologies in areas with depths between 50 and 1000 meters. In this study, offshore wind farms—which have increasingly been used in energy production worldwide in recent years—have been examined. The main objective is to highlight the importance of utilizing Türkiye's existing offshore wind potential for electricity generation.

Keywords :

Wind energy, Offshore wind turbines, The situation in Türkiye.



EVALUATION OF PUMICE-BASED BUILDING MATERIALS IN TERMS OF STRUCTURAL LIGHTNESS, THERMAL INSULATION AND ENERGY EFFICIENCY

Nusret BOZKURT ^{1,*} , Ünal TUNÇ ² , Erden Ozan KARACA ¹

¹ Bitlis Eren University, Civil Engineering Department, Bitlis, Türkiye

² Bitlis Eren University, Institute of Graduate Education, Department of Civil Engineering, Bitlis, Türkiye

*Corresponding Author: nbozkurt@beu.edu.tr

ABSTRACT

Pumice is a volcanic-origin, silica-rich, and highly porous material that stands out as a natural lightweight aggregate in the construction sector. This distinctive porous structure imparts low bulk density and superior insulating capability to pumice-based concrete and cementitious materials. This review focuses on the structural lightness, thermal performance, and insulation characteristics of pumice and its derivatives, assessing this natural resource's contribution to modern design and energy efficiency goals. Türkiye, with its vast pumice deposits, holds a strategic position in the global market. Lightweight concretes incorporating pumice aggregates substantially reduce the building's dead load compared to normal concrete. This lightening effect decreases foundation loads and allows for the scaling down of structural element dimensions, generating savings in material and labor costs. Furthermore, the glassy texture and mostly non-connected pore system of pumice provide a low thermal conductivity coefficient (k-value). Experimental studies confirm that pumice concrete offers 4 to 6 times better thermal insulation than conventional concrete, significantly lowering the energy consumption for heating and cooling in buildings. Beyond thermal performance, pumice's high sound absorption capacity and intrinsic fire resistance elevate structures' comfort and safety standards. Current research efforts concentrate on innovative solutions, such as modification with polymer coatings or chemical admixtures, to mitigate pumice aggregates' high water absorption while simultaneously improving mechanical strength. The high pozzolanic activity of finely ground pumice plays a critical role in developing sustainable and high-performance construction materials. Consequently, pumice-based materials are positioned as an indispensable component for future lightweight and insulated structural designs due to their low environmental impact and substantial energy savings potential. This material ensures that the resulting structure contributes significantly to global energy conservation efforts and sustainable construction practices.

Keywords: Pumice stone, Energy efficiency, Thermal insulation, Structural lightness



CHRONOLOGICAL EVOLUTION OF BUILDING HEALTH MONITORING AND PREDICTION SYSTEMS IN TÜRKİYE

Nusret BOZKURT ^{1,*} , Orhan DURAK ²

¹ Bitlis Eren University, Department of Civil Engineering, Bitlis, Türkiye

² Bitlis Eren University, Institute of Graduate Education, Department of Civil Engineering, Bitlis, Türkiye

* **Corresponding Author:** nbozkurt@beu.edu.tr

ABSTRACT

Given Türkiye's position within a high-seismicity belt, the continuous and reliable monitoring of critical engineering infrastructure, such as large bridges and high-rise structures, is a necessity for both safety and economic considerations. Structural Health Monitoring (SHM) systems serve as a fundamental tool for the rapid, remote, and objective assessment of structural performance and damage progression by analyzing dynamic responses, including modal periods and damping ratios, under seismic and environmental loading. The mandatory implementation of these systems in high-rise buildings has been legally supported by the Turkish Earthquake Building Code (TBDY 2018).

The progression of SHM applications in Türkiye has evolved chronologically, aligning with global technological advancements. Initial applications prioritized highly accurate geodetic monitoring techniques; early studies using Global Navigation Satellite Systems (GNSS) demonstrated the potential to provide displacement measurements superior in accuracy to those derived from accelerometers. With the operational status of national GNSS reference networks (such as CORS-TR and İSKİ-UKBS), the Network RTK GNSS method has become widely utilized for high-precision displacement detection (approaching ± 2 -3 cm horizontal accuracy) in large structures. SHM systems installed in high-rises in Istanbul continuously collect high-frequency vibration data (e.g., 200 Hz), facilitating the real-time analysis of dynamic properties; developed software provides automated alerts when predefined threshold levels are exceeded.

Furthermore, complex infrastructure like the Haliç Metro Crossing Bridge (2014) is equipped with a permanent SHM system encompassing 61 diverse sensors, including GPS and accelerometers. For these large structures, the objective extends beyond current condition assessment to integrating prognosis systems, which rely on non-linear analysis and fragility assessments to rapidly determine post-earthquake usability. To effectively manage the epistemic uncertainties (e.g., modeling and measurement errors) inherent in structural identification, advanced smart computation techniques like Genetic Algorithms and Fuzzy Logic are employed to optimize model parameters. These findings are crucial for establishing a robust, reliability-based Life-Cycle Management (LCM) framework. This review details the chronological and technical advancement of SHM and prognosis systems within Türkiye.

Keywords:

Building Health Systems (SHS), Global Positioning Systems (GNSS), Life Cycle Management (LCM).



CHRONOLOGICAL DEVELOPMENT OF GREEN BUILDING TECHNOLOGIES IN TÜRKİYE AND A REGIONAL PERSPECTIVE ON SUSTAINABILITY CRITERIA

Nusret BOZKURT ^{1*} , Saffet SOYUGÜZEL ²

¹ Bitlis Eren University, Civil Engineering Department, Bitlis, Türkiye

² Bitlis Eren University, Graduate School of Civil Engineering, Bitlis, Türkiye

* **Corresponding Author:** nbozkurtl@beu.edu.tr

ABSTRACT

The accelerating global climate crisis and the rapid depletion of finite natural resources necessitate a fundamental transition in the construction sector towards sustainable practices. Buildings are responsible for approximately 40% of the world's total energy consumption and a substantial share of resource use, making designs that minimize environmental impact critically important. In this context, green buildings are defined as structures prioritizing environmental sustainability, efficient resource management, and high levels of occupant health and comfort. Given Türkiye's rapidly increasing energy demand—driven by population growth, urbanization, and industrialization—and its high external energy dependency, adopting energy efficiency measures in buildings has become a strategic national imperative.

The development of green building technologies in Türkiye has been primarily spurred by legal processes that gained momentum after 2007. These regulations aimed to standardize building energy performance, mandate the Energy Identity Document, and incentivize the use of renewable energy sources. Energy efficiency approaches have emphasized the implementation of thermal insulation standards and the integration of passive design principles into architectural planning. Internationally recognized certification systems, such as LEED and BREEAM, serve as crucial benchmarks in Türkiye for measuring environmental performance and promoting sustainable construction. This study chronologically reviews the evolution of green building technologies and related policies within the Turkish framework, starting from foundational legal regulations through to institutional efforts and the practical integration of technology. This analysis aims to contribute to defining the necessary roadmap for future sustainable construction policies in the frame of civil engineering.

Keywords: Green building technologies, Energy efficiency, Sustainability.



CHRONOLOGICAL EVOLUTION OF SMART CONCRETE AS A SPECIAL COMPOSITE MATERIAL: A JOURNEY FROM SELF-SENSING AND REPAIR SYSTEMS TO ARTIFICIAL INTELLIGENCE INTEGRATION

Nusret BOZKURT ^{1*} Nidahi SOYUGÜZEL ²

¹ Bitlis Eren University, Civil Engineering Department, Bitlis, Türkiye

² Bitlis Eren University, Institute of Graduate Education Department of Civil Engineering, Bitlis, Türkiye

* Corresponding Author: nbozkurt@beu.edu.tr

ABSTRACT

Concrete is the most widely utilized man-made material globally, with annual production surpassing 30 billion tons, forming the backbone of modern infrastructure. Yet, conventional concrete inherently suffers from low tensile strength and brittleness, making cracking due to shrinkage or excessive loads inevitable. These cracks compromise structural integrity, accelerating the ingress of deleterious substances, leading to reinforcement corrosion, shortened service life, and substantial maintenance expenditures. To overcome these pervasive limitations, concrete technology has rapidly advanced towards developing specialized concretes that offer performance beyond mere load-bearing capacity. The development of smart concretes represents the pinnacle of this technological evolution.

The chronological progression of smart concrete commenced with the introduction of fiber reinforcements (such as steel, glass, or polymer fibers) aimed at improving ductility and controlling crack propagation, a concept dating back to early applications like straw in adobe, formalized in modern contexts since the early 1900s. The subsequent key phase involved developing the material's ability for self-sensing through the piezoresistive effect. This is achieved by incorporating electrically conductive fillers like carbon microfibers, graphene nanoplatelets, or brass fibers into the cementitious matrix. By monitoring changes in electrical resistance, this smart material can provide real-time, distributed data on strain, stress, and damage accumulation, offering a robust and economical alternative to localized, fragile traditional sensors used in Structural Health Monitoring (SHM). Studies have confirmed that materials like brass fiber concrete exhibit high sensitivity, with resistance decreasing under compression and increasing under tension, both showing a strong linear correlation ($R^2 \approx 0.99$).

Further advancing its multi-functionality, smart concrete technology now encompasses self-healing capabilities, enabling autonomous repair of induced damage. Self-healing mechanisms range from autogenous healing (effective for cracks less than 50µm), to engineered autonomous methods utilizing encapsulated polymers or mineral admixtures, and bio-based techniques such as Microbially Induced Calcium Carbonate Precipitation (MICP). Most recently, the integration of Artificial Intelligence (AI) and the Internet of Things (IoT) has revolutionized concrete management. Machine learning models (e.g., Fuzzy Logic, ANN) are used for highly accurate prediction and optimization of material properties, curing processes, and mix designs, yielding results 99% similar to experimental data. This integrated approach establishes smart concrete as a cornerstone for safe, resilient, and sustainable infrastructure development.

Keywords: Smart Concrete, Self-Sensing, Self-Healing, Piezoresistivity, Structural Health Monitoring (SHM), Artificial Intelligence (AI), Special Concrete, Fiber Reinforcement.



THE EFFECT OF TRAINING DATA ORDER ON MODEL PERFORMANCE IN DEEP LEARNING: A SYSTEMATIC ANALYSIS ON CIFAR-10

Mehmet MOLU 

*Bitlis Eren University, Institute of Graduate Education Department of Computer Engineering, Bitlis, Türkiye,
molu.mehmet@gmail.com*

ABSTRACT

In traditional approaches, it is common to randomly shuffle the dataset at the beginning of each epoch. However, in this study, the impact of data ordering on the performance of deep learning models was examined. In this context, nine different data ordering strategies were experimentally evaluated using the CIFAR-10 dataset with SimpleCNN, ResNet20, and VGG11 architectures. The ordering strategies include: original ordering, class-based block ordering, random ordering, 1-item mix, 10-item mix, 50-item mix, 100-item mix, and image complexity-based approaches (K2Z: easy-to-difficult, Z2K: difficult-to-easy).

To quantitatively measure image complexity, a multi-component difficulty metric was used, combining entropy, edge density, color diversity, and features based on HOG and LBP. Experimental results show that the 1-item mix strategy, which maximizes class diversity within a batch, achieved the highest average test accuracy. In contrast, class-based block ordering led to a significant performance drop across all architectures, consistent with catastrophic forgetting-like behavior. Furthermore, it was observed that curriculum learning approaches (K2Z and Z2K) did not provide the expected performance improvement compared to random and homogeneous mixing strategies.

The findings suggest that data ordering is an important hyperparameter in deep learning training and that batch-level diversity plays a decisive role in generalization performance.

Keywords: Deep learning, Model performance, Data ordering, CIFAR-10.



PROPOSED MANAGEMENT SYSTEM TO ENHANCE THE EFFICIENCY OF MATERIAL AND TECHNICAL HUMAN RESOURCES IN PUBLIC INSTITUTIONS

Mehmet MOLU 

*Bitlis Eren University, Institute of Graduate Education Department of Computer Engineering, Bitlis, Türkiye,
molu.mehmet@gmail.com*

ABSTRACT

Efficient utilization of public resources holds strategic importance for national economic stability and the reduction of current account deficits. In public institutions, the ineffective management of assets such as durable equipment, spare parts, and consumables—along with the suboptimal use of technical human resources—further exacerbates productivity losses. Inadequate utilization of surplus materials, unnecessary procurement activities, and the failure to systematically recover functional components from decommissioned devices result in additional financial burdens. This study proposes an integrated structural and software-based management system architecture designed to address these challenges, aiming to improve institutional efficiency in both material management and the effective deployment of technical expertise.

The proposed system is built on the integrated operation of two primary components: the Material Announcement System (MİS) and the Regional Technical Service and Warehouse Management System (BDYS). MİS is designed to facilitate the exchange of surplus materials among public institutions. When necessary, the system can share data with existing institutional procurement platforms via API connections, enabling procurement personnel to view available surplus items before initiating purchasing processes. This capability prevents unnecessary acquisitions, increases inter-institutional material circulation, and significantly enhances budget efficiency.

BDYS aims to digitalize storage operations and centralize technical service processes. Within warehouse management, racks are identified and associated with material categories, each item is uniquely registered, and malfunction statuses are systematically recorded. Device–spare part relationships are managed through rule-based structures, while subcomponents of devices are modeled using tree-based hierarchies to track complex dependencies. With cross-warehouse stock visibility, the system can recommend appropriate parts for repairs, ensure the systematic recovery of reusable components, and propose optimization strategies such as maximizing the number of functional devices using parts from multiple faulty units.

In the technical service module, unresolved malfunctions in institutions are directed to specialized units, where standardized fault categories are linked with predefined solution methods. Technical specifications, error codes, and all related documents are stored within a digital institutional memory. This module enables more efficient task allocation based on personnel expertise and allows complete traceability of repair histories, part replacements, and overall device lifecycle information.

The extensible structure of the proposed system allows further enhancement through the integration of artificial intelligence and data analytics. Functions such as material demand forecasting, fault probability modeling, predictive maintenance recommendations, and resource optimization can increase device lifespan, improve stock rationalization, and automate maintenance processes.

Overall, this study introduces an innovative system architecture aimed at restructuring material and technical human resource management in public institutions through a holistic approach, contributing significantly to institutional efficiency, sustainability, and cost optimization. The extensible structure of the proposed system allows further enhancement through the integration of machine learning models, such as Random Forest and Gradient Boosting, along with data analytics components.

Keywords: Machine learning, Material management, Technical human resources, enterprise Software integration, Centralized management systems, Resource optimization.



A CONCEPTUAL TWO-LAYER EMOTION CHAIN MODEL FOR IN-STORE CUSTOMER SATISFACTION ANALYSIS

Mehmet MOLU 

Bitlis Eren University, Institute of Graduate Education Department of Computer Engineering, Bitlis, Türkiye,
molu.mehmet@gmail.com

ABSTRACT

Customer experience in retail environments is critical for improving service quality and optimizing sales performance. Existing methods often measure customer satisfaction indirectly through surveys or sales data; however, these approaches fail to sufficiently capture the customer's real-time emotional experience inside the store. This study proposes a two-layer emotion chain system designed to analyze customers' in-store emotional journeys.

The proposed framework consists of two core components: the Regional Emotion Chain (REC) and the Master Emotion Chain (MEC). Within this system, the store management defines specific regions where customer experience will be monitored, including but not limited to store entrance and exit areas. The Regional Emotion Chain records emotion scores as a time series while the customer remains within a specific store region, enabling detailed analysis of emotional changes at each location. Importantly, when a customer revisits the same region, a new and independent regional chain is initiated. For example, if a customer's movement within the store follows the sequence Section1 → Section2 → Section1 → Section3 → Section1, five distinct regional emotion chains will be generated.

The Master Emotion Chain aggregates the single representative scores derived from each regional chain in sequential order. This structure makes it possible to observe the overall emotional flow throughout the customer's journey and to interpret these findings in conjunction with regional emotional variations. Together, the two-layer design enables both spatial and temporal analysis, offering a holistic evaluation of the customer experience.

The system is currently at the conceptual stage, and no prototype or data collection has yet been conducted. The originality of the proposed model lies in its ability to monitor customer satisfaction in real time, at both regional and journey-based levels. Potential contributions include supporting data-driven decision-making processes in areas such as store layout design, product placement, and personnel management, and providing a new analytical framework for customer experience studies. Future work will detail the emotion detection algorithms, regional chain analysis methods, regional score extraction models, and master chain interpretation approaches.

Keywords: Emotion analysis, Time-series analysis, Emotion chain, Retail analytics.



INTEGRATING GEOSPATIAL ANALYSIS, TEMPORAL MODELING, AND MACHINE LEARNING FOR SEISMIC HAZARD ASSESSMENT: A 24-YEAR EARTHQUAKE STUDY IN CHILE (2000–2024)

Cansu AKYÜREK ANACUR ^{1*} , Özlem ŞEKER ¹

¹ Bitlis Eren University, Computer Engineering Department, Bitlis, Türkiye

* **Corresponding Author:** caanacur@beu.edu.tr

ABSTRACT

A comprehensive analysis of the region's seismic behaviour was conducted using 133,590 earthquake events that took place in Chile between 2000 and 2024. The spatial distribution, temporal trends, and magnitude-depth relationships of the earthquakes were analysed in detail. Random Forest, XGBoost, LightGBM, and SVM models were also applied to predict events with a magnitude of ≥ 5.0 Mw. The study compared the models' discriminatory power using ROC-AUC, F1, sensitivity, and specificity metrics after integrating spatial and temporal features from the raw data into machine learning models. Furthermore, the newly engineered spatial indicators derived from raw catalogue texts contributed significantly to model performance, highlighting the value of enriched feature sets in seismic classification tasks. The findings show that seismic activity in Chile exhibits high spatial clustering along the Nazca–South America plate boundary, and particularly the spatial components (latitude, longitude and epicentre distance) play a decisive role in large earthquake prediction. The study reveals that integrated analytics of long-term seismic data will make a significant contribution to seismic hazard assessments.

Keywords: Seismic hazard assessment; Machine learning; Spatiotemporal analysis; Earthquake prediction; Feature engineering; Seismic catalog analysis



MULTIMODAL DEEP LEARNING-BASED CLASSIFICATION OF HANDWRITING DATA: THE CASE OF ALZHEIMER'S DISEASE

Cansu AKYÜREK ANACUR ^{1*} , Asuman GÜNAY YILMAZ ² , Bekir DİZDAROĞLU ³

¹ Bitlis Eren University, Computer Engineering Department, Bitlis, Türkiye

² Karadeniz Technical University, Artificial Intelligence and Data Science Department, Trabzon, Türkiye

³ Karadeniz Technical University, Computer Engineering Department, Trabzon, Türkiye

* **Corresponding Author:** caanacur@beu.edu.tr

ABSTRACT

Handwriting analysis is becoming more significant for neurodegenerative disease assessment. This work calculated 18 literature-defined features (temporal, kinematic, geometric, etc.) from the DARWIN handwriting database's raw data to build a feature set. First, a 1D Convolutional Neural Network (1D-CNN) was used to assess handwriting patterns' Alzheimer's disease detection potential. The second stage transformed this feature set to a 2D picture format and evaluated the visual representations using 2D-CNN models. By translating the numerical feature set into alternative representational formats, the study could examine how different modelling approaches respond to the same handwriting information. The findings show that deep learning models can usefully process handwriting dynamics' discriminative information for neurodegenerative disease categorization.

Keywords: Handwriting analysis; Feature extraction; Deep learning; Alzheimer detection



ANALYSIS OF SOCIETAL EMOTIONAL RESPONSES TO MPOX DISEASE BASED ON X (TWITTER) DATA

Kübra ÇETİN YILDIZ ^{1,*} , Emine AYAZ ²

¹Bitlis Eren University, Institute of Graduate Education Department of Computer Engineering, Bitlis, Türkiye

²Bitlis Eren University, Computer Engineering Department, Bitlis, Türkiye

* **Corresponding Author:** kubracetin13@gmail.com

ABSTRACT

This study examines societal sentiment and perception changes regarding mpox (monkeypox) disease through social media data on the X (Twitter) platform. The ability of digital communication platforms to allow individuals to express their emotions, anxieties, and risk perceptions quickly and openly has made such data sources more dynamic compared to traditional epidemiological tools. In this context, English user content from X between January and June 2025 was categorized into seven emotions: fear, surprise, joy, sadness, anger, disgust, and neutral, and classified using the DistilBERT model. The dataset was pre-processed, noise was reduced, and the model was optimized for sentiment classification. The pre-processing involved spam filtering, language verification, lemmatization, and symbol cleaning.

The model's performance was evaluated by training it on 17,483 tweets pulled from X using 3-fold cross-validation in Python 3.11.1, resulting in an average accuracy of 76.36% and a weighted F1 score of 75.06%. The findings suggest that online discussions about mpox are largely shaped by fear and neutral emotions. The predominance of fear and neutral emotions indicates that the public experiences uncertainty and anxiety regarding mpox.

Keywords: Mpox, Sentiment analysis, Natural language processing, DistilBERT, X.



LAND COVER SEGMENTATION AND FOREST LOSS ANALYSIS FROM SATELLITE IMAGES USING VISION TRANSFORMERS

Yaren YALÇINKAYA ¹ , Emine AYAZ ² Vedat TÜMEN ²

¹Bitlis Eren University, Institute of Graduate Education Department of Computer Engineering, Bitlis, Türkiye

² Bitlis Eren University, Computer Engineering Department, Bitlis, Türkiye

* **Corresponding Author:** yrynkaya@gmail.com

ABSTRACT

Today, rapid urbanization, agricultural activities, and industrialization are causing a significant decline in forest areas. This decline not only threatens the sustainability of the ecosystem but also negatively affects the oxygen balance in the atmosphere, increasing the risk of climate change. In this study, a deep learning-based semantic segmentation approach is proposed for the detection and classification of forested areas from satellite images.

The study uses the “Augmented Forest Segmentation” dataset available on the Kaggle platform, which is based on high-resolution satellite images containing various soil and land use types. The Transformer-based SegFormer (b0) model was chosen for the segmentation process. The model was adapted by retraining it for the forest class on specific pre-training weights and optimized the training process with an increased number of epochs.

As a result of model training, we achieved a pixel accuracy of 87% and a weighted F1 score of 86%. Tests conducted on sample satellite images after training showed that the model successfully distinguished forest areas. This study aims to contribute to AI-supported decision-making systems for the protection of natural areas and the analysis of environmental risks.

Keywords: Semantic segmentation, Forest area detection, Satellite images, Deep learning, Environmental monitoring, Vision transformer.



ADAPTIVE MULTI-COEFFICIENT QUANTIZATION INDEX MODULATION IN DCT-BASED STEGANOGRAPHY

Mehtap ÜLKER 

Bitlis Eren University, Civil Engineering Department, Bitlis, Türkiye, m.ulker@beu.edu.tr

ABSTRACT

In digital image steganography, the primary objective is to transmit embedded information imperceptibly while ensuring that the hidden data can still be reliably recovered despite degradations encountered during storage, processing, or transmission. However, conventional DCT-based approaches commonly used in the literature exhibit structural fragility, as they embed each information bit into a single transform coefficient. Consequently, these single-coefficient modulation strategies are highly susceptible to random and transform-domain distortions such as Gaussian noise, JPEG compression, blurring, and resampling. Even a slight perturbation in the selected coefficient may directly invert the extracted bit decision, resulting in low robustness, high error rates, and unstable decision behavior. To address this fundamental weakness and enhance statistical reliability under degradation, this study proposes a multi-component hybrid embedding method. The proposed approach is built upon a multi-coefficient embedding structure in which each information bit is distributed across multiple mid-frequency DCT coefficients within the same 8×8 block. This design statistically reduces the impact of coefficient-level distortions and significantly lowers decision variance during extraction by employing majority-vote fusion. The embedding strength is controlled via a content-adaptive quantization mechanism (adaptive QIM), where the quantization step is determined based on second-order block statistics—particularly variance. Accordingly, larger modulation intervals are used in highly textured blocks to improve robustness, whereas smaller intervals are employed in smooth regions to preserve perceptual fidelity. In addition, the embedded bitstream is pre-processed using a key-derived XOR-based lightweight scrambling operation and encoded with a Hamming error correction code to mitigate random single-bit errors during extraction. The robustness of the method was evaluated under a challenging scenario in which strong Gaussian noise ($\sigma = 5$) was intentionally applied to the stego images to emulate real-world distortions. Experimental results demonstrate that the proposed system maintains high perceptual quality, achieving PSNR values in the range of 46–59 dB, while still enabling meaningful data recovery with bit error rates between 9% and 15% even under severe degradation. The combined effect of multi-coefficient modulation, adaptive QIM dynamics, and forward error correction yields substantially higher stability, flexibility, and distortion resistance compared with traditional single-coefficient DCT-based embedding schemes. In conclusion, this study introduces a content-aware, multi-coefficient, and error-corrected embedding architecture that offers a robust alternative to conventional transform-based steganography methods, which are typically vulnerable to various forms of degradation. The performance results indicate that the proposed framework provides a technically viable and reliable solution for robust steganography and transform-domain digital watermarking applications that require high tolerance to noise and distortion.

Keywords:

Adaptive QIM, DCT, Steganography, Multi-Coefficient modulation, Gauss noise.



ULUSLARARASI AKILLI SİSTEMLER, TASARIM VE ENERJİ KONFERANSI

International Conference on Intelligent Systems, Design and Energy



INVESTIGATION OF THE APPLICABILITY OF FUZZY LOGIC METHOD IN ESTIMATING LOAD-DISPLACEMENT DATA OF LIGHTWEIGHT CONCRETE BEAMS

Erden Ozan KARACA^{1,*} , Nusret BOZKURT¹

¹ Bitlis Eren University, Civil Engineering Department, Bitlis, Türkiye

* **Corresponding Author:** eokaraca@beu.edu.tr

ABSTRACT

In the context of this study, a fuzzy logic model was developed using flexural tensile strength data obtained from lightweight concrete beams reinforced with carbon fiber polymer (CFRP) material. The beams produced in the experimental study measured 10x10x50 cm and exhibited three distinct crack depths. The beams were reinforced by bonding CFRP material with four different surface areas to the bottom surfaces of the beams. The load-displacement data obtained during the three-point bending tensile strength test applied to the beams were used to create the fuzzy logic model. The fuzzy output results obtained from the model and the experimental results were compared with the load-displacement values at the moment of beam failure to determine the correlation relationships. The correlation values obtained for load and displacement demonstrated an accuracy rate of 99%. This will enable the final load-displacement values provided by CFRP surface areas that could not be examined within the scope of the experimental study to be predicted with a high degree of accuracy in the reinforcement of beams.

Keywords:

Fuzzy logic, Concrete beam, CFRP, Load-displacement.



BLE BASED IOT APPLICATION FOR LIFE DETECTION UNDER DEBRIS

Özlem ŞEKER^{1,*} , Cennet AKÇAKAYA² , Nurullah AKARSLAN²

¹ Bitlis Eren University, Department of Computer Engineering, Bitlis, Türkiye

² Bitlis Eren University, Institute of Graduate Education Department of Computer Engineering, Bitlis, Türkiye

*Corresponding Author: oyerlikaya@beu.edu.tr

ABSTRACT

Earthquakes represent a major global hazard due to their unpredictable nature and destructive consequences. The rapid and reliable detection of individuals trapped under collapsed structures is a decisive factor that directly influences the effectiveness of search and rescue operations. However, conventional manual search techniques often fall short, particularly in time-critical situations. This study presents a multi-sensor network based on ESP32 microcontrollers that communicates via the Bluetooth Low Energy (BLE) protocol and operates entirely without internet infrastructure, together with an integrated mobile application. The proposed system aggregates data from an infrared (IR) thermal camera, accelerometer, vibration sensor, and passive infrared (PIR) motion detectors through multi-hop BLE Mesh routing, forwards these data to a Raspberry Pi gateway using the Message Queuing Telemetry Transport (MQTT) protocol, and displays them to search and rescue teams in real time via the mobile interface. When a living subject is detected, the mobile application highlights the corresponding area, assisting team navigation and providing real-time vital-signal analyses through its user interface. The developed prototype was evaluated under three representative scenarios, that are unobstructed, partially obstructed, and node-failure conditions. Results showed that sensor fusion produced clear increases in temperature, vibration, and acceleration magnitudes during live tests, while non-live scenarios exhibited a completely static profile. Centroid-based analysis of normalized sensor features demonstrated that the feature-space energy in live cases was approximately 35–50% higher compared to non-live conditions. Regarding communication performance, the BLE Mesh topology remained stable; time-to-live (TTL) values consistently ranged between 6 and 7 hops, and the sustained data transmission rate of 1.5–2.1 kB/s in live scenarios confirmed the robustness of the MQTT communication chain. The findings indicate that the proposed Internet of Things (IoT) based framework can accurately detect living individuals in confined and complex environments following an earthquake, while reliably delivering critical information to search and rescue teams through the mobile application. Furthermore, its infrastructure-independent operation suggests that the system can be readily adapted to other disaster contexts, including floods, landslides, mining accidents, and confined-space emergencies following explosions.

Keywords:

Bluetooth Low Energy (BLE), Disaster, Earthquake, Internet of Things (IoT), Message Queuing Telemetry Transport (MQTT), Mesh network.



EFFECT ON DECISION MAKING PROCESSES OF PYTHAGOREAN FUZZY SET

Feride TUĞRUL 

Munzur University, Department of Computer Engineering, Tunceli, Türkiye
feridetugrul@munzur.edu.tr

ABSTRACT

The Pythagorean Fuzzy Set concept is a more flexible approach that encompasses fuzzy sets and intuitionistic fuzzy sets in the uncertainty modeling process. The concept was first introduced by Yager (2013) and offers a new approach for jointly evaluating membership and non-membership degrees. While Atanassov's intuitionistic fuzzy set, this relationship was defined as the sum of the squares of membership and non-membership degrees to be less than or equal to 1 in Pythagorean fuzzy sets. This approach allows decision makers to express uncertainty over a wider range. Therefore, Pythagorean fuzzy sets offer higher representational power than intuitionistic fuzzy sets and are particularly effective in solving complex problems such as multi-criteria decision making, risk analysis, expert systems, and information processing. Decision making is an approach that aims to systematically analyze decision problems that consider multiple criteria. This method allows the decision maker to evaluate both qualitative and quantitative factors to make the most appropriate choice among alternatives. Among the most commonly used methods, AHP, TOPSIS, VIKOR, and PROMETHEE are prominent, aiming to determine the relative advantages of alternatives under different assumptions. Today, fuzzy logic and its extended forms, intuitionistic and Pythagorean fuzzy approaches, are frequently integrated into decision making processes to reduce the influence of uncertainty, expert judgment, and subjective assessments. This allows decision models to more effectively represent the complex and uncertain situations encountered in real life problems. This study presents a numerical example of the impact of Pythagorean fuzzy sets on decision-making processes.

Keywords: Fuzzy set, Pythagorean fuzzy set, Decision making.



SHORT-TERM ELECTRICITY LOAD FORECASTING WITH HOLT-WINTERS, XGBOOST AND EXTENDED HYBRID HOLT-WINTERS AND XGBOOST MODEL: EVIDENCE FROM THE AEP HOURLY DATASET

Murat BİNİCİ ^{1,*} , Nebi SUDAY ²

¹ Bitlis Eren University, Department of Mechanical Engineering, Bitlis, Türkiye

² Bitlis Eren University, Institute of Graduate Education Department of Mechanical Engineering, Bitlis, Türkiye

* Corresponding Author: mbinici@beu.edu.tr

ABSTRACT

Short-term load forecasting is a key input for the secure and economical operation of modern power systems. In this study we investigate the performance of a classical statistical model, a machine learning model, and an extended hybrid approach for one-hour-ahead forecasting of hourly electricity demand. The case study uses the AEP_hourly dataset, which contains American Electric Power's hourly load measurements from 2004 to 2018. After aggregating duplicated timestamps and resampling to a regular hourly frequency, the data are split into a training period (2004–2016) and an out-of-sample test period (2017–2018). As a statistical baseline, we estimate an additive Holt–Winters exponential smoothing model with a 24-hour seasonal component. The machine learning model is an XGBoost regressor trained on lagged load values (1, 24 and 168 hours) and calendar features (hour of day, day of week, month and weekend indicator). The proposed extended hybrid model first fits the Holt–Winters specification and then trains XGBoost on the resulting residuals using both residual and load lags together with the same calendar variables; final forecasts are obtained by adding the residual predictions to the Holt–Winters forecasts. Results on the test set show that the hybrid model clearly improves upon pure Holt–Winters (reducing MAE from about 1741 MW to 1216 MW and MAPE from 11.0% to 7.5%), but remains dominated by the pure XGBoost model, which achieves an MAE of roughly 160 MW and a MAPE close to 1.1%. The visual analysis confirms that XGBoost captures both the daily pattern and short-term fluctuations more accurately, while Holt–Winters tends to underestimate peaks. These findings suggest that, for high-frequency load data with strong nonlinearities, feature-rich gradient boosting models provide substantial accuracy gains over traditional exponential smoothing, and that residual-based hybrids may require additional extensions (e.g., multi-step training or exogenous variables) to fully exploit their potential.

Keywords:

Short-term load forecasting, Holt–Winters; XGBoost, Hybrid forecasting model, Time series analysis, Electricity demand.



ADAPTIVE REPRESENTATION-FEATURE SELECTION FOR EFFICIENT AND INTERPRETABLE TIME SERIES CLASSIFICATION

Celal ALAGÖZ^{1*} , Farhan AADIL¹

¹ Sivas Science and Technology University, Department of Computer Engineering, Sivas, Türkiye

* **Corresponding Author:** celal.alagoz@gmail.com

ABSTRACT

The CFIRE (Cross-domain Feature Integration for Robust Extraction) framework has demonstrated the efficacy of fusing features from multiple mathematical representations—including temporal, spectral, and time-frequency domains—for time series classification. However, its original feature selection strategy employed a global, one-size-fits-all approach, which may not adapt optimally to the unique characteristics of individual datasets. This work introduces a significant enhancement to CFIRE by implementing a dataset-specific feature selection mechanism that dynamically tailors the feature set for each unique classification problem.

Our improved framework automates the selection of the most discriminative representation-feature pairs by evaluating multiple selection criteria—including top-k percentage and mutual information thresholds—directly on the training data of each dataset. This allows the model to adapt its feature space to the specific temporal patterns, noise characteristics, and discriminative needs of a given problem, moving beyond a fixed configuration. The selected feature subsets are then used to transform both training and test data, ensuring consistency while maximizing relevance.

We present a preliminary evaluation of CFIRE on a curated suite of five diverse datasets from the UCR Time Series Archive. The results demonstrate that our method successfully reduces feature space dimensionality while maintaining, and in some cases improving, classification accuracy compared to using the full feature set. The selected features consistently originate from multiple domains, validating the hypothesis that complementary representations contribute unique discriminatory information. These findings underscore the potential of CFIRE as a scalable and effective solution for multi-domain TSC, providing a solid foundation for future large-scale benchmarking.

Keywords: Time series classification, Feature selection, Multi-Domain features, Mutual information, UCR Archive.



HYBRID OPTIMIZATION-BASED DEEP LEARNING MODEL DESIGN FOR ENERGY-EFFICIENT INTELLIGENT SYSTEMS

İlayda AKSOY 

Bitlis Eren University, Institute of Graduate Education Department of Computer Engineering, Bitlis, Türkiye
aksoyilayda56@gmail.com

ABSTRACT

The design and optimization of energy-efficient deep learning models represent a critical challenge in developing sustainable intelligent systems, particularly for edge computing and resource-constrained environments. This paper introduces a novel hybrid optimization framework that systematically integrates evolutionary algorithms with gradient-based optimization techniques to automate both neural architecture search and hyperparameter tuning while explicitly optimizing energy consumption. The proposed two-stage approach leverages the global exploration capabilities of evolutionary algorithms and the local refinement strengths of gradient-based methods, addressing fundamental limitations in existing automated machine learning (AutoML) frameworks by incorporating energy efficiency as a primary optimization objective alongside model accuracy.

Our methodology employs a genetic algorithm for global architecture exploration, followed by gradient-based fine-tuning using adaptive optimizers. The framework simultaneously optimizes network architecture (layer count, neuron count, activation functions, dropout rates) and hyperparameters (learning rate, batch size, regularization parameters) through an integrated search process. A multi-objective fitness function explicitly balances model accuracy, computational efficiency, and energy consumption, enabling the discovery of architectures that achieve superior performance while maintaining strict energy constraints suitable for edge devices and sustainable computing applications.

Extensive experimental validation was conducted on multiple benchmark datasets (MNIST, CIFAR-10, CIFAR-100, Fashion-MNIST) using convolutional and fully connected neural networks. The proposed hybrid method was rigorously compared against baseline approaches including random search, grid search, Bayesian optimization, and standard gradient descent. Statistical analysis using t-tests confirmed significant improvements ($p < 0.001$) across all evaluated metrics.

The experimental results demonstrate that our hybrid optimization approach consistently outperforms traditional methods, achieving 15-20% higher accuracy rates while reducing energy consumption by 25-35% compared to baseline methods. Specifically, on CIFAR-10, the method achieved 82% accuracy with 2.1W average power consumption, compared to 75% accuracy with 3.8W for Bayesian optimization and 72% accuracy with 4.5W for grid search, representing improvements of 9.3% in accuracy and 45% in energy efficiency. The automated design process reduced manual development effort by approximately 80% while producing architectures that are 18% more accurate and 30% more energy-efficient than manually designed baselines. These findings establish the effectiveness of hybrid optimization strategies in automated energy-

efficient deep learning model design and provide a foundation for sustainable intelligent system development.

Keywords: Deep learning, Neural architecture search, Hybrid optimization, Energy-efficient computing, Automated machine learning, Edge computing.



SELFIE2BFP: A DEEP LEARNING APPROACH FOR BODY FAT PERCENTAGE ESTIMATION FROM FACIAL IMAGES

Yusuf UZ¹ , Zafer SERİN¹ , Ugur YUZGEC^{1,*}

¹ Bilecik Şeyh Edebali University, Computer Engineering Department, Bilecik, Türkiye,
* **Corresponding Author:** ugur.yuzgec@bilecik.edu.tr

ABSTRACT

This study investigates the feasibility of estimating body fat percentage (BFP) using only facial images through deep learning techniques and mathematical modeling. A multi-stage prediction model was developed, which first extracts gender, age, and body mass index (BMI) from facial images using pre-trained deep learning models, and subsequently applies a gender- and age-adjusted BFP estimation formula. The results indicate that the facial image quality, expression, and lighting significantly affect the performance of deep learning models, thereby influencing the overall prediction accuracy. Despite the limitations in dataset balance and model generalizability, this study demonstrated that facial features can provide meaningful indicators of body composition. These findings suggest that facial image analysis combined with Artificial Intelligence (AI) and mathematical models can serve as a noninvasive and accessible tool for preliminary health assessments.

Keywords: Body fat percentage, Deep learning, Facial image analysis, Artificial intelligence, Obesity, BMI estimation.



CROSS-PLATFORM HATE SPEECH DETECTION IN TURKISH

Mehmet Emin BAKIR ¹ , Sezer DÖYMAZ ^{2,*} , Vedat TÜMEN ³

¹ Izmir Katip Çelebi University, Computer Engineering Department, Izmir, Türkiye

² Bitlis Eren University, Institute of Graduate Education Department of Computer Engineering, Bitlis, Türkiye

³ Bitlis Eren University, Computer Engineering Department, Bitlis, Türkiye

* Corresponding Author: sezerdoymaz13@gmail.com

ABSTRACT

The rapid growth of social media has amplified the spread of harmful content, such as hate speech, which undermines individual dignity and societal cohesion. Automated detection is crucial for creating safer digital spaces; however, Turkish hate speech detection remains underexplored, with prior work limited to platform-specific datasets that restrict scalability and generalizability. This study investigates whether models trained on aggregated multi-platform data can match or exceed the performance of models trained separately for each platform.

We introduce a novel dataset spanning four social media platforms: Reddit, Instagram, Facebook, and X (formerly Twitter), containing 8,186 samples with approximately balanced representation of around 2,000 entries per platform. The dataset is annotated for multi-class classification into five hate speech categories and binary classification (hate versus non-hate). Three machine learning algorithms were evaluated: Support Vector Machine (SVM), Random Forest (RF), and K-Nearest Neighbors (KNN). In platform-specific experiments, models were trained and tested independently on each platform. For binary classification, RF achieved an average F1-score of 72% across platforms (85% on Reddit, 76% on X, 70% on Facebook, 58% on Instagram). In multi-class classification, the best platform-specific model (SVM) averaged 33% F1. We then trained unified models on the combined corpus. The unified RF model improved binary classification to 74% F1 and multi-class classification to 40% F1, matching or exceeding the platform-specific results.

These findings confirm that a single model trained on diverse data generalizes effectively across platforms. The study makes three contributions: (1) the first Turkish hate speech dataset spanning four platforms; (2) empirical evidence that unified training reduces the need for redundant platform-specific solutions; and (3) benchmark results for future research. Future work may extend the corpus and evaluate transformer-based architectures for cross-platform Turkish hate speech detection.

Keywords:

Hate speech detection, Turkish natural language processing, Cross-platform classification, Social media, Machine learning.



A STUDY ON WEBASSEMBLY-BASED CRYPTO MINING

Fikri AĞGÜN¹ , Raif SİME^{2,*}

¹ Bitlis Eren University, Adilcevaz Vocational School, Department of Computer Technologies, Bitlis, Türkiye

² Bitlis Eren University, Department of Information Technology, Bitlis, Türkiye

* Sorumlu Yazar: rsime@beu.edu.tr

ABSTRACT

WebAssembly (Wasm) is a low-level execution environment that delivers near-native performance in modern web browsers. Although it was originally developed to support web applications requiring high performance, it has increasingly been adopted by malicious actors for cryptomining (cryptojacking) applications. This study examines WebAssembly's architectural characteristics, performance advantages, security limitations, and suitability for mining algorithms, and investigates the technical structure, detection methods, and impacts of WebAssembly-based coin-mining applications.

With the expansion of the cryptocurrency ecosystem, interest in mining algorithms used to generate these currencies has grown. Mining typically requires substantial computational power and is often performed on specialized hardware. However, recent developments have enabled mining to be conducted via web browsers using WebAssembly.

Due to its near-CPU performance and flexible memory management, WebAssembly provides a significant performance advantage over JavaScript. This advantage has given rise to both legitimate and malicious mining applications. WebAssembly's high performance and portability make it an attractive environment for cryptocurrency mining, but it also introduces security concerns. Alongside legitimate use cases, malicious cryptojacking attacks have become widespread.

In this paper, the technical aspects, benefits, risks, and detection methods of WebAssembly-based mining applications are analyzed.

An experimental methodology was employed to evaluate in-browser, WebAssembly-based coin-mining performance. Sample hashing functions written in C and Rust were compiled to WebAssembly (WASM) and integrated into the browser via JavaScript. Equivalent pure JavaScript implementations and native C implementations of the same algorithms were also prepared to enable a three-way comparison. The results indicate that WebAssembly is both performance-capable and security-sensitive for browser-based crypto mining. WASM provides substantial advantages for computation-intensive tasks but can cause noticeable resource consumption on user devices when misused.

During WebAssembly's ongoing development, more effective and secure solutions for mining-related use cases are expected to emerge.

Keywords:

WebAssembly, Cryptocurrency mining, Cryptojacking, WASI, Browser security.



DETECTING SPECULAR SURFACES WITH LIDAR–SONAR SENSOR FUSION

Berat Demirkan¹ , Tolga Özaslan^{1,*}

¹ Ankara Yıldırım Beyazıt University, Department of Mechanical Engineering, Ankara, Türkiye

* **Corresponding Author:** tozaslan@aybu.edu.tr

ABSTRACT

Autonomous flight of mobile robotic platforms, such as micro unmanned aerial vehicles (UAV), relies on lightweight onboard sensors that enable mapping, localization, and obstacle avoidance. Among these sensors, 2D time-of-flight (ToF) laser scanners are widely used for operating in indoor 2.5D environments such as office buildings, warehouses, and shopping centers. These environments often contain glass doors, panels, and windows, as well as shiny or metallic surfaces. Due to the highly specular or transparent nature of these surfaces, performance of laser scanner perception pipelines degrades dramatically. A 2D LiDAR operates by emitting laser beams across the sensor plane and relies on diffuse surface reflections for point measurements which are then aggregated into a point cloud of the surroundings. Transparent and specular surfaces, however, either produce no return (such as glass), reflect the beam away from the receiver (such as mirrors), or allow the beam to pass through and be reflected by objects behind them which effectively renders the laser scanner blind to such surfaces. This fails the downstream perception pipeline causing it to model occupied space as free or free space as occupied. This poses a critical issue for tasks that depend on reliable spatial awareness, including exploration, obstacle avoidance, and mapping.

In this work, we study the characteristics of a 2D ToF laser scanner by collecting and analyzing measurements from various objects with different surface qualities at different viewing angles. These objects include highly specular objects such as mirrors, glossy floor tiles and whiteboards; clean and slightly dirty glass windows; and diffuse surfaces such as drywall. Our observations show that, independent of the viewing angle, all diffuse surfaces are detected accurately with low intensity values. Specular surfaces, on the other hand, fail the scanner in most cases, except when the beams hit the surface close to the right angle. Spatially isolated lines or clusters of detections with individual measurements rapidly appearing and disappearing caused by speckle reflections on glass are distinctive features that can be utilized to detect glass. However, this behavior alone is not sufficient to ensure consistent detection, especially when the UAV tilts even slightly and the laser strikes the glass at non-right angles. To enhance robustness, we utilize a sonar sensor to obtain point-range measurements within the scanners field of view. Due to its operating principle the sonar consistently detects the presence of obstacles even when the laser provides weak, ambiguous, or zero returns. By considering intensity peaks with sonar readings, we obtain a reliable cue of glass regions. These seed points are then used to grow a linear region along the corresponding portion of the scan, enabling the system to mark the transparent surface within the scan.

Keywords:

Laser scanner, Glass detection, Sonar sensor, Mapping, Mobile robots.



DATA-DRIVEN SCORING OF A CONTINUOUS WATER QUALITY INDEX USING NONLINEAR TREE BASED MACHINE LEARNING MODELS

Ridvan Firat CINAR 

Batman University, Department of Computer Engineering, Batman, Türkiye
ridvanfirat.cinar@batman.edu.tr

ABSTRACT

Ensuring access to safe drinking water requires accurate assessment methods that go beyond binary decisions of potability. Traditional Water Quality Index (WQI) formulations provide continuous scores but are often reduced to categorical labels, leading to a loss of nuanced information. In this study, we introduce a data-driven approach to reconstruct a continuous WQI using physicochemical parameters from the publicly available Kaggle dataset. Unlike the original dataset, which provides only a binary potable/non-potable label, our method generates a continuous score by mapping normalized sub-indices into a weighted aggregation framework and training nonlinear machine learning models. Three algorithms, Decision Tree, Random Forest, and Gradient Boosting are evaluated for predicting the reconstructed score. Experimental results show that ensemble-based methods significantly outperform a single decision tree, achieving lower error rates and higher coefficients of determination. Feature importance analysis further indicates that pH, Sulphate, and Solids are the most influential parameters, consistent with domain knowledge. By extending binary classification into a continuous scoring scheme, the proposed framework improves the interpretability of model outputs and provides decision-makers with finer resolution information for water quality assessment and monitoring.

Keywords: Water quality index, Water quality score, Potability prediction, Decision tree, Random Forest, Gradient boosting, Machine learning, KNN Imputation.



RECOVERING DELETED DATA ON THERMAL PAPER USING UV LIGHT AND IMAGE PROCESSING IN DIGITAL FORENSICS

Onur KAYA¹ , Songül KARAKUŞ^{2*}

¹Bitlis Eren University, Institute of Graduate Education Department of Computer Engineering, Bitlis, Türkiye

²Bitlis Eren University, Computer Engineering Department, Bitlis, Türkiye

*Corresponding Author: skarakuş@beu.edu.tr

ABSTRACT

Thermal printer outputs such as receipts, labels, and barcodes contain legally and commercially valuable data; however, over time—or due to heat, light, and other environmental factors—the text on these materials often fades or disappears completely. This creates a significant risk of permanent loss of critical evidence and information. This study presents a forensic imaging and digital processing-oriented methodology developed to non-destructively reveal erased text on thermal paper. In the first stage of the study, erased thermal paper samples were illuminated under UV-A light at a wavelength of 365 nm—commonly used in forensic document examinations—using various light intensities, and captured in high-resolution digital format. Several image processing techniques were then applied to the digitized images to enhance the readability of the degraded documents and to distinguish the text from the background. The proposed methodology combines UV-based imaging with the analytical power of digital image processing, successfully making faded or erased text residues on thermal paper visible. This approach provides a reliable and digitally reproducible solution that enables the non-destructive recovery of valuable information, particularly in cases where traditional examination methods fall short. Furthermore, the similarity of the techniques employed to advanced methods used in the digital restoration of historical or heavily damaged documents demonstrates their adaptability to modern evidence materials.

Keywords: Forensic document examination, Evidence, Thermal paper, Ultraviolet, Image processing, Non-Destructive method.



FACIAL RECOGNITION-BASED SECURITY VERIFICATION IN MOBILE BANKING: AN INNOVATIVE ARTIFICIAL INTELLIGENCE-BASED APPROACH

Eyyüp KARDEŞ^{1,*} , İrfan ÖKTEN² , Uğur YÜZGEÇ³

¹Bitlis Eren University, Institute of Graduate Education Department of Computer Engineering, Bitlis, Türkiye

²Bitlis Eren University, Department of Computer Engineering, Bitlis, Türkiye

³Bilecik Şeyh Edebali University, Department of Computer Engineering, Bilecik, Türkiye

*Corresponding Author: eyyupkardes47@gmail.com

ABSTRACT

Technological advances that enable the manipulation of images transferred to digital media are contributing to the rapid advancement of image processing methods. The combination of artificial intelligence techniques with high computational power has, particularly in recent years, enabled more efficient and reliable large-scale data analysis. Image processing technologies are widely used in many critical fields such as medicine, security, automotive, and agriculture, and deep learning-based methods are increasingly preferred due to their multiple input processing capacity and minimal human intervention requirement.

This research proposal presents an innovative security architecture that aims to increase the security of mobile banking transactions and improve the user experience. The proposed system aims to protect user accounts against unauthorized access through a facial recognition verification module integrated into mobile banking applications. Even if user passwords are compromised, transactions can only be processed with the account owner's approval, thanks to the requirement for biometric verification. This approach significantly enhances the reliability of banking services by providing an additional layer of protection, particularly for financial transactions requiring high security, such as money transfers, EFTs, wire transfers, deposits, and withdrawals. The integration of the facial recognition-based security module into mobile banking applications aims to provide banks with a modern, user-friendly, and high-security service infrastructure. This will enable users to manage financial transactions more securely and contribute to banks' competitive advantage in the field of digital security.

Keywords: Facial recognition, Mobile banking security, Artificial intelligence, Biometric verification, Image processing.



AUTOMATED POST-EARTHQUAKE WALL DAMAGE DETECTION AND CLASSIFICATION USING YOLOV8

Erkan DEVECİ^{1,*} , Burhan ERGEN²

¹ *Osmaniye Korkut Ata University, Dijital Transformation and Software Office, Osmaniye, Türkiye*

² *Fırat University, Department of Computer Engineering, Elazığ, Türkiye*

* **Corresponding Author:** erkandeveci@osmaniye.edu.tr

ABSTRACT

This study presents a novel approach for the automatic detection and classification of post-earthquake structural damage on building walls using the YOLOv8 deep learning algorithm. Post-disaster damage assessment is critical for timely intervention and rehabilitation planning; however, current manual inspection methods are time-consuming and subjective. To overcome these challenges, we developed a comprehensive real-time detection system that can classify wall conditions into three categories: normal, cracked, and perforated. A specialized dataset consisting of 2000 high-resolution images from buildings affected by the February 6 earthquakes in Türkiye was compiled. The dataset was meticulously preprocessed and split into 80% for training and 20% for testing. The YOLOv8 model architecture was optimized with hyperparameter tuning and trained for 100 steps with a batch size of 16 and a learning rate of 0.001. Experimental results show outstanding performance with class-specific accuracy values of 0.999 for normal, 0.777 for crack, and 0.849 for hole. The model achieved 0.875 overall accuracy, 0.852 recall, 0.903 precision (mAP@0.5), and 0.707 mAP@0.5:0.95. The model's F1-score based on confidence threshold analysis reached 0.86 at the optimal threshold. The system maintains real-time processing capabilities at 31 frames per second on mid-range GPU hardware (NVIDIA Quadro M2000), making it suitable for field use. The proposed methodology offers significant progress in post-disaster structural assessment by providing fast, objective, and scalable damage assessment. This technology can greatly improve emergency response efficiency, resource allocation, and safety assessment procedures following seismic events. Future work will focus on expanding the model to detect additional types of damage and on its use as a mobile application for on-site assessment by emergency response teams.

Keywords:

Post-Earthquake building inspection, YOLOv8, Wall damage classification, Deep learning, Crack and hole classification.



PLANNING, OPTIMIZATION, AND GRID INTEGRATION OF ELECTRIC VEHICLE CHARGING INFRASTRUCTURE: A SYSTEMATIC LITERATURE REVIEW

Fatih İLKBAHAR ^{1,*} , Şahin KARA ² , Muhammed Zekeriya GÜNDÜZ ³

¹ Düzce University, Department of Computer Technologies, Düzce, Türkiye

² Sakarya University of Applied Sciences, Department of Computer Technologies, Sakarya, Türkiye

³ Bingöl University, Department of Computer Technologies, Bingöl, Türkiye

*Corresponding Author: fatihilkbahar@duzce.edu.tr

ABSTRACT

Electric vehicles are spreading fast. This increase in electric vehicle use has led to problems such as infrastructure issues, planning of charging stations, and efficient use of charging stations. In sustainable transportation, charging stations and electric vehicles are connected. In sustainable transportation, charging stations and electric vehicles are connected. Therefore, scientific studies on electric vehicle charging station networks have increased significantly. A systematic literature review on electric vehicle charging stations examined peer-reviewed studies published in major academic databases, including IEEE Xplore, ScienceDirect, Scopus, and DergiPark, aimed at improving electric vehicle charging infrastructure. Three main topics were identified for the review: (a) Planning and Location Determination of Charging Stations, (b) Grid Integration and Smart Charging Strategies, and (c) Optimization-Based Routing. When spatial studies are examined in detail, Geographic Information Systems (GIS) are integrated with multi-criteria decision-making features and optimization models to determine the most suitable station location in densely populated areas with high traffic flow, considering the adequacy of energy infrastructure. Optimization-based studies present research that combines artificial intelligence methods in demand forecasting, resource management, pricing determination, and charging planning processes. The literature shows that there are significant problems related to grid infrastructure such as voltage drops, load imbalances, and demand increases in regions where electric vehicles are heavily used. Smart charging software, regional dynamic pricing, bidirectional charging technologies, and simulation-based studies are highlighted as solutions to these problems. In addition, the increasing use of renewable energy sources and the increase in efficiency in energy storage systems, as well as the durability of charging stations and the reduction of carbon intensity, are among the areas of research. The studies emphasize scalability, safety, and sustainability in low-carbon transportation.

Keywords: Smart charging, EV charging infrastructure, Spatial optimization, Distribution grid impact.



EVALUATING METEOROLOGICAL EFFECTS ON WIND TURBINE PERFORMANCE: ANOMALY DETECTION AND ENERGY LOSS QUANTIFICATION

Gökhan YÜKSEK 

Batman University, Department of Electrical and Electronics Engineering, Batman, Türkiye
gokhan.yuksekbattman.edu.tr

ABSTRACT

This study evaluates the influence of key meteorological parameters on wind turbine performance with a specific focus on power curve anomalies and the quantification of energy losses. Using operational data containing wind speed, wind direction, air temperature, air density, cloud cover, solar irradiation, and actual turbine output, the analysis explores how atmospheric variability alters the expected behavior defined by the theoretical power curve. Deviations between theoretical and measured power values are used to detect performance anomalies linked to meteorological conditions, revealing the circumstances under which turbines operate below their expected efficiency. Energy loss metrics are then derived by aggregating the gap between theoretical and actual power across the dataset, allowing a detailed examination of how temperature fluctuations, density variations, and wind regime inconsistencies contribute to short-term and cumulative production losses. The findings underscore the importance of integrating meteorological information into both performance assessment and predictive maintenance strategies, demonstrating that comprehensive atmospheric monitoring significantly enhances the accuracy of energy yield estimations and supports more reliable operational planning.

Keywords:

Wind turbine performance, Power curve anomaly detection, Energy loss quantification, Atmospheric effects, Wind energy assessment, Operational data analysis.



STELLAR OSCILLATION OPTIMIZER-BASED PARAMETER IDENTIFICATION FOR PHOTOWATT PWP201 AND STM6-40/36 PV MODULES

Serdar EKİNCİ ¹ , Davut İZCİ ^{2*} , Burcu BEKTAŞ GÜNEŞ ³ , İlayda AKSOY ⁴ ,
Mohit BAJAJ ⁵ , Laith ABUALIGAH ⁶

¹ Bitlis Eren University, Department of Electric and Electronic Engineering, Bitlis, Türkiye

² Bursa Uludağ University, Department of Electric and Electronic Engineering, Bursa, Türkiye

³ İstanbul Gedik University, Department of Computer Engineering, İstanbul, Türkiye

⁴ Bitlis Eren University, Institute of Graduate Education Department of Computer Engineering, Bitlis, Türkiye

⁵ Graphic Era University, Department of Electrical Engineering, Dehradun, India

⁶ Al al-Bayt University, Department of Artificial Intelligence and Software Engineering, Amman, Jordan

*Corresponding Author: davutizci@gmail.com

ABSTRACT

Accurate parameter identification of photovoltaic (PV) modules plays a critical role in performance prediction, system design, and maximum power extraction, particularly as renewable energy systems continue to grow in scale and complexity. However, the nonlinear characteristics of PV modules often make parameter estimation a challenging task that requires powerful and reliable optimization techniques. In this study, the recently developed stellar oscillation optimizer (SOO) is employed to estimate the unknown electrical parameters of two widely used commercial PV modules, namely Photowatt-PWP201 and STM6-40/36. The optimization process aims to improve model fidelity by minimizing the mismatch between experimentally measured and simulated current-voltage characteristics under standard test conditions. To thoroughly evaluate its performance, SOO is benchmarked against several well-established metaheuristic algorithms reported in the literature. Comparative analyses demonstrate that SOO achieves superior accuracy, faster convergence, and enhanced numerical stability for both test modules. These results confirm that the Stellar Oscillation Optimizer provides a competitive and robust solution for PV parameter identification, offering significant potential for integration into advanced modeling, real-time monitoring, and performance forecasting applications in solar energy systems.

Keywords:

Photowatt PWP201, STM6-40/36, PV parameter estimation, Stellar oscillation optimizer, Parameter identification.



ENHANCED TRANSIENT PERFORMANCE OF MICRO-ROBOTIC SYSTEMS VIA SFOA-BASED PID TUNING

Muhammet İsmail GÜNGÖR¹ , Davut İZCİ^{1,*} , Serdar EKİNCİ² , Ehab GHITH³

¹ Bursa Uludağ University, Department of Electric and Electronic Engineering, Bursa, Türkiye

² Bitlis Eren University, Department of Electric and Electronic Engineering, Bitlis, Türkiye

³ Ain Shams University, Department of Electric and Electronic Engineering, Cairo, Egypt

*Corresponding Author: davutizci@gmail.com

ABSTRACT

In this study, the parameters of a proportional–integral–derivative (PID) controller are automatically tuned using the starfish optimization algorithm (SFOA) to improve the transient performance of a micro-robotic position control system. The optimization is carried out by minimizing the integral of squared time multiplied by the squared error (ISTES), which emphasizes both rapid response and disturbance attenuation over time. To validate the effectiveness of the proposed approach, SFOA is benchmarked against several reported methods, including JSO, HHO, AOA, and HAOARSO, under identical simulation conditions. The comparative results reveal that SFOA attains the smallest ISTES value, accompanied by the shortest rise time (6.8838 s) and settling time (12.0729 s), while fully eliminating overshoot. These outcomes highlight that SFOA offers rapid convergence, high solution accuracy, and a robust global search capability for PID parameter tuning. Owing to its simplicity and computational efficiency, the proposed method shows strong potential for real-time implementation and future extensions to multi-objective control optimization.

Keywords:

Micro-robotic position control. Starfish optimization algorithm, Transient response enhancement, PID controller.



NUMERICAL INVESTIGATION OF THE COOLING PERFORMANCE OF PHOTOVOLTAIC PANELS EQUIPPED WITH SQUARE FINS

Abdullatif YILMAZ ^{1,*} , Cengiz YILDIZ ²

¹Firat University, Graduate School of Natural and Applied Sciences, Department of Mechanical Engineering, Elazığ, Türkiye

² Firat University, Department of Mechanical Engineering, Elazığ, Türkiye

*Corresponding Author: abltf_ylmz@hotmail.com

ABSTRACT

The increase in operating temperature of photovoltaic (PV) panels is a critical problem that significantly reduces energy conversion efficiency. The main objective of this study is to numerically investigate the thermal performance of different passive cooling systems integrated onto the bottom surface of PV panels and compare their effects on panel efficiency. In this context, a flat panel without fins (control model) and a panel geometry with square-section fins were analyzed. Aluminum was selected as the fin material. Computational Fluid Dynamics (CFD) analyses were performed using ANSYS Fluent software under different air speeds (0.5 m/s and 2.5 m/s) and solar radiation conditions at different times of the day (09:00, 14:00, 18:00). The findings showed that the finless panel was insufficient, especially under high solar irradiance, and that increasing air velocity alone was not effective in reducing the temperature. The square-fin geometry panel significantly reduced the panel temperature compared to the case without fins by changing the flow structure and creating local turbulence. Analysis revealed that the pressure differences and swirling flow created by the fins are the primary mechanisms that enhance convective heat transfer. At the highest irradiance and temperature conditions studied (14:00), the square-finned design was found to reduce surface temperature by approximately 7°C compared to the panel without fins, resulting in a 1% increase in panel efficiency. In conclusion, passive cooling strategies with square-finned geometry in photovoltaic panels play a critical role in improving the efficiency and stability of PV systems.

Keywords: Photovoltaic panel, Passive cooling, Fin, Computational Fluid Dynamics (CFD), Heat transfer, Panel efficiency.



SINGLE-ENDED FAULT DETECTION AND FAULT LOCATION IN TRANSMISSION LINES USING THE APPROXIMATE DERIVATIVE

Mustafa AKDAĞ^{1,*} , Mehmet Salih MAMIŞ²

¹ Bitlis Eren University, Department of Electrical and Electronics Engineering, Bitlis, Türkiye

² İnönü University, Department of Electrical and Electronics Engineering, Malatya, Türkiye

* Corresponding Author: makdag@beu.edu.tr

ABSTRACT

Fault-location estimation methods for power transmission lines (PTL) are generally classified as impedance-based methods and travelling-wave (TW)-based methods. TW-based approaches exhibit significantly lower sensitivity to factors such as fault resistance and therefore typically provide higher accuracy. Consequently, most recent studies in literature focus on TW-based fault-location algorithms. When a fault occurs, current and voltage travelling waves propagate toward both ends of the line. Two-ended methods determine the fault location from the arrival-time difference of these waves but require precise time synchronization between the line terminals. In contrast, single-ended methods use only the current or voltage signal measured at one terminal, extracting the arrival times of the initial TW launched by the fault and the TWs reflected from the fault point and the remote terminal. Although they do not require any synchronization hardware, they must correctly distinguish between the incident and reflected waves.

A wide range of signal-processing techniques has been proposed to extract TW arrival times and amplitudes from fault transients. In this study, the Approximate Derivative (AD) method is employed to detect TW arrivals and their magnitudes. The AD operator simply computes the difference between consecutive samples of the measured transient signal. This operator, which has previously been investigated for two-ended applications, is computationally simple and has proven effectiveness. In the present work, it is adapted for single-ended fault detection and fault-location estimation using current or voltage measurements from one terminal.

Because TWs generated during a fault propagate not only in the faulted phase but also in the healthy phases, modal transformation is applied to obtain a single modal component with a dominant TW signature. The Karrenbauer modal transformation is used in this study. Under normal operating conditions, applying the AD operator to modal signals yields values near zero, whereas during faults it produces clear and abrupt transitions. By comparing each AD sample with a predefined threshold, fault detection is achieved. After detecting the fault, the samples required for fault location are selected based on the line geometry, conductor parameters, propagation velocity, sampling frequency, and line length. Modal transformation and the AD operator are then applied, and the arrival index of the initial TW is determined. Using TW theory, the indices of the waves reflected from the fault point and the remote terminal are separated based on their polarity. The distance to the fault is computed from the index difference between the initial TW and the fault-reflected TW, considering the propagation velocity and sampling frequency.

The effectiveness of the proposed method is verified through ATP/EMTP simulations of a 400-kV, 50-Hz, 300-km double-ended transmission line. A total of 35 fault scenarios, covering various fault types and locations, are simulated. Despite using a sampling frequency (250 kHz) significantly lower than that required by many methods in the literature, the proposed approach achieves highly accurate fault-location results. Furthermore, the impact of noise is analyzed, and the minimum signal-to-noise ratio required for reliable performance is identified.

Keywords: Transmission line faults, Fault detection, Fault location, Travelling waves (TW), Approximate derivative (AD).



INVESTIGATION OF THE THERMAL PERFORMANCE OF AIR-COOLED LITHIUM-ION BATTERY SYSTEMS IN ELECTRIC VEHICLES

Fatih OKTAY ^{1,*} , Emin EL ²

¹ Bitlis Eren University, Graduate Education Institute, Department of Mechanical Engineering, Bitlis, Türkiye

² Bitlis Eren University, Department of Mechanical Engineering, Bitlis, Türkiye

*Corresponding Author: ftokty4913@gmail.com

ABSTRACT

Today, electric vehicles (EVs) are considered the most suitable solution to replace internal combustion engine vehicles. The development of EV technologies is progressing rapidly, and battery technology plays a critical role in the performance of electric vehicles.

Lithium-ion batteries offer significant advantages over other battery technologies, including high specific energy, high energy density, long durability, low self-discharge rate, and long shelf life. However, battery temperature has become one of the most critical parameters that must be carefully addressed in the development and widespread adoption of Lithium-ion battery-powered electric vehicles. Both high and low temperature conditions can significantly affect battery capacity and service life. In high-temperature environments, Lithium-ion batteries may pose a thermal runaway risk, which can lead to short circuits, fires, explosions, and other safety issues. In low-temperature conditions, lithium dendrites may form, which can cause short circuits, startup failures, and other operational malfunctions.

To maximize the efficiency of a Lithium-ion battery pack, the temperature must be kept constant between 15°C and 35°C. Therefore, a reliable and robust battery thermal management system is required to effectively distribute heat and keep the battery pack temperature under control. In electric vehicles (EV), the Battery Thermal Management System (BTMS) plays a critical role in extending the life of the Lithium-ion battery pack by optimizing the operating temperature of the batteries and reducing the risk of thermal runaway. A good Battery Thermal Management System (BTMS) should keep the Lithium-ion battery pack's temperature between 15°C and 35°C, be light and small, use energy efficiently, be affordable, evenly distribute temperature across all battery cells, and allow enough airflow to release toxic gases if there is a Lithium-ion battery fire.

This study compared and evaluated the performances of various air-cooled Lithium-ion battery systems used in electric vehicles. The results indicate that air-cooled battery systems provide both a feasible and cost-effective thermal management solution for electric and hybrid electric vehicles, serving as a guide for future battery designs.

Keywords:

Electric vehicles, Lithium-ion battery, Battery temperature, Air cooling, Battery thermal management system, Battery performance.



A DEEP LEARNING-BASED APPROACH FOR A TWO-WAY SIGN LANGUAGE TRANSLATION SYSTEM

Dilan ÖZEK^{1,*} , İrfan ÖKTEN² , Lokman DOĞAN³ 

¹ Computer Engineer, Bitlis, Türkiye

² Bitlis Eren University, Department of Computer Engineering, Bitlis, Türkiye

³ Kütahya Health Sciences University, Kütahya Vocational School, Artificial Intelligence Operator Pr. Kütahya, Türkiye

* Corresponding Author: dilanozek34@gmail.com

ABSTRACT



This study presents a bidirectional sign language translation system developed using VideoMAE-based deep learning techniques to mitigate communication barriers experienced by hearing-impaired individuals in healthcare settings. Communication challenges in clinical environments can negatively affect diagnostic accuracy, treatment quality, and patient involvement in the care process. Existing sign language translation solutions often lack robustness in recognizing dynamic gestures, supporting extensive vocabularies, and operating with real-time performance. In this research, a large-scale dataset comprising 20,000 videos and over 7,000 distinct Turkish Sign Language (TSL) medical terms was utilized to train a high-performance sign language recognition model based on the Video Masked Autoencoder (VideoMAE) architecture. The masked video modeling strategy of VideoMAE enables effective learning of both spatial and temporal dependencies, offering significant advantages in recognizing complex and dynamic gestures. Due to the computational demands of the model, training was optimized using distributed parallel programming techniques, including Distributed Data Parallel (DDP), multi-threaded data processing, and GPU-accelerated pipelines. The proposed system supports both sign → text/speech translation and text → sign conversion, forming a comprehensive bidirectional communication framework. Generated signs are visualized through a motion-driven avatar interface, facilitating natural and intuitive user interaction. The originality of this study lies in integrating advanced video representation learning, large-scale data processing, and bidirectional translation to offer a real-time, accurate, and user-centered communication solution for healthcare environments. Performance evaluation will focus on translation accuracy, processing speed, usability, and applicability in real-world clinical scenarios. The findings are expected to significantly improve accessibility in emergency units, outpatient clinics, and consultation areas.

Keywords:

Sign language translation, VideoMAE, Deep learning, Masked autoencoder, Parallel programming, Turkish sign language.



RESNET-50 BASED CNN MODEL FOR GRAPE LEAF IMAGE CLASSIFICATION IN MATLAB

Seda YETKİN YESİL^{1,*} , Olcay PALTA¹ 

^{1*} Bitlis Eren University, Vocational School of Technical Sciences, Department of Electronics and Automation, Bitlis, Türkiye

* Corresponding Author: syetkin@beu.edu.tr

ABSTRACT

The primary aim of this study is to investigate the effectiveness of a Convolutional Neural Network (CNN) architecture, specifically ResNet-50, in accurately classifying grapevine leaves belonging to five different species (Ak, Ala Idris, Buzgulu, Dimnit, and Nazli). Thanks to its capacity to extract rich and detailed features from images, the ResNet-50 architecture enables the high-accuracy differentiation of leaf species that are morphologically very similar. To this end, a comprehensive dataset comprising a total of 500 grapevine leaf images, representing the five species, was created. Each species is represented by 100 images, all of which were captured under similar lighting and environmental conditions to enhance data consistency and minimize noise. Prior to model training, various preprocessing steps were applied to the dataset. The ResNet-50-based CNN model was implemented in MATLAB, and both training and validation were conducted through custom MATLAB scripts. In the experimental setup, the dataset was divided into training (70%) and test (30%) subsets. Additionally, due to the limited amount of data, a 5-fold cross-validation technique was employed. The average results from this cross-validation process indicated that the model achieved an accuracy of 75.40%.

Keywords: Convolutional neural network, Grape leaf, Resnet-50, Image, classification.



SENTIMENT ANALYSIS OF MONKEYPOX TWEETS USING A HYBRID CNN-BIGRU BASED DEEP LEARNING MODEL

Ümit CAN 

Munzur University, Computer Engineering Department, Tunceli, Türkiye
ucan@munzur.edu.tr

ABSTRACT

Recently, epidemics have disrupted people's lives. Following the COVID-19 pandemic, cases of monkeypox, a rare disease, began to appear worldwide. These incidents raised societal tension and anxiety. Understanding public attitudes, sentiments, and perceptions regarding the epidemic is essential for developing effective policies and implementing effective countermeasures. Online social media platforms are essential venues for expressing feelings and views. In particular, Twitter provides valuable information for measuring societal sentiment. Machine learning and deep learning methods have recently been widely used in social network analysis. Deep learning models, which deliver strong performance, particularly on complex and nonlinear problems, are used in natural language processing and text mining. In this study, a CNN-BiGRU hybrid deep learning model was developed by combining a CNN and a BiGRU and applied for the first time to monkeypox sentiment analysis. The dataset was labeled as positive, negative, or neutral with VADER. In addition, FastText, and TF-IDF word embedding methods were used for feature extraction, and the performance of the machine and deep learning methods was tested separately. As a result of the experimental studies, the FastText-CNN-BiGRU model obtained the highest results with 0.9400 accuracy, 0.9404 precision, 0.9400 recall, and 0.9401 F-score. The FastText-BiGRU model was the second most successful, achieving 0.9351 accuracy, 0.9372 precision, 0.9351 recall, and 0.9356 F-score. The third most successful model was the TF-IDF-CNN-BiGRU model, achieving 0.9138 accuracy, 0.9088 precision, 0.9100, recall, and 0.9093 F-score.

Keywords: Deep learning, Machine learning, Monkeypox, Sentiment analysis, Social network.



MONITORING AND ANALYSIS OF EMPLOYEE PRODUCTIVITY WITH ARTIFICIAL INTELLIGENCE: AN APPLICATION USING THE YOLO ALGORITHM

Hasan ÖNDER ^{1*} , İlknur ÇEVİK TEKİN ¹ 

¹ Selçuk University, Beyşehir Ali Akkanat Faculty of Business Administration / Department of Management Information Systems, Konya, Türkiye

* **Corresponding Author:** honder1903@gmail.com

ABSTRACT

Rapid and remarkable developments in the field of artificial intelligence are directly impacting today's business world. It is predicted that in the future, artificial intelligence will become a critical competitive factor for businesses, significantly transforming business lines, content, management styles, organizational structures, and corporate cultures. One of the most fundamental elements in a business's success is employee performance. Therefore, managers are inclined to develop new methods to motivate employees and evaluate their performance more efficiently. In institutions with a large number of employees, how personnel use their time, the extent to which they contribute to work processes, and the activities they focus on play a decisive role in performance evaluation. Studying and analyzing employee behaviors is of great importance in human resource management. This research aims to monitor and analyze employees' workplace activities using AI-supported image processing methods. The developed system enables decision-makers in businesses to make more objective and data-driven evaluations, facilitating the measurement of employee productivity. In this context, the deep learning-based YOLOv8 object detection model was used to classify different employee activities. During the training process, the gradual decrease in Box Loss, Class Loss, and DFL Loss values indicates that the learning process is progressing steadily. According to experimental results, the obtained 95.6% mAP@0.5 average accuracy rate demonstrates the model's high classification performance. While high accuracy rates were observed in some classes in the precision-recall and precision-confidence curves, the error rate increased in other classes. Confusion matrix analysis revealed that most of these errors were caused by similar behavior patterns between classes.

Keywords: Artificial Intelligence, YOLO, Employee productivity, Image processing, Object detection, Deep learning.



A MACHINE LEARNING AND CLUSTERING-BASED FRAMEWORK FOR ASSESSING ENVIRONMENTAL EFFECTS IN THE TEXTILE INDUSTRY

İsmail ÇALIKUŞU^{1,*} , Kadir HALTAŞ²

¹ Nevşehir Hacı Bektaş Veli University, Department of Electronics and Automation, Nevşehir, Türkiye

² Nevşehir Hacı Bektaş Veli University, Department of Computer Technologies, Nevşehir, Türkiye

* **Corresponding Author:** ismailcalikusu@nevsehir.edu.tr

ABSTRACT

The objective of this study is to comprehensively assess the environmental impacts of the textile and ready-to-wear clothing industry and to establish a machine learning-based multivariate framework for predicting the Air Quality Index (AQI). In this context, 21 years of monthly data obtained from the city of Surat in India were utilized. Eight different machine learning models were evaluated to predict the AQI using the aforementioned data: Long Short-Term Memory (LSTM), Linear Regression, Ridge, Lasso, Support Vector Regression–Radial Basis Function (SVR-RBF), K-Nearest Neighbor (KNN), Decision Tree, and Gradient Boosting. The analysis results showed that LSTM achieved the best performance ($R^2 = 0.2932$, MAE = 22.87) due to its sensitivity to patterns that change over time, while the Gradient Boosting model was the second most successful model. In contrast, the SVR-RBF, KNN, and Decision Tree models showed lower accuracy. Principal Component Analysis (PCA) was applied for dimension reduction to examine seasonal pollution trends, followed by the Density-Based Clustering in Noise-Affected Applications (DBSCAN) method. The clustering resulted in five clusters and one noise segment. Cluster 3, in particular, stood out with consistently high pollution levels (AQI = 241) despite low variance. This study demonstrates that there is a non-linear relationship between production volume and pollution, and that industrial modernization has the potential to reduce environmental damage. Overall, the findings reveal that machine learning models are effective tools for environmental monitoring, risk classification, and developing data-driven sustainability strategies.

Keywords:

Machine learning, Air Quality Prediction (AQI), Environmental Impacts, Principal Component Analysis (PCA), Clustering (DBSCAN).



ENHANCING SITUATIONAL AWARENESS AGAINST RANSOMWARE ATTACKS: ANALYSIS, DETECTION, AND PREVENTION APPROACHES

Muhammed Zekeriya GÜNDÜZ ^{1,*} , Şahin KARA ² , Fatih İLKBAHAR ³

¹ Bingöl University, Department of Computer Technologies, Bingöl, Türkiye

² Sakarya University of Applied Sciences, Department of Computer Technologies, Sakarya, Türkiye

³ Düzce University, Department of Computer Technologies, Düzce, Türkiye

* Sorumlu Yazar: mzgunduz@bingol.edu.tr

ABSTRACT

There has been an exponential increase in the frequency of cyberattacks. Among these attack types, ransomware constitutes one of the most common and impactful threats, as it prevents users from accessing their systems by locking device screens or encrypting files. In ransomware attacks, the victim's data remains encrypted until the demanded ransom is paid, and the consequences of such attacks are often permanent. Therefore, recovering data without the intervention of the attackers is extremely difficult. To establish an effective defense against these attacks, it is critically important to enhance end-users' situational awareness within the context of cybersecurity. Indeed, cybersecurity awareness activities directed toward end-users will make the early detection of ransomware threats more comprehensible, faster, and more feasible. Furthermore, the severe negative impacts of ransomware attacks on user data highlight the necessity of proactive security measures. In this review study, the structure of ransomware attacks, as well as existing detection and prevention mechanisms, are examined; additionally, several improvement suggestions regarding current approaches are presented.

Keywords: Ransomware attacks, Cybersecurity, Situational awareness, User awareness.



SMART DOOR SECURITY SYSTEM WHIT FACE RECOGNITION: A LOW-COST IOT-BASED APPROACH

Elif ERCEL ^{1,*} , İrfan ÖKTEN ²

¹ Bitlis Eren University, Graduate Education Institute, Department of Computer Engineering, Bitlis, Türkiye

² Bitlis Eren University, Department of Computer Engineering, Bitlis, Türkiye

* **Corresponding Author:** elifercelakademik@gmail.com

ABSTRACT

This study aims to develop an Internet of Things (IoT)-based smart door security system with facial recognition capabilities using image processing technologies. Today's rapidly developing smart systems have the potential to revolutionize home security by replacing traditional physical security methods. This research aims to contribute to this change by offering an advanced, secure solution that minimizes the risk of unauthorized access. The method involves setting up a system that detects and processes the face of a person approaching the door. This process involves capturing the image with a camera, detecting the face using image processing techniques, and finally comparing it with the registered authorized faces. If the identity verification is successful, the door opens automatically; if unsuccessful, access is denied and an instant notification is sent. Integration has been achieved with the mobile application developed for the system's remote control and notification capabilities.

Compared to existing security systems, this study offers faster and more accurate identity verification, which is its primary original aspect. Furthermore, the use of low-cost hardware components such as the ESP32-CAM, rather than microcontrollers like the Raspberry Pi which are costly, enables the system to be widely adopted, creating a significant difference. This system not only performs the door opening function but also provides a comprehensive security solution by sending instant notifications to the user, enabling remote live monitoring, and recording entry attempts. This developed prototype will enable widespread use by offering a cost-effective, modern, and high-tech solution for home and office security, especially in today's world where smart home technologies are rapidly spreading.

Keywords: Security, Embedded systems, ESP32 CAM, Face recognition, Mobile application.



SPEAKER DETECTION IN DIALOGUE-HEAVY TEXTS: A COMPARATIVE ANALYSIS OF BABELSCAPE AND SAVASYBERT NER MODELS

Tuğçe DENİZ ¹ , Pınar ÜNVER ¹ , Beytullah TÜTÜNCÜ ¹ , Barış ASLAN ¹ , **Pakize ERDOĞMUŞ ^{1,*}**

¹ Düzce University, Department of Computer Engineering, Düzce, Türkiye

* **Corresponding Author:** pakizeerdogmus@duzce.edu.tr

ABSTRACT

This study addresses the problem of assigning dialogues to the correct speaker in literary texts for multi-speaker text-to-speech (TTS) systems and proposes a hybrid method combining machine learning and rule-based approaches. The method consists of two layers: identification of 'Person' entities using SavasyBERT and the multilingual Babelscape models, and rule-based dialogue detection based on dashes and quotation marks. The concept of "Speaker" is defined as the intersection of these two layers. The findings indicate that the Turkish-specific SavasyBERT model identifies fictional characters more consistently and produces lower noise. In contrast, the Babelscape model exhibited a tendency to generate more false positives due to its limited alignment with Turkish language characteristics. Consequently, it is evaluated that the proposed hybrid approach, when used with SavasyBERT, offers a reliable character detection infrastructure for Turkish multi-speaker TTS applications.

Keywords: Named Entity Recognition (NER), Speaker detection, Hybrid approach, SavasyBERT, Babelscape, Multi-Speaker Text-to-Speech.



CONDUCTIVE ASPHALT PAVEMENTS FOR SNOW AND ICE MANAGEMENT ON ROADS

Alev AKILLI EL 

Bitlis Eren University Vocational School of Technical Sciences, Department of Construction, Bitlis, Türkiye
aakilli@beu.edu.tr

ABSTRACT

In cold climate regions, snow and ice accumulation on road surfaces significantly reduces skid resistance, posing a serious threat to traffic safety. Traditional de-icing and snow removal methods, such as mechanical clearing, manual intervention, and the use of chemical de-icing salts, often lead to operational delays, pavement deterioration, and environmental pollution. In recent years, conductive pavement technologies have emerged as an environmentally friendly alternative that effectively melts snow and ice while enhancing road safety. This study investigates the potential application of conductive pavements on roads that experience heavy ice formation and snow accumulation. The fundamental principles of conductive asphalt concrete, types of conductive materials (e.g., graphite, carbon fiber, steel powder), heating mechanisms, and energy efficiency aspects are examined. Moreover, recent studies from the literature are reviewed to compare the performance of various conductive fillers in terms of electrical conductivity, heating efficiency, mechanical strength, and environmental sustainability. The findings indicate that conductive asphalt pavements provide an effective solution for preventing icing and reducing snow accumulation, while ensuring long-term road safety without causing environmental harm. Therefore, conductive pavement technologies hold significant potential for developing safe and sustainable transportation systems under winter conditions.

Keywords: Conductive asphalt concrete, Snow melting, Road safety, Sustainable pavement technologies.



GEOPOLIMER BRICK TECHNOLOGY IN TERMS OF ENERGY AND SUSTAINABILITY

Aykut TUNTAŞ¹ , Namık YALTAY^{1,*}

¹ Van Yüzüncü Yıl University, Civil Engineering Department, Van, Türkiye

* **Corresponding Author:** namikyaltay@yyu.edu.tr

ABSTRACT

Today, the construction industry is recognized as one of the major contributors to global carbon emissions and energy consumption; particularly due to the production processes of construction materials, which require high temperatures and intensive fossil fuel usage, posing significant environmental risks. The production of fired clay bricks is also considered unsustainable because of its high energy demand. Since the manufacturing of traditional fired bricks requires elevated temperatures, the process results in substantial energy consumption and considerable CO₂ emissions. This situation has increased global interest in sustainable geopolymer brick production, positioning these materials as a promising alternative solution. Geopolymer bricks can be produced at considerably lower temperatures compared to fired bricks, making them a more sustainable and energy-efficient option. Moreover, geopolymer brick production provides significant advantages in terms of environmental waste management. These bricks are formed through the alkali activation of industrial by-products and wastes rich in silica and alumina, resulting in chemical bonding. Utilizing industrial by-products in construction materials reduces natural clay consumption, decreases the need for landfill space, and lowers the carbon footprint by eliminating the use of cement. Due to these advantages, numerous studies have been conducted in this field. This research focuses on reviewing and compiling various experimental studies in the literature related to geopolymer brick production. Many researchers have demonstrated that curing temperature, activator molarity, molding pressure, and the Si/Al ratio play critical roles in the mechanical and physical performance of geopolymer bricks. However, acceptable mechanical properties have also been achieved even with low molarity and ambient-temperature curing processes. Based on the findings of all reviewed studies, geopolymer bricks have emerged as a promising construction material both environmentally and economically, owing to their potential for waste utilization, lower curing temperatures compared to fired bricks, reduced carbon emissions, and improved thermal performance.

Keywords: Geopolymer brick, CO₂ emission, Waste utilization.



EVALUATION OF HEAT TRANSFER BEHAVIOUR IN A MINICHANNEL WITH ELECTRONIC CHIPS USING DIFFERENT FLUIDS

Fatih TAŞDELEN 

Bitlis Eren University, Vocational School of Technical Sciences, Bitlis, Türkiye
ftasdelen@beu.edu.tr

ABSTRACT

This study investigates the cooling performance of two heat-generating chips located within a mini-channel measuring 2 mm in height and 20 mm in length, across different Reynolds numbers ($Re = 1 \times 10^3 - 5 \times 10^3$). A constant heat flux of 100 kW/m^2 was applied to the chip surfaces, and all other surfaces were modelled as adiabatic. Air, water, and a 5% Al_2O_3 -water nanofluid served as coolant fluids. Numerical models were developed using the ANSYS FLUENT programme in 2D dimensions. At $Re = 1 \times 10^3$, the surface temperatures for chip 1 and chip 2 were 830.53 K and 884.35 K for air, 309.50 K and 308.84 K for water, and 307.42 K and 306.15 K for the 5% Al_2O_3 -water nanofluid, respectively. At $Re = 5 \times 10^3$, the average surface temperatures of chip 1 and chip 2 were measured as 518.62 K and 503.75 K, respectively, under air cooling conditions. In contrast, when water and a 5% Al_2O_3 -water nanofluid were used as the cooling medium, the temperatures of chip 1 and chip 2 became much closer, reaching approximately 302 K and 301 K, respectively. A decrease in chip surface temperatures was noted for all fluids as the Reynolds number increased, with the lowest temperatures recorded for water and a 5% Al_2O_3 -water nanofluid. The 5% Al_2O_3 -water nanofluid was the most effective of the coolant fluids, and air was the least effective.

Keywords: Chip surface temperature, Reynolds number, 5% Al_2O_3 -water nanofluid.



AN EXAMINATION OF THE EFFECT OF CHANNEL HEIGHT ON HEAT TRANSFER WITHIN A CHIP-EMBEDDED MINICHANNEL

Fatih TAŞDELEN 

Bitlis Eren University, Vocational School of Technical Sciences, Bitlis, Türkiye
ftasdelen@beu.edu.tr

ABSTRACT

This study aims to examine how channel height influences the heat transfer efficacy of a chip within minichannels. A two-dimensional computational fluid dynamics (CFD) analysis was performed to investigate the effect of channel height on heat transfer in a chip situated within rectangular minichannels of varying heights. Air at an inlet temperature of 300 K was used as the cooling fluid, with a continuous heat flux of 50 kW/m² applied to the chip surface. For a more precise assessment of convective heat transfer, the channel walls were considered adiabatic. Numerical calculations were conducted for different Reynolds numbers (Re = 100, 200, and 300) and for different channel heights (H = 1, 1.5, and 2 mm). The evaluation of thermal performance involved analysing differences between the local and average Nusselt numbers, as well as temperature distributions across the chip surface. The results show that increasing the Reynolds number lowers the chip surface temperature and raises the average Nusselt number, while increasing the channel height leads to higher chip surface temperatures. When the Reynolds number increased from 100 to 300, at a channel height of 1 mm, the chip surface temperature dropped from 499.15 K to 456.88 K, while the average Nusselt number increased from 11.08 to 13.15. Similarly, at a channel height of 2 mm, the chip surface temperature decreased from 607.72 K to 528.12 K, and the average Nusselt number rose from 9.89 to 13.32. The results indicate that channel height and flow conditions are essential in influencing the cooling efficacy of a chip's minichannel design.

Keywords: Mini-channel cooling, Heat transfer, CFD, Nusselt number, Reynolds number.



INVESTIGATION OF THE USE OF WASTE MATERIALS IN SOIL IMPROVEMENT METHODS

Özge Nur ÇETKİN 

Bitlis Eren University, Vocational School of Technical Sciences, Bitlis, Türkiye
oncetkin@beu.edu.tr

ABSTRACT

With the growing population, the needs in the construction industry are rapidly increasing. As a result of this increase and the resulting needs, the goal is to create safer and more comfortable structures. The creation of these structures depends on the engineering properties of the soil on which they will be built. Therefore, the soil used as the foundation or material for a building is of great importance. Because soils have different properties, they do not always meet the desired engineering specifications. Soils are improved to eliminate soil-related problems and to complete the structure more safely and economically. A review of literature and field studies reveals that one of the most frequently preferred methods recently is to improve the soil by adding various industrial waste materials such as fly ash, silica fume, and blast furnace slag. Industrial waste, in particular, is increasing with the development of technology and industry. Landfilling this waste is becoming an ever-increasing problem. Therefore, as in other fields, the use of industrial waste has gained significant importance in various applications in the construction industry. This use of waste products alleviates landfill problems to some extent. Furthermore, the use of these products is considered an environmentally and economically sound endeavor.

Keywords: Soil, Soil improvement, Industrial waste.



EFFECT OF DIFFERENT FLOW RATE VARIATION ON CALCIUM CARBONATE PRECIPITATION IN SAND SOILS TREATED BY MICP METHOD

Zehra ERTOSUN KARABULUT^{1,*} , Sabriye Banu İKİZLER²

¹ Muş Alparslan University, Department of Architecture, Muş, Türkiye

² Karadeniz Technical University, Civil Engineering Department, Trabzon, Türkiye

* Corresponding Author: z.ertosun@alparslan.edu.tr

ABSTRACT

MICP is a technique based on the principle that bacteria improve the mechanical properties of a soil or porous material by precipitating calcium carbonate (CaCO_3) through their biochemical activity. MICP is mainly used in geotechnical and civil engineering for increasing soil strength, reducing liquefaction risk, reducing permeability, slope and foundation improvement, and environmentally friendly alternative soil stabilization. MICP has been developed as an environmentally friendly alternative to traditional soil improvement methods. In contrast to the high energy consumption and carbon emissions of methods such as cement and lime, MICP provides calcium carbonate precipitation through biological processes, creating a natural bond between soil particles. Soil strength and stiffness are increased, permeability is reduced and soil behavior is homogeneously improved at the micro-scale. Low environmental impact, controlled applicability and the potential to improve dynamic soil performance make MICP an important alternative for sustainable geotechnical applications. In this study, three different sand specimens are considered and improved by MICP method. In order to see the effect of flow rate on the cured sand samples, 0.2, 0.6 and 1.8 ml/min rates of the curing solution were applied. *Sporosarcina pasteurii* bacteria is used in the treatment with MICP. After the treated sand samples are dried in an oven for 14 days, unconfined compression tests are performed. In the experiments, it is seen that all three different sand types gained strength. When the effect of flow rate was analyzed, the highest strength was obtained at high flow rate in fine-grained AFS 65/70 sand and at low flow rate in coarse-grained CEN sand. In addition, it was determined that the calcite bonds formed at high flow rate were weaker than the calcite bonds formed at low flow rate in the experimental setup where coarse and fine grained soils were considered. As the flow rate increased, calcite precipitation decreased for all three different sand types.

Keywords: Flow rate, MICP, Unconfined compressive strength.

TAM METİN BİLDİRİLER



SHORT-TERM ELECTRICITY LOAD FORECASTING WITH HOLT-WINTERS, XGBOOST AND EXTENDED HYBRID HOLT-WINTERS AND XGBOOST MODEL: EVIDENCE FROM THE AEP HOURLY DATASET

Murat BİNİCİ^{1,*} , Nebi SUDAY²

¹ Bitlis Eren University, Department of Mechanical Engineering, Bitlis, Türkiye

² Bitlis Eren University, Institute of Graduate Education Department of Mechanical Engineering, Bitlis, Türkiye

* Corresponding Author: mbinici@beu.edu.tr

ÖZET

Short-term load forecasting is a key input for the secure and economical operation of modern power systems. In this study we investigate the performance of a classical statistical model, a machine learning model, and an extended hybrid approach for one-hour-ahead forecasting of hourly electricity demand. The case study uses the AEP_hourly dataset, which contains American Electric Power's hourly load measurements from 2004 to 2018. After aggregating duplicated timestamps and resampling to a regular hourly frequency, the data are split into a training period (2004–2016) and an out-of-sample test period (2017–2018). As a statistical baseline, we estimate an additive Holt–Winters exponential smoothing model with a 24-hour seasonal component. The machine learning model is an XGBoost regressor trained on lagged load values (1, 24 and 168 hours) and calendar features (hour of day, day of week, month and weekend indicator). The proposed extended hybrid model first fits the Holt–Winters specification and then trains XGBoost on the resulting residuals using both residual and load lags together with the same calendar variables; final forecasts are obtained by adding the residual predictions to the Holt–Winters forecasts. Results on the test set show that the hybrid model clearly improves upon pure Holt–Winters (reducing MAE from about 1741 MW to 1216 MW and MAPE from 11.0% to 7.5%), but remains dominated by the pure XGBoost model, which achieves an MAE of roughly 160 MW and a MAPE close to 1.1%. The visual analysis confirms that XGBoost captures both the daily pattern and short-term fluctuations more accurately, while Holt–Winters tends to underestimate peaks. These findings suggest that, for high-frequency load data with strong nonlinearities, feature-rich gradient boosting models provide substantial accuracy gains over traditional exponential smoothing, and that residual-based hybrids may require additional extensions (e.g., multi-step training or exogenous variables) to fully exploit their potential.

Anahtar Kelimeler: Short-term Load Forecasting; Holt–Winters; XGBoost; Hybrid Forecasting Model; Time Series Analysis; Electricity Demand

1 INTRODUCTION

Electricity load forecasting plays a crucial role in the balanced and reliable operation of power systems. Energy utilities may experience difficulties in meeting electricity demand during certain periods. Anticipating such adverse situations in advance and managing them strategically makes load forecasting an essential tool. Through accurate forecasts, utilities can optimize their operational and managerial decision-making processes [1]. Load forecasting can be conducted over different time horizons, namely short-term, medium-term, and long-term forecasting. Short-

term load forecasting typically covers periods ranging from one hour to one week, whereas medium-term load forecasting spans from one week to one year. Long-term load forecasting, on the other hand, is performed for time horizons exceeding one year [2].

Short-term load forecasting plays a critical role in the efficient operation of energy systems. Such forecasts are typically performed at minute-level, hourly, or daily intervals. This study focuses on one-hour-ahead forecasting, with the objective of accurately predicting the electricity load for the subsequent hour. Hourly forecasts are particularly important for optimizing the daily operations of generation and distribution systems, as short-term forecasts enable the effective management of processes such as reserve planning, energy trading, and hydrothermal unit commitment. Consequently, short-term forecasting horizons emerge as a key factor for ensuring system reliability and economic operation in the energy sector [2].

A review of the literature on electricity demand and consumption forecasting indicates that classical statistical time series methods, machine learning techniques, and deep learning approaches have been widely employed. In a study focusing on short-term load forecasting, day-ahead hourly load predictions were performed. The study utilized hourly load data from the ISO New England and PJM electricity markets covering the period from 2007 to 2011, and an Artificial Neural Network (ANN) was applied for forecasting purposes. The trained ANN model was tested using data from 2012. Model accuracy was evaluated using the Mean Absolute Percentage Error (MAPE) metric, yielding MAPE values of 3.14% and 1.59% for the PJM and ISO New England datasets, respectively [3].

In another study proposing a statistical SARIMAX-based framework for hourly electricity load forecasting, weather variables, calendar variables, and the interactions among these factors were explicitly considered. The study utilized hourly electricity consumption data from Japan covering the period from 2012 to 2015, with the data from 2015 designated as the test dataset. A conventional SARIMAX model including only main effects was compared with an extended SARIMAX model incorporating interaction terms, and the inclusion of interaction effects was shown to yield improvements exceedingly approximately 20% in the MAPE, MAE, and RMSE error metrics [4].

In a study using hourly electricity consumption data from Australia, Portugal, and Spain for the years 2010 and 2011, the Iterative Neural Network (INN) method was employed for forecasting, and model performance was evaluated using the Mean Absolute Error (MAE) and MAPE metrics. The data from 2010 were used for training (70%) and validation (30%), while the data from 2011 served as the test set. Forecasts were also generated using the Weighted Nearest Neighbor (WNN), Pattern Sequence-Based Forecasting (PSF), and Iterative Linear Regression (ILR) methods, and the results were compared with those obtained from the INN model. A 24-hour forecasting horizon was adopted, and it was reported that the INN-based forecasts achieved over 90% agreement across all three datasets, outperforming the other forecasting methods [5].

In an ultra-short-term electricity consumption forecasting study, 15-minute interval data from the Paris region covering the period from December 2006 to November 2010 were utilized. The study applied a hybrid Holt–Winters (HW) and Extreme Learning Machine (ELM) approach. Initially, the dataset was decomposed into stationary linear and fluctuating nonlinear residual components. The HW method was used to model the linear component, while the ELM method was applied to the nonlinear component. Model accuracy and comparative performance were evaluated using the Root Mean Square Error (RMSE), MAE, and R^2 metrics. For comparison purposes, HW, ELM, and Long Short-Term Memory (LSTM) models were also implemented, and the proposed hybrid approach was reported to yield superior forecasting performance [6].

In a study proposing a Dynamic Multi-Domain (DMD)-based forecasting framework for short-term load forecasting (STLF) in the European energy market, multiple datasets covering the period from 2019 to 2024 were utilized. Using real-world hourly load datasets, comparative

analyses were conducted against tree-based ensemble methods and deep learning models. To enhance model speed and energy efficiency, a SHAP-based forward feature selection (SFFS) algorithm was employed. The results demonstrated that the DMD-XGBoost model achieved improvements in MAPE ranging from 69% to 79% compared to other DMD-based models, while also accelerating training time by a factor of 3.7 to 15 [7].

In [8], hybrid forecasting models based on the CatBoost and XGBoost algorithms, enhanced through different optimization techniques, were evaluated using hourly electricity load and temperature data. Model performance was compared on training and test datasets using statistical error metrics. The results indicated that the CatBoost-Arithmetic Optimization Algorithm (AOA) hybrid model performed better on the training dataset, whereas the XGBoost-AOA hybrid model exhibited superior performance on the test dataset. Furthermore, importance and sensitivity analyses revealed that temperature was the most influential variable in load forecasting, while the month variable also had a statistically significant impact on forecasting performance.

In a study proposing a hybrid machine learning model for electricity demand forecasting based on Bayesian Clustering by Dynamics (BCD) and Support Vector Regression (SVR), hourly electricity load and temperature data from New York City were used to train and test the model. First, the load series were partitioned into subclusters using the BCD method, which accounts for piecewise stationary dynamics. Subsequently, SVR models were developed for each cluster to forecast the day-ahead 24-hour load profile. Model performance was evaluated using the MAE and MAPE metrics, and the proposed hybrid approach was compared with the standalone SVR model and the forecasts published by the New York ISO. The results demonstrated that, particularly on abnormal days such as weekends and holidays, the hybrid model produced lower error values than all comparison methods and achieved superior performance in hourly short-term load forecasting [9].

In another study, a hybrid approach combining the Haar wavelet transform (WT), Holt-Winters triple exponential smoothing (TES), and the Weighted Nearest Neighbor (WNN) method was proposed for short-term hourly electricity load forecasting. The study employed hourly load data from the California (2000) and Spain (2002) electricity markets to perform day-ahead 24-hour load forecasting. Using the wavelet transform, the load series was decomposed into deterministic and fluctuation components; the deterministic component was modeled using the Holt-Winters method, while the rapidly varying fluctuation component was forecast using the WNN model. Model performance was evaluated using MAPE, weekly MAPE, and error variance metrics, and the proposed hybrid approach was compared with the standalone Holt-Winters model, the standalone WNN model, and the WT+WNN model. The results demonstrated that the proposed WT + Holt-Winters + WNN model achieved lower error values across both markets and all seasons, thereby exhibiting superior forecasting performance compared to the benchmark methods [10].

Although classical time series approaches, machine learning methods, and deep learning-based models have been widely applied in electricity demand forecasting, studies that simultaneously consider a classical statistical model, a powerful tree-based machine learning model, and a residual-based hybrid approach under the same dataset and evaluation framework remain relatively limited, particularly for high-frequency hourly data. Hourly load series typically exhibit pronounced daily and weekly cycles, sudden peaks, and nonlinear variations; therefore, methods relying solely on trend and seasonality may fail to adequately capture level changes and peak demands during certain periods. In contrast, gradient-boosted tree models supported by appropriate feature engineering are capable of representing short-term fluctuations more effectively. Consequently, there is a clear need to compare different model families under identical conditions using long-term hourly load data such as the AEP_hourly dataset [11], and to assess the practical contribution of residual-based hybridization approaches.

The primary objective of this study is to develop and comparatively evaluate, for one-hour-ahead load forecasting using the AEP_hourly dataset, (i) a Holt–Winters model with additive trend and additive seasonality components, (ii) an XGBoost regression model constructed using lagged load values (1, 24, and 168 hours) and calendar-based variables, and (iii) an extended hybrid Holt–Winters + XGBoost approach in which the residuals obtained from the Holt–Winters forecasts are modeled using both residual and load lags. In this context, the dataset was divided into a training period (2004–2016) and a test period (2017–2018). Model performance on the test period was evaluated using the MAE, RMSE, and MAPE metrics, and the improvement achieved by the hybrid approach over the classical model, as well as its relative position with respect to the pure machine learning approach, was examined both quantitatively and visually.

The remainder of this paper is organized as follows. The second section introduces the dataset used in the study and describes the applied preprocessing steps. The third section presents the methodological framework of the Holt–Winters (HW), XGBoost, and residual-based hybrid HW–XGBoost models. The fourth section describes the implementation of the models and discusses the obtained findings. The fifth section provides a discussion of the results. Finally, the last section summarizes the main conclusions and outlines recommendations for future research.

2 DATASET AND PREPROCESSING

The data used in this study were obtained from the AEP_hourly subset of the Hourly Energy Consumption dataset published on the Kaggle platform [11]. The AEP_hourly dataset contains hourly electricity load/consumption values for a specific region and has a univariate time series structure consisting of a timestamp (Datetime) and load values measured in megawatts (MW). Due to its high-frequency (hourly) nature, the dataset provides a suitable test environment for short-term load forecasting applications.

During the preprocessing stage, the timestamps were first converted into a datetime format, and the observations were ordered chronologically. Subsequently, duplicate timestamps were identified at certain time points. Since this issue poses challenges when constructing a regular hourly frequency, cases with multiple observations for the same hour were handled by averaging the corresponding load values and aggregating them into a single observation. As a result, a unique load value was obtained for each hour.

In the subsequent step, the data were resampled to a regular hourly time index, and missing hours along the series were examined. When missing time points were detected, the missing values were filled using a time-based interpolation approach in order to preserve the continuity of the series. As a result of these procedures, a regular hourly time series suitable for use in the training and test stages was obtained.

Due to temporal dependence in the time series, random shuffling was not applied during model evaluation; instead, a chronological split was adopted. Accordingly, the dataset was divided into a training period covering 2004–2016 and a test period covering 2017–2018. This partitioning was intended to realistically assess the models’ forward-looking forecasting capability and to prevent time leakage. After the models were developed using the training period, their one-hour-ahead forecasting performance was comparatively examined on the test period.

3 PREDICTION MODELS

In this study, a classical time series model (Holt–Winters), a tree-based machine learning model (XGBoost), and a residual-based extended hybrid Holt–Winters + XGBoost approach were compared under the same evaluation framework for hourly electricity load forecasting.

3.1 Holt-Winters

The Holt-Winters method is one of the fundamental techniques of the exponential smoothing (ETS) family, which models a time series through three components: level, trend, and seasonality [12]. In this study, additive trend and additive seasonality assumptions were adopted. To represent the daily cycle in hourly load data, the seasonal period was set to $m = 24$.

For the additive Holt-Winters model, the component update equations are given in Eqs. (1)-(3) [12].

$$\ell_t = \alpha(y_t - s_{t-m}) + (1 - \alpha)(\ell_{t-1} + b_{t-1}) \quad (1)$$

$$b_t = \beta(\ell_t - \ell_{t-1}) + (1 - \beta)b_{t-1} \quad (2)$$

$$s_t = \gamma(y_t - \ell_t) + (1 - \gamma)s_{t-m} \quad (3)$$

Here, y_t denotes the observed load value, ℓ_t represents the level component, b_t denotes the trend component, and s_t represents the seasonal component. The parameters α, β, γ , with values in the interval $[0,1]$, are the smoothing parameters. The h -step-ahead forecast is given in Eq. (4).

$$\hat{y}_{t+h|t} = \ell_t + hb_t + s_{t-m+h_m} \quad (4)$$

3.2 XGBoost Regression

XGBoost is a powerful ensemble method belonging to the family of gradient-boosted decision trees (GBDT), designed to reduce overfitting through regularization terms and to achieve scalability on large-scale datasets [13].

In XGBoost, the prediction can be expressed as the sum of K decision trees, as shown in Eq. (5). The objective function is minimized using the formulation given in Eq. (6), where L denotes the loss function and Ω represents the regularization term that penalizes model complexity.

$$\hat{y}_t = \sum_{k=1}^K f_k(x_t), \quad f_k \in F \quad (5)$$

$$\min \sum_t L(y_t, \hat{y}_t) + \sum_{k=1}^K \Omega(f_k) \quad (6)$$

In this study, XGBoost was formulated as a supervised learning problem for one-hour-ahead load forecasting. The model inputs were constructed using lagged load values and calendar-based variables. Specifically, lag terms y_{t-1} and y_{t-24} (the daily cycle) and y_{t-168} (the weekly cycle) were included, along with calendar features such as hour of the day, day of the week, month and a weekend indicator. The use of a 168-hour window to capture weekly patterns has also been emphasized in the literature as an effective representation for load time series [14].

3.3 Extended Residual-Based Hybrid Holt-Winters + XGBoost Model

Hybrid forecasting approaches generally aim to reduce prediction error by combining structural components that are well captured by one method (e.g., trend and seasonality) with nonlinear patterns in which another method performs strongly. The extended hybrid structure proposed in this study is based on a residual modeling framework. In this approach, a baseline forecast is first generated using the Holt-Winters method, after which the residuals, representing the components not explained by Holt-Winters, are learned using XGBoost to refine the final forecast. The proposed hybrid framework consists of five steps.

Step 1 - Baseline forecasting with Holt-Winters: During the training period, the Holt-Winters model is fitted and the baseline forecast \hat{y}_t^{HW} is obtained.

Step 2 - Residual computation: The residual series associated with the Holt–Winters model is computed using Eq. (7).

$$r_t = y_t - \hat{y}_t^{HW} \quad (7)$$

Step 3 - Feature set expansion for residual modeling: The “extended” aspect of this study lies in incorporating not only residual lags but also load lags and calendar-based variables into the residual forecasting process. Accordingly, the input vector for the XGBoost residual model is defined as in Eq. (8).

$$z_t = [y_{t-1}, y_{t-24}, y_{t-168}, r_{t-1}, r_{t-24}, r_{t-168}, \text{hour}, \text{dayofweek}, \text{month}, \text{is_weekend}] \quad (8)$$

Step 4 - Residual forecasting with XGBoost: The XGBoost model learns the residual series r_t as the target variable and generates the predicted residuals \hat{r}_t^{XGB} for the test period.

Step 5 - Final hybrid forecast: The final forecast is obtained by Eq. (9), which combines the Holt–Winters forecast with the residual correction of XGBoost.

$$\hat{y}_t^{HYB} = \hat{y}_t^{HW} - \hat{y}_t^{XGB} \quad (9)$$

This structure preserves the “regular” components captured by the Holt–Winters model through trend and seasonality, while simultaneously aiming to capture nonlinear short-term fluctuations via the residual channel using XGBoost.

4 IMPLEMENTATION AND FINDINGS

In this section, the Holt–Winters (HW), XGBoost, and residual-based hybrid HW–XGBoost approaches were implemented, and their one-hour-ahead forecasting performances were compared. Due to the dependence among observations in time series data, the dataset was divided chronologically, with the period from 2004 to 2016 used for training and the period from 2017 to 2018 used for testing. This design allowed the models’ forward-looking forecasting capability to be evaluated under a realistic scenario. All three models were implemented using the Python programming language in the Google Colab environment, where all analyses and evaluations were also conducted.

Table 1. Performance metrics of Holt–Winters, XGBoost ve hybrid HW + XGBoost models

Model	MAE (MW)	RMSE (MW)	MAPE (%)
Holt–Winters	1741.0616	2351.9936	11.04 %
XGBoost	159.7382	210.1693	1.08 %
Hybrid HW + XGBoost	1216.1578	1836.4475	7.54 %

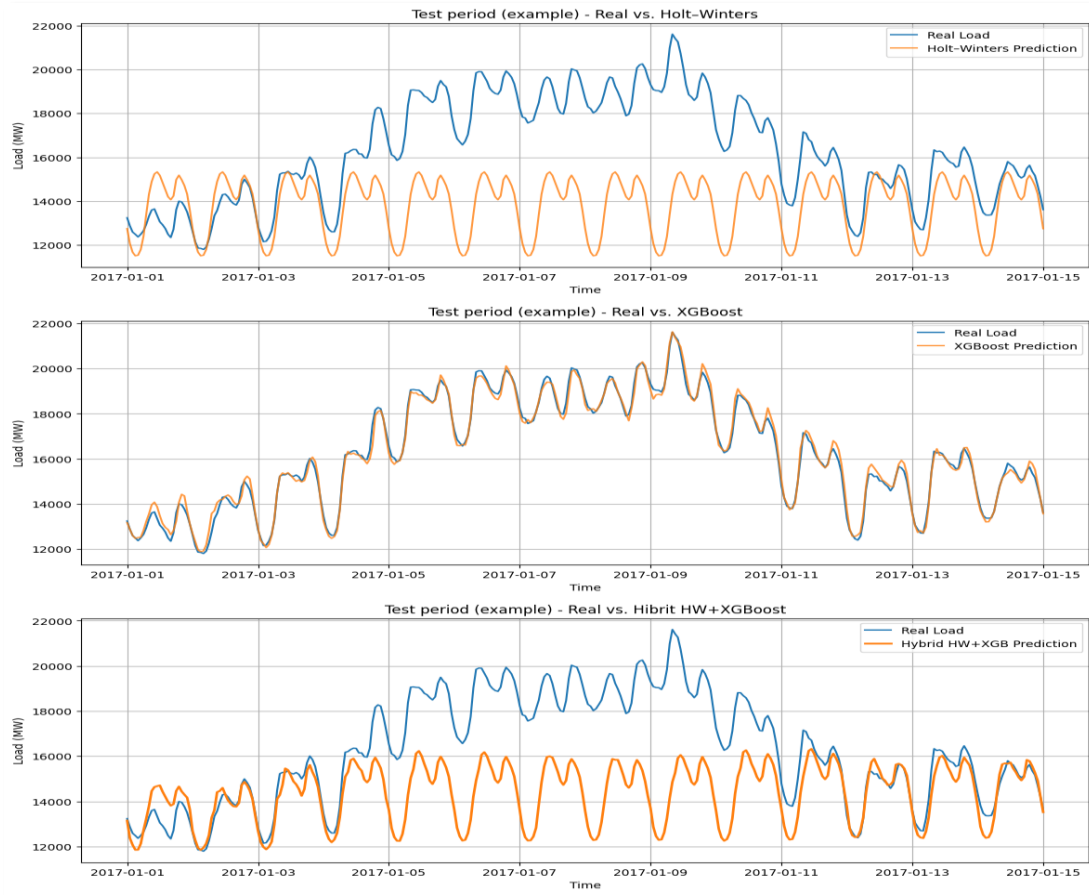


Figure 1. Comparison of real load and model predictions (HW, XGBoost, Hibrit).

During the implementation stage, the Holt–Winters model was fitted to the training data, with the seasonal period set to 24 in order to capture the daily cycle. The XGBoost model was formulated as a supervised learning problem and trained using lagged load values (1, 24, and 168 hours) together with calendar-based variables, including hour of the day, day of the week, month, and a weekend indicator. In the hybrid model, Holt–Winters forecasts were first obtained, after which the residual series was constructed and modeled using XGBoost. The final forecast was then calculated as the sum of the Holt–Winters forecast and the residual correction.

Model accuracy was evaluated on the test period using the MAE, RMSE, and MAPE metrics (Table 1). The results indicate that the Holt–Winters model was generally able to capture daily patterns; however, its errors increased particularly during peak demand periods, as it tended to underestimate load levels and peak values. The XGBoost model, supported by lagged observations and calendar-based variables, represented short-term fluctuations as well as daily and weekly patterns more effectively, yielding the lowest error values among the compared models. The hybrid approach partially corrected the systematic errors of the Holt–Winters model and achieved a notable improvement relative to Holt–Winters; however, it remained inferior to the pure XGBoost model for one-hour-ahead forecasting. Visual comparisons (Figure 1) further show that XGBoost follows the actual load values more closely, while the hybrid model produces results closer to Holt–Winters but is unable to fully compensate for sudden level changes during certain periods.

5 DISCUSSION

The findings of this study indicate that, even in hourly electricity load series with strong daily and weekly cycles, nonlinear short-term fluctuations and level shifts can pose significant

challenges for classical exponential smoothing-based methods. Although the Holt–Winters model generally captures daily seasonality, it produces systematic deviations, particularly during sudden level changes and high peak demand periods. In contrast, the XGBoost model, constructed using lagged load values (1-24-168) and calendar-based variables, more effectively represents both periodic structures and short-term irregularities, thereby achieving the highest forecasting accuracy.

The residual-based hybrid approach achieved a notable improvement over the classical Holt–Winters model by learning the remaining errors after Holt–Winters; however, it was unable to match the performance of the pure XGBoost model at a very short forecasting horizon such as one hour ahead. One possible explanation is that the residuals extracted by the Holt–Winters model are relatively small and noisy, limiting the amount of additional information available for residual learning. Another explanation is that when XGBoost directly targets the load series, it can already learn a substantial portion of the underlying structure through lagged values and calendar-based features. Consequently, the “additional information” provided by hybridization may be limited at this forecasting horizon.

6 CONCLUSIONS AND RECOMMENDATIONS

In this study, Holt–Winters, XGBoost, and a residual-based extended hybrid Holt–Winters + XGBoost approach were compared for one-hour-ahead short-term load forecasting using the AEP_hourly dataset. The findings indicate that the Holt–Winters model is able to capture daily seasonality in general, but its errors increase particularly during periods of level shifts and peak demand. In contrast, the XGBoost model, leveraging lagged load values (1, 24, and 168 hours) together with calendar-based variables, more effectively represents short-term fluctuations and achieves the lowest error values. Although the residual-based hybrid approach provides a meaningful improvement over Holt–Winters, it remains inferior to the pure XGBoost model for one-hour-ahead forecasting.

For future research, it is recommended to evaluate multi-step forecasting strategies (direct and recursive) for 24-hour and longer horizons, to incorporate exogenous variables such as temperature, humidity, and public holidays into the models, to test generalizability across different PJM regions or alternative datasets, and to conduct further comparisons with deep learning-based methods such as LSTM and TCN.

Conflict of Interest Statement

There are no conflicts of interest among the authors.

Statement of Research and Publication Ethics

This study was conducted in accordance with the principles of research and publication ethics.

Artificial Intelligence (AI) Contribution Statement

Artificial intelligence tools were used to support the translation of the manuscript into English and to assist in the technical merging and formatting of figures generated as a result of the analyses. The use of AI was limited to language editing and visual arrangement support, and all scientific interpretations, analyses, and final decisions were performed by the authors.

Contributions of the Authors

Murat Binici conceptualized the study, designed the methodology, performed the analyses, and drafted the original manuscript. Nebi Suday contributed to data curation, validation of results, literature review, and manuscript revision. Both authors reviewed the final version of the manuscript and approved it for submission.

REFERENCES

- [1] Vivas, E., Allende-Cid, H., and Salas, R., “A systematic review of statistical and machine learning methods for electrical power forecasting with reported MAPE score,” *Entropy*, vol. 22, no. 12, p. 1412, 2020. <https://doi.org/10.3390/e22121412>.
- [2] Filik, Ü. B., Gerek, Ö. N., and Kurban, M., “A novel modeling approach for hourly forecasting of long-term electric energy demand,” *Energy Conversion and Management*, vol. 52, no. 1, pp. 199–211, 2011. <https://doi.org/10.1016/j.enconman.2010.06.059>.
- [3] Sahay, K. B. and Tripathi, M. M., “Day ahead hourly load forecast of PJM electricity market and ISO New England market by using artificial neural network,” in *Proc. IEEE Innovative Smart Grid Technologies (ISGT)*, Feb. 2014, pp. 1–5. DOI: 10.1109/ISGT.2014.6816486
- [4] Elamin, N., and Fukushima, M., “Modeling and forecasting hourly electricity demand by SARIMAX with interactions,” *Energy*, vol. 165, pp. 257–268, 2018. <https://doi.org/10.1016/j.energy.2018.09.157>.
- [5] Rana, M., Koprinska, I., and Troncoso, A., “Forecasting hourly electricity load profile using neural networks,” *Proceedings of the International Joint Conference on Neural Networks (IJCNN)*, pp. 824–831, 2014. DOI: 10.1109/IJCNN.2014.6889489.
- [6] Liu, C., Sun, B., Zhang, C., and Li, F., “A hybrid prediction model for residential electricity consumption using Holt–Winters and extreme learning machine,” *Applied Energy*, vol. 275, p. 115383, 2020. <https://doi.org/10.1016/j.apenergy.2020.115383>.
- [7] Moesmann, M., Khanal, S., and Pedersen, T. B., “Energy-efficient short-term load forecasting for responsive demand-side analytics for the European electricity market,” *Proceedings of the 16th ACM International Conference on Future and Sustainable Energy Systems*, pp. 177–190, 2025. <https://doi.org/10.1145/3679240.3734612>.
- [8] Zhang, L., and Jánošík, D., “Enhanced short-term load forecasting with hybrid machine learning models: CatBoost and XGBoost approaches,” *Expert Systems with Applications*, vol. 241, p. 122686, 2024. <https://doi.org/10.1016/j.eswa.2023.122686>.
- [9] Fan, S., Mao, C., Zhang, J., and Chen, L., “Forecasting electricity demand by hybrid machine learning model,” in *Advances in Neural Networks – ICONIP 2006, Lecture Notes in Computer Science*, vol. 4233, pp. 952–963, 2006. https://doi.org/10.1007/11893257_105.
- [10] Sudheer, G., and Suseelatha, A., “Short term load forecasting using wavelet transform combined with Holt–Winters and weighted nearest neighbor models,” *Electrical Power and Energy Systems*, vol. 64, pp. 340–346, 2015. <https://doi.org/10.1016/j.ijepes.2014.07.043>.
- [11] R. Mulla, “Hourly Energy Consumption,” Kaggle dataset. [Online]. Available: <https://www.kaggle.com/datasets/robikscube/hourly-energy-consumption>. Accessed: Nov. 15, 2025.
- [12] Kramar, V., and Alchakov, V., “Time-series forecasting of seasonal data using machine learning methods,” *Algorithms*, vol. 16, no. 5, p. 248, 2023. <https://doi.org/10.3390/a16050248>.
- [13] Chen, T., and Guestrin, C., “XGBoost: A scalable tree boosting system,” in *Proceedings of the 22nd ACM SIGKDD International Conference on Knowledge Discovery and Data Mining (KDD)*, pp. 785–794, 2016. <https://doi.org/10.1145/2939672.2939785>.
- [14] Filik, Ü. B., Gerek, Ö. N., and Kurban, M., “A novel modeling approach for hourly forecasting of long-term electric energy demand,” *Energy Conversion and Management*, vol. 52, no. 1, pp. 199–211, 2011. <https://doi.org/10.1016/j.enconman.2010.06.059>.



DERİN ÖĞRENMEDE EĞİTİM VERİSİNİN SIRALAMASININ MODEL PERFORMANSINA ETKİSİ: CIFAR-10 ÜZERİNDE SİSTEMATİK BİR ANALİZ

Mehmet MOLU

Bitlis Eren Üniversitesi, Lisansüstü Eğitim Enstitüsü, Bilgisayar Mühendisliği Bölümü, Bitlis, Türkiye
molu.mehmet@gmail.com

ÖZET

Geleneksel yaklaşımlarda veri setinin her epoch başında rastgele karıştırılması yaygındır; bu çalışmada, veri sıralamalarının derin öğrenme modellerinin performansında ne gibi etkilere sahip olduğu incelenmiştir. Bu kapsamda, CIFAR-10 veri seti üzerinde SimpleCNN, ResNet20 ve VGG11 mimarileri kullanılarak dokuz farklı veri sıralama stratejisi deneysel olarak değerlendirilmiştir. Sıralama stratejileri; orijinal sıralama, sınıf bazlı blok sıralama, karışık sıralama, 1'li karışım, 10'lu karışım, 50'li karışım, 100'lü karışım ve görüntü karmaşıklığına dayalı göre kolaydan zora(K2Z) ve zordan kolay(Z2K) yaklaşımlarıdır. Görüntü karmaşıklığını nicel olarak ölçmek amacıyla entropi, kenar yoğunluğu, renk çeşitliliği, HOG ve LBP tabanlı özellikleri birleştiren çok bileşenli bir zorluk metriği kullanılmıştır. Deneysel sonuçlar, Batch içindeki sınıf çeşitliliğini en yüksek oranda sağlayan 1'li karışım stratejisinin en yüksek ortalama test doğruluğunu elde ettiğini göstermektedir. Buna karşılık, sınıf bazlı blok sıralamanın catastrophic forgetting benzeri bir davranışla uyumlu şekilde tüm mimarilerde ciddi performans çöküşüne yol açtığı gözlemlenmiştir. Curriculum learning (K2Z ve Z2K) yaklaşımlarının ise rastgele ve homojen karışım stratejilerine kıyasla beklenen performans artışını sağlayamadığı tespit edilmiştir. Elde edilen bulgular, veri sıralamasının derin öğrenme eğitiminde önemli bir hiperparametre olduğunu ve batch içi çeşitliliğin genelleme performansı açısından belirleyici rol oynadığını ortaya koymaktadır.

Anahtar Kelimeler: Derin öğrenme, model performansı, veri sıralaması, CIFAR-10

1 GİRİŞ

Birçok alanda derin öğrenme modelleri gün geçtikçe daha çok kullanılmaktadır. Derin öğrenme modellerinin eğitim maliyetleri (donanım giderleri, eğitim süresi vb.) ve performansı (doğruluk oranı) kullanım oranı üzerinde olumsuz etki edebilmekte ya da istenen verimin azalmasına sebep olabilmektedir. Derin öğrenme modellerinin eğitim maliyetlerinin azaltılması ve performansının artırılması alanlarındaki çalışmalar değerlidir. Bu alanda yapılabilecek her bir olumlu değişim, sadece tekil bir fayda sağlamayacak, ilgili modeli, yapıyı veya stratejiyi kullanan her bir işlem kadar fayda sağlamış olacaktır. Model eğitiminde veri seti sıralaması da önemlidir. Geleneksel yaklaşım, her epoch başında veri kümesinin rastgele karıştırılması üzerinedir. Bu yöntem, ardışık örnekler arasındaki korelasyonu azaltarak stochastic gradient descent(SGD)'nin istatistiksel ve yakınsama davranışını iyileştirebilir [1]. Verilerin zorluk düzeyine göre sıralanmasının öğrenmeyi kolaylaştırabileceği Bengio ve arkadaşlarının Curriculum learning çalışmasında gösterilmiştir [2].

Bu çalışmada, model eğitiminde kullanılan verilerin modele girdi sıralamasının, eğitim maliyeti ve model performansı üzerindeki etkisi deneysel olarak incelenmiştir.

2 İLGİLİ ÇALIŞMALAR

2.1 Curriculum Learning

Curriculum learning ilk defa Bengio ve ark. [1] tarafından ortaya atılmış ve “kolaydan zora doğru düzenlenmiş verilerin model eğitimini kolaylaştırdığı” gösterilmiştir. Sonraki çalışmalar Curriculum learning’nin özellikle düşük kapasiteli modellerde avantaj sağladığını [3], aynı zamanda yanlış kurgulandığında öğrenmeyi yavaşlattığını [4] göstermiştir.

2.2 Veri Sırasının Optimizasyona Etkisi

Gürbüzbalaban ve ark. [1], karışık veri sıralamasının geleneksel SGD’ye kıyasla matematiksel olarak neden daha hızlı yakınsadığını ve daha iyi genelleme sağladığını açıklamıştır.

3 YÖNTEM

Bu çalışmada, veri sıralamasının etkisini izole edebilmek amacıyla, optimizör türü, öğrenme oranı, batch boyutu ve epoch sayısı dahil olmak üzere tüm eğitim hiperparametreleri sabit tutulmuş ve yalnızca veri sıralaması değiştirilmiştir. Tüm karşılaştırmalar, aynı optimizör ve aynı hiperparametreler altında, yalnızca veri sıralamasının değiştirilmesi yoluyla gerçekleştirilmiştir.

3.1 Veri Seti ve Ön İşleme

Bu çalışmada, CIFAR-10 [5] veri seti kullanılmıştır. Veri seti, 32x32 piksel RGB görüntülerden oluşmaktadır. Veri seti, 10 sınıftan oluşmakta olup her bir sınıftan 5000 eğitim ve 1000 test görüntüsü bulunmaktadır. Görüntüler [-1, 1] aralığına normalize edilmiştir ve herhangi bir veri artırma uygulanmamıştır.

3.2 Model Mimarileri

Tüm modeller Adam optimizör ile 0,001 learning rate’de, batch size 32 olacak şekilde 5 epoch boyunca eğitilmiştir.

3.3 SimpleCNN Mimarisi

Bu model, yaklaşık 2,1 milyon parametreye sahip, iki konvolüsyon katmanı, iki tam bağlı katman ve dropout içeren basit bir CNN mimarisidir.

3.4 ResNet20 Mimarisi

Bu model, CIFAR-10 veri seti için optimize edilmiş, yaklaşık 272 bin parametreye sahip, 20 katmanlı bir mimaridir.

3.5 VGG11 Mimarisi

Bu model de, CIFAR-10 veri seti için optimize edilmiş, yaklaşık 9,75 milyon parametreye sahip, 11 katmanlı bir mimaridir.

3.6 Veri Sıralama Stratejileri

Dokuz farklı sıralama stratejisi kullanılmıştır:

- **Orijinal Sıra:** CIFAR-10 veri setinin orijinal sıralaması
- **Blok Sınıf Sıralama:** Orijinal sıradaki görüntülerin sınıf içi sıralamaları değiştirilmeden, her sınıfın 5000 örneğinin ardışık bloklar halinde sıralanması (0-9)
- **Karışık Sıralama:** Orijinal sıralamanın seed 825 ile karıştırılmış hali

- **1'li Karışım:** Blok sınıf sıralamasında, her sınıftan sırasıyla birer örnek alınarak, ardışık olarak yapılmış sıralama.
- **10'lu Karışım:** Blok sınıf sıralamasında, her sınıftan sırasıyla onar örnek alınarak, ardışık olarak yapılmış sıralama.
- **50'li Karışım:** Blok sınıf sıralamasında, her sınıftan sırasıyla elliser örnek alınarak, ardışık olarak yapılmış sıralama.
- **100'lü Karışım:** Blok sınıf sıralamasında, her sınıftan sırasıyla yüzer örnek alınarak, ardışık olarak yapılmış sıralama.
- **K2Z 1'li:** 1'li Karışım sonucunda oluşan sıralamanın, her sınıftaki görüntülerin kendi içinde kolaydan zora sıralanmış halinin, 1'li karışım biçimi.
- **Z2K 1'li:** 1'li Karışım sonucunda oluşan sıralamanın, her sınıftaki görüntülerin kendi içinde zordan kolaya sıralanmış halinin, 1'li karışım biçimi.

Bu çalışmada, bir görüntünün zorluk seviyesini nicel olarak ölçmek amacıyla, piksel tabanlı metrikler ile doku tanımlayıcılarını birleştiren çok bileşenli zorluk ölçütü geliştirilmiştir. Önerilen yöntem, üç temel bileşenin kademeli olarak birleştirilmesine dayanmaktadır.

İlk aşamada; (1) numaralı denklemde gösterildiği gibi, dört adet piksel tabanlı metrik hesaplanmaktadır. Gri-seviye görüntünün bilgi içeriğini temsil eden Shannon entropisi (SE), kenar karmaşıklığını yansıtan Sobel filtresi çıktısının varyansı (SF), doku pürüzlülüğünü ölçen Laplacian filtresi çıktısının varyansı (LF) ve renk çeşitliliğini gösteren kanallar arası piksel varyansının ortalaması (PV) elde edilmektedir. Bu metrikler, ampirik olarak belirlenmiş referans değerler (sırasıyla 8,0, 0,1, 0,05 ve 0,1) ile normalize edilmekte ve önceden tanımlanan ağırlıklarla birleştirilerek piksel tabanlı bir skor (pixel_score) üretilmektedir.

$$pixel_score = 0.35 \left(\frac{SE}{8.0} \right) + 0.25 \left(\frac{SF}{0.1} \right) + 0.20 \left(\frac{LF}{0.1} \right) + 0.20 \left(\frac{PV}{0.05} \right) \quad (1)$$

İkinci bileşen, görüntünün yapısal karmaşıklığının değerlendirilmesine yöneliktir. Bu amaçla, yönelim ve kenar düzenlerini temsil eden Histogram of Oriented Gradients (HOG) öznetelik vektörü çıkarılmakta ve bu vektörün varyansı (hog_score), yapısal örüntü çeşitliliğinin bir göstergesi olarak kullanılmaktadır. Elde edilen değer, 0,05'e bölünerek normalize edilmektedir.

Üçüncü bileşen ise yerel doku değişkenliğinin ölçülmesine dayanmaktadır. Uniform Local Binary Patterns (LBP) operatörü ile üretilen doku haritasının varyansı (lbp_score), görüntüdeki yerel doku heterojenliğini nicel olarak ifade etmektedir ve bu değer 0,5 referansına bölünerek normalize edilmektedir.

Son aşamada; (2) numaralı denklemde gösterildiği gibi, görüntünün nihai karmaşıklık (zorluk) skoru, üç ana bileşenin ağırlıklı doğrusal birleşimi yoluyla elde edilmektedir.

$$Karmaşıklık\ Skoru = 0.4pixel_score + 0.3hog_score + 0.3lbp_score \quad (2)$$

Bu çok bileşenli yaklaşım, entropi, kenar yoğunluğu, renk çeşitliliği, yapısal örüntüler ve yerel doku özelliklerini tek bir sayısal değerde birleştirerek kapsamlı, açıklanabilir ve yeniden üretilebilir bir görsel karmaşıklık ölçümü sunmaktadır. Bu metrik en uygun olduğunu iddia etmez; karşılaştırmalı analiz amacıyla kullanılmıştır.

3.7 Eğitim Protokolü

Tekrarlanabilirlik için tüm deneylerde random seed 42 kullanılmıştır. Tüm model ve sıralama kombinasyonları için hiperparametreler sabittir.

- **Optimizer:** Adam
- **Learning Rate:** 0,001
- **Batch Boyutu:** 32
- **Epoch Sayısı:** 5
- **Kayıp Fonksiyonu:** Çapraz Entropi (Cross-Entropy)
- **Donanım:** NVIDIA T4 GPU
- **Weight Decay:** 0 (SimpleCNN, ResNet20), 0,0001 (VGG11)

Eğitim süresi, hesaplama maliyetlerini sınırlamak amacıyla 5 epoch ile sınırlandırılmıştır. Bu nedenle elde edilen sonuçlar, uzun vadeli yakınsama davranışından ziyade, belirlenen deney koşulları altındaki performans karşılaştırmasını yansıtmaktadır.

4 DENEYSEL BULGULAR VE ANALİZ

Tablo 1. Modellere göre Sıralama Stratejilerinin Test Doğrulukları(%).

Sıralama Stratejisi	SimpleCNN	ResNet20	VGG11	Ortalama
Orijinal Sıra	71,06	74,23	74,10	73,13
Blok Sınıf Sıralama	10,00	10,11	10,00	10,04
Karışık Sıralama	72,63	74,89	73,81	73,78
1'li Karışım	73,25	73,64	74,54	73,81
10'lu Karışım	72,35	55,55	64,98	64,29
50'li Karışım	63,81	28,95	15,79	36,18
100'lü Karışım	58,72	12,72	13,85	28,43
K2Z 1'li Karışım	56,72	54,11	53,93	54,92
Z2K 1'li Karışım	50,00	43,63	47,55	47,06
Ortalama	58,72	47,53	47,61	

4.1 Genel Performans Analizi

Tablo 1'de sunulan sonuçlar, maksimum batch içi sınıf çeşitliliği sağlayan 1'li Karışım stratejisinin, SimpleCNN, ResNet20 ve VGG11 mimarilerinin tamamında yüksek ve tutarlı test doğrulukları ürettiğini göstermektedir. Bu strateji, hem orijinal hem de rastgele karıştırılmış sıralamaya kıyasla daha kararlı bir performans sergileyerek %73,81 ortalama doğruluğa ulaşmıştır.

4.2 Homojen Dağılımın Üstünlüğü

1'li karışım en yüksek ortalama performansı sağlamıştır. Her batch'te tüm sınıflardan örnekler bulunması, gradient güncellemelerinin daha dengeli olmasını sağlamıştır [1].

4.3 Blok Sınıf Sıralamasının Başarısızlığı

Blok sınıf sıralaması, tüm modellerde yaklaşık %10 test doğruluğu ile ciddi bir başarısızlık göstermiştir. Bu durum, derin öğrenme literatüründe catastrophic forgetting [6] olarak tanımlanan mekanizmalarla benzer bir davranış sergilemektedir. Model, bir sınıfı tamamen gördükten sonra diğer sınıfa geçtiğinde, önceki sınıfa ait bilgileri hızla unutmaktadır.

4.4 Ardışık Sınıf Elemanı Sayısının Etkisi

Ardışık olarak sunulan aynı sınıfa ait örnek sayısı arttıkça (1→10→50→100), veri sıralaması giderek mini-blok sınıf yapısına yaklaşmakta ve buna paralel olarak tüm modellerde test doğruluğunda belirgin bir düşüş gözlemlenmektedir.

- **SimpleCNN:** %73,25 → %72,35 → %63,81 → %58,72.
- **ResNet20:** %73,64 → %55,55 → %28,95 → %12,72.
- **VGG11:** %74,54 → %64,98 → %15,79 → %13,85.

4.5 Zorluk Bazlı Sıralamanın Analizi

K2Z ve Z2K stratejileri, sınıflar arası homojen dağılıma sahip olmalarına rağmen, 1’li karışım stratejisinin gerisinde kalmıştır. SimpleCNN modelinde 100’lü karışım stratejisinin dahi gerisinde kalmıştır (100’lü Karışım: %58,72, K2Z 1’li Karışım: %56,72, Z2K 1’li Karışım: %50,00).

- **K2Z:** %56,72 (SimpleCNN), %54,11 (ResNet20), %53,93 (VGG11).
- **Z2K:** %50,00 (SimpleCNN), %43,63 (ResNet20), %47,55 (VGG11).

Genel olarak, "Kolaydan Zora" (K2Z) yaklaşımı, "Zordan Kolaya" (Z2K) yaklaşımına göre daha kararlı ve yüksek bir doğruluk oranı sergilemiştir.

4.6 Model Duyarlılığı

- **SimpleCNN:** İncelenen sıralama stratejileri altında görece olarak daha kararlı sonuçlar üretmiştir.
- **ResNet20:** Orijinal sıralama (%74,23) ve karışık sıralamada (%74,89) en yüksek doğruluk oranına sahipken, karışım seviyesinin artmasından olumsuz etkilenmiştir.
- **VGG11:** Sıralama stratejilerinden ResNet20’e benzer şekilde etkilenmiştir.

5 TARTIŞMA

5.1 Batch Çeşitliliğinin Önemi

Çalışma sonuçları, en iyi performansın “Karışık Sıralama” ve “1’li Karışım” senaryolarında alınması, mini-batch içerisindeki sınıf çeşitliliğinin, stabil bir gradyan inişi için önemli olduğunu doğrulamaktadır. Blok sınıf sıralama ve yüksek bloklu (50’li Karışım/100’lü Karışım) sıralamalarda, model her batch’te sadece tek bir sınıfın özelliklerini görebilmekte ve optimizasyon vektörü sürekli o sınıfın yönüne sapmaktadır. Bu durum, önceki sınıfların tamamen unutulmasına yol açmaktadır.

5.2 Karmaşıklık Sıralamasının Verimsizliği

Curriculum learning literatüründe bildirilen sonuçların aksine, bu çalışmada kullanılan zorluk metriği ve deney koşulları altında K2Z ve Z2K yöntemlerinin tam rastgele yöntemden daha kötü sonuç vermesi ilginçtir.

Bu çalışmada kullanılan zorluk metriği ve kısa eğitim süresi altında curriculum learning [2] beklenen iyileşmeyi sağlayamamıştır. Geliştirilen zorluk metriği sıralama için verimli olmamış olabilir.

6 SINIRLILIKLAR VE GELECEK ÇALIŞMALAR

6.1 Çalışmanın Sınırlılıkları

- Bulgular sadece CIFAR-10 ile sınırlıdır.
- 5 epoch'luk kısa eğitim, başlangıç dinamiğini yakalamak için uygundur ancak uzun vadeli yakınsama ve genelleme açığı üzerindeki etkiyi tam olarak yansıtamayabilir.
- Model çeşitliliği sınırlıdır (SimpleCNN, ResNet20 ve VGG11).
- Zorluk metriği önceden hesaplanmıştır, dinamik değildir.
- Optimizer türü bu çalışmada sabit tutulmuştur.

6.2 Gelecek Çalışmalar

Aşağıdaki çalışmalarla daha aydınlatıcı sonuçlar elde edilebilir.

- Büyük ölçekli veri setlerinin kullanılması.
- Karmaşıklık sıralaması dahil, farklı veri sıralama stratejilerinin kullanılması.
- Model sayısı ve çeşitliliği artırılması.
- Eğitim süresinin artırılması.

7 SONUÇ

Bu çalışma, veri sıralama stratejilerinin derin öğrenme modellerinin performansı üzerindeki etkisini göstermeye çalışmıştır. Yapılan deneyler, maksimum batch içi sınıf çeşitliliğinin (1'li Karışım) daha yüksek test doğruluğu sağladığını, sınıf bazlı blok sıralamanın ise unutma benzeri etkilerle ilişkili ciddi bir performans çöküşü sergilediği gözlemlenmiştir. Curriculum learning literatürünün aksine, zorluk bazlı sıralama stratejileri beklenen performans iyileştirmesini sağlayamamıştır. Elde edilen sonuçlar, derin öğrenme modellerinin eğitimi sırasında veri sıralamasının dikkate alınması gereken önemli bir parametre olduğunu ortaya koymaktadır. Bu sonuçlar, belirtilen eğitim süresi ve deney koşulları altında geçerlidir.

Araştırma ve Yayın Etiği Beyanı (Statement of Research and Publication Ethics)

Bu çalışma, araştırma ve yayın etiği ilkelerine uygun olarak hazırlanmıştır.

Yapay Zekâ (AI) Katkı Beyanı (Artificial Intelligence (AI) Contribution Statement)

Yapay zekâ (AI) araçları araştırma, yazım, düzenleme, veri analizi vb. alanlarda kullanılmıştır.

KAYNAKÇA

- [1] M. Gürbüzbalaban, A. Ozdaglar, and P. Parrilo, "Why random reshuffling beats stochastic gradient descent," Mathematical Programming, 2021. <https://doi.org/10.1007/s10107-019-01440-w>.
- [2] Y. Bengio, J. Louradour, R. Collobert, and J. Weston, "Curriculum learning," Proceedings of the 26th International Conference on Machine Learning (ICML), 2009. <https://doi.org/10.1145/1553374.1553380>.
- [3] D. Weinshall, G. Cohen, and D. Amir, "Curriculum learning by transfer learning: Theory and experiments with deep networks," Proceedings of the 35th International Conference on Machine Learning (ICML), 2018. <https://doi.org/10.48550/arXiv.1802.03796>.
- [4] G. Hacohen and D. Weinshall, "On the power of curriculum learning in training deep networks," Proceedings of the 36th International Conference on Machine Learning (PMLR), 2019. <https://doi.org/10.48550/arXiv.1904.03626>.

- [5] A. Krizhevsky, "Learning multiple layers of features from tiny images," University of Toronto Technical Report, 2009.
- [6] M. Toneva, A. Sordoni, et al., "An empirical study of example forgetting during deep neural network learning," International Conference on Learning Representations (ICLR), 2019.
<https://doi.org/10.48550/arXiv.1812.05159>



SELFIE2BFP: A DEEP LEARNING APPROACH FOR BODY FAT PERCENTAGE ESTIMATION FROM FACIAL IMAGES

Yusuf UZ¹ , Zafer SERİN¹ , Ugur YUZGEC^{1,*}

¹ Bilecik Şeyh Edebali University, Computer Engineering Department, Bilecik, TÜRKİYE

* **Corresponding Author:** ugur.yuzgec@bilecik.edu.tr

ABSTRACT

This study investigates the feasibility of estimating body fat percentage (BFP) using only facial images through deep learning techniques and mathematical modeling. A multi-stage prediction model was developed, which first extracts gender, age, and body mass index (BMI) from facial images using pre-trained deep learning models, and subsequently applies a gender- and age-adjusted BFP estimation formula. The results indicate that the facial image quality, expression, and lighting significantly affect the performance of deep learning models, thereby influencing the overall prediction accuracy. Despite the limitations in dataset balance and model generalizability, this study demonstrated that facial features can provide meaningful indicators of body composition. These findings suggest that facial image analysis combined with Artificial Intelligence (AI) and mathematical models can serve as a noninvasive and accessible tool for preliminary health assessments.

Keywords: Body Fat Percentage, Deep Learning, Facial Image Analysis, Artificial Intelligence, Obesity, BMI Estimation.

1 INTRODUCTION

Obesity has become a global health crisis that significantly affects millions of people worldwide and contributes to a wide range of chronic diseases such as cardiovascular disorders, diabetes, and hypertension. According to recent statistics, one in eight people globally lives with obesity, and it is projected that by 2035, half of the world's population will face obesity or overweight-related health issues [1], [2], [3]. In adult males, 15–18% of body fat is considered normal, whereas in females, the healthy range is 20–25%. Obesity occurs when these values exceed 25% in men and 30% in women. As illustrated in Figure 1, obesity rates have been rising rapidly, with adult obesity more than doubling, and adolescent obesity nearly quadrupling since 1990.

Accurate assessment of obesity is critical for effective health management, and Body Fat Percentage (BFP) is a more reliable indicator of body composition than traditional metrics such as Body Mass Index (BMI). While BMI is widely used due to its simplicity, it fails to distinguish between fat mass and lean body mass, often leading to misleading interpretations, particularly for individuals with high muscle mass [4]. Therefore, developing accessible, noninvasive, and cost-effective methods for estimating BFP is essential for both individual health monitoring and large-scale public health interventions.

Obesity has significant negative impacts on both the quality and duration of life, while also increasing the risk of various serious health complications. Extensive research has demonstrated a strong causal relationship between obesity and chronic diseases such as cardiovascular disorders [5], type 2 diabetes [6], and hypertension [7]. These findings underscore the critical role of obesity in improving overall public health outcomes.

Several recent studies have explored the use of artificial intelligence, machine learning, and image analysis techniques to estimate body fat percentage (BFP) in a more accessible and noninvasive manner.

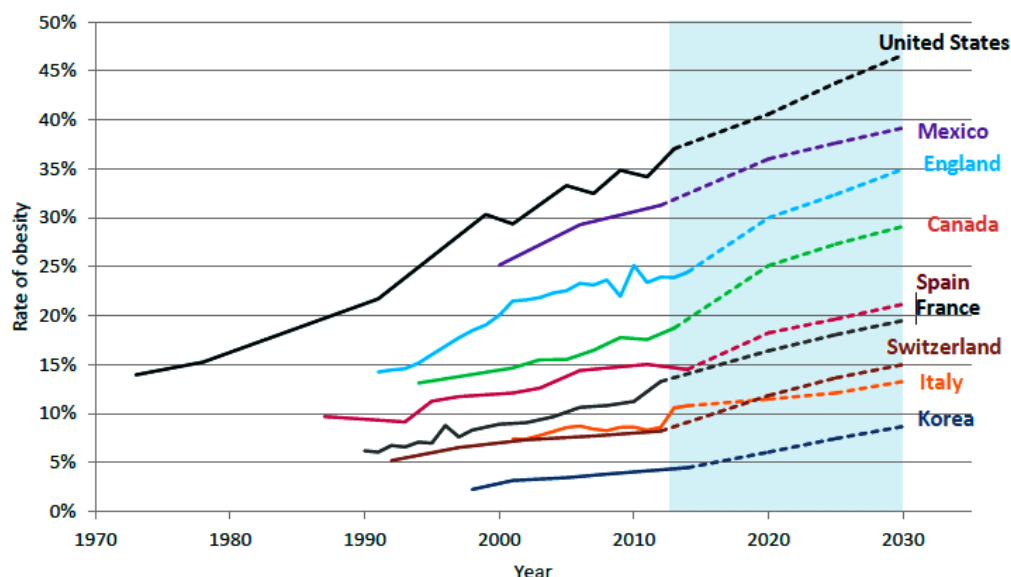


Figure 1. Global obesity trends by country (1970–2030) [8]

These studies demonstrate the growing interest in leveraging computational models to provide cost-effective and user-friendly alternatives to the traditional BFP measurement methods.

A survey by Uçar et al. [9] utilized electrocardiography (ECG) signals as input features for gender-based BFP prediction models. The researchers applied various filters to extract the QRS components within different frequency ranges, generating a total of nine ECG signals per subject. A set of 25 time-domain features, including age, weight, height, and BMI, was extracted and combined with additional demographic and anthropometric data. Spearman's feature selection method was applied to enhance the performance of the model. The resulting models demonstrated high correlation coefficients of 0.94 for males, 0.93 for females, and 0.91 overall, indicating the potential of ECG-based BFP estimation when combined with gender-specific modeling approaches.

In another study by Uçar et al. [10], a hybrid machine learning approach was proposed for estimating BFP using anthropometric measurements. The system was trained on a real-world dataset and evaluated using a correlation analysis. The results showed that the BFP could be predicted with a correlation coefficient of 0.788 using only a single anthropometric measurement. This finding suggests that simplified models can yield meaningful results, making this method suitable for practical applications without the need for complex measurement devices.

Kupusinac et al. focused on predicting BFP using artificial neural networks (ANNs), with inputs including gender, age, and BMI [11]. The dataset consisted of 2,755 individuals, with ages ranging from 18 to 88 years and BMI values between 16.60 and 64.60 kg/m². The BFP values were obtained using bioelectrical impedance measurements. The ANN-based model achieved a

prediction accuracy of 80.43%, demonstrating the effectiveness of neural networks in capturing the complex relationships between basic demographic and physical parameters and body fat levels.

Finally, in a study by Alves et al., a sex-based deep learning and computer vision approach was introduced to estimate BFP from 2D images captured using smartphones [12]. The method leverages anatomical knowledge to identify key body landmarks and estimate body segment dimensions, such as arm, waist, thigh, and hip circumferences. These measurements were then used to infer the body fat percentage, offering a low-cost and scalable solution for body composition analysis.

These studies collectively highlight the potential of AI and image-based modeling in estimating body fat percentage, with most approaches relying on body measurements or specialized sensors. A more recent trend involves leveraging facial images for health-related predictions, including age, sex, BMI, and even cardiovascular risk factors, suggesting that facial features contain subtle but meaningful information about an individual's overall health and body composition. However, to the best of our knowledge, there are currently no studies that directly estimate the BFP solely from facial images using deep learning models. This represents a significant research gap, particularly in the context of developing user-friendly and mobile-accessible tools for preliminary health assessments.

In this study, we aimed to address this gap by proposing a novel deep learning-based framework, Selfie2BFP, which estimates body fat percentage using only a single facial image. Our approach combines pre-trained deep learning models for gender, age, and BMI prediction with a validated BFP estimation formula. Unlike previous studies that relied on specialized hardware or extensive body measurements, our method offers a non-invasive, accessible, and efficient way to assess body fat percentage.

2 METHODOLOGY

This study proposes Selfie2BFP, a deep-learning-based framework for estimating body fat percentage (BFP) from a single facial image. The methodology consists of a sequential pipeline that first extracts demographic and anthropometric features (gender, age, and BMI) from the input image using pre-trained deep learning models and then applies a validated BFP estimation formula. The overall architecture is illustrated in Figure 2.

2.1 Overview of the Proposed Framework

The proposed framework operates in a cascaded manner as follows:

1. Input: Single facial image (e.g., a selfie).
2. Feature Extraction: The image is processed using three separate deep learning models to predict an individual's gender, age, and BMI.
3. BFP Estimation: The predicted values are used as inputs to the formula of Deurenberg et al. [13] to compute the estimated BFP.
4. Output: The estimated BFP is presented to the user, along with categorical interpretation (e.g., "Normal", "High") based on age- and gender-specific thresholds [14].

This approach eliminates the need for specialized equipment or manual measurements and offers a scalable and mobile-accessible solution for preliminary body composition assessment.

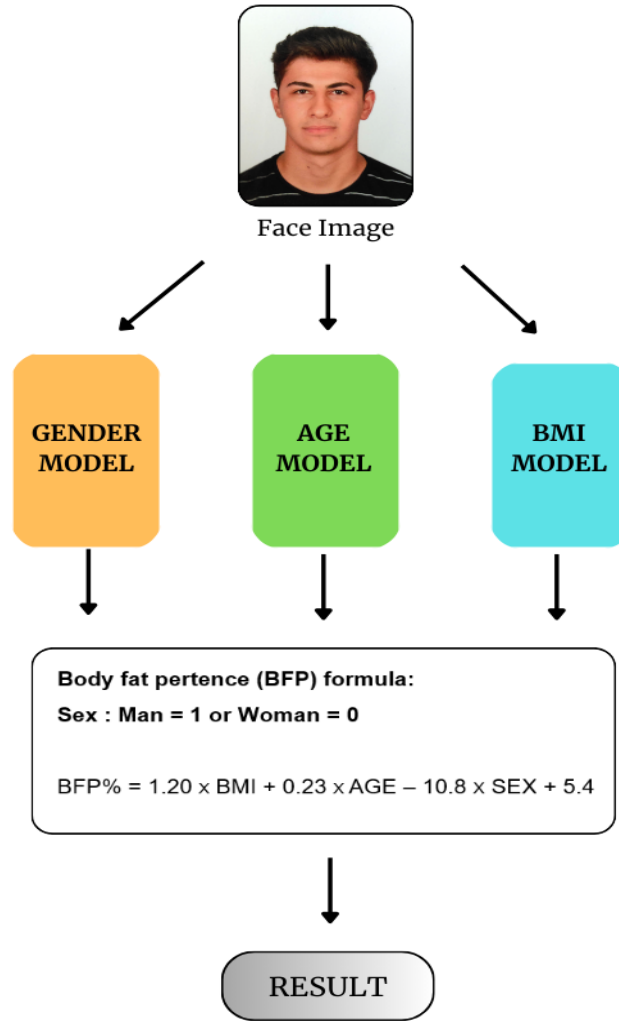


Figure 2. Proposed Selfie2BFP model

2.2 Deep Learning Models for Facial Feature Prediction

Three state-of-the-art deep learning models were selected and integrated into the pipeline because of their high performance on large-scale datasets and availability as pre-trained models.

- **Gender Prediction:** The SmallerVGGNet architecture implemented in Keras was used for binary gender classification. The model was trained on 2,200 facial images (80% training and 20% validation) and achieved 96% and 90% training and validation accuracies, respectively. The input size was $96 \times 96 \times 3$, and the final layer used a sigmoid activation function for binary output [15].
- **Age Prediction:** An SE-ResNeXt50-32x4d model pre-trained on the APPA-REAL dataset (7,591 images) was employed. This architecture combines the ResNeXt structure with Squeeze-and-Excitation (SE) blocks to enhance feature representation. The model outputs a 101-class distribution (ages 0–100) and achieves a Mean Absolute Error (MAE) of 4.800 on the validation set [16].
- **BMI Prediction:** A Vision Transformer (ViT-H_14) model, pre-trained on ImageNet1K and fine-tuned on a private dataset of 4,207 facial images, was used. The model processed the image in 14×14 patches and used a 32-layer transformer encoder. A custom BMIHead module (five fully connected layers with GELU activation and dropout) is added to the final feature vector to regress the BMI value. The base ViT weights were frozen during training to preserve the learned visual representations [17].

2.3 Gender Prediction using SmallerVGGNet

For gender classification from facial images, this study employs a lightweight Convolutional Neural Network (CNN) architecture known as SmallerVGGNet, implemented using the Keras deep-learning framework. The model is specifically designed for binary classification tasks and is optimized for real-time performance and deployment in resource-constrained systems. It consists of 11 convolutional layers, three max-pooling layers, two fully connected (dense) layers, a flattened layer, and additional regularization components including Batch Normalization and Dropout layers.

The input layer accepts facial images resized to 96×96 pixels with three-color channels (RGB). The initial convolutional layer applies 32 filters, followed by layers with 64 and 128 filters in subsequent blocks. Each convolutional operation is followed by a ReLU activation function and Batch Normalization, which stabilize the learning process and accelerate convergence by reducing the internal covariate shift. MaxPooling2D layers are strategically placed to downsample feature maps, reducing the spatial dimensions and computational load without significant loss of critical information.

After the convolutional base, the feature maps were flattened into a one-dimensional vector and passed through a dense layer with 1,024 neurons. This was followed by a final 2-neuron Dense layer with a Sigmoid activation function, enabling binary classification (male/female). To prevent overfitting during training, dropout layers with an appropriate dropout rate were incorporated at key stages of the network, randomly setting a fraction of the input units to zero during training.

The model was trained on a dataset of 2,200 facial images, with 80% training and 20% validation splits. It achieved a training accuracy of 96% and a validation accuracy of 90%, demonstrating a strong generalization capability for gender prediction. Due to its compact architecture and high efficiency, SmallerVGGNet is well-suited for integration into real-time applications and web-based systems. The model was used in its pre-trained form within the Selfie2BFP pipeline to provide reliable gender estimates as inputs for subsequent body fat percentage calculations.

2.4 Age Prediction with SE-ResNeXt50-32x4d

For age estimation from facial images, this study employed the SE-ResNeXt50-32x4d architecture, a deep convolutional neural network that combines the strengths of ResNeXt and Squeeze-and-Excitation (SE) blocks. This model is based on the ResNeXt framework, which utilizes a “split-transform-merge” strategy through grouped convolutions to increase cardinality, thereby enabling the network to learn more diverse and discriminative features via multiple parallel pathways. The “50” in the name refers to the total number of layers, while “32x4d” indicates 32 groups, each processing 4-dimensional filter channels.

A key enhancement in this architecture is the integration of Squeeze-and-Excitation (SE) blocks, which adaptively recalibrate channel-wise feature responses by explicitly modeling inter-channel dependencies. These blocks use global average pooling to generate channel-wise statistics, followed by a bottleneck mechanism that learns the channel-specific importance weights. This allows the model to emphasize informative facial features related to aging, such as wrinkles, skin texture, and facial sagging, while suppressing less-relevant regions.

The model was pre-trained on the ImageNet dataset and further fine-tuned on the APPA-REAL dataset, which contained 7,591 facial images annotated with both chronological and perceived age labels, covering a broad age spectrum. This dataset enables robust training for real-world age distributions. The final classification layer was restructured to produce a 101-class output, corresponding to ages ranging from 0 to 100. Additionally, an adaptive average pooling layer was incorporated to ensure compatibility with the variable input dimensions, thereby enhancing model flexibility.

Model performance was evaluated using the Mean Absolute Error (MAE) metric, which measures the average deviation between predicted and actual ages. SE-ResNeXt50-32x4d achieved an MAE of 4.800 on the training dataset and 4.51 on the evaluation dataset used in this study, demonstrating its effectiveness in capturing age-related facial patterns. The model was implemented in PyTorch and integrated into a pipeline to provide reliable age estimates as inputs for subsequent BFP calculations.

2.5 BMI Prediction Using Vision Transformer (ViT-H_14)

Body Mass Index (BMI) prediction was performed using a Vision Transformer (ViT-H_14) architecture, representing a modern attention-based alternative to convolutional networks. Unlike CNNs, which process images through local receptive fields, ViT treats an image as a sequence of patches and applies self-attention mechanisms to model the global dependencies across the entire face.

The model is based on the ViT-H_14 variant, pre-trained on ImageNet1K_SWAG_E2E_V1 weights, ensuring strong generalization capabilities. The input facial images were divided into 14×14 patches, each linearly embedded into a fixed-dimensional vector. These patch embeddings, along with a learnable class token, are fed into a deep transformer encoder consisting of approximately 32 layers, each containing multihead self-attention and feed-forward neural network modules. This structure enabled the model to capture both fine-grained local features (e.g., facial fullness and jawline definition) and holistic facial proportions associated with BMI.

To adapt ViT for regression-based BMI prediction, a custom BMIHead module was attached to the output of the class token. This module consists of five fully connected layers: the first reduces the 1280-dimensional feature vector to 640 dimensions, followed by progressive downsampling to 320, 160, 80, and finally to one dimension (the predicted BMI value). Each layer (except the last) applies the GELU activation function and includes a 50% dropout rate to prevent overfitting and enhance the generalization.

Crucially, the weights of the base ViT model were frozen during training, ensuring that the rich visual representations learned from large-scale datasets were preserved. Only the BMIHead module was trained on a private dataset of 4,207 facial images with the corresponding BMI labels. This transfer learning strategy allows efficient and effective fine-tuning with limited domain-specific data.

The model achieved a Mean Absolute Error (MAE) of 6.10 on the Face-to-BMI dataset, with a lower error for male subjects (5.84) compared to females (7.13), indicating potential gender-related biases in facial-BMI correlations. Despite this, the ViT-based approach demonstrates strong potential for noninvasive BMI estimation from facial cues.

2.6 Body Fat Percentage (BFP) Estimation

The predicted gender, age, and BMI values were used as inputs to the Deurenberg et al. [13] formula for estimating the BFP. This formula has been widely validated in diverse populations and demonstrates a high coefficient of determination ($R^2 = 0.79$), indicating that 79% of the variance in body fat percentage is explained by BMI, age, and gender. A standard error of estimate (SEE) of 4.0% suggests clinically acceptable prediction accuracy, comparable to other indirect methods such as skinfold thickness and bioelectrical impedance analysis. Given that the dataset consists of adult individuals, the adult-specific formula (Equation 1) was applied:

$$BFP = (1.20 \times BMI) + (0.23 \times A) - (10.8 \times G) - 5.4 \quad (1)$$

where G is coded as 1 for males and 0 for females, A represents age. This formula has been validated in diverse populations and provides a reliable estimate of body fat percentage when direct measurement methods are unavailable. The estimated BFP is then categorized into "Low", "Ideal", "Normal", or "High" ranges based on age- and gender-specific thresholds from the U.S. Army Standards [17] (see Tables 1 and 2).

Table 1. Age-based categorized body fat percentage table for men [17].

Age Range	Low (%)	Ideal (%)	Normal (%)	High (%)
18 - 20	2.0 - 3.9	6.2 - 12.5	14.3 - 18.9	20.2 +
21 - 25	2.5 - 4.9	7.3 - 13.6	15.4 - 21.2	22.3 +
26 - 30	3.5 - 8.4	10.6 - 16.4	18.1 - 22.3	23.4 +
31 - 35	4.5 - 9.4	11.7 - 17.5	19.2 - 23.4	24.5 +
36 - 40	5.6 - 10.5	12.7 - 18.6	20.2 - 24.4	25.6 +
41 - 45	6.7 - 13.8	15.9 - 21.3	22.8 - 25.6	27.6 +
46 - 50	7.7 - 14.8	16.9 - 22.4	23.9 - 27.7	28.7 +
51 - 55	8.8 - 15.9	18.0 - 23.4	25.0 - 28.7	29.7 +
56 +	9.9 - 17.0	19.1 - 24.5	26.0 - 30.8	31.6 +

Table 2. Age-based categorized body fat percentage table for women [17].

Age Range	Low (%)	Ideal (%)	Normal (%)	High (%)
18 - 20	11.3 - 15.7	17.7 - 21.5	23.2 - 29.0	30.2 +
21 - 25	11.9 - 18.4	20.3 - 23.8	25.5 - 29.6	30.8 +
26 - 30	12.5 - 19.0	20.9 - 24.6	26.1 - 31.5	32.5 +
31 - 35	13.2 - 19.6	21.5 - 25.1	26.7 - 32.1	33.2 +
36 - 40	13.8 - 22.2	24.0 - 27.3	28.8 - 32.7	33.8 +
41 - 45	14.4 - 22.8	24.6 - 27.9	29.4 - 34.4	35.4 +
46 - 50	15.0 - 23.4	25.2 - 28.6	30.1 - 35.0	36.0 +

2.7 Dataset for Model Evaluation

The performance of the deep learning models was evaluated on the Face-to-BMI dataset [18], which contains 1,544 facial images labeled with gender, age, and BMI values. The dataset was imbalanced, with approximately 80% male and 20% female participants. This imbalance is acknowledged as a limitation and may contribute to performance disparities between genders in the results. Figure 3 shows some facial images from this dataset.

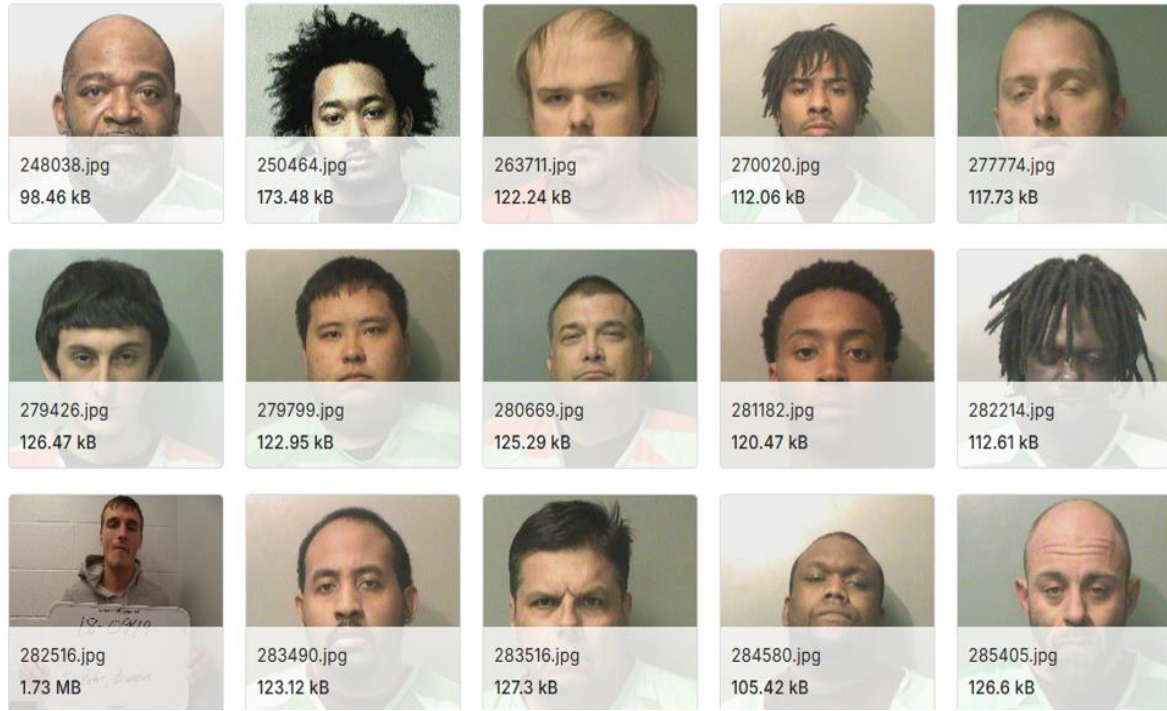


Figure 3. Some face images from Face-to-BMI Dataset [18]

3 RESULTS AND DISCUSSION

The proposed Selfie2BFP framework was evaluated on a dataset of 1,544 facial images (Face-to-BMI dataset) to assess the performance of its sequential deep learning models and the overall feasibility of estimating body fat percentage (BFP) from facial cues. The results highlight both the potential and limitations of this approach, particularly with respect to gender-based performance disparities and error propagation in the prediction pipeline.

3.1 Performance of Facial Attribute Prediction Models

The first stage of the evaluation focused on the individual deep learning models used to predict gender, age, and BMI from facial images. The SmallerVGGNet model achieved an overall accuracy of 83.14% (Table 3). However, a significant performance gap was observed between genders; while the model correctly classified 94.97% of male subjects, its accuracy for female subjects was only 37.00%. This substantial disparity is primarily attributed to the class imbalance in the evaluation dataset, which consists of approximately 80% male and 20% female participants. Such an imbalance can lead to a model bias, where the classifier becomes overly optimized for the majority class (male), resulting in poor generalization for underrepresented groups. This finding underscores the critical importance of balanced and diverse training datasets for facial analysis.

Table 3. Gender prediction model (SmallerVGGNet) performance results for Face-to-BMI dataset.

Gender	Total Number of People	Correct Predictions	Incorrect Predictions	Gender Accuracy (%)
Male	1233	1171	62	94.97
Female	300	111	189	37.00
Overall	1533	1282	251	83.14

The SE-ResNeXt50-32x4d model demonstrated a Mean Absolute Error (MAE) of 4.51 across the entire dataset (Table 4). The error was lower for the male subjects (MAE=4.33) than for the female subjects (MAE=5.27). This suggests that the ability of the model to extract age-related facial features (e.g., wrinkles, skin texture) may be less effective for female faces, potentially due to differences in facial morphology, makeup usage, or lighting sensitivity. The MAE value of 4.51 is comparable to state-of-the-art age estimation models, indicates robust performance, although further refinement for female subjects is required.

Table 4. Age prediction model (SE-ResNeXt50-32x4d) performance results for Face-to-BMI dataset.

Gender	Total Number of People	MAE
Male	1233	4.33
Female	300	5.27
Overall	1533	4.51

The Vision Transformer (ViT-H_14) model achieved an overall MAE of 6.10 (Table 5). Similar to the other models, a gender-based performance gap was evident, with a lower error for males (MAE=5.84) and a higher error for females (MAE=7.13). This discrepancy may arise from the fact that facial adiposity correlates differently with BMI across genders, and the model may not have fully captured the subtler facial cues associated with BMI in women. The relatively high MAE, particularly for female subjects, indicates that BMI estimation from facial images remains a challenging task.

Table 5. BMI prediction model (ViT-H_14) performance results for Face-to-BMI dataset.


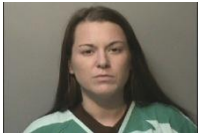
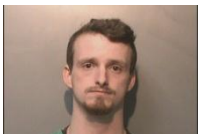


Gender	Total Number of People	MAE
Male	1233	5.84
Female	300	7.13
Overall	1533	6.10

3.2 Body Fat Percentage Estimation and Error Analysis

The final BFP estimates were derived by applying the predicted gender, age, and BMI values to Deurenberg's formula. Because the ground truth BFP values were not available for the dataset, direct calculation of the BFP MAE was not possible. However, by analyzing the error propagation through the pipeline, an estimated overall MAE of approximately 8% for the BFP prediction can be inferred. This estimation is based on the cumulative errors from the individual models and the standard error of estimate (SEE = 4.0%) of Deurenberg's formula.






Qualitative analysis of the predictions was conducted using the sample results (Tables 6 and 7). Table 6 presents cases where the predicted BFP values are close to expected ranges based on the real BMI and age. For instance, in a male subject with a real BMI of 39.5, the predicted BFP was 42.6%, which was reasonably close to the expected value of 43.6%. These results demonstrate the potential of the framework when underlying models perform accurately.

Table 6. Examples of BFP predictions with high agreement to expected values.

Image	Real Gender	Prediction Gender	Real Age	Prediction Age	Real BMI	Prediction BMI	Real BFP	Prediction BFP
	Male	Male	54	52	39.5	39.1	%43.6	%42.6
	Female	Female	27	24	24.8	30.2	%30.5	%36.5
	Male	Male	25	30	22.1	25.0	%16.1	%20.1
	Male	Male	31	28	32.8	37.0	%30.3	%34.6
	Female	Female	33	29	27.3	34.9	%36	%43.1

In contrast, Table 7 shows cases with significant deviations from the expected values. For example, a male subject with a real BMI of 16.0 (indicating underweight) was predicted to have a BMI of 29.6 (obese), leading to a BFP prediction of 23.4% instead of 8.1%. Such large errors typically result from cascading failures. For instance, a minor error in age or significant error in BMI prediction can be amplified by the BFP formula, leading to clinically misleading results.

Table 7. Examples of BFP Predictions with Significant Deviation from Expected Values.

Image	Real Gender	Prediction Gender	Real Age	Prediction Age	Real BMI	Prediction BMI	Real BFP	Prediction BFP
	Male	Male	22	17	16.0	29.6	%8.1	%23.4
	Female	Female	37	32	17.7	31.2	%24.3	%39.3
	Male	Male	20	18	32.6	41.1	%27.5	%37.2
	Male	Male	48	40	29.9	30.2	%30.7	%36.2
	Female	Male	25	22	19.7	25.1	%24.0	%19.1

4 CONCLUSIONS

This study presents Selfie2BFP, a novel deep-learning-based framework for estimating body fat percentage (BFP) using only a single facial image. By integrating pre-trained models for gender, age, and BMI prediction with the Deurenberg et al. formula, the proposed system offers a noninvasive, accessible, and user-friendly approach to preliminary body composition assessment. The results demonstrated the feasibility of deriving meaningful health indicators from facial images, positioning Selfie2BFP as a promising tool for large-scale health screening and personal wellness monitoring.

Despite its potential, its current implementation has several limitations. First, the performance of the AI models, particularly for gender and BMI prediction, was significantly affected by the class imbalance in the evaluation dataset, which consisted of approximately 80% male and 20% female subjects. This imbalance leads to lower accuracy for female users, raising concerns about model fairness and generalizability across demographic groups. Second, errors in the intermediate predictions (gender, age, and BMI) were propagated through the pipeline and amplified by the BFP estimation formula, resulting in an estimated overall MAE of approximately 8% for the BFP. Third, the accuracy of the system is sensitive to the image quality, facial

expression, and lighting conditions, which can lead to unreliable predictions in suboptimal capture scenarios.

To address these limitations and enhance the robustness of the system, several directions for future research were proposed. First, the model should be retrained and evaluated on a larger, balanced, and diverse dataset that includes equal representation across gender, age, and ethnic groups, to ensure equitable performance. Second, end-to-end training of a unified deep learning model, trained directly on facial images and BFP labels (if available), could reduce error propagation and improve the overall accuracy. Third, the integration of additional input modalities, such as multiple facial views or metadata (e.g., height and activity level), can refine the predictions. Fourth, real-time feedback mechanisms and personalized health recommendations (e.g., diet or exercise suggestions) can be added to increase user engagement. Finally, the system can be extended to mobile platforms and evaluated in real-world settings to assess its long-term impact on health behavior.

Acknowledgements

This study was funded by TÜBİTAK under the 2209-A program. We would like to thank TÜBİTAK for their valuable contributions to this study.

Declaration of Competing Interest

The authors declare that they have no known competing financial interests or personal relationships that could have influenced the work reported in this paper.

Statement of Research and Publication Ethics

This study has been prepared in accordance with the principles of research and publication ethics.

Contributions of the Authors

Yusuf UZ: Research, Conceptualization, Methodology development, Software development, Writing– original draft.

Zafer SERİN: Formal analysis, Research, Software development, Supervision.

Uğur YÜZGEÇ: Project management, Supervision, Formal analysis, Writing–review and editing.

Data Availability

Gender prediction model: <https://github.com/arunponnusamy/gender-detection-keras/tree/master>

Age prediction model: <https://github.com/yu4u/age-estimation-pytorch>

Body mass index (BMI) prediction model: <https://github.com/liujie-zheng/face-to-bmi-vit>

Face to BMI datasets: <https://www.kaggle.com/datasets/gaikwadvishal114/face-to-bmi>

Figure 2 is a schematic diagram of the proposed Selfie2BFP model. The facial image shown in the "Face Image" block is a photograph of the first author, Yusuf Uz, used with personal consent for scientific publication. Figure 3 includes sample facial images from the publicly available Face-to-BMI dataset [18], which can be used for academic purposes under its open license.

REFERENCES

- [1] Ma, H., Wang, M., Qin, C., Shi, Y., Mandizadza, O. O., Ni, H., and Ji, C., “Trends in the burden of chronic diseases attributable to diet-related risk factors from 1990 to 2021 and the global projections through 2030: a population-based study,” *Frontiers in Nutrition*, vol. 12, p. 1570321, 2025.
- [2] Dong, C., Ji, Y., Fu, Z., Qi, Y., Yi, T., Yang, Y., Sun, Y., and Sun, H., “Precision management in chronic disease: An AI empowered perspective on medicine-engineering crossover,” *iScience*, vol. 28, no. 3, 2025.
- [3] Li, H., Liang, L., Song, Z., and Li, Y., “Global, regional, and national burden of cardiovascular disease attributable to high body mass index from 1990 to 2021 and projection to 2045,” *Frontiers in Endocrinology*, vol. 16, p. 1546176, 2025.
- [4] Yaemsiri, S., Slining, M. M., and Agarwal, S. K., “Perceived weight status, overweight diagnosis, and weight control among U.S. adults: NHANES 2003–2008 study,” *International Journal of Obesity*, vol. 35, pp. 1063–1070, 2011.
- [5] Saliba, L. J., and Maffett, S., “Hypertensive heart disease and obesity: A review,” *Heart Failure Clinics*, vol. 15, no. 4, pp. 509–517, 2019.
- [6] Klein, S., Gastaldelli, A., Yki-Järvinen, H., and Scherer, P. E., “Why does obesity cause diabetes?” *Cell Metabolism*, vol. 34, no. 1, pp. 11–20, 2022.
- [7] Jiang, S. Z., Lu, W., Zong, X. F., Ruan, H. Y., and Liu, Y., “Obesity and hypertension,” *Experimental and Therapeutic Medicine*, vol. 12, no. 4, pp. 2395–2399, 2016.
- [8] Lee, M., “Research trends in obesity & obesogenic environments in Korea,” *Nutrition Research and Practice*, vol. 13, no. 6, pp. 461–472, 2019.
- [9] Uçar, M. K., Ucar, Z., Uçar, K., Akman, M., and Bozkurt, M. R., “Determination of body fat percentage by electrocardiography signal with gender based artificial intelligence,” *Biomedical Signal Processing and Control*, vol. 68, p. 102650, 2021.
- [10] Uçar, M. K., Ucar, Z., Köksal, F., and Daldal, N., “Estimation of body fat percentage using hybrid machine learning algorithms,” *Measurement*, vol. 167, p. 108173, 2021.
- [11] Kupusinac, A., Stokić, E., and Doroslovački, R., “Predicting body fat percentage based on gender, age and BMI by using artificial neural networks,” *Computer Methods and Programs in Biomedicine*, vol. 113, no. 2, pp. 610–619, 2014.
- [12] Alves, S. S., Ohata, E. F., Junior, P. C. S., Barroso, C. B., Nascimento, N. M., Loureiro, L. L., and Rebouças Filho, P. P., “Sex-based approach to estimate human body fat percentage from 2D camera images with deep learning and machine learning,” *Measurement*, p. 113213, 2023.
- [13] Deurenberg, P., Weststrate, J. A., and Seidell, J. C., “Body mass index as a measure of body fatness: age- and sex-specific prediction formulas,” *British Journal of Nutrition*, vol. 65, no. 2, pp. 105–114, 1991.
- [14] U.S. Department of the Army, Army Regulation 600-9: The Army Body Composition Program, 28 June 2013. [Online]. [Accessed: Apr. 5, 2025].
- [15] Rosebrock, A., “Keras and Convolutional Neural Networks (CNNs),” *PyImageSearch*, Apr. 16, 2018. [Online]. Available: <https://pyimagesearch.com/2018/04/16/keras-and-convolutional-neural-networks-cnns/>
- [16] Wang, K., Niu, X., Dou, Y., Xie, D., and Yang, T., “A siamese network with adaptive gated feature fusion for individual knee OA features grades prediction,” *Scientific Reports*, vol. 11, no. 1, p. 16833, 2021.
- [17] Ambita, A. A. E., Boquio, E. N. V., and Naval, P. C. Jr., “Covit-gan: Vision transformer for covid-19 detection in CT scan images with self-attention GAN for data augmentation,” in *Proc. Int. Conf. Artificial Neural Networks*, pp. 587–598, Cham: Springer International Publishing, Sep. 2021.
- [18] Face to BMI datasets. Accessed: Nov. 2, 2023. [Online]. Available: <https://www.kaggle.com/datasets/gaikwadvishal114/face-to-bmi>

Enerji ve Sürdürülebilirlik Açısından Geopolimer Tuğla Teknolojisi

Aykut TUNTAŞ¹ , Namık YALTAY^{1,*} 

¹ Van Yüzüncü Yıl Üniversitesi, İnşaat Mühendisliği Bölümü, Van, Türkiye

* Sorumlu Yazar: namikyaltay@yyu.edu.tr

ÖZET

Günümüzde inşaat sektörü, küresel karbon salımlarının ve enerji tüketiminin en büyük kaynaklarından biri olarak bilinmekte; özellikle yapı malzemelerinin üretim süreçleri, yüksek sıcaklık gereksinimleri ve yoğun fosil yakıt kullanımı nedeniyle çevresel açıdan ciddi riskler oluşturmaktadır. Pişmiş tuğla üretimi de yoğun enerji harcamasından dolayı sürdürülebilir gözükmemektedir. Geleneksel pişmiş tuğlaların üretimi yüksek sıcaklıkları gerektirdiği için bu süreç hem yüksek enerji tüketimine hem de önemli miktarda CO₂ emisyonuna yol açmaktadır. Bu durum, küresel ölçekte sürdürülebilir geopolimer tuğla üretimine olan ilgiyi artırmış ve bu yapı malzemeleri öne çıkan yeni bir çözüm olarak dikkat çekmiştir. Geopolimer tuğlaların pişmiş tuğlalara kıyasla daha düşük sıcaklıklarda üretilmesi enerji verimliliği açısından daha sürdürülebilir bir yöntemdir. Geopolimer tuğla üretimi aynı zamanda çevresel atık yönetimi açısından da önemli bir kazanım sunmaktadır. Bu tuğlalar yüksek silika ve alümina içerikli endüstriyel yan ürünlerin ve atıkların alkali aktivasyon yoluyla kimyasal olarak bağlanmasıyla elde edilmektedir. Endüstriyel yan ürünlerin yapı malzemesine dönüştürülmesi doğal kil tüketimini azaltmakta, depolama alanı ihtiyacını düşürmekte ve çimento kullanımının ortadan kalkmasıyla karbon ayak izini düşürmektedir. Tüm bu artılardan dolayı bu alanda çok sayıda çalışma yapılmıştır. Bu araştırma, geopolimer tuğla üretimine ait literatürdeki çeşitli deneysel çalışmaları inceleyip derlenmesine odaklanmaktadır. Birçok araştırmacı, kür sıcaklığı, aktivatör molaritesi, kalıplama basıncı ve Si/Al oranının geopolimer tuğlaların mekanik ve fiziksel performansı üzerinde kritik rol oynadığını ortaya koymuştur. Ancak düşük molarite ve oda sıcaklığında kürleme işlemiyle dahi tuğlalar kabul edilebilir mekanik özellikler göstermiştir. Tüm çalışmaların sonucu olarak; atık malzemelerin değerlendirilmesi, pişmiş tuğlaya kıyasla daha düşük sıcaklıklı kür işlemleri, azaltılmış karbon salınımı ve daha iyi termal performans gibi olumlu yönleriyle geopolimer tuğlalar hem çevresel hem de ekonomik açıdan gelecek vaat eden bir yapı malzemesi olmuştur.

Anahtar Kelimeler: Sürdürülebilirlik, Geopolimer, Tuğla, Karbon Emisyonu, Enerji Verimliliği

1 GİRİŞ

Günümüzde inşaat sektörü, enerji tüketimi ve çevresel etkiler bakımından dünyadaki karbon salınımının baş aktörlerinden biridir. Özellikle yapı malzemelerinin üretimi sırasında yüksek miktarda enerji harcanmakta ve sera gazı emisyonları açığa çıkmaktadır [1]. Pişmiş tuğla ve Geleneksel kiremit üretimi de yüksek sıcaklıklarda fırınlama gerektirdiği için yoğun enerji tüketmekte ve önemli ölçüde karbon salımı ile çevresel zararlara yol açmaktadır [2]. Bu bağlamda geopolimer tuğla üretimi, atık malzemeleri değerlendirerek daha düşük enerjiyle tuğla üretme

potansiyeliyle dikkat çekmektedir. Bu çalışmada, literatürdeki güncel bulgular ışığında geopolimer tuğlaların enerji verimliliği ve çevresel sürdürülebilirlik avantajları ele alınacak; Farklı kaynaklardan elde edilen geopolimer tuğla üretim çalışmaları derlenerek sunulacaktır.

1.1 Geopolimer Tuğla Teknolojisinin Enerji ve Sürdürülebilirlik Açısından Önemi

Geopolimer tuğlalar, alkali aktivasyon yöntemiyle, genellikle uçucu kül, cüruf, seramik atığı, kırmızı çamur, bor atığı gibi yüksek silika ve alümina içeren endüstriyel yan ürünlerin kimyasal bağlanması sonucu oluşan yeni nesil yapı malzemeleridir. Bu tuğlaların en önemli avantajlarından biri, üretimleri sırasında yüksek sıcaklıklarda fırınlamaya ihtiyaç duymamalarıdır [3]. Örneğin, Zeybek (2009) tarafından yapılan bir çalışmada, Class F tipi uçucu külden üretilen geopolimer tuğlaların 60°C sıcaklıkta 24 saatlik kürleme ile optimum 45 MPa basınç dayanımına ulaştığı rapor edilmiştir [4]. Bu derece düşük sıcaklıklı işlem, geleneksel tuğla üretimindeki 900-1000°C fırınlama ile kıyaslandığında ciddi bir enerji tasarrufu anlamına gelmektedir.

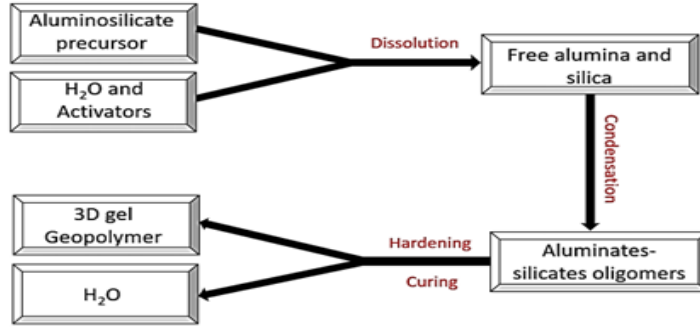
Geopolimer tuğlaların çevresel sürdürülebilirlik açısından bir diğer kritik avantajı, atık malzemelerin yeniden kullanımıdır. Uçucu kül, yüksek fırın cürufu, metalurji cürufları gibi atıklar normalde depolama alanlarında birikerek çevreye zarar verebilirken, geopolimer teknolojisi bu atıkları değerlendirip katma değerli ürünlere dönüştürebilmektedir. Literatürdeki bir derleme, son yıllarda yayınlanmış çalışmalar ışığında endüstriyel atıkların geopolimer tuğla üretiminde yaygın ve başarılı biçimde kullanıldığını, atık kullanımının tuğla dayanımını olumsuz etkilemeden doğal kil tüketimini azalttığını göstermiştir [5]. Böylece geopolimer tuğla üretimi, döngüsel ekonomi prensiplerine uygun olarak atık yönetimine katkı sunar. Ayrıca Portland çimentosu kullanımına gerek kalmaması sayesinde karbon ayak izinin azaltılmasına yardımcı olur [6]. Singh ve Sengupta (2022) tarafından yapılan kapsamlı bir derleme, geopolimer tuğlaların hem atık değerlendirme yoluyla çevresel fayda sağladığını hem de üretim süreçlerinde geleneksel malzemelere kıyasla daha düşük sera gazı emisyonu bıraktığını vurgulamıştır. Bu nedenle geopolimer tuğlalar, enerji verimliliği yüksek ve çevre dostu bir yapı malzemesi alternatifi olarak gün geçtikçe önem kazanmaktadır [7].

Geopolimer tuğlalar konusunda son yıllarda yapılan akademik çalışmalar, farklı atık malzemelerin kullanımı, üretim koşulları ve elde edilen performanslar hakkında zengin bir birikim oluşturmuştur.

Horel (2012), termik santral taban külünü alkali çözelti ile alkali aktivasyona tabi tutmuştur. Basınç dayanımı ve mikro yapı analizleriyle, taban külünden imal edilen geopolimer tuğlaların mekanik açıdan yeterli performansı sağlayabildiği gösterilmiştir. Bu çalışma, taban külünün hem çimento harçlarına aktif bir katkı malzemesi olabileceğini hem de geopolimer tuğla üretiminde kullanılabileceğini göstermiştir[8].

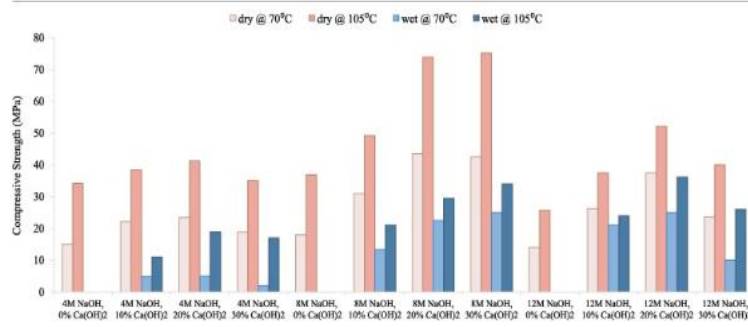
Ibrahim ve ark. (2015), Uçucu kül bazlı hafif geopolimer tuğlalar üzerine yaptığı derlemede, literatürde bildirilen farklı kürleme koşulları, karışım oranları ve gözeneklilik azaltma yöntemlerini incelemiştir. Derlemede, kür şartlarının tuğla özelliklerinde kritik önemde olduğu özellikle vurgulanmaktadır. Örneğin, 80°C’de 6 saat kürlenen numunelerin yaklaşık 27 MPa basınç dayanımı ve 0.34 W/mK ısı iletkenliği ile optimum sonuçları verdiği rapor edilmiştir. Bu da kür süresi ve sıcaklığının optimize edilmesiyle geopolimer tuğla performansının geleneksel tuğlalara yaklaşabildiğini ortaya koymaktadır[9].

Amin ve ark. (2017) yaptıkları çalışmada, seramik karo üretim tesislerinden çıkan ince toz atığı (spreydryer siklon tozu) geopolimer tuğla üretiminde bağlayıcı malzeme olarak değerlendirmiştir. 1M NaOH çözeltisi ve %6–10 sönmüş kireç (Ca(OH)_2) ilavesiyle hazırlanan karışım, oda sıcaklığında 90 gün kürlenmiştir. Elde edilen tuğlaların yaklaşık 10 MPa basınç dayanımına ulaştığı ve üretim maliyetinin ciddi miktarda düştüğü belirtilmiştir. Bu çalışma, seramik endüstrisi atıklarının da geopolimer tuğla için uygun bir hammadde olabileceğini göstermiştir[10].

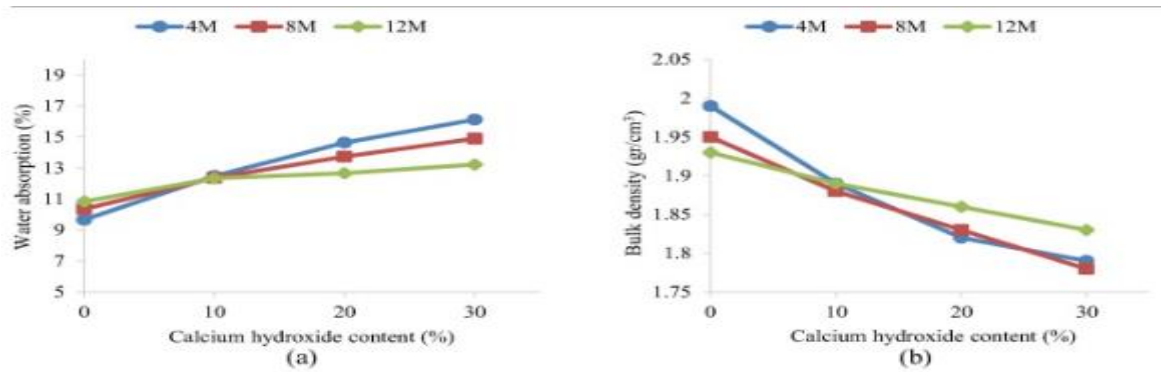


Şekil 1. Polimerizasyon sürecinin reaksiyon mekanizması [10]

Madani ve ark. (2020) yaptıkları çalışmada agrega yıkama atıklarını ana malzeme olarak kullanmıştır. NaOH konsantrasyonu (4, 8, 12 M), $\text{Ca}(\text{OH})_2$ katkı oranı (%5–15) ve kür sıcaklığı (70°C vs 105°C) gibi parametreler üzerinde durulmuştur. Sonuçlar, daha yüksek molariteli çözeltilerin daha yoğun bir yapı oluşturup dayanımı arttırdığını; %15 $\text{Ca}(\text{OH})_2$ katkısıyla kuru kür koşulunda yaklaşık 75 MPa gibi çok yüksek basınç dayanımlarına ulaşıldığı görülmüştür. Ancak $\text{Ca}(\text{OH})_2$ oranı %20'yi aştığında dayanım ve yoğunlukta düşüş gözlenmiştir. Yine kür sıcaklığının 70°C 'den 105°C 'ye çıkarılmasının dayanımı belirgin biçimde artırdığı saptanmıştır. Bu çalışma, uygun aktivatör ve kür koşullarıyla atık malzemeleri değerlendirerek yüksek performanslı geopolimer tuğlalar üretilebileceğini göstermiştir[11].



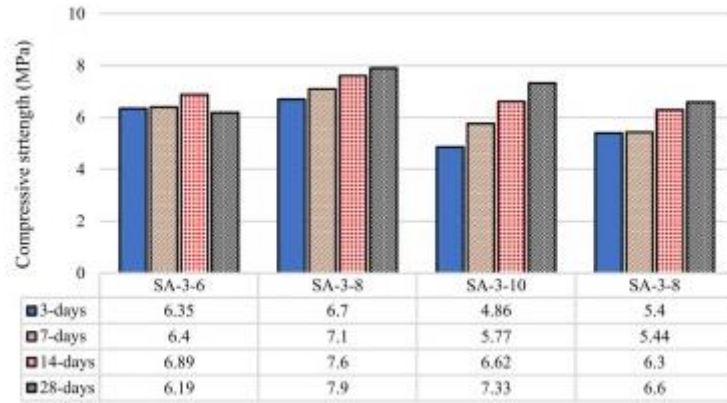
Şekil 2. Sıcaklık ve kürleme koşullarının basınç dayanımına etkisi [11]



Şekil 3. Kalsiyum hidroksit ve sodyum hidroksitin (a) su emilimi ve (b) hacim yoğunluğu üzerindeki etkisi [11]

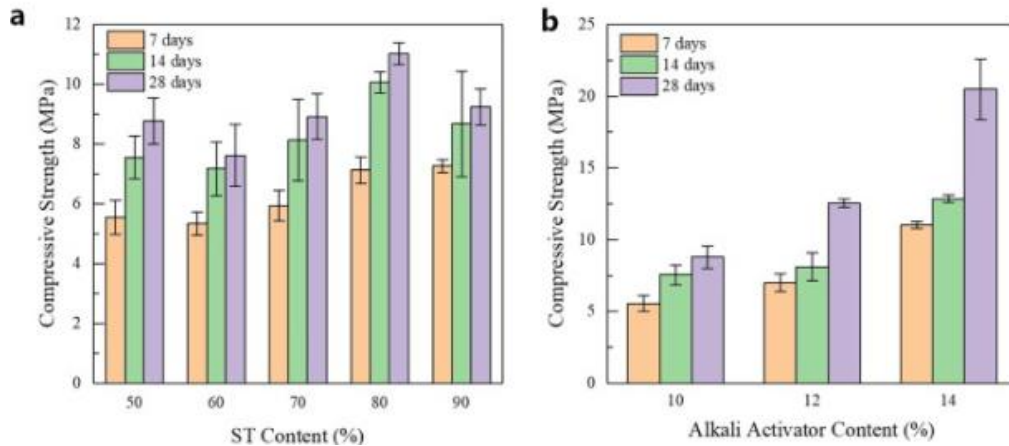
Ahmed ve ark. (2021) yüksek Si, düşük Al içeren ferrosilikon atığı ile alumina fabrikası atığını birlikte değerlendirdiği bir çalışmada, 6 ila 12 M arasında sodyum hidroksit ve sodyum silikat aktivatörü kullanılarak oda sıcaklığında 28 güne kadar kür yapılmıştır. Farklı Si/Al oranları elde etmek için alumina atığı ilavesi %0.5–4 aralığında değiştirilmiştir. En iyi sonuç 8 M NaOH ve Si/Al = 1 oranıyla elde edilmiş (28.gün 10.9 MPa basınç dayanımı ve yaklaşık %13 su emme). Bu sonuçlartuğla üretimi için kabul edilebilir değerlerdir. Ayrıca, alumina atığı ilavesinin tuğlaların

termal iletkenliğini düşürdüğü ve yalıtım özelliklerini iyileştirdiği belirlenmiştir (daha düşük ısı iletim katsayısı). Bu sonuç, metalurjik cüruf ve mineral atıkların birlikte kullanılmasının hem mekanik hem de termal açıdan avantaj sağlayabileceğini göstermektedir[12].



Şekil 4. Farklı NaOH konsantrasyonu ve Si/Al = 3,4'te geopolimer tuğlanın basınç dayanımı [12]

Kang ve ark. (2021) yaptıkları çalışmada, maden şisti artıklarını uçucu kül ve metakaolin ile yaklaşık %50'lere varan oranlarda karıştırarak fırınlanmamış (pres) tuğla üretimini incelemiştir. Alkali aktivatör miktarı ve kür süresi değişkenleri incelenmiştir. En iyi sonuçlar %50 şist artığı, %50 diğer bağlayıcılar ve 28 gün kür koşulları altında yaklaşık 20.5 MPa basınç dayanımı ve %13.4 su emme ile elde edilmiştir. Üretilen tuğlanın, kriterleri karşıladığı bildirilmiştir[13].



Şekil 5. (a) 7 günlük, 14 günlük ve 28 günlük kürleme koşullarında farklı ST içeriğine sahip numunelerin basınç dayanımı ve (b) 7 günlük, 14 günlük ve 28 günlük kürleme koşullarında farklı alkali içeriğine sahip numunelerin basınç dayanımı [13]

Ranjitham ve ark. (2021) yaptıkları bildiride, uçucu kül esaslı geopolimer harç ile üretilen pres tuğlaları incelemiştir. Çalışma sonucunda, 10 MPa'dan büyük basınç dayanımı ile uygun karışım tasarımı ve kürleme yöntemi sayesinde geopolimer tuğlaların gereksinimleri karşılayabildiğini kanıtlamıştır[14].

Al Amara (2022) yaptığı araştırmada, F sınıfı uçucu kül bazlı geopolimer harca farklı oranlarda (%10–60) bor atığı ekleyerek tuğla örnekleri üretmiştir. Numunelerin basınç dayanımı, eğilme dayanımı, yoğunluk, su emme ve ısı iletim özellikleri değerlendirilmiştir. Bulgular, bor atığı ikamesi %50'ye kadar arttıkça tuğlaların basınç dayanımının yükseldiğini ve optimum %50 ikamesinde maksimum dayanıma ulaşıldığını göstermiştir. Daha yüksek bor atığı oranlarında ise dayanımda düşüş görülmüştür. Ayrıca %50 bor atığı içeren numunede ısı iletim katsayısının belirgin şekilde azaldığı, yani yalıtım performansının iyileştiği saptanmıştır. Bu tez, bor madeni

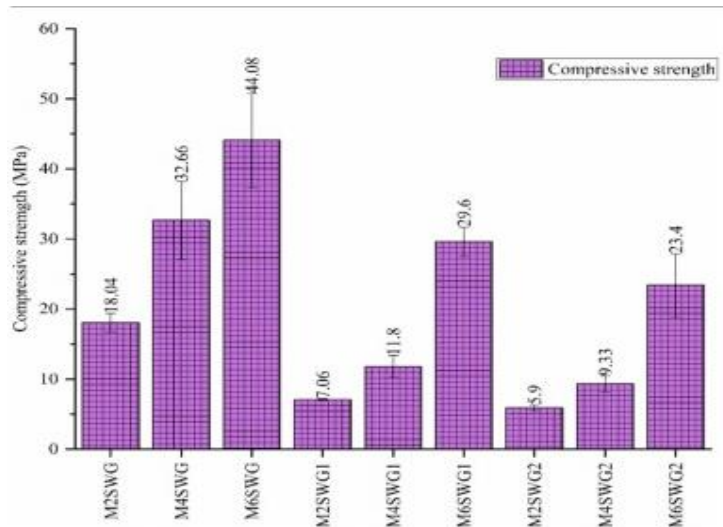
atıklarının geopolimer tuğla üretiminde değerlendirilebileceğine dair önemli bir kanıt sunmaktadır[15].

Al Amara & Çağlar (2022): yaptıkları derlemede, literatürde uçucu kül, yüksek fırın cürufu, seramik ve bor atığı gibi malzemelerin kullanımını kapsamlı biçimde özetlemiştir. Derleme, endüstriyel atıkların geopolimer tuğla üretiminde yaygın ve başarılı şekilde kullanılabildiğini, atık katkısının uygun oranlarda olması koşuluyla tuğlanın fiziksel-mekanik özelliklerini geliştirebildiğini ortaya koymaktadır. Ayrıca atık kullanımının doğal kaynak tüketimini azalttığı ve çevresel açıdan önemli yararlar sağladığı vurgulanmıştır. Bu makale, son yıllarda araştırmaların odağının atıkların verimli kullanımı ve tuğla performansına etkileri üzerinde yoğunlaştığını göstermesi bakımından değerlidir[16].

Ahmad & Rashid (2022) yaptıkları çalışmada, Killi bir toprağı doğrudan bağlayıcı malzeme olarak kullanmıştır. 4 M veya daha düşük molaritelerde NaOH kullanılarak oda koşulunda kür uygulanan tuğlalarda, kalıplama (presleme) basıncının dayanım üzerinde dramatik etkisi olduğu bulunmuştur. Örneğin, 20 MPa pres uygulanması dayanımı yaklaşık 5.9 kat, 40 MPa pres ise yaklaşık 7.4 kat artırmıştır. Optimum tasarım ile yalnızca kil toprak ve alkali aktivatör ile yaklaşık 10 MPa mukavemet ve düşük su emme değerlerine ulaşılabileceği gösterilmiştir. Bu sonuç, yerel killi toprakların bile uygun işlem ve presleme ile geopolimer tuğlaya dönüştürülerek pişmiş tuğla kalitesine erişebileceğine işaret etmektedir[17].

Singh & Sengupta (2022), Uçucu külü geopolimer tuğla üretiminde kullanmıştır. Farklı koşullarda üretilen tuğlaların performanslarını karşılaştırmıştır. Araştırma sonucunda, geopolimer tuğlaların uçucu kül başta olmak üzere birçok atığı değerlendirebildiği ve standart tuğla dayanımlarına ulaşabildiği belirtilmiştir. Dayanımı etkileyen başlıca faktörlerin; alkali aktivatör konsantrasyonu, kalıplama basıncı, kür sıcaklığı ve kür süresi olduğu özetlenmiştir. Ayrıca bu tuğlaların üretiminin, karbon ayak izini azaltmada ve atık yönetimde önemli rol oynayabileceği vurgulanarak geopolimer teknolojisinin sürdürülebilirlik boyutuna dikkat çekilmiştir[18].

Sher B. Singh ve ark. (2024), uçucu kül ve düşük molaritede alkali aktivatörler (1–4 M) kullanarak geopolimer tuğla üretmiştir. Numuneler oda sıcaklığında kürlenmiş ve tuğlaların hedeflenen sınıf-10 mukavemetine (≥ 10 MPa) ulaştığı görülmüştür. Özellikle 2 M NaOH + Na₂SiO₃ içeren karışımla yaklaşık 18 MPa basınç dayanımı ve %16.5 su emme elde edilerek standart pişmiş kil tuğlasına denk performans sağlanmıştır. Bu çalışma, çok düşük alkali içeriği ve tamamen oda koşulu kür ile dahi geopolimer tuğla üretiminin mümkün ve ekonomik olabileceğini göstermiştir[19].



Şekil 6. Aktifleştirici çözeltide %5, %6 ve %7 ilave su kullanılarak üretilen geopolimer tuğlaların 28 günlük basınç dayanımları [19]

2 SONUÇLAR

- Geleneksel pişmiş tuğla üretimi, yüksek sıcaklıklarda fırınlama gerektirdiği için yoğun enerji tüketir ve önemli ölçüde karbon salımı ile çevresel zararlara yol açmaktadır.
- Geopolimer tuğla üretimi daha düşük sıcaklıklarda gerçekleştirildiği için daha az enerji harcar ve karbon salınımı konusunda çevre dostudur.
- Yapılan çalışmalarda atık malzemelerin geopolimer tuğla için kullanımın uygun olduğu, bu sayede doğal kaynak tüketiminin azaltılabileceği görülmüştür.
- Geopolimer tuğlalar her ne kadar düşük aktivatör molaritesi ve düşük kür sıcaklığında da tatmin edici seviyelerde mekanik özelliklere sahip olsa da, aktivatör yoğunluğu ve kür sıcaklığı arttıkça tuğlaların basınç dayanımları iyileşmektedir.

Yazar Katkıları (Contributions of the Authors)

Kavramsallaştırma ve yazım Aykut TUNTAŞ tarafından gerçekleştirilmiştir.

Yorumlama, değerlendirme ve düzeltme Doç. Dr. Namık YALTAY tarafından gerçekleştirilmiştir.

KAYNAKLAR

- [1]-International Energy Agency, & United Nations Environment Programme. (2019). *2019 Global status report for buildings and construction: Towards a zero-emission, efficient and resilient buildings and construction sector*. IEA.
- [2]-Zhou, J., Yang, Y., & Wang, Z. (2021). Environmental impacts of fired clay bricks production: Energy consumption and CO₂ emissions assessment. *Journal of Cleaner Production*, 282, 124517. <https://doi.org/10.1016/j.jclepro.2020.124517>
- [3]-Singh, N., Kumar, S., & Rakesh, N. (2021). Utilization of industrial by-products for geopolimer brick manufacturing and assessment of mechanical and durability performance. *Construction and Building Materials*, 270, 121388. <https://doi.org/10.1016/j.conbuildmat.2020.121388>
- [4]-Zeybek, O. (2009). Fly ash based geopolimer brick production: Master of Science thesis. *Anadolu University, Turkey*.
- [5]- Liew, Y. M., Heah, C. Y., Kamarudin, H., & Mustafa Al Bakri, A. M. (2017). Processing and characterization of geopolimer bricks using industrial by-products: A review. *Reviews in Advanced Materials Science*, 48(1), 10–26.
- [6]- Yildizel, S. A., & Balaban, M. (2023). Geopolimer bricks within the concept of circular economy: Valorization of industrial wastes for sustainable construction materials. *Journal of Cleaner Production*, 412, 137314. <https://doi.org/10.1016/j.jclepro.2023.137314>
- [7]-Singh, B. K., & Sengupta, S. (2022). *An overview of fly ash utilization in production of geopolimer bricks*. Innovative Infrastructure Solutions, 7(1), 283. DOI: 10.1007/s41062-022-00713-0.
- [8]- Horel, C. (2012). *Sodyum Hidroksit ve Sodyum Silikat ile aktive edilmiş taban külünün çimentoya etkisi ve geopolimerik tuğla üretimi* (Lisans Tezi, Afyon Kocatepe Üniversitesi, Mühendislik Fakültesi).

- [9]- Wan Ibrahim, W. M., Hussin, K., Bakri, M. M. A., Binhussain, M., Kamarudin, H., & others. (2015). *A review of fly ash-based geopolymer lightweight bricks*. Applied Mechanics and Materials, 754-755, 452-456. DOI: 10.4028/www.scientific.net/AMM.754-755.452.
- [10]- El Sayed, A. M., Abdallah, H. M., Abdel-Goad, M., Abobeah, R., & Amin, S. K. (2024). Geopolymer and alkali-activated membranes opportunities and assessment of performance. *Journal of Membrane Science and Research*, 10(1).
- [11]- Madani, H., Ramezaniapour, A. A., Shahbazinia, M., & Ahmadi, E. (2020). *Geopolymer bricks made from less active waste materials*. Construction and Building Materials, 247, 118441. DOI: 10.1016/j.conbuildmat.2020.118441.
- [12]- Ahmed, M. M., El-Naggar, K. A. M., Hassan, D. T., & others. (2021). *Fabrication of thermal insulation geopolymer bricks using ferrosilicon slag and alumina waste*. Case Studies in Construction Materials, 15, e00737. DOI: 10.1016/j.cscm.2021.e00737.
- [13]- Kang, X., Gan, Y., Chen, R., & Zhang, C. (2021). *Sustainable eco-friendly bricks from slate tailings through geopolymerization: Synthesis and characterization analysis*. Construction and Building Materials, 278, 122337. DOI: 10.1016/j.conbuildmat.2021.122337.
- [14]- Ranjitham, M., Vishvapriya, K., & Pavya, L. U. V. (2021). *Experimental investigation on geopolymer bricks*. In **Proc. of the International Conference on Advances in Civil Engineering** (Springer, Advances in Materials Research, Vol. 29, pp. 129-136).
- [15]- Al Amara, S. N. A. (2022). *Uçucu kül tabanlı geopolimer tuğla üretiminde bor atığı kullanımının etkisi* (Yüksek Lisans Tezi, Kırşehir Ahi Evran Üniversitesi, Fen Bilimleri Enstitüsü).
- [16]- Al Amara, S. N. A., & Çağlar, A. (2022). *Geopolimer tuğla üretiminde atık kullanımı üzerine yapılan akademik çalışmalar (2017–2022)*. Sürdürülebilir Mühendislik Uygulamaları ve Teknolojik Gelişmeler Dergisi, 5(2), 171-176.
- [17]- Ahmad, M., & Rashid, K. (2022). Novel approach to synthesize clay-based geopolymer brick: Optimizing molding pressure and precursors' proportioning. Construction and Building Materials, 322, 126472.
- [18]- Singh, B. K., & Sengupta, S. (2022). *An overview of fly ash utilization in production of geopolymer bricks*. Innovative Infrastructure Solutions, 7(1), 283. DOI: 10.1007/s41062-022-00713-0.
- [19]- Singh, S. B., Maiti, P. R., & Mohanty, S. (2024). *Development of filler-free and ambient-cured fly ash geopolymer brick*. Case Studies in Construction Materials, 20, e018XX. DOI: 10.1016/j.cscm.2023.e018XX.



NUMERICAL INVESTIGATION OF THE COOLING PERFORMANCE OF PHOTOVOLTAIC PANELS EQUIPPED WITH SQUARE FINS

Abdullatif YILMAZ ^{1,*} , Cengiz YILDIZ ²

¹Firat University, Graduate School of Natural and Applied Sciences, Department of Mechanical Engineering, Elazığ, Türkiye

² Firat University, Department of Mechanical Engineering, Elazığ, Türkiye

* Corresponding Author: abltf_ylmz@hotmail.com

ABSTRACT

The increase in operating temperature of photovoltaic (PV) panels is a critical problem that significantly reduces energy conversion efficiency. The main objective of this study is to numerically investigate the thermal performance of different passive cooling systems integrated onto the bottom surface of PV panels and compare their effects on panel efficiency. In this context, a flat panel without fins (control model) and a panel geometry with square-section fins were analyzed. Aluminum was selected as the fin material. Computational Fluid Dynamics (CFD) analyses were performed using ANSYS Fluent software under different air speeds (0.5 m/s and 2.5 m/s) and solar radiation conditions at different times of the day (09:00, 14:00, 18:00). The findings showed that the finless panel was insufficient, especially under high solar irradiance, and that increasing air velocity alone was not effective in reducing the temperature. The square-fin geometry panel significantly reduced the panel temperature compared to the case without fins by changing the flow structure and creating local turbulence. Analysis revealed that the pressure differences and swirling flow created by the fins are the primary mechanisms that enhance convective heat transfer. At the highest irradiance and temperature conditions studied (14:00), the square-finned design was found to reduce surface temperature by approximately 7°C compared to the panel without fins, resulting in a 1% increase in panel efficiency. In conclusion, passive cooling strategies with square-finned geometry in photovoltaic panels play a critical role in improving the efficiency and stability of PV systems.

Keywords: Photovoltaic panel, Passive cooling, Fin, Computational fluid dynamics (CFD), Heat transfer, Panel efficiency.

1 INTRODUCTION

Photovoltaic (PV) systems, which enable the direct conversion of solar energy into electricity, play a central role among renewable energy technologies. However, the energy conversion efficiency of PV panels is adversely affected by the increase in surface temperature during operation. It is well known that each one-degree Celsius rise in surface temperature results in a reduction of approximately 0.25–0.5% in panel efficiency [1]. In regions with high solar irradiance, panel temperatures may reach 60–70 °C, which not only reduces instantaneous power generation but also shortens the long-term lifespan of the panel [2]. Therefore, the development of effective thermal management strategies for PV panels is of critical importance to enhance system performance and reliability.

Various cooling methods, categorized as active and passive, have been investigated in the literature to reduce PV panel temperatures [3–4]. Although active cooling techniques (such as fans or pumps) are effective, they involve additional energy consumption and increased system complexity. Passive cooling methods, on the other hand, offer a sustainable and economical alternative since they require no external energy input [5]. Among these methods, integrating fins that function as heat sinks on the rear surface of the panel has gained prominence. Heat sinks are fundamental heat transfer elements whose effectiveness has been demonstrated across a wide range of applications, from electronic cooling to industrial systems [6]. Relevant studies have shown that various fin configurations can reduce panel temperature and increase efficiency [7, 8]. For instance, Gotmare et al. (2015) reported a 4.2% reduction in panel temperature and a corresponding 5.5% increase in power output using perforated fins [9]. Moreover, recent CFD studies highlight the importance of optimizing geometric parameters such as fin spacing, height, and shape [10]. However, studies systematically comparing the combined effects of fin geometry (e.g., square fins) and fin material (e.g., aluminum) on cooling performance remain limited.

In this context, the present study aims to address this gap in the literature. The primary objective of this work is to systematically examine the combined effects of panel cooling geometry (finless and square-fin configurations) and fin material (aluminum) on passive cooling performance using Computational Fluid Dynamics (CFD). Beyond determining thermal performance and efficiency enhancement, the study also aims to analyze the underlying fluid dynamic mechanisms—including variations in velocity and pressure fields—that contribute to these improvements.

2 MATERIALS AND METHODS

In this study, the effect of square fin geometry on the passive cooling performance of a photovoltaic panel was investigated using the Computational Fluid Dynamics (CFD) method. Numerical analyses were performed with ANSYS Fluent software, which is based on the finite volume method. The analysis procedure consisted of geometric modeling, mesh generation, and the configuration of solution settings.

2.1 Geometric Models

In the analyses, a standard PV panel geometry with dimensions of 1800 × 1000 mm was used as the baseline. To enable a comparative assessment, both the finless configuration and the square-fin configuration were modeled (Figure 1):

1. **Finless Model (Control):** A standard panel with a flat rear surface and no cooling elements.
2. **Square-Fin Model:** A configuration in which 39 square-section fins, each measuring 100 × 100 mm, were uniformly distributed and mounted on the rear surface of the panel.

All fins were modeled with a thickness of 4 mm and attached to the back of the panel. The panel was positioned at a tilt angle of 40°, corresponding to the latitude of Ankara Province.

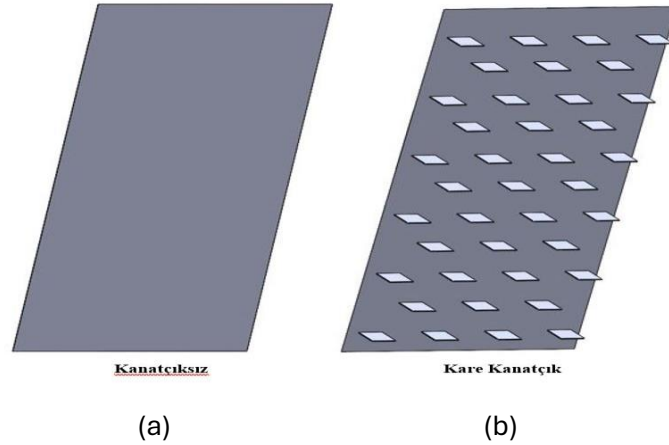


Figure 1. Geometric models used in the analyses: (a) Finless control model, (b) Square-fin model.

2.2 Numerical Method and Boundary Conditions

The airflow was assumed to be three-dimensional, incompressible, and steady-state. The standard k-ε turbulence model was employed for turbulence modeling [11]. The momentum and energy equations were solved simultaneously until a stable convergence was achieved.

The primary materials and operating conditions used in the study are summarized in Table 1. Since thermal conductivity is the material property that most significantly affects heat transfer, aluminum (237 W/mK) was selected as the fin material. To simulate atmospheric conditions, air was used as the working fluid, and two inlet velocities—0.5 m/s and 2.5 m/s—were defined to represent low and high wind speeds. To capture variations in thermal load throughout the day, separate analyses were conducted for three characteristic time periods (09:00, 14:00, 18:00), each corresponding to different solar irradiance and ambient temperature conditions.

The complex heat transfer occurring on the front surface of the panel exposed to solar radiation was modeled using the Sol-Air Temperature approach, which incorporates both radiative and convective effects, providing a more realistic boundary condition.

Table 1. Material Properties and Operating Conditions Used in the Analyses

Parameter	Values
Fin Material	Aluminium
Thermal Conductivity (k)	(Al/Cu) 237 W/m·K
Fluid	Air
Air Inlet Velocity	0.5 m/s, 2.5 m/s
Time / Ambient Temperature	09:00 (20 °C), 14:00 (25 °C), 18:00 (22 °C)
Time / Solar Irradiance	09:00 (689 W/m ²), 14:00 (775 W/m ²), 18:00 (453 W/m ²)

The panel efficiency (η) was calculated using Equation (1) based on the average cell temperature (T_{cell}) obtained from each analysis, together with the nominal efficiency under standard test conditions (η_{STC}) and the temperature coefficient (γ) [12].

$$\eta = \eta_{\text{STC}} \cdot [1 - \gamma \cdot (T_{\text{cell}} - 25)] \quad (1)$$

3 RESULTS AND DISCUSSION

In this section, the thermal performance of the finless and finned panels under varying operating conditions, as well as their effects on panel efficiency, are presented and compared.

3.1 Performance of the Finless Model (Reference Case)

The analyses revealed that the finless reference model is insufficient for passive cooling. Particularly at 14:00, when solar irradiance reaches its daily peak, the panel surface temperature rose to approximately 330 K (~57 °C). Under these conditions, increasing the air velocity from 0.5 m/s to 2.5 m/s did not yield a meaningful improvement in panel temperature or efficiency. This indicates that, on a flat surface exposed to high radiative loads, convective heat transfer alone is unable to provide effective cooling. Therefore, geometric enhancements that increase the heat transfer area become necessary.

3.2 Effect of Geometry on Flow Structure and Pressure Field

The primary reason fins enhance cooling performance is their influence on the flow structure and pressure distribution behind the panel. Figure 2 compares the pressure contours generated by the three different geometries at an air velocity of 2.5 m/s. In the finless model (Figure 2a), the pressure field formed by the incoming airflow remains relatively uniform, whereas in the square-fin model (Figure 2b), the fins disrupt the flow by acting as obstacles and generate localized pressure differences.

These pressure differences cause flow separation and lead to the formation of small-scale vortices. Such vortex-dominated and turbulent flow enhances mixing between the hot panel surface and the cooler ambient air, thereby disrupting the stagnant and insulating boundary layer. As a result, the convective heat transfer coefficient increases. The three-dimensional flow structure generated by the square fins further intensifies this turbulence effect, which in turn contributes significantly to improved cooling performance.

These variations in the pressure field directly influence the velocity distribution as well. As shown in Figure 3, in the finless model (Figure 3a), the airflow progresses along the surface with minimal obstruction, whereas in the finned model, the presence of fins significantly slows and mixes the flow. In particular, the low-velocity and vortex-dominated regions that form between the fins in the finned model allow the air to remain in contact with the surface for a longer duration, thereby enhancing its ability to absorb heat. This slowed and mixed airflow is the primary mechanism responsible for the increase in convective heat transfer.

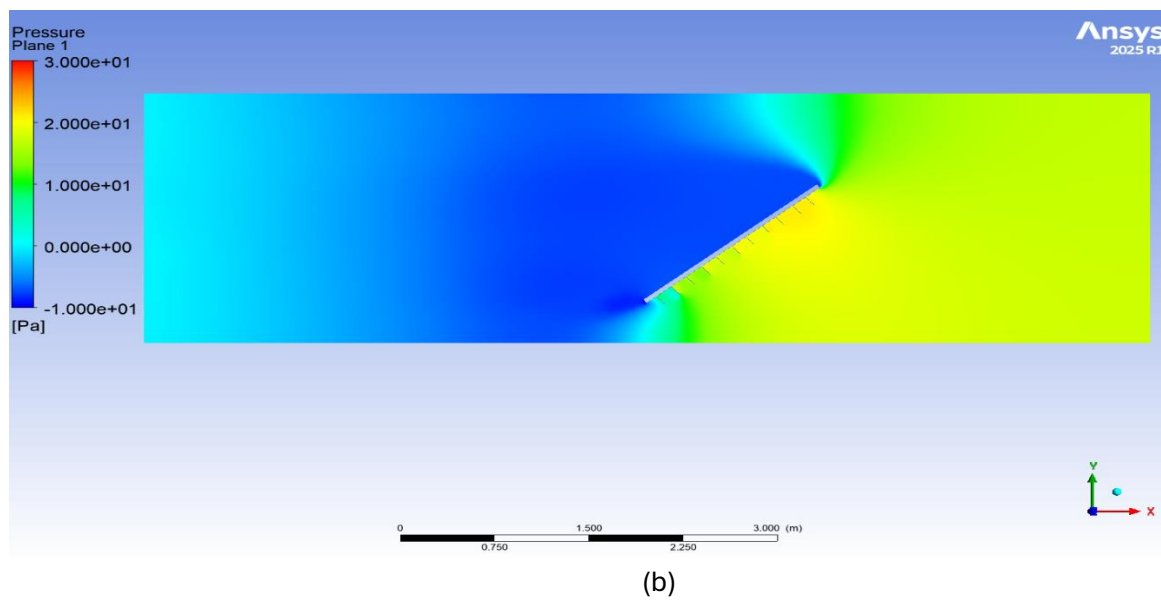
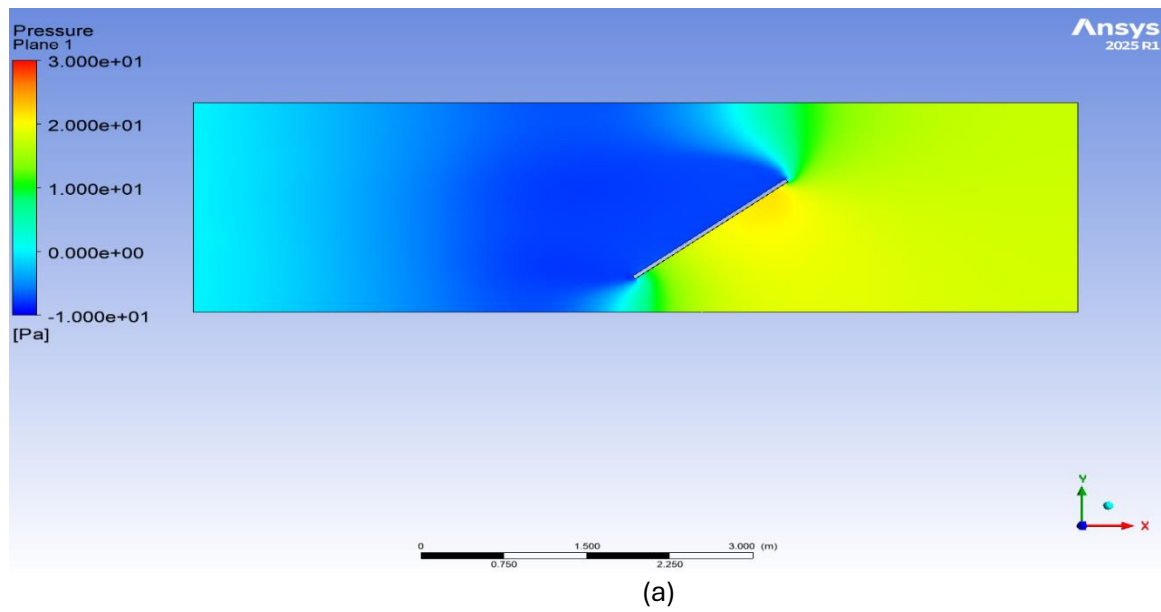


Figure 2. Effect of different geometries on surface pressure distribution (2.5 m/s): (a) Finless model, (b) Square-fin model

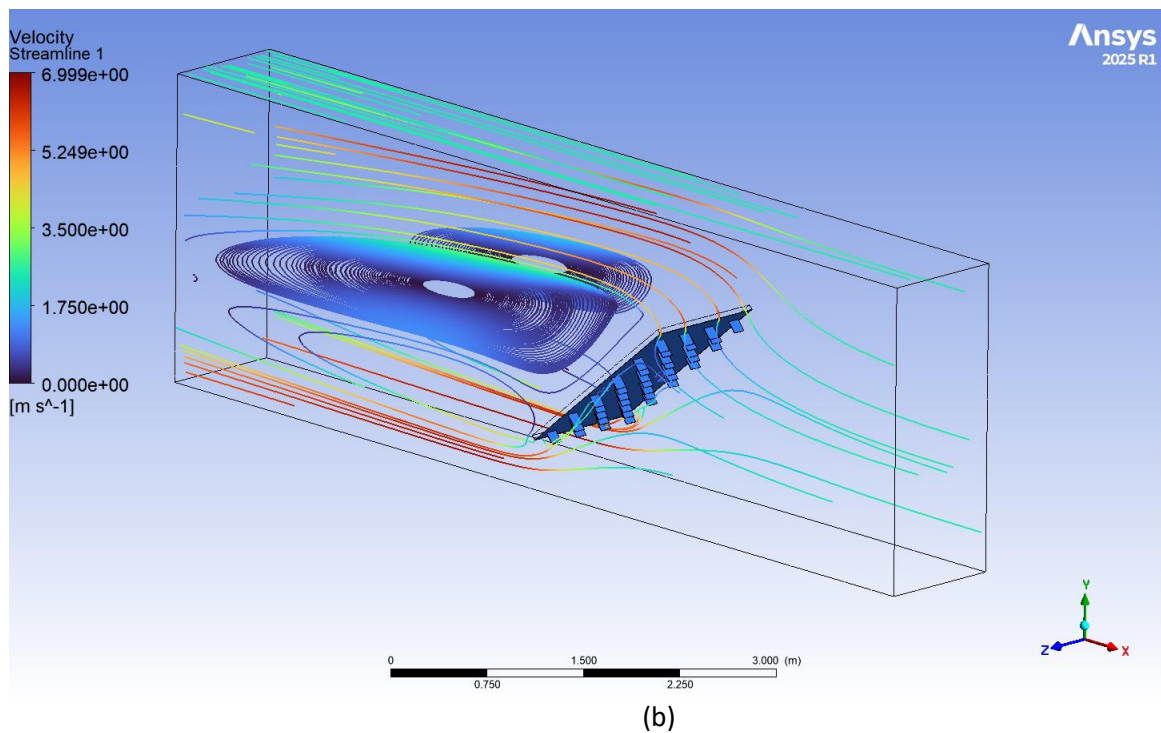
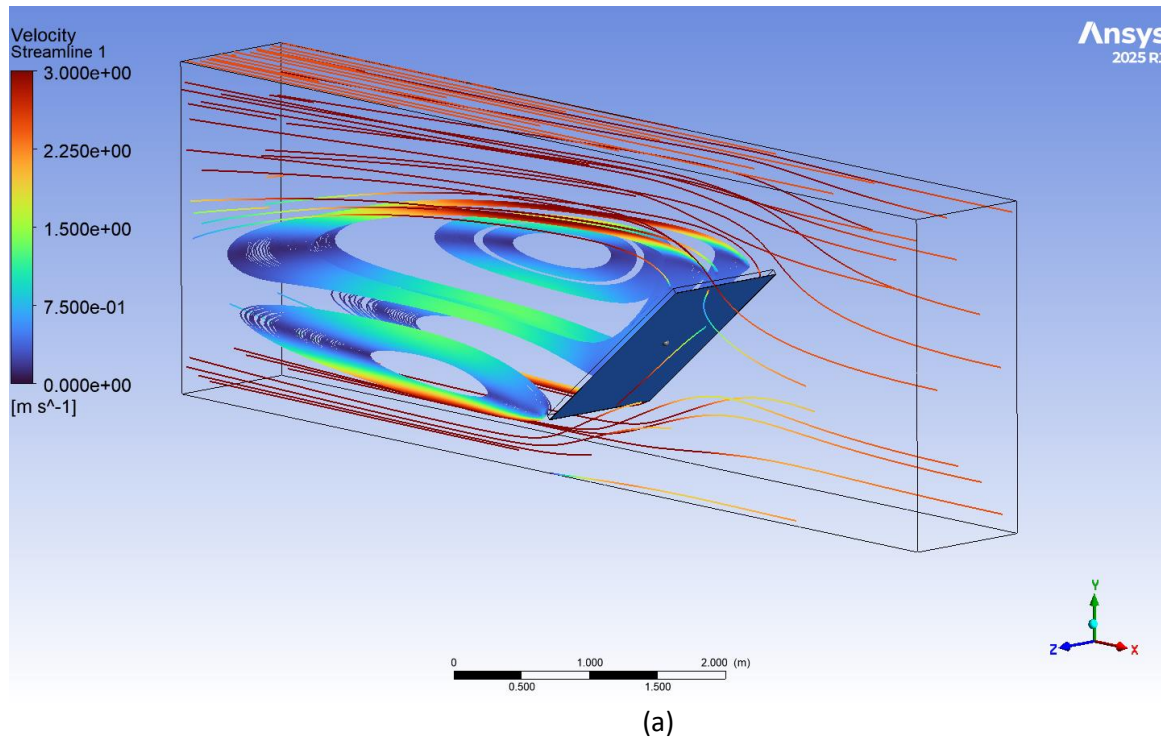


Figure 3. Effect of different geometries on velocity distribution (2.5 m/s, 14:00): (a) Finless model, (b) Square-fin model.

3.3 Effects on Flow Structure and Pressure Distribution

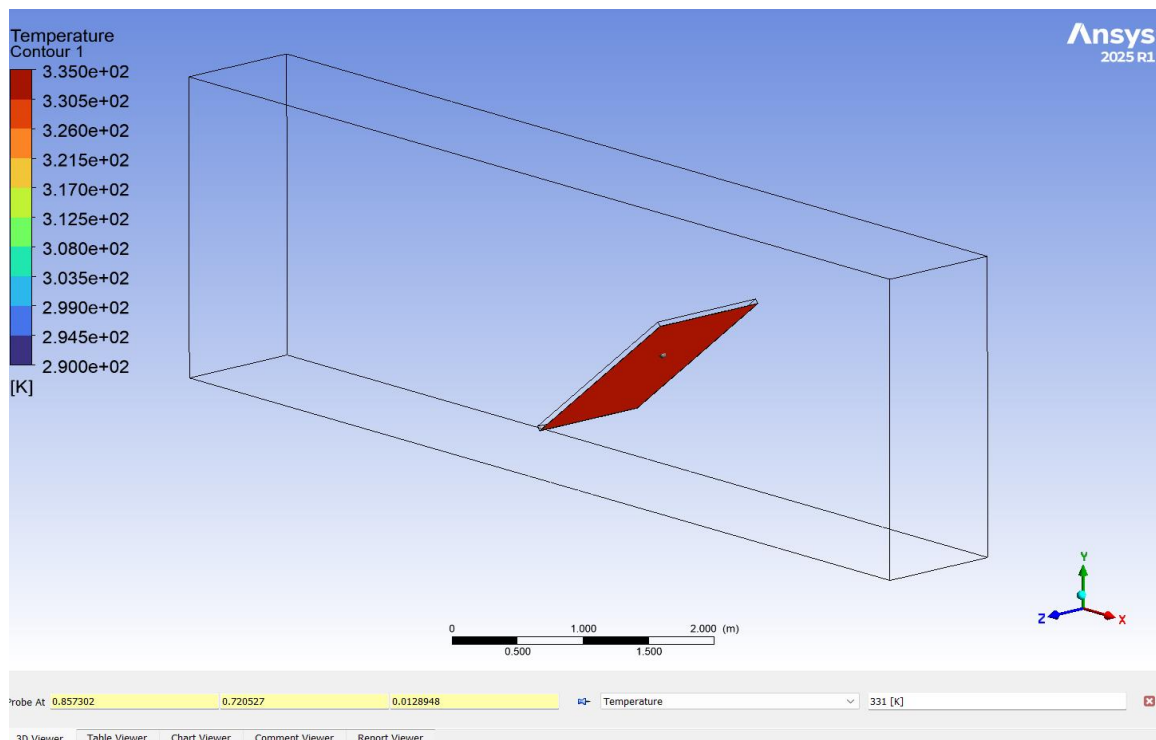
CFD analyses demonstrated that the fins fundamentally alter the flow structure behind the panel. While the flow remains largely laminar in the finless model, the square-fin geometry introduces obstacles along the flow path, generating localized vortices and turbulence. This behavior is confirmed by the complex pressure distribution formed around the fins. Particularly at the higher air velocity of 2.5 m/s, positive pressure regions develop on the wind-facing surfaces of

the fins, whereas negative pressure zones appear on their leeward sides. These pressure differences enhance fluid mixing, forming the primary mechanism that increases the convective heat transfer coefficient between the hot panel surface and the ambient air.

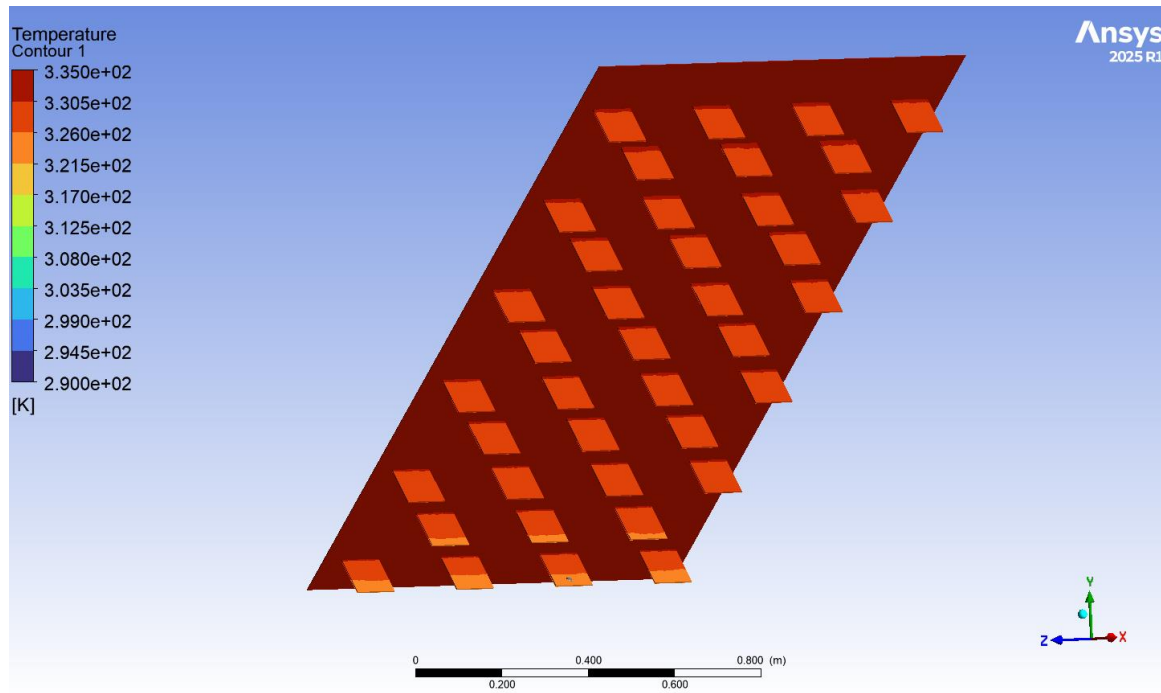
3.4 Effect of Fin Geometry on Cooling Performance

The square-fin model provided a noticeable improvement in cooling performance under all operating conditions compared to the finless configuration. By disturbing the airflow, the fins generated localized turbulence and increased the effective heat transfer surface area, enabling more efficient transfer of heat from the panel surface to the surrounding air.

In Figure 4, the temperature distributions of the finless and finned geometries using aluminum material are compared for the highest irradiance and ambient temperature condition of the day—14:00—at an air velocity of 2.5 m/s. The analyses clearly show that the finned configuration provides a significant improvement over the finless case, with the finned model exhibiting noticeably lower surface temperatures.



(a)



(b)

**Figure 4. Surface temperature distributions of the aluminum cooling plate geometry (14:00, 2.5 m/s):
(a) Finless model, (b) Square-fin model**

It was observed that the square-fin model enhances cooling compared to the finless configuration by directing the airflow through well-defined channels between the fins. Due to the presence of the fins, the flow gains a three-dimensional character, which more effectively disrupts the boundary layer and consequently improves the convective heat transfer coefficient.

3.5 Efficiency Analysis

It was determined that fin-enhanced panel cooling has a significant impact on overall performance. The fins facilitate faster and more uniform heat dissipation across the panel surface, preventing the formation of hot spots and reducing the overall panel temperature.

The efficiency results obtained for the finless panel are presented in Figure 5, while the efficiency values for the finned model are summarized in Figure 6. The graphs illustrate the panel efficiency at different times of the day (09:00, 14:00, and 18:00) and for varying air velocities. It is clearly observed that the square-fin model exhibits superior performance compared to the finless configuration, achieving higher efficiency levels. An improvement of approximately 1% in efficiency was obtained relative to the finless model. This result quantitatively demonstrates that passive cooling strategies can effectively enhance PV panel performance.

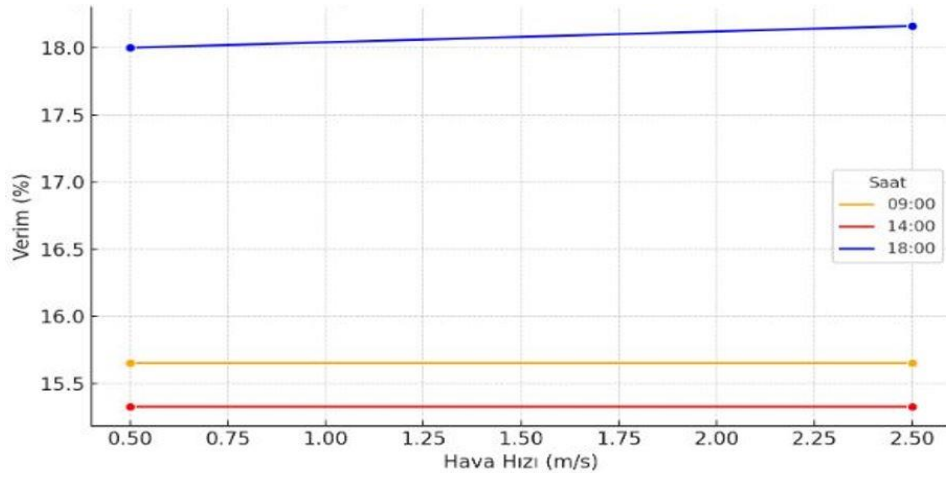


Figure 5. Effect of air velocity on panel efficiency for the finless aluminum-based photovoltaic panel

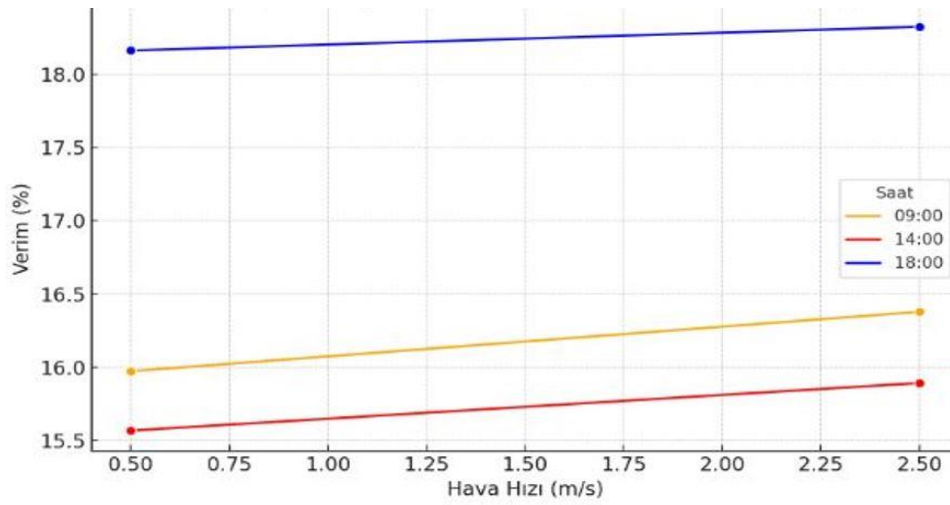


Figure 6. Effect of air velocity on panel efficiency for the square-fin aluminum-based photovoltaic panel

4 CONCLUSION

In this study, the passive cooling performance of photovoltaic panels was numerically investigated by comparing finless and square-fin geometries. The following key conclusions were obtained:

- The finless (flat) panel geometry was found to be insufficient for effective cooling. Under the most challenging condition (14:00), the panel surface temperature reached approximately 57 °C (330 K), and increasing the air velocity did not produce a meaningful reduction in temperature.
- The addition of fins to the rear surface of the panel disrupted the flow path, creating localized pressure differences and vortices. This increased both the effective heat transfer surface area and the level of turbulence, resulting in a significant improvement in cooling performance—and consequently efficiency—under all operating conditions compared to the finless configuration.
- When compared to the finless model, the square-fin geometry was found to establish a more effective mechanism for disrupting the boundary layer and enhancing fluid mixing by

imparting a three-dimensional motion to the flow. Owing to this enhanced heat transfer mechanism, the square-fin model demonstrated a superior cooling performance relative to the finless configuration.

In conclusion, the square-fin design made of aluminum, which demonstrated strong performance, effectively enhanced the flow dynamics and reduced the surface temperature by approximately 7 °C compared to the finless panel. In this context, passive cooling emerges as a promising strategy for improving PV panel efficiency by more than 1%. These findings highlight the critical importance of geometric enhancements in thermal management for PV panel design.

Conflict of Interest Statement

The authors declare that there is no conflict of interest among them.

Research and Publication Ethics Statement

This study was conducted in accordance with the principles of research and publication ethics.

Artificial Intelligence (AI) Contribution Statement

This manuscript was written, edited, analyzed, and prepared entirely by the authors without the use of any artificial intelligence (AI) tools. All content, text, data analysis, and figures were produced solely by the authors.

Author Contributions

Abdullatif YILMAZ: Methodology, Numerical Modeling, Analysis, Writing – Original Draft.

Cengiz YILDIZ: Methodology, Conceptualization, Supervision, Writing – Review and Editing.

REFERENCES

- [1] E. Radziemska, "The effect of temperature on the power drop in crystalline silicon solar cells," *Renewable Energy*, vol. 28, no. 1, pp. 1-12, 2003. doi: 10.1016/S0960-1481(02)00015-0.
- [2] L. M. Shaker, A. A. Al-Amiery, M. M. Hanoon, W. K. Al-Azzawi, A. A. H. Kadhum, Examining the influence of thermal effects on solar cells: a comprehensive review. *Sustainable Energy Research*, 11(1), 6, 2024.
- [3] D. H. El-Nagar, M. Emam, A. A. El-Betar, S. A. Nada, Combining active and passive cooling techniques for maximizing power generation and thermal utilization of photovoltaic panels. *Renewable Energy*, 123310, 2025.
- [4] A. Basem, A. Mukhtar, Z. M. Salem Elbarbary, F. Atamurotov, N. E. Benti, Experimental study on the various varieties of photovoltaic panels (PVs) cooling systems to increase their electrical efficiency. *PLoS One*, 19(9), 2024.
- [5] C. Wang, F. Guo, H. Liu, G. Wang, A Comprehensive Review of Research Works on Cooling Methods for Solar Photovoltaic Panels. *Energies*, 18(16), 4305, 2025.
- [6] O. Yemenici, Üçgen Kanatlı Yüzeylerin Isı Transfer Performansının Taguchi Yöntemiyle Deneysel İncelenmesi. *Karadeniz Fen Bilimleri Dergisi*, 15(1), 406-418, 2025.
- [7] E. Cuce, T. Bali, and S. A. Sekucoglu, "Effects of passive cooling on performance of silicon photovoltaic cells," *International Journal of Low-Carbon Technologies*, vol. 6, no. 4, pp. 299-308, 2011. doi: 10.1093/ijlct/ctr012.
- [8] A. El Mays, R. Ammar, M. Hawa, M. Abou Akroush, F. Hachem, M. Khaled, and M. Ramadan, "Improving photovoltaic panel using finned plate of aluminum," *Energy Procedia*, vol. 119, pp. 812-817, 2017. doi: 10.1016/j.egypro.2017.07.100.

- [9] J. A. Gotmare, D. S. Borkar, and P. R. Hatwar, "Experimental investigation of PV panel with fin cooling under natural convection," *International Journal of Advanced Technology in Engineering and Science*, vol. 3, no. 2, pp. 447-454, 2015.
- [10] G. Ömeroğlu, Fotovoltaik-termal (PV/T) sistemin sayısal (CFD) ve deneysel analizi. *Fırat Üniversitesi Mühendislik Bilimleri Dergisi*, 30(1), 161-167, 2018.
- [11] G. Abril-Macias, J. Peralta-Jaramillo, E. Delgado-Plaza, I. Sosa-Tinoco, D. Avilés, Simulation of the fluid dynamic and thermal behavior of an experimental passive cooling system of photovoltaic panels. *Heliyon*, 10(3), 2024.
- [12] S. Dubey, J. N. Sarvaiya, B. Seshadri, Temperature dependent photovoltaic (PV) efficiency and its effect on PV production in the world—a review. *Energy procedia*, 33, 311-321, 2013.

5 ÇİFT YÖNLÜ İŞARET DİLİ TERCÜME SİSTEMİ İÇİN DERİN ÖĞRENME TABANLI BİR YAKLAŞIM

Dilan ÖZEK^{1,*} , İrfan ÖKTEN² , Lokman DOĞAN³ 

¹ Bilgisayar Mühendisi, Bitlis, Türkiye

² Bitlis Eren Üniversitesi, Bilgisayar Mühendisliği Bölümü, Bitlis, Türkiye

³ Kütahya Sağlık Bilimleri Üniversitesi, Kütahya Meslek Yüksek Okulu, Yapay Zeka Operatörlüğü Pr., Kütahya, Türkiye

* Sorumlu Yazar: dilanozek34@gmail.com

ÖZET

Bu çalışma, sağlık hizmetlerine erişim sürecinde duyma engelli bireylerin yaşadığı iletişim güçlüklerini azaltmak amacıyla VideoMAE tabanlı derin öğrenme yöntemleri kullanılarak geliştirilen çift yönlü bir işaret dili tercüme sistemi sunmaktadır. Sağlık ortamlarında meydana gelen iletişim kopuklukları, tanınma doğruluğunun düşmesine, tedavi sürecinin gecikmesine ve hastaların klinik karar süreçlerine etkin katılımının sınırlanmasına neden olabilmektedir. Mevcut işaret dili tercüme sistemleri ise özellikle dinamik hareketlerin tanınması, yüksek doğruluk, gerçek zamanlı işleme ve geniş kapsamlı kelime dağarcığı desteği gibi açılardan yetersiz kalmaktadır. Bu çalışmada, Türk İşaret Dili (TİD) sağlık terminolojisini kapsayan 20.000 video ve 7.000'den fazla benzersiz işaretten oluşan büyük ölçekli bir veri seti üzerinde Video Masked Autoencoder (VideoMAE) mimarisi kullanılarak yüksek performanslı bir işaret dili tanıma modeli eğitilmiştir. VideoMAE'nin maskeli video modelleme stratejisi, hem uzamsal hem de zamansal bağımlılıkların güçlü bir şekilde öğrenilmesini sağlayarak dinamik işaretlerin tanınmasında önemli bir avantaj sunmuştur. Eğitim süreci, veri yoğunluğunun yüksekliği nedeniyle dağıtık paralel programlama yöntemleri (Distributed Data Parallel, çok iş parçacıklı veri işleme ve GPU tabanlı hızlandırma) ile optimize edilmiştir. Sistem, işaret → metin/ses dönüşümünün yanı sıra doktorlardan gelen yazılı ifadeleri işaret dizilerine çeviren metin → işaret modülünü de içermekte olup bu yönüyle tam işlevsel bir çift yönlü iletişim altyapısı sağlamaktadır. Üretilen işaretler hareket dizisi temelli bir avatar aracılığıyla görselleştirilmiş ve kullanıcı etkileşimi kolaylaştırılmıştır. Çalışmanın özgün değeri, derin öğrenme tabanlı video temsili, büyük ölçekli veri işleme ve çift yönlü çeviri bileşenlerini bir araya getirerek sağlık alanında gerçek zamanlı, doğru ve kullanıcı dostu bir iletişim sistemi sunmasıdır. Sistem performansı çeviri doğruluğu, işlem süresi ve klinik uygulanabilirlik ölçütleri kapsamında değerlendirilecek olup elde edilen çıktılar, özellikle acil servis ve poliklinik ortamlarında erişilebilirliğin artırılmasına önemli katkı sağlayacaktır.

Anahtar Kelimeler: İşaret Dili Tercümesi, VideoMAE, Derin Öğrenme, Masked Autoencoder, Paralel Programlama, Türk İşaret Dili.

1 GİRİŞ

İşaret dili, yalnızca bir iletişim aracı olmanın ötesinde, işitme engelli bireylerin sağlık hizmetlerine erişimde bağımsızlıklarını ve mahremiyetlerini koruyabilmeleri açısından da büyük önem taşımaktadır. Sağlık profesyonelleri ile hastalar arasındaki iletişimde yaşanan kopukluklar, tanı ve tedavi süreçlerinin etkinliğini olumsuz yönde etkileyebilmekte; özellikle acil müdahale gerektiren durumlarda ciddi riskler doğurabilmektedir. Bu nedenle, işaret dili tercüme sistemleri sağlık alanında sosyal kapsayıcılığı artıran kritik teknolojik çözümler arasında yer almaktadır.

Mevcut uygulamalarda çoğunlukla insan tercümanlara başvurulmakta; ancak tercüman erişiminin her zaman mümkün olmaması, maliyet, zaman ve gizlilik gibi faktörler bu yaklaşımı sınırlamaktadır. Ayrıca, her sağlık kurumunda Türk İşaret Dili'ne hâkim uzman personelin bulunmaması, duyma engelli bireylerin sağlık hizmetlerinden eşit koşullarda yararlanmasını güçleştirmektedir. Bu durum, otomatik işaret dili tanıma ve çeviri sistemlerine olan ihtiyacı daha da belirgin hâle getirmektedir [1].

Literatürde geliştirilen erken dönem işaret dili tanıma sistemleri genellikle el hareketlerine odaklanan kural tabanlı veya klasik makine öğrenmesi yöntemlerine dayanmaktadır. Ancak bu yaklaşımlar, işaret dilinin doğasında bulunan çoklu modaliteyi (el şekli, el hareketi, yüz ifadesi ve beden duruşu) yeterince temsil edememektedir. Derin öğrenme tabanlı yöntemlerin yaygınlaşmasıyla birlikte, bu sınırlılıkların aşılmasına yönelik önemli adımlar atılmıştır [2].

Bununla birlikte, sağlık alanına özgü işaret dili uygulamaları, genel amaçlı işaret dili sistemlerine kıyasla daha karmaşık gereksinimler içermektedir. Sağlık terminolojisi; soyut kavramlar, ardışık hareketler ve ince motor beceriler gerektiren işaretlerden oluşmakta olup, bu durum modelin hem uzamsal hem de zamansal bağımlılıkları güçlü biçimde öğrenmesini zorunlu kılmaktadır. Bu noktada, Video tabanlı Transformer mimarileri, uzun menzilli bağımlılıkları modelleme yetenekleri sayesinde önemli bir avantaj sunmaktadır [3].

Video Masked Autoencoder (VideoMAE) mimarisi, videonun büyük bir kısmını maskeleyerek yalnızca sınırlı sayıda görünür yama üzerinden öğrenme gerçekleştiren self-supervised bir yaklaşım sunmaktadır. Bu özellik, büyük ölçekli video veri setleri üzerinde etiketleme maliyetini azaltırken, modelin daha genelleştirilebilir ve sağlam temsiller öğrenmesini mümkün kılmaktadır. VideoMAE'nin sunduğu bu veri verimliliği, sağlık alanına yönelik işaret dili uygulamaları için özellikle uygun bir yapı oluşturmaktadır [4],[5].

Bu çalışmada, Türk İşaret Dili sağlık terminolojisini kapsayan geniş ölçekli bir video veri seti kullanılarak VideoMAE tabanlı bir işaret dili tanıma modeli geliştirilmiştir. Önerilen sistem, yalnızca işaret → metin/ses dönüşümünü değil, aynı zamanda metin → işaret dönüşümünü de destekleyen çift yönlü bir iletişim altyapısı sunmayı hedeflemektedir. Böylece, sağlık personeli ile duyma engelli bireyler arasında daha doğal, hızlı ve güvenilir bir iletişim ortamının oluşturulması amaçlanmaktadır.

2 MATERYAL VE METOTLAR

Bu bölümde, önerilen VideoMAE tabanlı çift yönlü işaret dili tercüme sisteminin geliştirilme sürecinde izlenen yöntemsel yaklaşım ayrıntılı olarak açıklanmaktadır. Çalışmanın metodolojisi; veri setinin oluşturulması ve ön işlenmesi, model mimarisinin tasarımı, eğitim süreci ve başarımların değerlendirme adımlarından oluşmaktadır. Sunulan yöntemsel çerçeve, literatürde önerilen güncel derin öğrenme tabanlı işaret dili tanıma yaklaşımlarıyla uyumlu olacak şekilde yapılandırılmıştır.

Çift Yönlü İşaret Dili Tercüme Sistemi



Şekil 2. Çift Yönlü İşaret Dili Tercüme Sisteminin Genel İş Akışı.

Şekil 2’de, Türk İşaret Dili sağlık terminolojisine yönelik geliştirilen çift yönlü işaret dili tercüme sisteminin genel mimarisi ve işlem adımları gösterilmektedir. Sunulan iş akışı; veri toplama ve ön işleme, VideoMAE tabanlı model eğitimi, performans değerlendirme ve sistem çıktılarının üretilmesi aşamalarını kapsamaktadır. Bu bütüncül yapı, hem işaret → metin/ses hem de metin → işaret dönüşümünü destekleyen çift yönlü bir iletişim altyapısının oluşturulmasına olanak tanımaktadır.

2.1 Veri Seti

Bu çalışmada kullanılan veri seti, Türk İşaret Dili’nin sağlık alanında kullanılan terminolojisini kapsayacak şekilde özel olarak hazırlanmıştır. Veri seti, farklı yaş gruplarından ve fiziksel özelliklere sahip işaretleyiciler tarafından kaydedilmiş 20.000’den fazla video içermekte olup, 7.000’in üzerinde benzersiz sağlık terimini kapsamaktadır. Bu terimler; hastalık adları, semptom ifadeleri, tedavi süreçlerine yönelik kavramlar ve hasta-doktor iletişiminde sık kullanılan yönlendirici ifadelerden oluşmaktadır.

Veri toplama sürecinde, gerçek klinik ortamlarda karşılaşılabilecek varyasyonları yansıtmak amacıyla kayıtlar farklı hızlarda, kamera açıları ve aydınlatma koşullarında gerçekleştirilmiştir. Ayrıca işaretleyicilerin el baskınlığı, yüz ifadeleri ve beden duruşlarındaki bireysel farklılıklar özellikle gözetilmiştir. Bu çeşitlilik, modelin farklı kullanıcı profillerine karşı genelleme yeteneğini artırmayı hedefleyen önemli bir tasarım tercihidir [2].

Veri setine uygulanan ön işleme adımları aşağıdaki aşamalardan oluşmaktadır:

Zamansal yeniden örnekleme: Video sekansları belirli kare uzunluklarına normalize edilmiştir.

Uzamsal yeniden boyutlandırma: Tüm kareler VideoMAE giriş formatına uygun olacak şekilde 224×224 piksel çözünürlüğe ölçeklendirilmiştir.

Normalizasyon: Piksel değerleri standartlaştırılarak modelin öğrenme süreci stabilize edilmiştir.

Patch bölütleme: VideoMAE mimarisine uygun olarak videolar uzamsal ve zamansal yamalara ayrılmıştır.

Bu ön işleme süreci, modelin hem uzamsal hem de zamansal özellikleri daha etkili bir biçimde öğrenmesine katkı sağlamaktadır.

2.2 VideoMAE Mimarisi

VideoMAE mimarisi, Vision Transformer (ViT) tabanlı bir encoder ve yalnızca ön eğitim (pretraining) aşamasında kullanılan hafif bir decoder yapısından oluşmaktadır. Encoder bileşeni, maskelenmemiş video yamaları üzerinden öğrenme gerçekleştirerek uzamsal ve zamansal bağımlılıkları yüksek boyutlu gizil temsiller hâlinde kodlamaktadır. Decoder ise maskelenmiş bölgelerin yeniden inşası amacıyla kullanılarak self-supervised öğrenme sürecini desteklemektedir [6], [7].

Bu çalışmada VideoMAE'nin tercih edilmesinin temel nedeni, yüksek maskeleme oranlarına rağmen anlamlı video temsilleri öğrenebilme yeteneğidir. Bu özellik, özellikle işaret dili gibi uzun süreli ve karmaşık hareket dizilerini içeren uygulamalarda önemli avantajlar sunmaktadır. Çok başlı dikkat mekanizmaları sayesinde, el, kol ve yüz hareketleri arasındaki uzun menzilli ilişkiler etkili bir biçimde modellenenmektedir.

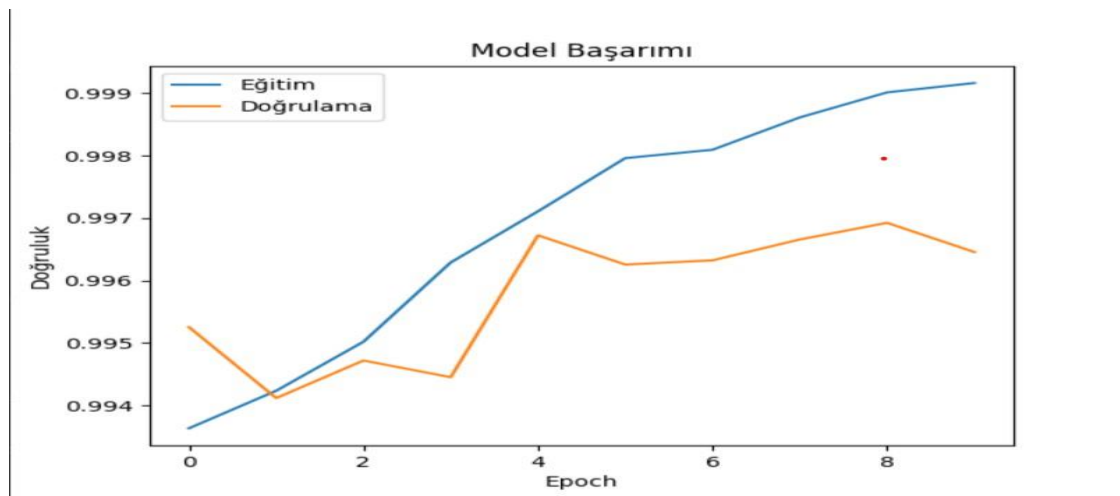
Klasik CNN ve RNN tabanlı yöntemlerle karşılaştırıldığında, VideoMAE mimarisi uzun video sekanslarında bilgi kaybını azaltmakta ve daha küresel bir bağlam öğrenimi sağlamaktadır. Bu yönüyle mimari, sağlık alanına özgü dinamik işaretlerin temsil edilmesi için uygun bir yapı sunmaktadır [8],[9].

2.3 Model Eğitimi ve Başarım Analizi

Model eğitimi sürecinde doğruluk (accuracy) ve kayıp (loss) metrikleri temel performans ölçütleri olarak kullanılmıştır. Eğitim ve doğrulama aşamalarında elde edilen metrikler, modelin öğrenme sürecini izlemek ve genelleme yeteneğini değerlendirmek amacıyla düzenli olarak analiz edilmiştir.

Şekil 2.3'te, modelin eğitim süreci boyunca gösterdiği doğruluk ve kayıp eğrileri sunulmaktadır. Eğitim ve doğrulama doğruluk eğrilerinin birbirine yakın seyretmesi, modelin aşırı öğrenme eğilimi göstermediğini ve genelleme yeteneğini koruduğunu ortaya koymaktadır. Benzer şekilde kayıp değerlerindeki istikrarlı azalış, ön işleme adımlarının ve seçilen mimarinin model performansına olumlu katkı sağladığını göstermektedir.

Model başarımı yalnızca nicel metrikler üzerinden değil, aynı zamanda dinamik işaretlerin ayırt edilebilirliği açısından yapılan nitel gözlemlerle de değerlendirilmiştir. Özellikle ardışık el hareketleri ve yüz ifadeleri içeren karmaşık sağlık işaretlerinde modelin tutarlı ve kararlı tahminler üretebildiği gözlemlenmiştir.



Şekil 2.3. Model Başarım Grafiği.

Eğitim ve doğrulama doğruluk eğrileri, modelin epoklar ilerledikçe artan bir performans sergilediğini ve genelleme yeteneğini koruduğunu göstermektedir.

3 BULGULAR VE TARTIŞMA

Deneyisel sonuçlar, VideoMAE tabanlı modelin sağlık alanına özgü dinamik işaretleri temsil etme konusunda yüksek bir potansiyele sahip olduğunu göstermektedir. Maskeli video modelleme yaklaşımı, özellikle el, kol ve yüz hareketlerinin zamansal bütünlüğünü koruyarak anlamlı temsil öğrenimine katkı sağlamaktadır. Elde edilen bulgular, literatürdeki benzer çalışmalarla uyumlu olup VideoMAE'nin işaret dili tanıma uygulamaları için uygun bir mimari olduğunu desteklemektedir [10], [11].

Modelin eğitim süreci boyunca doğruluk ve kayıp metriklerinde gözlemlenen istikrarlı iyileşme, kullanılan veri setinin kalitesini ve uygulanan ön işleme adımlarının etkinliğini ortaya koymaktadır. Eğitim ve doğrulama doğruluk eğrilerinin birbirine yakın seyretmesi, modelin aşırı öğrenme (overfitting) eğilimi göstermediğini ve genelleme yeteneğini koruduğunu göstermektedir. Bu durum, sağlık alanında farklı kullanıcı profilleri ve işaretleme stilleriyle karşılaşılması beklenen gerçek dünya senaryoları açısından önemli bir avantaj sunmaktadır[12].

Maskeli video modelleme stratejisinin sağladığı en önemli katkılardan biri, modelin sınırlı görünür bilgi üzerinden bağlamsal ilişkileri öğrenebilmesidir. Sağlık terminolojisine ait işaretlerde sıklıkla karşılaşılan ardışık ve ince motor hareketler, VideoMAE mimarisinin sunduğu uzun menzilli bağımlılık modelleme yeteneği sayesinde daha etkili bir biçimde temsil edilebilmektedir. Bu durum, geleneksel CNN ve RNN tabanlı yöntemlerde sıkça karşılaşılan Zamansal bilgi kaybının azaltılmasına katkı sağlamaktadır [13],[14].

Elde edilen bulgular, Transformer tabanlı mimarilerin işaret dili tanıma alanında sunduğu avantajları doğrular niteliktedir. Özellikle çok başlı dikkat mekanizmaları, el hareketleri ile yüz ifadeleri arasındaki ilişkilerin bütüncül olarak değerlendirilmesine olanak tanımaktadır. Bu özellik, sağlık alanında anlam değişimine yol açabilecek küçük hareket farklılıklarının daha doğru biçimde ayırt edilmesini mümkün kılmaktadır.

Büyük ölçekli veri setleri üzerinde eğitimin mümkün hâle gelmesi için paralel programlama ve GPU hızlandırmalı eğitim altyapılarının kullanılması, sistemin ölçeklenebilirliğini önemli ölçüde artırmaktadır. Dağıtık eğitim yaklaşımları sayesinde, modelin eğitim süresi makul seviyelerde tutulurken, daha geniş veri setleriyle çalışma imkânı elde edilmiştir. Bu durum, ilerleyen aşamalarda veri setinin genişletilmesi ve model performansının daha da iyileştirilmesi açısından önemli bir avantaj sunmaktadır.

Son olarak, elde edilen sonuçlar yalnızca teknik performans açısından değil, aynı zamanda uygulama potansiyeli açısından da değerlendirildiğinde, önerilen sistemin sağlık alanında duyma engelli bireylerin iletişim deneyimini iyileştirebilecek güçlü bir altyapı sunduğu görülmektedir. VideoMAE tabanlı yaklaşımın sunduğu temsil gücü ve ölçeklenebilirlik, sistemin gerçek klinik ortamlarda uygulanabilirliğini destekleyen önemli bulgular arasında yer almaktadır.

4 SONUÇ

Bu çalışmada, sağlık alanında duyma engelli bireylerin karşılaştığı iletişim engellerini azaltmaya yönelik olarak Video Masked Autoencoder (VideoMAE) tabanlı çift yönlü bir Türk İşaret Dili tercüme sistemi önerilmiştir. Sunulan yaklaşım, video tabanlı derin öğrenme mimarilerinin sunduğu uzamsal ve zamansal temsil gücünden yararlanarak sağlık terminolojisine özgü dinamik işaretlerin etkili bir biçimde modellenmesini amaçlamaktadır.

Elde edilen deneyisel bulgular, VideoMAE tabanlı modelin işaret dili tanıma görevinde anlamlı ve ayırt edici temsiller öğrenebildiğini göstermektedir. Maskeli video modelleme yaklaşımının sağladığı veri verimliliği, büyük ölçekli video veri setleri üzerinde eğitim yapılmasını

mümkün kılarken, modelin genelleme yeteneğini de olumlu yönde etkilemiştir. Bu yönüyle önerilen sistem, sağlık alanına yönelik işaret dili uygulamaları için güçlü bir teknik temel sunmaktadır.

Çalışmanın önemli katkılarından biri, yalnızca işaret → metin/ses dönüşümüne odaklanmakla kalmayıp, aynı zamanda metin → işaret dönüşümünü de destekleyen çift yönlü bir iletişim altyapısını hedeflemesidir. Bu yaklaşım, sağlık personeli ile duyma engelli bireyler arasında daha doğal, hızlı ve güvenilir bir iletişim ortamının oluşturulmasına olanak tanımaktadır. Özellikle acil servis ve poliklinik gibi zamanın kritik olduğu sağlık ortamlarında, bu tür sistemlerin erişilebilirliği artırma potansiyeli bulunmaktadır.

Bununla birlikte, çalışma bazı sınırlılıklar içermektedir. Model performansı bu aşamada sınırlı sayıda metrik üzerinden değerlendirilmiş olup, gerçek klinik ortamlarda elde edilecek kullanıcı geri bildirimleri henüz dâhil edilmemiştir. Ayrıca, sistemin gerçek zamanlı çalışabilirliği ve farklı donanım yapılandırmaları üzerindeki performansı kapsamlı biçimde test edilmemiştir.

Gelecek çalışmalarda, önerilen sistemin gerçek klinik senaryolarda uygulanması, kullanıcı deneyimi odaklı değerlendirmelerin yapılması ve gerçek zamanlı performansının analiz edilmesi planlanmaktadır. Bunun yanı sıra, veri setinin genişletilmesi, farklı işaretleyici profillerinin eklenmesi ve avatar tabanlı metin → işaret modülünün geliştirilmesiyle sistemin pratik kullanım değerinin artırılması hedeflenmektedir. Sonuç olarak, bu çalışma VideoMAE tabanlı derin öğrenme yaklaşımlarının sağlık alanına özgü işaret dili tercüme sistemleri için umut vadeden bir çözüm sunduğunu ortaya koymaktadır.

KAYNAKÇA

- [1] O. Koller, “Deep learning-based sign language recognition and translation: A review,” *Machine Learning*, c. 109, s. 9–10, ss. 1811–1831, 2020.
- [2] N. C. Camgoz, O. Koller, S. Hadfield ve R. Bowden, “Neural sign language translation,” *Proc. IEEE Conf. Comput. Vis. Pattern Recognit. (CVPR)*, 2018.
- [3] A. Arnab, M. Dehghani, G. Heigold ve C. Sun, “ViViT: A video vision transformer,” *Proc. IEEE/CVF Int. Conf. Comput. Vis. (ICCV)*, 2021.
- [4] K. He, X. Chen, S. Xie, Y. Li, P. Dollár ve R. Girshick, “Masked autoencoders are scalable vision learners,” *Proc. IEEE/CVF Conf. Comput. Vis. Pattern Recognit. (CVPR)*, 2022.
- [5] A. Dosovitskiy, L. Beyer, A. Kolesnikov *et al.*, “An image is worth 16×16 words: Transformers for image recognition at scale,” *Int. Conf. Learn. Representations (ICLR)*, 2021.
- [6] N. C. Camgoz, O. Koller, H. Ney ve R. Bowden, “Sign language transformers: Joint end-to-end sign language recognition and translation,” *Proc. IEEE/CVF Conf. Comput. Vis. Pattern Recognit. (CVPR)*, 2020.
- [7] A. Graves, *Supervised Sequence Labelling with Recurrent Neural Networks*. Berlin, Germany: Springer, 2012.
- [8] J. Martinez, M. J. Black ve J. Romero, “On human motion prediction using recurrent neural networks,” *Proc. IEEE Conf. Comput. Vis. Pattern Recognit. (CVPR)*, 2017.
- [9] H. Fang, S. Xie, C. Wang, Y. Fang ve C. Lu, “RMPE: Regional multi-person pose estimation,” *Proc. IEEE Int. Conf. Comput. Vis. (ICCV)*, 2017.
- [10] D. Bragg, O. Koller, M. Bellard *et al.*, “Sign language recognition, generation, and translation: An interdisciplinary perspective,” *Proc. 21st Int. ACM SIGACCESS Conf. Comput. Accessibility*, 2019.
- [11] M. Müller, T. Röder ve M. Clausen, *Motion Capture for Animation*. San Francisco, CA, USA: Morgan Kaufmann, 2005.

- [12] J. Pu, W. Zhou ve H. Li, “Iterative alignment network for continuous sign language recognition,” *Proc. IEEE/CVF Conf. Comput. Vis. Pattern Recognit. (CVPR)*, 2019.
- [13] J. Shotton, A. Fitzgibbon, M. Cook *et al.*, “Real-time human pose recognition in parts from a single depth image,” *Proc. IEEE Conf. Comput. Vis. Pattern Recognit. (CVPR)*, 2011.
- [14] H. Zhou, W. Zhou ve H. Li, “Dynamic pseudo labels for continuous sign language recognition,” *Proc. IEEE/CVF Conf. Comput. Vis. Pattern Recognit. (CVPR)*, 2020.



AN EXAMINATION OF THE EFFECT OF CHANNEL HEIGHT ON HEAT TRANSFER WITHIN A CHIP-EMBEDDED MINICHANNEL

Fatih TAŞDELEN 

Bitlis Eren University, Vocational School of Technical Sciences, Bitlis, Türkiye
ftasdelen@beu.edu.tr

ABSTRACT

This study aims to examine how channel height influences the heat transfer efficacy of a chip within minichannels. A two-dimensional computational fluid dynamics (CFD) analysis was performed to investigate the effect of channel height on heat transfer in a chip situated within rectangular minichannels of varying heights. Air at an inlet temperature of 300 K was used as the cooling fluid, with a continuous heat flux of 50 kW/m² applied to the chip surface. For a more precise assessment of convective heat transfer, the channel walls were considered adiabatic. Numerical calculations were conducted for different Reynolds numbers (Re = 100, 200, and 300) and for different channel heights (H = 1, 1.5, and 2 mm). The evaluation of thermal performance involved analysing differences between the local and average Nusselt numbers, as well as temperature distributions across the chip surface. The results show that increasing the Reynolds number lowers the chip surface temperature and raises the average Nusselt number, while increasing the channel height leads to higher chip surface temperatures. When the Reynolds number increased from 100 to 300, at a channel height of 1 mm, the chip surface temperature dropped from 499.15 K to 456.88 K, while the average Nusselt number increased from 11.08 to 13.15. Similarly, at a channel height of 2 mm, the chip surface temperature decreased from 607.72 K to 528.12 K, and the average Nusselt number rose from 9.89 to 13.32. The results indicate that channel height and flow conditions are essential in influencing the cooling efficacy of a chip's minichannel design.

Keywords: Mini-channel cooling, Heat transfer, CFD, Nusselt number, Reynolds number.

1 INTRODUCTION

The rising thermal output from diverse electronic devices and components has necessitated the development of sophisticated cooling technologies that provide optimal performance and improved dependability. To avert system problems caused by overheating, it is crucial to implement effective and creative cooling techniques to keep chip temperatures within safe parameters [1]. Consequently, researchers have created multiple thermal management techniques and cooling mechanisms to regulate the rising temperature. Yu et al. [2] developed an innovative approach for the construction of microchannel heat sinks to reduce hot spot temperatures. Following the assessment of microchannel performance by the CFD, they corroborated the findings with analytical results. They illustrated the method for decreasing the hot spot temperature in a rectangular flow channel. Kozłowska et al. [3] conducted computational modelling and an experimental investigation of a small microchannel cooler using micropipes for

coolant transport. They built mathematical and three-dimensional numerical models of the proposed cooler design and conducted a series of numerical simulations for different mass flow rates of the cooling medium. Zehtabiyani-Rezaie et al. [4] undertook a numerical and analytical investigation into the heat transfer and entropy generation during both the developing and fully developed stages of stratified two-phase flow within a mini-channel. The researchers explored the effects of various parameters, including the Reynolds number, heat flux ratio, and volumetric flow rate ratio, on the flow field, heat transfer, and entropy generation. Mehta and Khandekar [5] examined the effect of imposed vibrations on laminar, thermally developing, single-phase flow and heat transfer in a square-section mini-channel. The frequency was regarded as the only variable, while the amplitude and Reynolds number of the flow vibrations were held constant. Spizzichino et al. [6] experimentally investigated the flow field in small-scale channels with different geometries. By varying the Reynolds number and the wall temperature, they aimed to analyse and improve thermal performance under different flow velocities, temperatures, and geometric configurations. Mehta and Khandekar [7] conducted an experimental study on the thermohydrodynamics of a thermally developed single-phase laminar flow of water in a square-section mini-channel. They reported that the developing flows, by exhibiting high heat transfer coefficients in the inlet regions, are suitable for mini/micro-scale applications that remove high heat flux. Kaushik et al. [8] performed a comparative analysis utilising experimental and simulation data to evaluate the $\text{Al}_2\text{O}_3 + \text{CuO} + \text{ZnO} + \text{H}_2\text{O}$ nanofluid against water as the sole fluid. The $\text{CuO} + \text{ZnO} + \text{H}_2\text{O}$ nanofluid demonstrated superior performance relative to water regarding fluid flow, thermal behaviour, and heat conduction parameters. Wu et al. [9] conducted simulations of water flow utilising nano-encapsulated phase change material for the purpose of cooling a CPU located within a mini-channel. The increase in Reynolds number and CPU heat flux resulted in a decrease and an increase in the melting fraction, respectively. Abed et al. [10] conducted an integrated experimental and numerical investigation into the characteristics of laminar flow and forced convection heat transfer within a square cross-section wavy microchannel. The study concluded that the serpentine microchannel improves heat transfer performance relative to a straight microchannel across the full spectrum of Dean numbers. Ghasemian et al. [11] conducted a numerical investigation of laminar forced convection heat transfer in a water-based Fe_3O_4 ferrofluid within a mini-channel featuring isothermal surfaces. Vortices were found to disrupt the thermal boundary layer, resulting in enhanced heat transfer. Sandler et al. [12] considered flow-boiling in mini- and microchannels as an effective method for cooling mobile devices and electronic components and examined in detail the low-pressure refrigerants R236fa and R245fa, with particular emphasis on the influence of saturation temperature on flow-boiling behaviour. Sajith et al. [13] performed studies on convective heat transfer in channels with hydraulic diameters of 3 mm and 4 mm. The experiments were conducted with varying heat inputs and mass flow rates, while temperature profiles were analysed across different Reynolds numbers and heating levels. Ho et al. [14] conducted an experimental investigation into the cooling characteristics of mini-channel heat sinks using water-based emulsions of nano-phase change materials. Increasing the Reynolds number within the range of 960-1381 led to a reduction in average convective heat transfer efficiency. Mortean and Mantelli [15] conducted a theoretical and experimental thermal analysis of laminar and transition flows in a diffusion-bonded cross-flow compact heat exchanger, proposing a novel Nusselt number correlation for the transition regime. Oyinlola et al. [16] conducted experimental studies to investigate the effects of micro-channel geometry on the thermal and hydraulic performance of absorber plates. As a result, they found that the heat transfer coefficient is strongly dependent on fluid velocity, and the Nusselt number depends on the Reynolds number.

The primary objective of this study is to investigate the influence of different channel heights on fluid flow and thermal transfer within the mini-channel. Consequently, flow and thermal evaluations of a mini-channel housing a heated electronic chip were conducted for varying channel heights ($H = 1, 1.5, \text{ and } 2 \text{ mm}$) using varied Reynolds number values ($\text{Re} = 100, 200, \text{ and}$

300). The mini-channel was developed as a two-dimensional model, and numerical studies were performed using the ANSYS FLUENT software under CFD-based laminar flow conditions. The present study thoroughly examined the critical influence of channel heights on the flow regime and heat transfer. The results offer direction for engineering solutions by demonstrating the impact of varying channel heights on cooling efficacy.

2 NUMERICAL METHODOLOGY

2.1 Geometric Framework and Boundary Condition Parameters

A two-dimensional mini-channel configuration was developed in the DesignModeler module of the simulation software. The configuration of the two-dimensional constructed channel is illustrated in Figure 1. After designing the channel geometry, it is essential to determine the boundary conditions for the established geometry before commencing the numerical analysis.

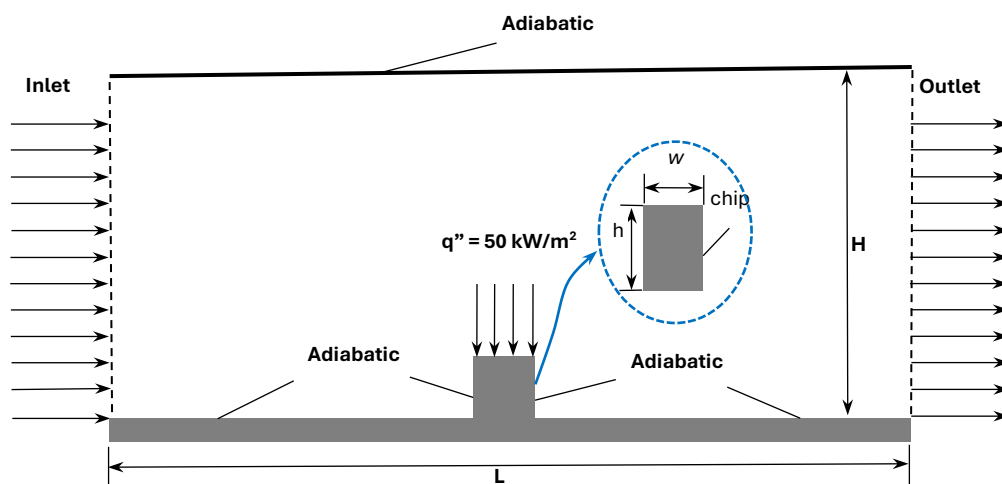


Figure 1. A schematic depiction of the mini-channel containing the chip

Figure 1 displays that the mini-channel has a length of $L = 10$ mm, while the chip is designed with a height of $h = 0.5$ mm and a surface width of $w = 1$ mm. The mini-channel's top and bottom walls, along with the chip side surfaces, are considered adiabatic, while the chip surface exhibits a heat flux of $q'' = 50$ kW/m². Silicon was selected as the channel and chip material due to its mechanical durability and compatibility with microfabrication techniques. The numerical analyses examined heat transfer on the chip surface across various channel heights ($H = 1, 1.5$, and 2 mm) for different Reynolds numbers ($Re = 100, 200$, and 300), using air with an inlet temperature of $T = 300$ K. Table 1 presents the thermophysical properties of the silicon and air used in the simulation.

Table 1. Thermophysical parameters of the silicon and air

Parameters	Units	Values
Density of silicon	[kg/m ³]	2330
Specific heat capacity of silicon	[J/kgK]	710
Thermal conductivity of silicon	[W/mK]	148
Density of air	[kg/m ³]	1.176

Specific heat capacity of air	[J/kgK]	1007
Thermal conductivity of air	[W/mK]	0.02566
Dynamic viscosity of air	[kg/(ms)]	1.858×10^{-5}

The material properties outlined in Table 1 serve as the inlet boundary conditions for the simulation model.

2.2 Grid Independence Study

Grid independence analysis thoroughly evaluated the independence of the numerical solution from the grid structure. The results for various grid densities were compared to identify the best grid structure, where the solution stabilised. Figure 2 illustrates the best grid configuration for the two-dimensional planned channel. To enhance the precision of the heat transfer resulting from the heat flux supplied to the chip's surface, a finer, optimised grid was utilised in this area, as illustrated in Figure 2.

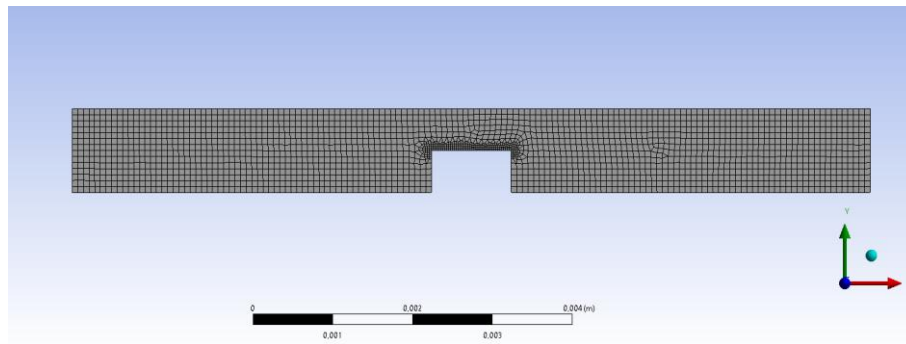


Figure 2. The grid structure of the mini-channel containing the chip

Table 2 displays the mean Nusselt number values on the chip surface for various node numbers. It indicates that the mean Nusselt number is 11.08 for node numbers 2060 and 2330, with convergence of the solution observed. As a result, a node number of 2330 was chosen for the flow and heat transfer solution within the channel.

Table 2. Mean Nusselt numbers on the chip surface for different node numbers

Node number	Mean Nu Number
1066	10.56
1305	10.62
1639	10.61
1945	10.89
2060	11.08
2330	11.08

2.3 Governing Equations

This study assumes that the flow within a mini-channel is two-dimensional, steady, incompressible, Newtonian, and laminar. Fluid properties are considered constant. The governing equations (Eqs. 1-3) are presented below.

Continuity Equation

$$\frac{\partial u}{\partial x} + \frac{\partial v}{\partial y} = 0 \quad (1)$$

Navier–Stokes Equations

$$\rho \left(u \frac{\partial u}{\partial x} + v \frac{\partial u}{\partial y} \right) = -\frac{\partial p}{\partial x} + \mu \left(\frac{\partial^2 u}{\partial x^2} + \frac{\partial^2 u}{\partial y^2} \right) \quad (2a)$$

$$\rho \left(u \frac{\partial v}{\partial x} + v \frac{\partial v}{\partial y} \right) = -\frac{\partial p}{\partial y} + \mu \left(\frac{\partial^2 v}{\partial x^2} + \frac{\partial^2 v}{\partial y^2} \right) \quad (2b)$$

Energy Equation

$$\rho c_p \left(u \frac{\partial T}{\partial x} + v \frac{\partial T}{\partial y} \right) = k \left(\frac{\partial^2 T}{\partial x^2} + \frac{\partial^2 T}{\partial y^2} \right) \quad (3)$$

3 RESULTS AND DISCUSSION

3.1 Examination of the Velocity Distribution in Mini-Channels

This section assesses the velocity distributions within the channel at varying heights for Reynolds numbers of 100, 200, and 300. Figures 3-5 depict the velocity distributions for these Reynolds numbers, specifically at a channel height of 1 mm.

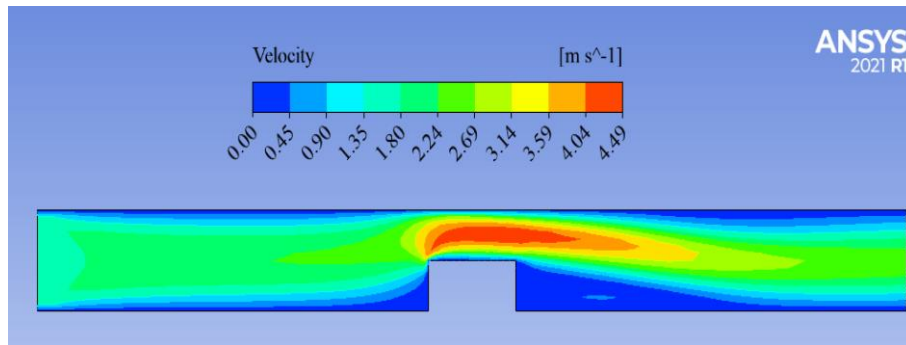


Figure 3. Velocity distributions within the channel ($H = 1$ mm, $Re = 100$)

Figures 3-5 indicate that flow velocity increases as the air fluid approaches the chip surface, attaining its maximum at the top surfaces of the chip. The maximum air flow velocities recorded at the top of the chip for 1 mm channel heights were 4.49 m/s, 8.49 m/s, and 12.54 m/s, corresponding to Reynolds numbers of 100, 200, and 300, respectively. Figures 6-8 illustrate the velocity distributions at Reynolds numbers of 100, 200, and 300 for channel heights of 1.5 mm.

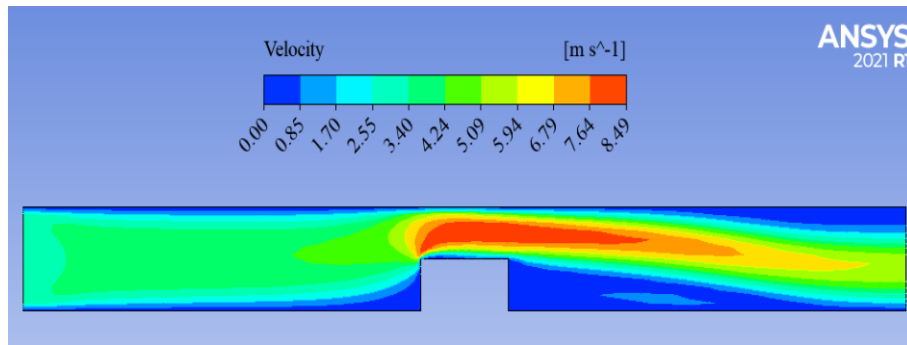


Figure 4. Velocity distributions within the channel ($H = 1$ mm, $Re = 200$)

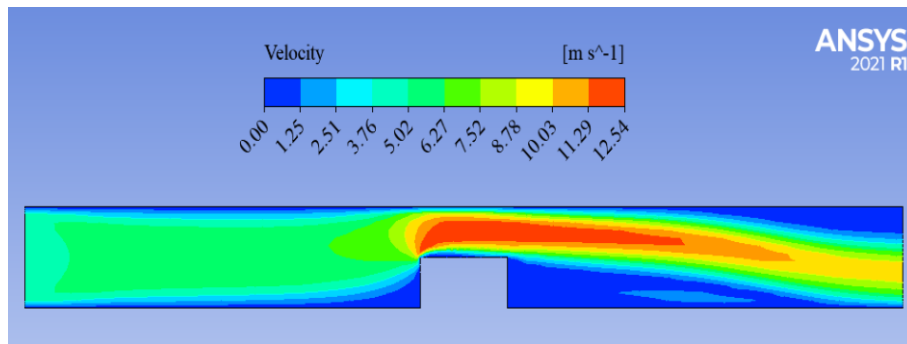


Figure 5. Velocity distributions within the channel ($H = 1$ mm, $Re = 300$)

Analysis of Figures 6-8 indicates that, similar to a 1 mm channel height, the air velocity increases as the chip nears the surface, achieving maximum air velocity above the chip. The observed maximum velocities at the top of the chip were 2.71 m/s, 5.11 m/s, and 7.51 m/s for Reynolds numbers of 100, 200, and 300, respectively.

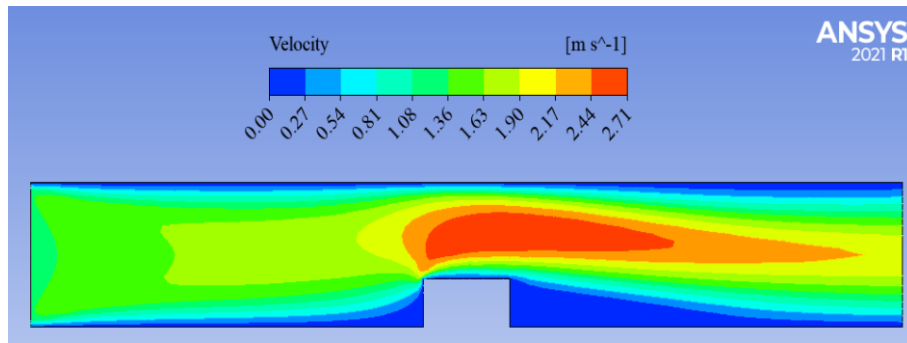


Figure 6. Velocity distributions within the channel ($H = 1.5$ mm, $Re = 100$)

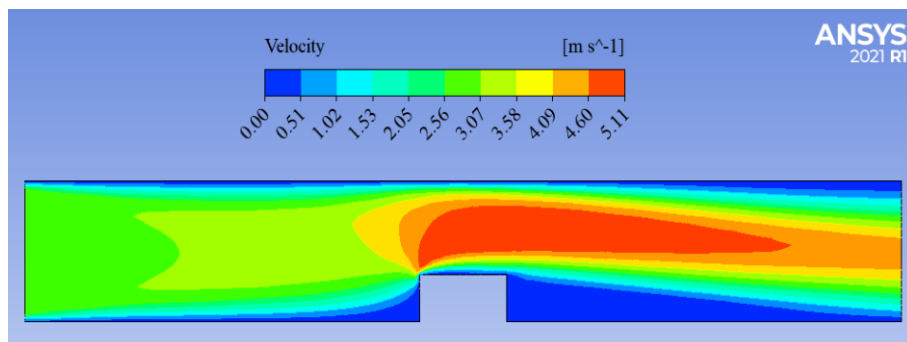


Figure 7. Velocity distributions within the channel ($H = 1.5$ mm, $Re = 200$)

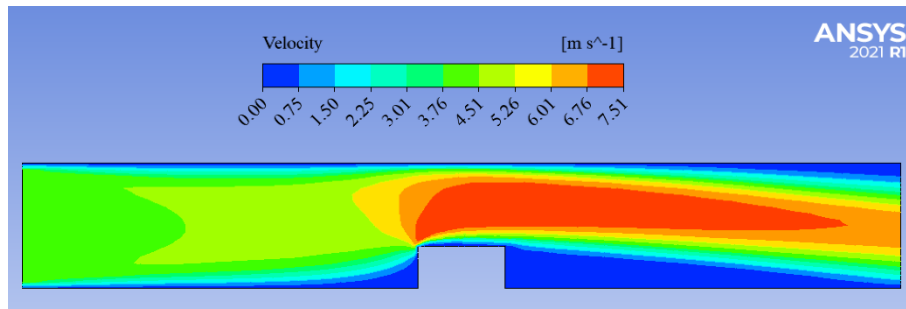


Figure 8. Velocity distributions within the channel ($H = 1.5$ mm, $Re = 300$)

Figures 9-11 present the velocity distributions at Reynolds numbers of 100, 200, and 300, respectively, for a channel height of 2 mm. The analysis of Figures 9-11 indicates that, similar to other channel heights, air velocity increases as the chip approaches the surface, achieving its peak directly above it. The highest recorded velocities at the top of the chip were 2.10 m/s, 3.99 m/s, and 5.89 m/s, corresponding to Reynolds numbers of 100, 200, and 300, respectively. Moreover, velocity analyses conducted at Reynolds numbers of 100, 200, and 300 revealed that velocity distributions within the channel diminished with increasing channel heights.

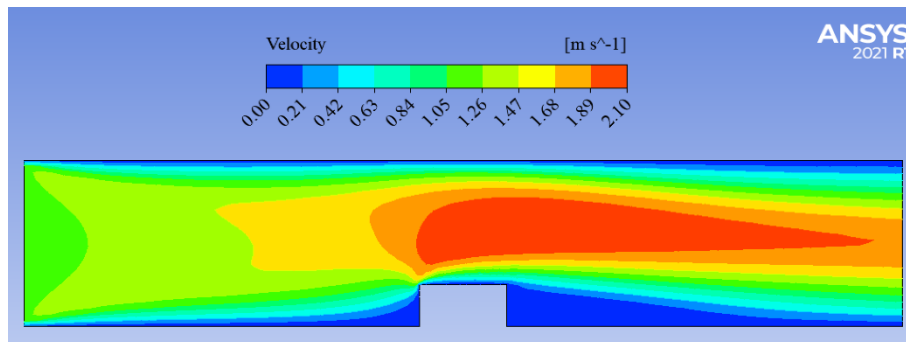


Figure 9. Velocity distributions within the channel ($H = 2$ mm, $Re = 100$)

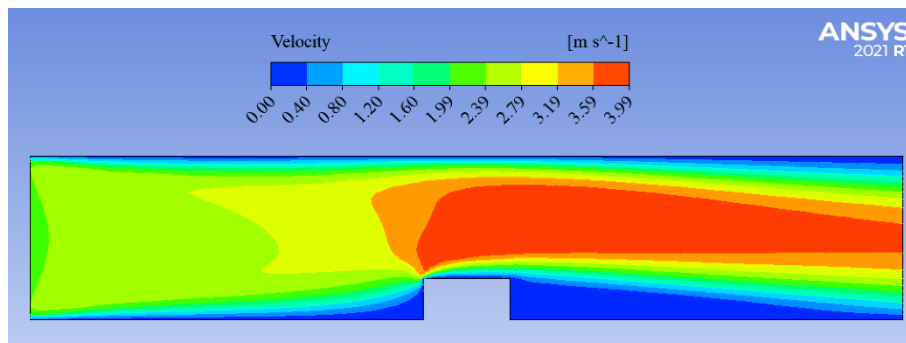


Figure 10. Velocity distributions within the channel ($H = 2$ mm, $Re = 200$)

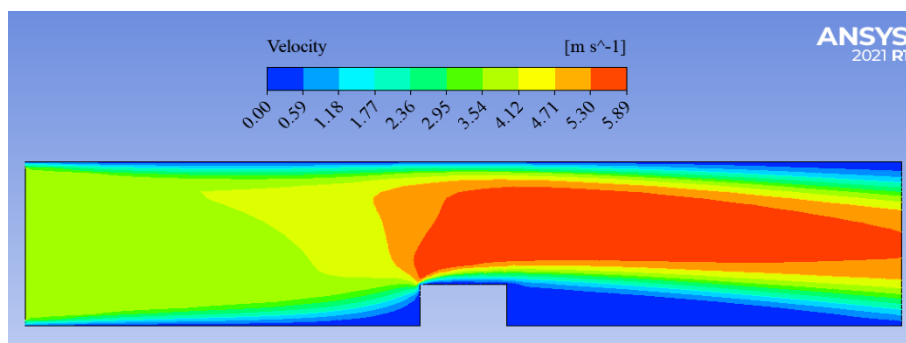


Figure 11. Velocity distributions within the channel ($H = 2$ mm, $Re = 300$)

3.2 Examination of Heat Transfer Behaviour in Mini-Channels

This section examines the temperature distributions within the channel and the heat transfer characteristics at the chip surface in detail. Numerical analyses conducted using ANSYS FLUENT assessed the temperature contours for Reynolds numbers of 100, 200, and 300, local temperature variations on the chip surface, and Nusselt number distributions across various channel heights ($H = 1$ mm, 1.5 mm, and 2 mm) to illustrate the thermal performance of the channels. Figures 12-14 present the temperature distributions for a channel height of $H = 1$ mm.

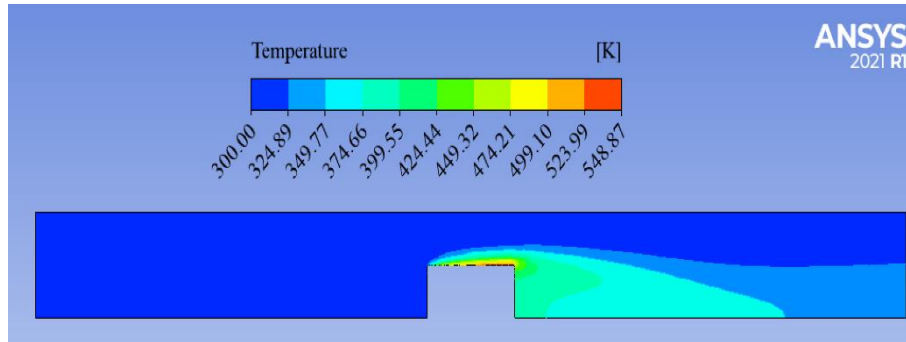


Figure 12. Temperature distributions within the channel ($H = 1$ mm, $Re = 100$)

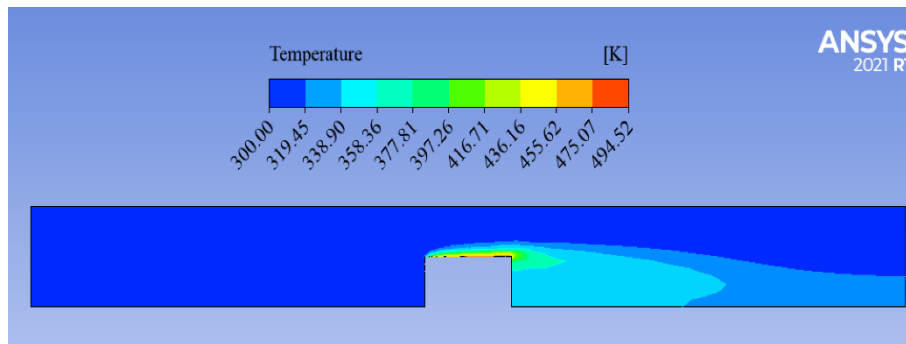


Figure 13. Temperature distributions within the channel ($H = 1$ mm, $Re = 200$)

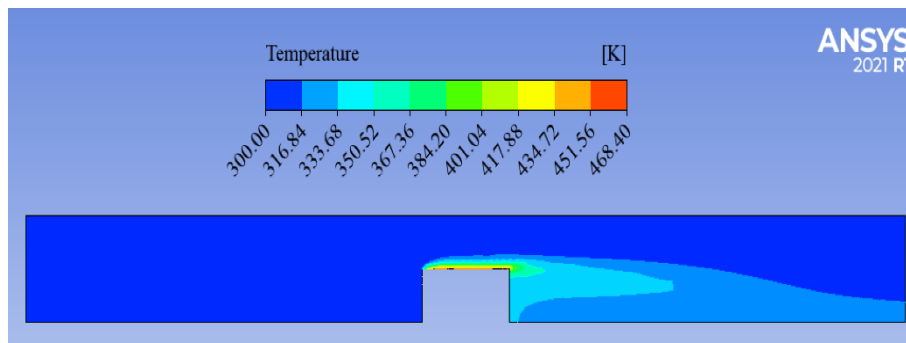


Figure 14. Temperature distributions within the channel ($H = 1$ mm, $Re = 300$)

Figures 12-14 demonstrate that heat transfer at the chip top surfaces is positively correlated with an increase in Reynolds number. At a channel height of $H = 1$ mm, maximum temperatures of 548.87 K, 494.52 K, and 468.40 K were observed at the chip top surfaces for Reynolds numbers of 100, 200, and 300, respectively. Figures 15-17 illustrate the temperature distributions for a channel height of $H = 1.5$ mm.

Figures 15-17 illustrate that heat transfer within the channel increased, resulting in decreased temperatures on the chip surfaces as the Reynolds number increased. At a channel

height of $H = 1.5$ mm, the maximum temperatures recorded at the chip surfaces were 648.04 K, 578.77 K, and 549.19 K for Reynolds numbers of 100, 200, and 300, respectively. Adjusting the channel height from $H = 1$ mm to $H = 1.5$ mm resulted in maximum temperature increases of 99.17 K, 84.25 K, and 80.79 K on the chip surface for Reynolds numbers of 100, 200, and 300, respectively. The observed temperature increases decreased concurrently with the rise in the Reynolds number. Figures 18-20 illustrate the temperature distributions for a channel height of $H = 2$ mm.

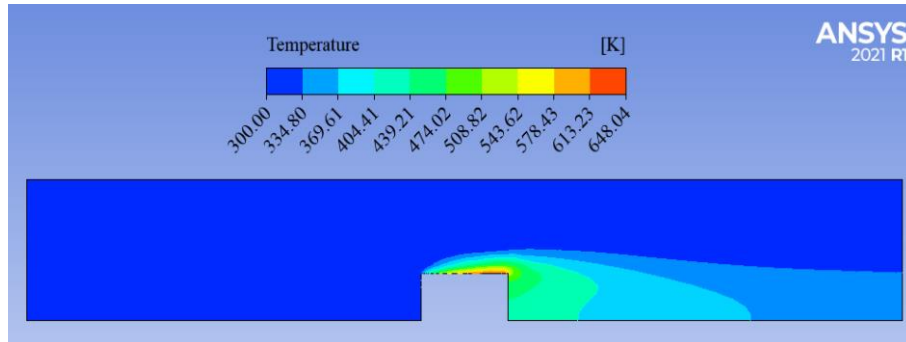


Figure 15. Temperature distributions within the channel ($H = 1.5$ mm, $Re = 100$)

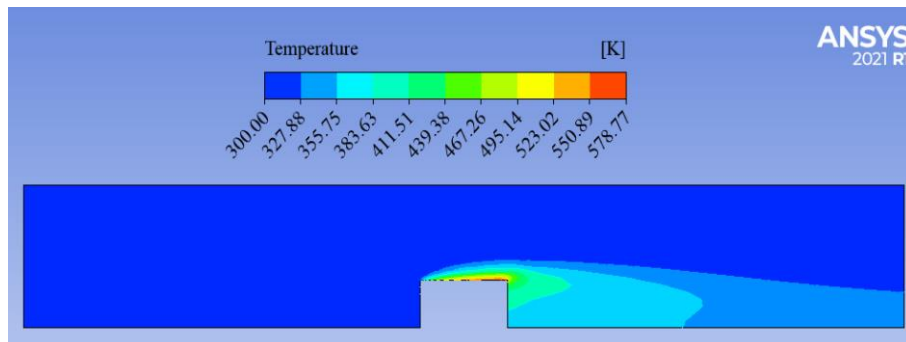


Figure 16. Temperature distributions within the channel ($H = 1.5$ mm, $Re = 200$)

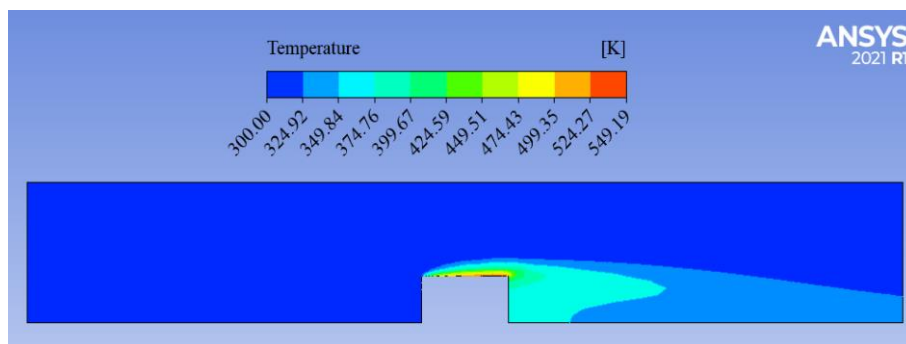


Figure 17. Temperature distributions within the channel ($H = 1.5$ mm, $Re = 300$)

As shown in Figures 18–20, similar to the channel heights of $H = 1$ mm and $H = 1.5$ mm, at a channel height of $H = 2$ mm, the heat transfer within the channel increases with increasing Reynolds number, and the temperatures on the chip surfaces decrease. For a channel height of $H = 2$ mm, the maximum temperatures observed on the chip surfaces at Reynolds numbers of 100, 200, and 300 were 701.90 K, 623.44 K, and 591.05 K, respectively. The results indicate that chip

surface temperatures rise as channel height increases. When the channel height is increased from $H = 1$ mm to $H = 2$ mm, the maximum temperature rises observed on the chip surfaces are 153.03 K, 128.92 K, and 122.65 K for Reynolds numbers of 100, 200, and 300, respectively. Figures 21 and 22 illustrate the graphs of the local Nusselt numbers and the temperature variations on the chip surface for a channel height of $H = 1$ mm at the same Reynolds numbers.

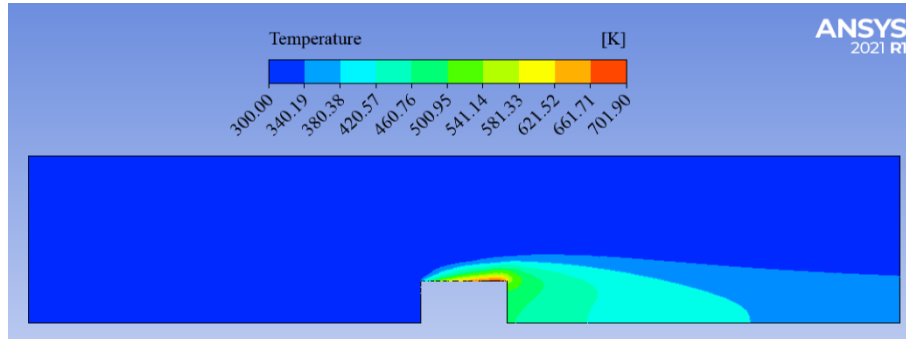


Figure 18. Temperature distributions within the channel ($H = 2$ mm, $Re = 100$)

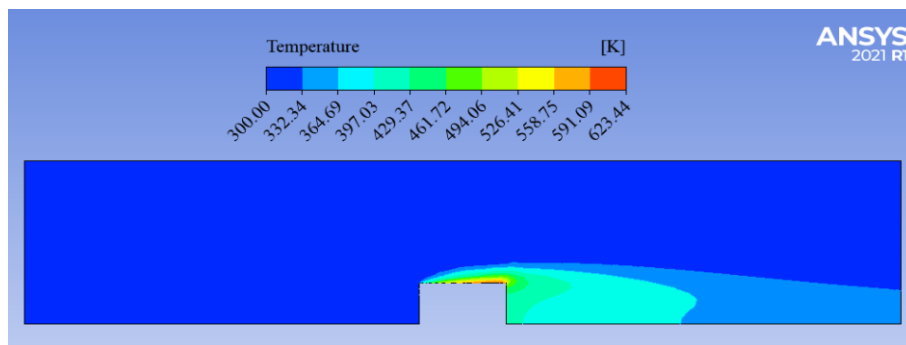


Figure 19. Temperature distributions within the channel ($H = 2$ mm, $Re = 200$)

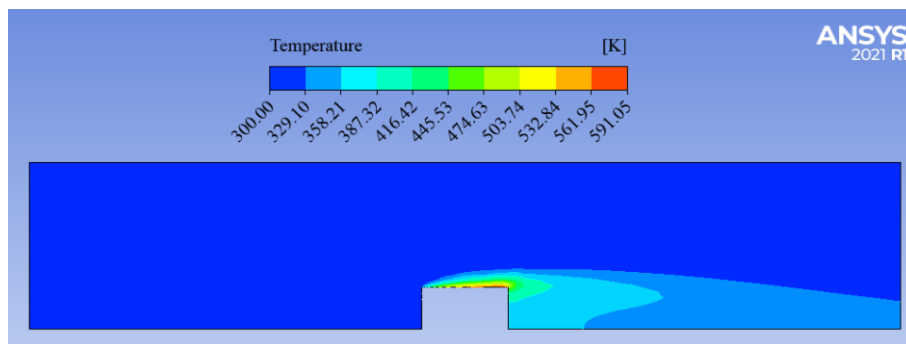


Figure 20. Temperature distributions within the channel ($H = 2$ mm, $Re = 300$)

Figure 21 illustrates that across all Reynolds number values, the local Nusselt numbers are elevated at the initial contact point between the air and the chip. Subsequently, these values decrease along the chip surface before attaining a stable state. Figure 22 corroborates Figure 21, demonstrating that elevated Nusselt numbers at the initial air-chip interface result in reduced chip surface temperatures in the contact area. Figure 22 illustrates that an increase in Reynolds number correlates with a decrease in temperatures on the chip surface of the air fluid.

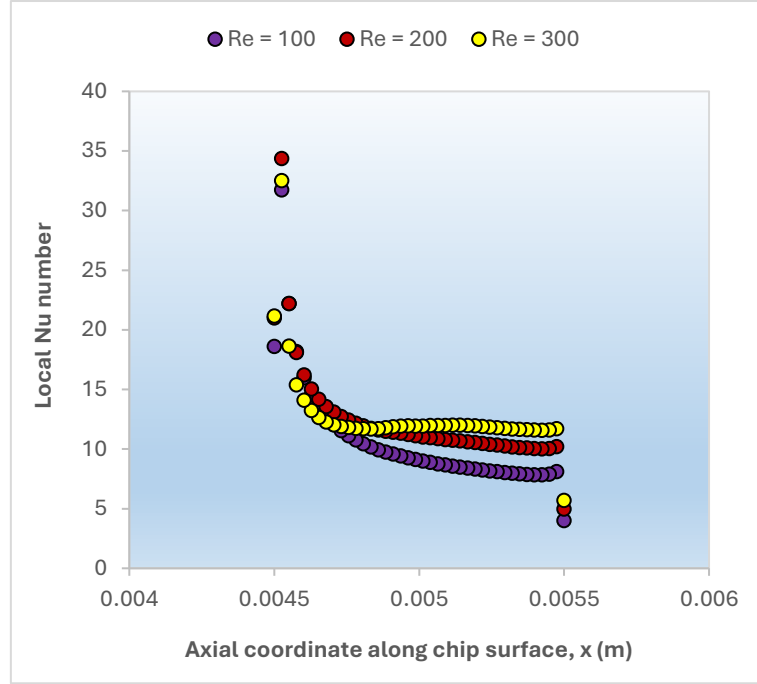


Figure 21. Local Nu number variations on the chip surface ($H = 1$ mm)

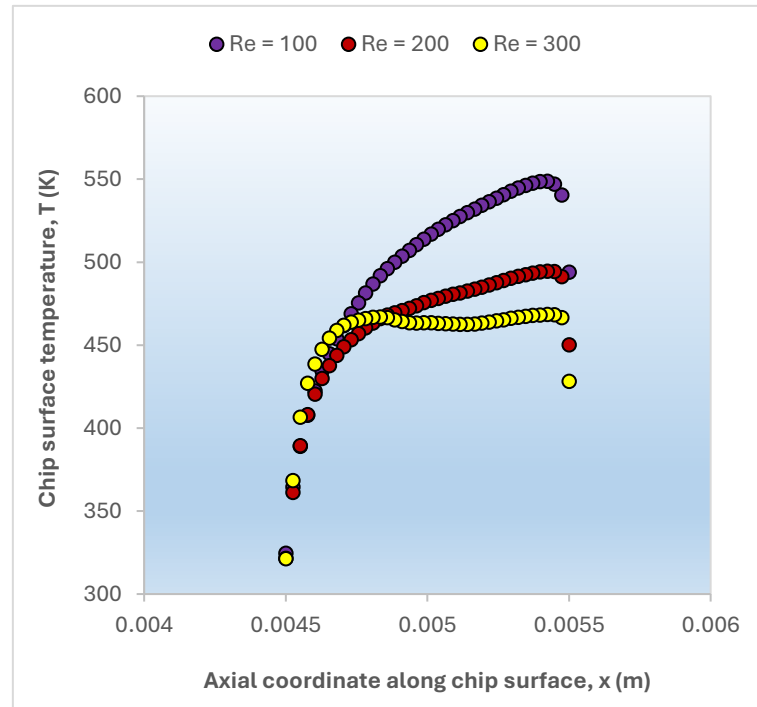


Figure 22. Temperature changes on the chip surface ($H = 1$ mm)

Figures 23 and 24 illustrate the graphs of local Nusselt numbers and temperature variations on the chip surface for a channel height of $H = 1.5$ mm at Reynolds numbers of 100, 200, and 300. Figure 23 illustrates that upon initial contact of the air with the chip, the local Nusselt numbers are elevated across all three Reynolds numbers, subsequently decreasing along the chip surface and demonstrating a more stable condition towards the end of the surface. Figure 24 demonstrates that a reduction in Reynolds number results in elevated chip surface temperatures.

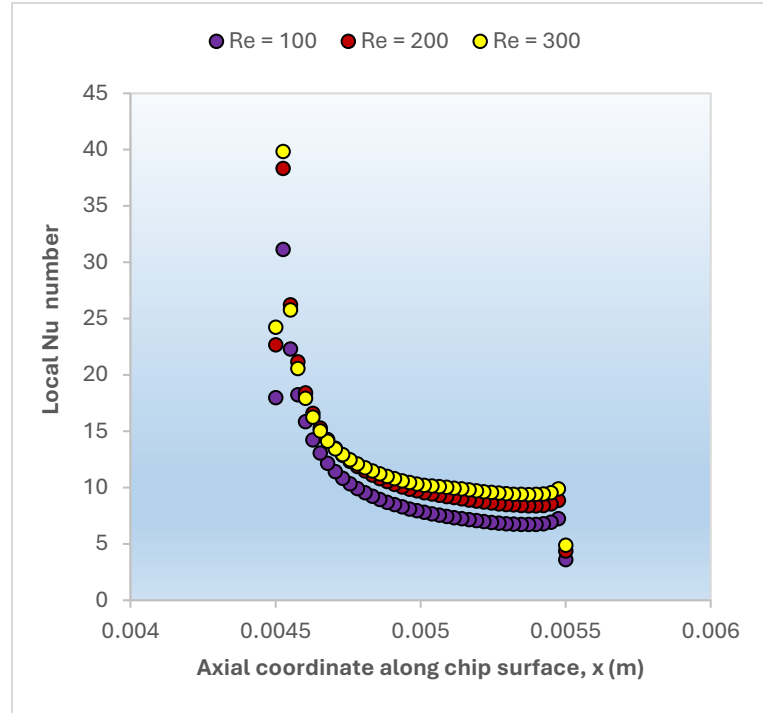


Figure 23. Local Nu number variations on the chip surface ($H = 1.5$ mm)

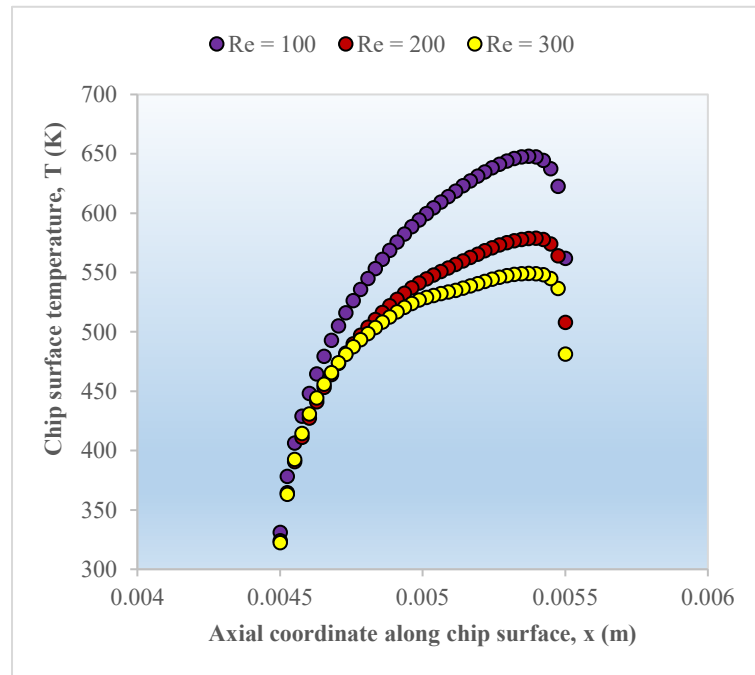


Figure 24. Temperature changes on the chip surface ($H = 1.5$ mm)

Figures 25 and 26 present the graphs of local Nusselt numbers and temperature variations on the chip surface for a channel height of $H = 2$ mm at Reynolds numbers of 100, 200, and 300, respectively. In Figure 25, similar to the channel heights of $H = 1$ mm and 1.5 mm, the high Nusselt numbers at the initial contact of the air fluid with the chip show a decreasing trend along the chip surface, while exhibiting a more stable condition toward the end of the chip surface.

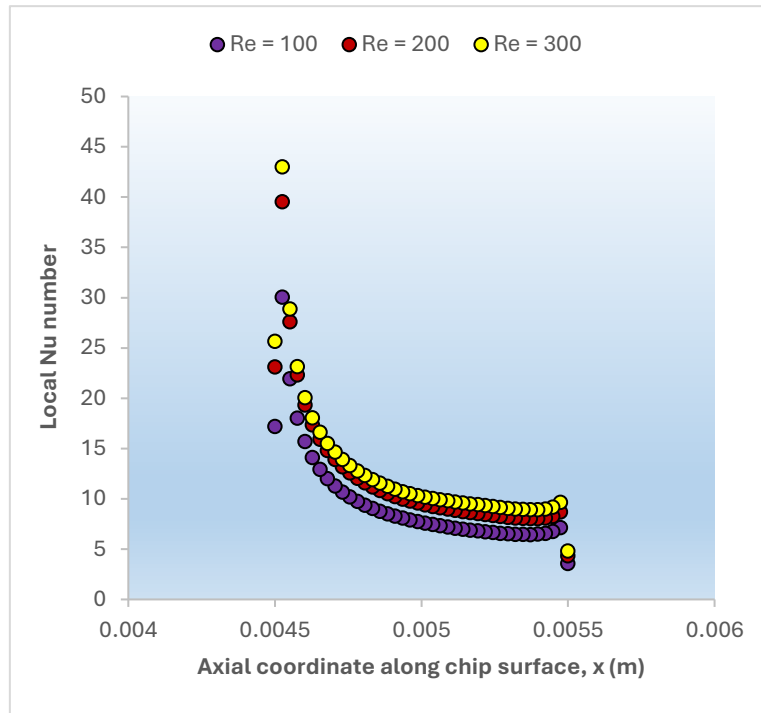


Figure 25. Local Nu number variations on the chip surface ($H = 2$ mm)

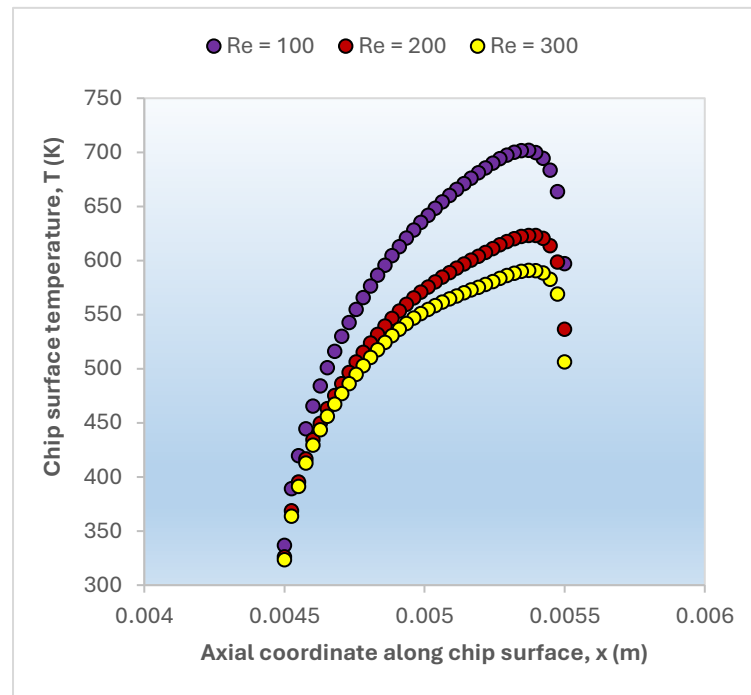


Figure 26. Temperature changes on the chip surface ($H = 2$ mm)

Figure 26 illustrates that the temperature values within the range of 300–350 K at the chip's starting point achieve peak temperatures of 701.90 K, 623.44 K, and 591.05 K for Reynolds numbers of 100, 200, and 300, respectively. The findings indicate that an increase in Reynolds number leads to a decrease in chip surface temperature, while an increase in channel height results in elevated chip surface temperatures.

4 CONCLUSION

This study investigates the heat transfer performance of an electronic chip situated within a mini-channel at different channel heights ($H = 1, 1.5, \text{ and } 2 \text{ mm}$) for Reynolds numbers of 100, 200, and 300. This study examined the temperature distributions and Nusselt numbers on the chip surface through CFD analyses of the 2D-designed mini-channels using ANSYS FLUENT. The key findings from this study are summarised below.

- With an increase in the Reynolds number, heat transfer within the channel is enhanced, leading to a reduction in chip surface temperatures and an increase in the Nusselt numbers on the chip surface.
- With an increase in channel height, the heat transfer within the channel diminishes, resulting in elevated chip surface temperatures.
- At a channel height of $H = 1 \text{ mm}$, an increase in the Reynolds number from 100 to 300 resulted in a decrease in chip surface temperature from 499.15 K to 456.88 K, accompanied by an increase in the average Nusselt number from 11.08 to 13.15.
- As the Reynolds number increased from 100 to 300 at a channel height of $H = 1.5 \text{ mm}$, the chip surface temperature decreased from 569.61 K to 505.97 K, while the average Nusselt number rose from 10.15 to 12.89.
- As the Reynolds number increased from 100 to 300 at a channel height of $H = 2 \text{ mm}$, the chip surface temperature decreased from 607.72 K to 528.12 K, while the average Nusselt number rose from 9.89 to 13.32.

The findings indicate that channel height and flow conditions have a significant impact on the cooling efficiency of a chip within a mini-channel. Optimising the design parameters of mini-channels is essential for the efficient cooling of chip surfaces.

Conflict of Interest Statement

The author declares that there is no conflict of interest regarding this study.

Statement of Research and Publication Ethics

This study has been conducted following the principles of research and publication ethics.

Artificial Intelligence (AI) Contribution Statement

This article was written, edited, analysed, and prepared entirely by the author without the use of any artificial intelligence (AI) tools. All content, text, data analysis, and figures were produced solely by the author.

4.1 Contributions of the Authors

The author was solely responsible for conceptualising the study, developing the methodology, executing the investigation, conducting data analyses, and writing the manuscript.

REFERENCES

- [1] H. A. Hussein, "Numerical hydrothermal evaluation of heat transfer in a multi-mini-channel heat sink: effect of square pin fins," *Results Eng.*, vol. 20, p. 101403, 2023. <https://doi.org/10.1016/j.rineng.2023.101403>
- [2] L. Yu, X. Wu, M. Song, and K. Chen, "Hot spot temperature optimization of micro-channel heat sinks enabled by designing vortex generators and realizing optimal flow pattern," *Int. J. Heat Mass Transf.*, vol. 247, p. 127181, 2025. <https://doi.org/10.1016/j.ijheatmasstransfer.2025.127181>
- [3] A. Kozłowska, P. Łapka, M. Seredyński, M. Teodorczyk, and E. Dąbrowska-Tumańska, "Experimental

- study and numerical modeling of micro-channel cooler with micro-pipes for high-power diode laser arrays,” *Appl. Therm. Eng.*, vol. 91, pp. 279–287, 2015. <http://dx.doi.org/10.1016/j.applthermaleng.2015.08.019>
- [4] N. Zehtabiyani-Rezaie, M. Saffar-Avval, and M. Mirzaei, “Analytical and numerical investigation of heat transfer and entropy generation of stratified two-phase flow in mini-channel,” *Int. J. Therm. Sci.*, vol. 90, pp. 24–37, 2015. <http://dx.doi.org/10.1016/j.ijthermalsci.2014.11.032>
- [5] B. Mehta and S. Khandekar, “Local experimental heat transfer of single-phase pulsating laminar flow in a square mini-channel,” *Int. J. Therm. Sci.*, vol. 91, pp. 157–166, 2015. <http://dx.doi.org/10.1016/j.ijthermalsci.2015.01.008>
- [6] M. Spizzichino, G. Sinibaldi, and G. P. Romano, “Experimental investigation on fluid mechanics of micro-channel heat transfer devices,” *Exp. Therm. Fluid Sci.*, vol. 118, p. 110141, 2020. <https://doi.org/10.1016/j.expthermflusci.2020.110141>
- [7] B. Mehta and S. Khandekar, “Infra-red thermography of laminar heat transfer during early thermal development inside a square mini-channel,” *Exp. Therm. fluid Sci.*, vol. 42, pp. 219–229, 2012. <http://dx.doi.org/10.1016/j.expthermflusci.2012.05.007>
- [8] S. Kaushik *et al.*, “Comparative analysis of fluid flow in mini channel with nano fluids and base fluid,” *Mater. Today Proc.*, 2023. <https://doi.org/10.1016/j.matpr.2023.05.363>
- [9] H. Wu, X. Wu, L. Feng, and M. M. Youshanlouei, “Cooling a central processing unit by installing a mini channel and flowing nanofluid, and investigating economic efficiency,” *Case Stud. Therm. Eng.*, vol. 30, p. 101719, 2022. <https://doi.org/10.1016/j.csite.2021.101719>
- [10] W. M. Abed, R. D. Whalley, D. J. C. Dennis, and R. J. Poole, “Numerical and experimental investigation of heat transfer and fluid flow characteristics in a micro-scale serpentine channel,” *Int. J. Heat Mass Transf.*, vol. 88, pp. 790–802, 2015. <http://dx.doi.org/10.1016/j.ijheatmasstransfer.2015.04.062>
- [11] M. Ghasemian, Z. N. Ashrafi, M. Goharkhah, and M. Ashjaee, “Heat transfer characteristics of Fe₃O₄ ferrofluid flowing in a mini channel under constant and alternating magnetic fields,” *J. Magn. Magn. Mater.*, vol. 381, pp. 158–167, 2015. <http://dx.doi.org/10.1016/j.jmmm.2014.12.078>
- [12] S. Sandler, B. Zajackowski, and Z. Krolicki, “Review on flow boiling of refrigerants R236fa and R245fa in mini and micro channels,” *Int. J. Heat Mass Transf.*, vol. 126, pp. 591–617, 2018. <https://doi.org/10.1016/j.ijheatmasstransfer.2018.05.048>
- [13] V. Sajith, D. Haridas, C. B. Sobhan, and G. R. C. Reddy, “Convective heat transfer studies in macro and mini channels using digital interferometry,” *Int. J. Therm. Sci.*, vol. 50, no. 3, pp. 239–249, 2011. [doi:10.1016/j.ijthermalsci.2010.04.005](http://dx.doi.org/10.1016/j.ijthermalsci.2010.04.005)
- [14] C. J. Ho, S.-T. Hsu, T.-F. Yang, B.-L. Chen, S. Rashidi, and W.-M. Yan, “Cooling performance of mini-channel heat sink with water-based nano-PCM emulsion-An experimental study,” *Int. J. Therm. Sci.*, vol. 164, p. 106903, 2021. <https://doi.org/10.1016/j.ijthermalsci.2021.106903>
- [15] M. V. V. Mortean and M. B. H. Mantelli, “Nusselt number correlation for compact heat exchangers in transition regimes,” *Appl. Therm. Eng.*, vol. 151, pp. 514–522, 2019. <https://doi.org/10.1016/j.applthermaleng.2019.02.017>
- [16] M. A. Oyinlola, G. S. F. Shire, and R. W. Moss, “Investigating the effects of geometry in solar thermal absorber plates with micro-channels,” *Int. J. Heat Mass Transf.*, vol. 90, pp. 552–560, 2015. <http://dx.doi.org/10.1016/j.ijheatmasstransfer.2015.06.087>



AUTOMATED POST-EARTHQUAKE WALL DAMAGE DETECTION AND CLASSIFICATION USING YOLOV8

Erkan DEVECİ^{1,*} , Burhan ERGEN²

¹ Osmaniye Korkut Ata University, Dijital Transformation and Software Office, Osmaniye, Türkiye

² Firat University, Department of Computer Engineering, Elazığ, Türkiye

* **Corresponding Author:** erkandeveci@osmaniye.edu.tr

ABSTRACT

This study presents a novel approach for the automatic detection and classification of post-earthquake structural damage on building walls using the YOLOv8 deep learning algorithm. Post-disaster damage assessment is critical for timely intervention and rehabilitation planning; however, current manual inspection methods are time-consuming and subjective. To overcome these challenges, we developed a comprehensive real-time detection system that can classify wall conditions into three categories: normal, cracked, and perforated. A specialized dataset consisting of 2000 high-resolution images from buildings affected by the February 6 earthquakes in Turkey was compiled. The dataset was meticulously preprocessed and split into 80% for training and 20% for testing. The YOLOv8 model architecture was optimized with hyperparameter tuning and trained for 100 steps with a batch size of 16 and a learning rate of 0.001. Experimental results show outstanding performance with class-specific accuracy values of 0.999 for normal, 0.777 for crack, and 0.849 for hole. The model achieved 0.875 overall accuracy, 0.852 recall, 0.903 precision (mAP@0.5), and 0.707 mAP@0.5:0.95. The model's F1-score based on confidence threshold analysis reached 0.86 at the optimal threshold. The system maintains real-time processing capabilities at 31 frames per second on mid-range GPU hardware (NVIDIA Quadro M2000), making it suitable for field use. The proposed methodology offers significant progress in post-disaster structural assessment by providing fast, objective, and scalable damage assessment. This technology can greatly improve emergency response efficiency, resource allocation, and safety assessment procedures following seismic events. Future work will focus on expanding the model to detect additional types of damage and on its use as a mobile application for on-site assessment by emergency response teams.

Keywords: Post-Earthquake Building Inspection, YOLOv8, Wall Damage Classification, Deep Learning, Crack and Hole Classification.

1 INTRODUCTION

Crack formation is a common structural defect observed in various man-made engineering structures such as sidewalk systems, bridge structures, nuclear facility containment walls, and tunnel ceilings found in metropolitan infrastructure. This condition is characterized by the process of a structural element breaking into discrete pieces and represents a mechanism that provides stress relief when concrete is subjected to stresses exceeding its tensile strength [1]. Crack formation is a morphological indicator of degradation processes that negatively affect the

integrity and structural performance of the concrete matrix, structurally weakening the concrete or exposing it to stress conditions that exceed design limits [2]. When crack propagation occurs, the stress tensors perpendicular to the crack plane approach zero [3]. Crack formation in concrete structures can create multidisciplinary problems such as degradation of strength and stiffness parameters in structural systems, deterioration of aesthetic integrity, reduction in long-term durability performance, and compromise of hydraulic isolation properties [4]. The reduction in stiffness resulting from crack formation causes additional deformation and displacement vectors in structural elements. The development of an effective, reliable, and economical algorithm for detecting surface anomalies is of primary importance for robust infrastructure management mechanisms [5, 6, 7].

Highway pavement inspection [8], underground pipeline inspection [9], bridge crack monitoring [10], and rail system assessment [11] have led to a recent surge in academic interest in automated crack detection mechanisms. In subsequent years, deep learning techniques have been widely implemented in various fields of expertise, particularly in engineering sciences, industrial applications, health sciences, natural language processing technologies, and autonomous vehicle systems [12, 13, 14, 15].

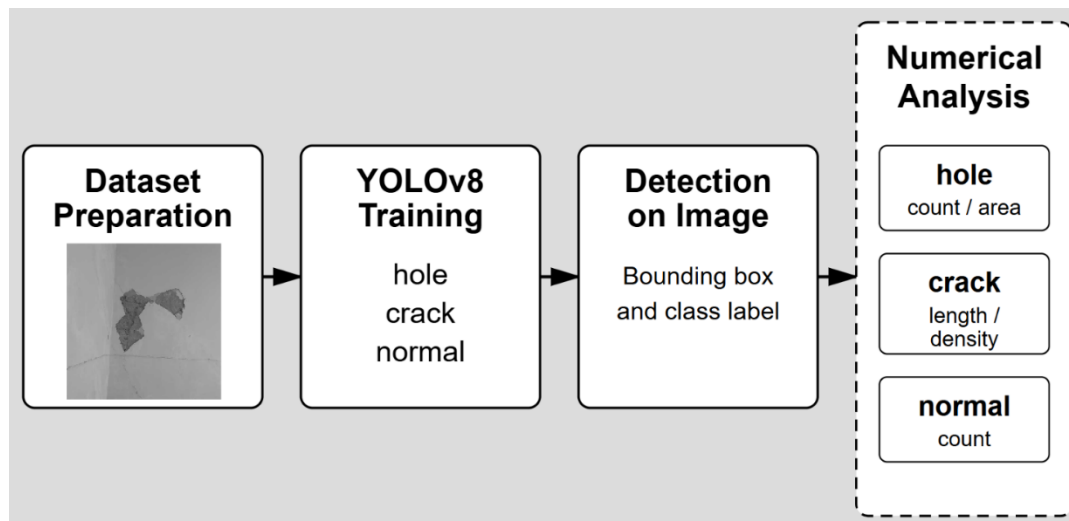


Figure 1. YOLOv8-Based Concrete Surface Defect Detection and Quantitative Analysis Process

Figure 1 schematically presents the general workflow of a damage detection process based on You Only Look Once version 8 (YOLOv8). In the first stage, the Data Set Preparation step collects and organizes the labeled, manually annotated images required to train and test the model. Then, in the Prediction Stage, the model detects normal, crack, and hole classes in the incoming images. The final stage is Analysis and Reporting, where numerical analyses are performed based on the model's findings, and comprehensive reports are generated according to the type and size of the detected defects. This workflow demonstrates the multi-class detection capability of the YOLOv8 architecture with a concrete application example and outlines the basic steps of an automated solution for damage detection.

This study presents a deep learning-based approach for detecting cracks on building surfaces. During the model training process, transfer learning was applied using the YOLOv8 architecture, which was pre-trained on the ImageNet dataset. An original dataset containing wall cracks and surface abnormalities recorded after the February 6 earthquakes was created and the model was trained on this dataset [16]. Based on the results obtained, the model's ability to detect surface defects such as cracks and holes with high accuracy was analyzed. In this context, the proposed method aims to provide an effective solution in structural health monitoring systems by demonstrating higher accuracy and generalization ability compared to classical image processing approaches.

2 MATERIALS AND METODS

2.1 Dataset

In this study, a specialized dataset consisting of 2000 images depicting cracks and holes on building surfaces, resulting from damage sustained by buildings following an earthquake, was utilized for the automatic detection of such defects. The dataset contains three different classes: normal, crack, and hole. Eighty percent of the images in the dataset (1,600 images) were randomly allocated for training, and 20% (400 images) for testing. The sample number distributions of the images in the dataset are shown in Figure 2. Accordingly, each image may contain more than one sample [16]. The labels for all images in the training and test datasets were prepared in YOLO format, and object annotations for the relevant class were provided for each image.

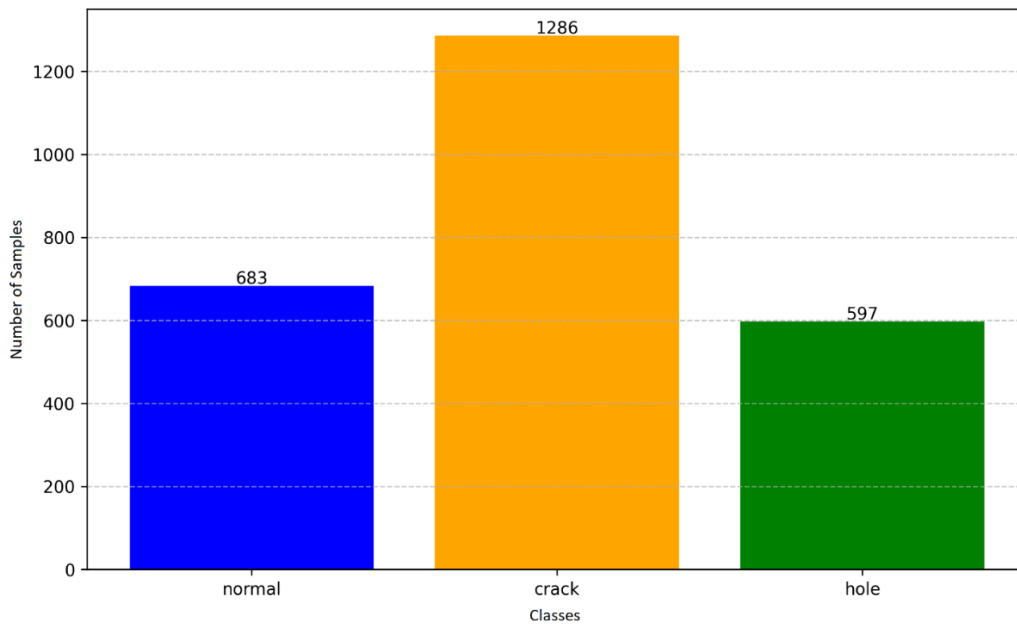


Figure 2. Dataset Distribution

The dataset structure is prepared in the standard YOLOv8 format, with images stored in the “images” folder and corresponding label files stored in the “labels” folder. Label files contain normalized coordinates in the form of object class and location information (class_id, x_center, y_center, width, height).

2.2 Model Architecture

The study utilized the YOLOv8 deep learning architecture, which offers state-of-the-art performance in object detection. Specifically, the You Only Look Once version 8 nano (YOLOv8n) model was chosen for this study as it provides a good balance between computational efficiency and accuracy. Pre-trained COCO weights were used for YOLOv8n, and then this model was retrained on the dataset specific to this study using transfer learning. In the first stage, convolutional layers were configured to extract low-level features from the input images and create representative features to be passed to subsequent layers. Subsequently, C2f (Cross-Stage Partial Connections with Full Bottleneck) blocks were incorporated, favoring an architectural design that minimizes information loss and improves gradient flow. These blocks both enhance the computational efficiency of the model and strengthen its representational power in the deep learning process.

The model has the ability to detect objects with a single pass over the image, making it an ideal choice for real-time applications. During training, mixed precision training was applied to increase memory efficiency and reduce training time.

3 FINDING AND DISCUSSION

This section provides a detailed analysis of the quantitative performance of the developed YOLOv8-based object detection model, offering a comprehensive evaluation in terms of both accuracy and inference efficiency. The model's class-based success levels are interpreted through general accuracy metrics, inference times, and learning trends; furthermore, its strengths and weaknesses are discussed with visual support using a confusion matrix, F1 score, and various curve analyses. The findings reveal that the model provides sufficient accuracy and speed for real-time applications.

Table 1. Class-Based Performance Indicators of the Model.

Class	Number of Images	Number of Samples	Precision	Recall	mAP50	mAP50-95
Normal	682	682	0.999	0.987	0.995	0.993
Crack	792	1285	0.777	0.707	0.799	0.498
Hole	403	596	0.849	0.862	0.916	0.631

Table 1 details the fundamental performance metrics achieved by the model for each class. The model demonstrated exceptional success in the normal class, achieving a mAP@0.5 value of 99.3%. This indicates that the model is highly successful in distinguishing surfaces without damage. The mAP@0.5 value obtained for the crack class was relatively lower at 79.9% compared to other classes. This situation may be attributed to the structural diversity of cracks and the high variation in the dataset. A high mAP@0.5 rate of 91.6% was recorded for the hole class; the model demonstrated strong performance in identifying surface holes.

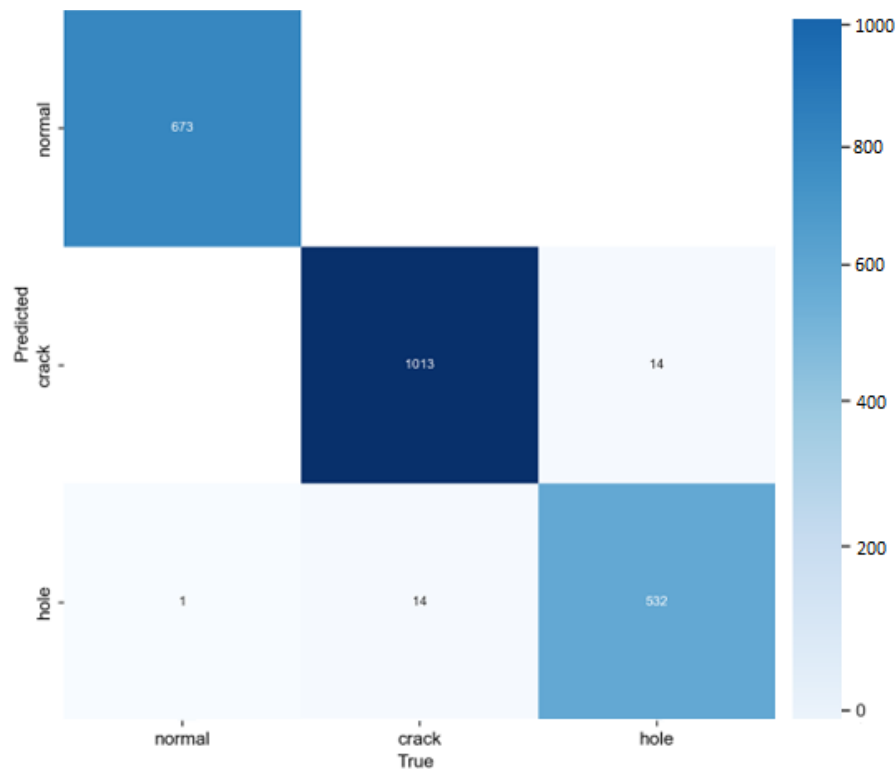


Figure 3. Confusion Matrix

The matrix showing the classification performance of the YOLOv8 object detection model in detecting surface defects is presented in Figure 3. When the data in the matrix is examined, the model exhibits heterogeneous performance in the three-class classification task, which includes the classes “normal,” “crack,” and “hole.”

The model for the normal class demonstrates nearly perfect classification capability with a 99.9% accuracy rate (673 correct classifications, only 1 misclassification). In the crack class, although a significant success was achieved with 1013 correct identifications, the misclassification of 258 examples as background is noteworthy and is likely due to the low-contrast characteristics of the cracks. For the hole class, 532 correct identifications were observed, while 14 examples were misclassified as cracks and 50 as background, indicating moderate classification confusion.

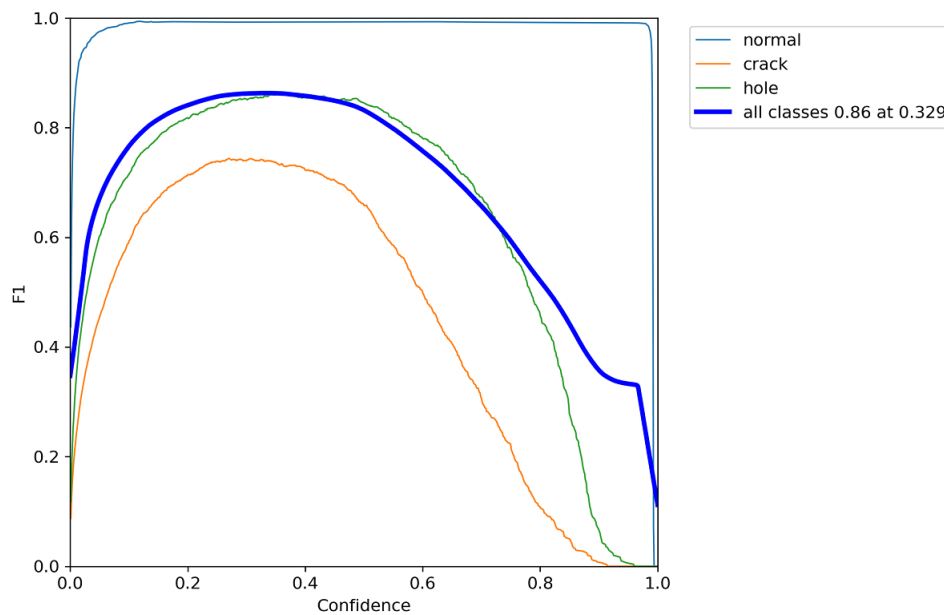


Figure 4. F1-Confidence Curve Graph

The F1 score, one of the most important metrics used to evaluate a model's classification capability, is the harmonic mean of precision and sensitivity values. The F1-Confidence Curve presented in Figure 4 shows the model's overall performance at different confidence scores and the optimal decision threshold (confidence threshold). In general, this analysis reveals that determining the model's optimal confidence threshold value to be around 0.329 is meaningful in terms of both all classes and overall F1 performance.

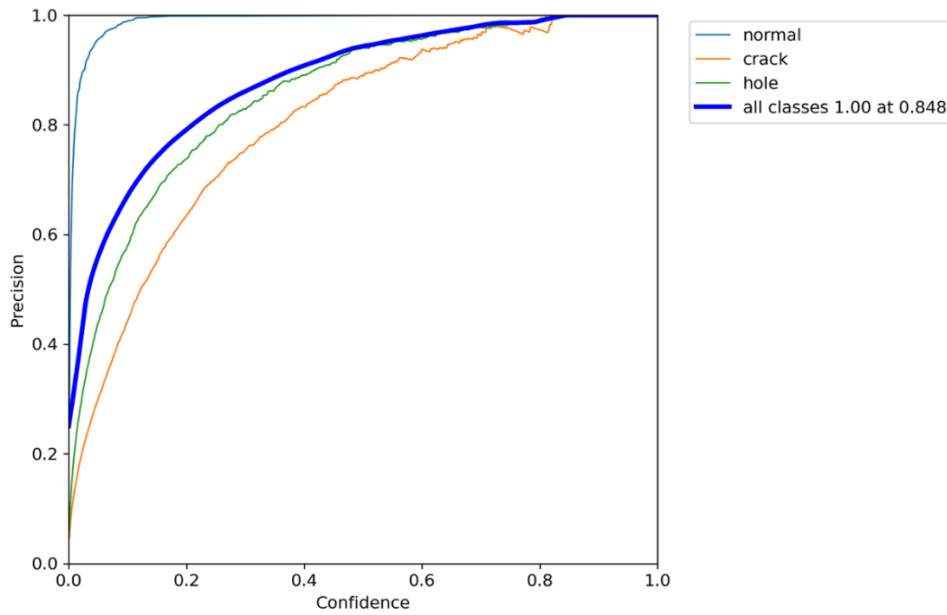


Figure 5. Precision-Confidence Curve Evaluation of the Model

The Precision-Confidence curve presented in Figure 5 evaluates the classification reliability of the trained YOLOv8n model across three different classes. When examining the model's overall accuracy curve (dark blue) for all classes, it can be seen that the model achieves maximum 100% accuracy at a confidence level of 84.8%. This clearly demonstrates the model's ability to make predictions with high accuracy.

The average accuracy value for all classes reaches 100% at a confidence threshold of 0.848. This finding indicates that the model is highly reliable in terms of accuracy at high confidence thresholds, but that this high accuracy is likely achieved at the expense of sensitivity. The distinct differentiation of accuracy curves at low confidence thresholds reflects the differences in the morphological and visual characteristics of the classes.

Overall, it was observed that the model showed steadily increasing accuracy curves for all classes and made highly successful predictions at high confidence thresholds. These results support the model's applicability in real-world applications, particularly in industrial inspection scenarios requiring high accuracy.

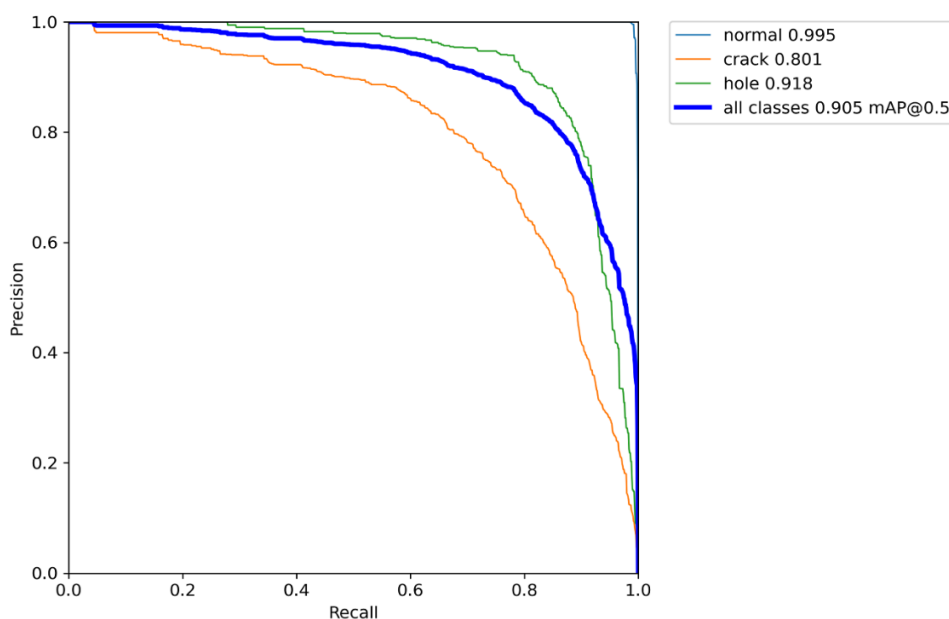


Figure 6. Precision-Recall Curve Evaluation of the Model

To quantitatively evaluate the class-based detection performance of the YOLOv8n model, a Precision-Recall (P-R) curve was created in Figure 6. The graph shows the variation in accuracy and sensitivity values of the model's predictions for the “normal,” “crack,” and “hole” classes. The curves also indicate the overall class performance and the 90.5% mAP@0.5 performance. This demonstrates that the model can classify with high accuracy and a low error rate.

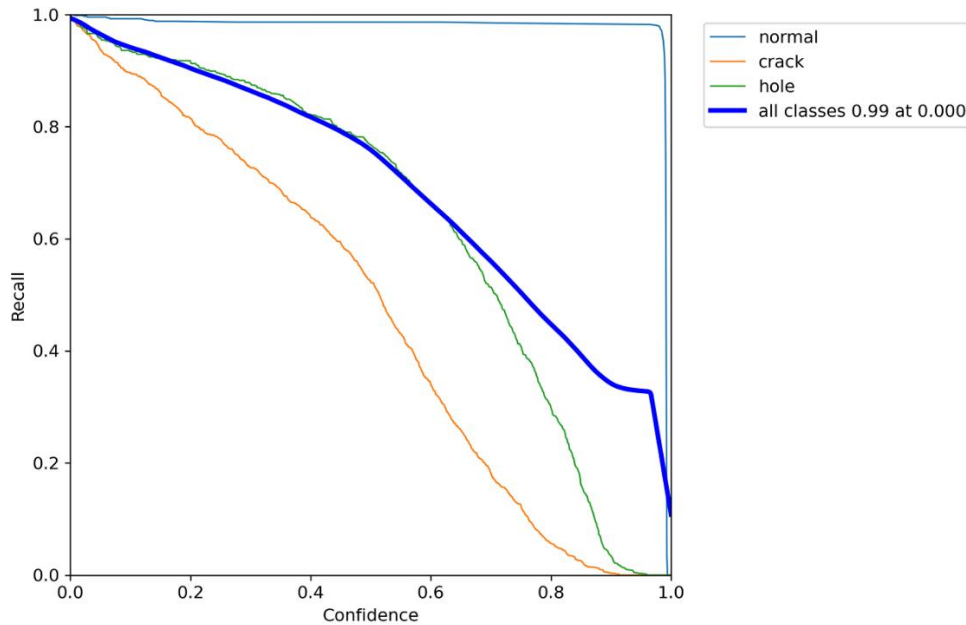


Figure 7. Recall-Confidence Curve Evaluation of the Model

Figure 7 shows the relationship between decision confidence and sensitivity regarding the predictions of the YOLOv8n model, both on a class-by-class basis and as an average across all classes. This analysis plays a critical role in determining the optimal threshold value and understanding class-based confidence behaviors. When all these metrics are evaluated together, it can be said that the YOLOv8n model offers fast learning capacity, a balanced training process with low loss values, high accuracy and sensitivity rates, and strong generalization ability. The limited number of sudden jumps in the training curves and the steady increase in metrics confirm that the training protocol has been properly optimized and that the model has been trained in a stable manner.

The images on the left side of Figure 8 show the original input fed into the system. The images on the right contain the detection results of the YOLOv8n model, with areas classified by the model as “hole,” “crack,” and “normal” marked. The model produced successful results by correctly classifying high-contrast areas. However, the large plaster fall area on the ceiling in the top image was not detected by the model. Possible reasons for this include insufficient representation of large plaster falls in the training dataset, such damage exhibiting visual characteristics different from the “hole” class, and the bounding box dimensions of large-area damage being significantly different from the examples encountered during training. Furthermore, in the bottom image, the large-scale concrete spillage area was detected as a single “hole,” and the variety of structural damage in this area (combination of cracks, holes, and plaster loss) caused the model to assign a single class label.

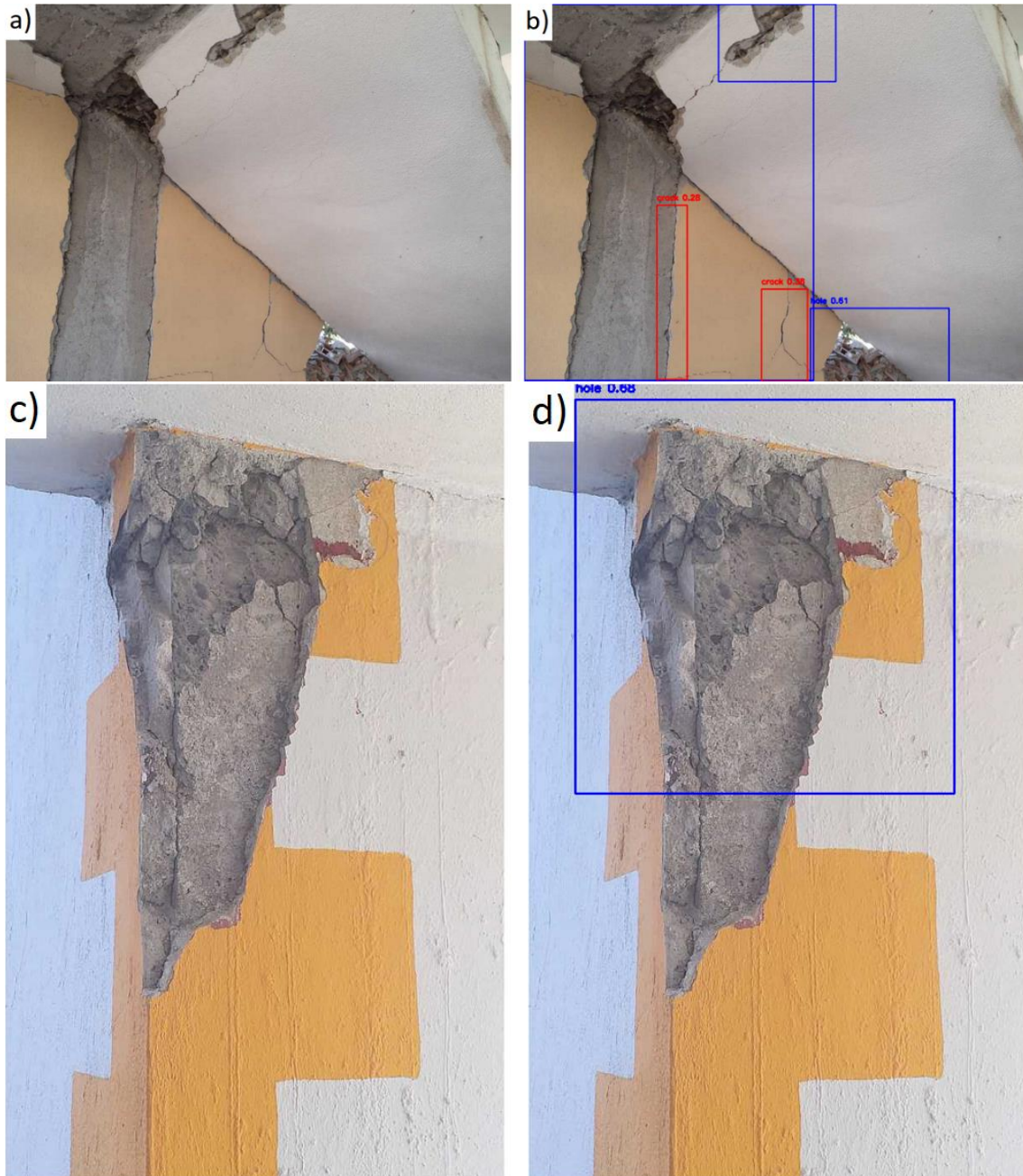


Figure 8. (a)(c) Wall image after the earthquake; (b)(d) Post-earthquake wall image showing the model's prediction result

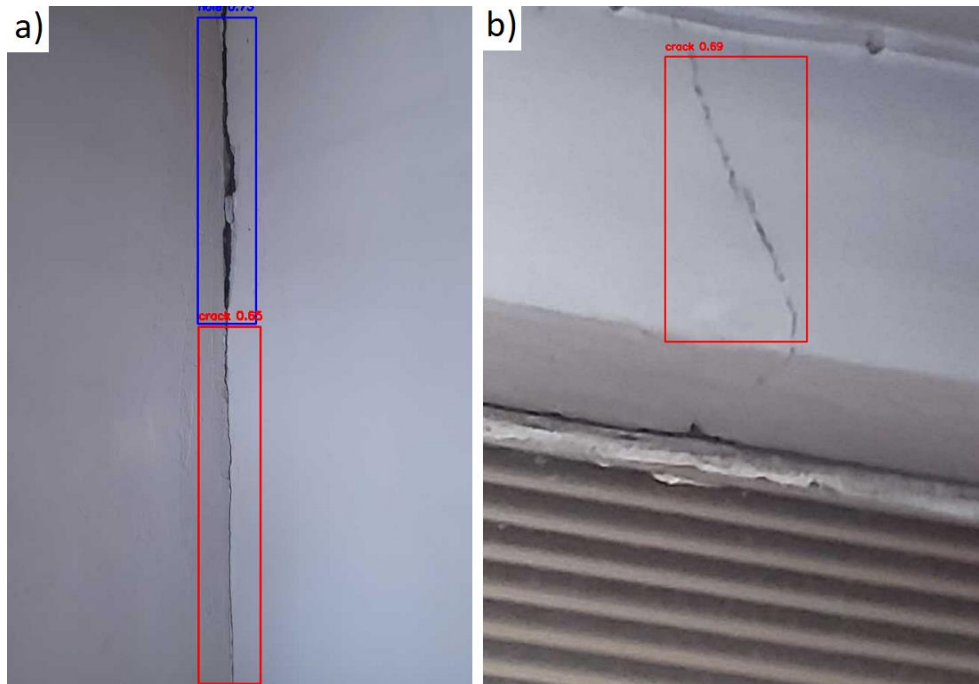


Figure 9. (a)(b) Estimates of Surface Defect Detection

Figure 9 (a) shows the image containing “crack” and ‘hole’ on the structure surface. Figure 9 (b) shows the “crack” defect detected by the YOLOv8n model with 0.69 accuracy. Despite the irregular morphology of the crack, the model correctly classified the area and achieved high accuracy in detection.

4 CONCLUSION

In this study, a customized object detection model was developed using the YOLOv8n architecture for the detection and classification of damage on building surfaces following an earthquake. The model was trained and evaluated to identify three different surface conditions: “normal,” “crack,” and “hole.” The training process was conducted over 100 epochs using a PyTorch and Ultralytics-based infrastructure on Quadro M2000 GPU hardware. Despite its lightweight structure, the model was shown to be capable of high-accuracy and low-latency predictions.

Performance evaluations were not limited to general accuracy levels; they were also detailed using multidimensional methods such as class-based analyses, complexity matrices, confidence threshold curves, and box plot analyses. Specifically, the model demonstrated exceptional performance in the “normal” class with a mAP@0.5 accuracy exceeding 99%, revealing the model's ability to recognize solid surfaces with high accuracy. On the other hand, the “crack” class was identified as the model's weakest link, with both a low mAP@0.5 (~79%) and a high false negative rate. This can be attributed to the visual diversity of crack structures and the high intra-class variance. The “hole” class showed strong accuracy with a mAP@0.5 success rate of 91.6%, but confusion was observed within certain confidence threshold ranges.

Various development strategies are proposed to further improve model performance in future studies. First, expanding the dataset and addressing imbalances between existing classes will positively impact the model's generalization capacity. Specifically, applying class-specific data augmentation techniques for the “crack” and “hole” classes can help the model learn these complex structures more effectively. Furthermore, there is a need for work on optimizing confidence threshold values to reduce false positive and negative classifications. However,

beyond the YOLOv8n architecture, a comparative evaluation of the YOLOv8m/s versions, which offer more complex and deep structures, and Transformer-based models would be useful in clarifying the limits of the achieved performance.

In conclusion, the YOLOv8n-based model developed in this study has demonstrated high accuracy and application potential in the automatic detection of damage on building wall surfaces. In this context, it is considered that the model provides a valuable contribution to academic research and establishes a solid foundation for use in engineering applications.

Conflict of Interest Statement

There is no conflict of interest among the authors.

Statement of Research and Publication Ethics

This study has been prepared in accordance with the principles of research and publication ethics.

Artificial Intelligence (AI) Contribution Statement

This article was written, edited, analyzed, and prepared entirely by the authors without the use of any artificial intelligence (AI) tools. All content, text, data analysis, and figures were produced solely by the authors.

Contributions of the Authors

“Erkan Deveci” Conceptualization, literature review, data collection and dataset creation, data preprocessing, training and optimization of the YOLOv8 model, hyperparameter tuning, conducting experimental studies, calculating and analyzing performance metrics, visualization, writing the article (introduction, materials and methods, results, and conclusion sections), article editing.

“Burhan Ergen” Project consulting, methodology design, determining the research direction, article review and critical feedback, final approval.

REFERENCES

- [1] Kovler, K., & Chernov, V. (2009). Types of damage in concrete structures. In N. Delatte, Failure, distress and repair of concrete structures (pp. 32-56). Boca Raton: Woodhead Publishing Limited.
- [2] Larosche, C. J. (2009). Types and causes of cracking in concrete structures. In N. Delatte, Failure, distress and repair of concrete structures (pp. 57-83). Boca Raton: Woodhead Publishing Limited.
- [3] Ghali, A., Favre, R., & Elbadry, M. (2002). Concrete Structures- Stresses and Deformation. Spon Press.
- [4] ACI Committee 201. (2001). Guide to Durable Concrete. In ACI Manual of Concrete Practice Part 1 -Materials and General Properties of Concrete (pp. 20 1.2R1-20 1.2R41). Farmington Hills: American Concrete Institute.
- [5] Daghighi, A. (2020). Full-Scale Field Implementation of Internally Cured Concrete Pavement Data Analysis for Iowa Pavement Systems. Creative Components. 638. [https:// lib. dr. iasta te. edu/ creat iveco mpone nts/ 638](https://lib.dr.iastate.edu/creativecomponents/638).
- [6] Hosseini, S., & Smadi, O. (2020). How prediction accuracy can affect the decision-making process in pavement management system. Infrastructures. [https:// doi. org/ 10. 31224/ osf. io/ t28ue](https://doi.org/10.31224/osf.io/t28ue).

- [7] Abukhalil, Y. B. (2019). Cross asset resource allocation framework for pavement and bridges in Iowa. Graduate Theses and Dissertations. 16951. [https:// lib. dr. iasta te. edu/ etd/ 16951](https://lib.dr.iastate.edu/etd/16951).
- [8] N. F. Hawks, and T. P. Teng. (2014). Distress identi_cation manual for the long-term pavement performance project. National academy of sciences.
- [9] R. Amhaz, S. Chambon, J. Idier, and V. Baltazart. (2016). Automatic crack detection on two dimensional pavement images: an algorithm based on minimal path selection," IEEE Trans. Intell. Transp. Syst., vol. 17, no. 10, pp. 2718-2729.
- [10] I. Abdel, O. Abudayyeh, and M. E. Kelly. (2003). Analysis of edge-detection techniques for crack identi_cation in bridges," J. Computer Civil Eng., vol. 17, no. 4, pp. 255-263.
- [11] P. Lad, and M. Pawar. (2016). Evaluation of railway track crack detection system," in Proc., IEEE ROMA, pp. 1-6.
- [12] E. Aslan ve Y. Özüpak, "Classification of Blood Cells with Convolutional Neural Network Model", Bitlis Eren Üniversitesi Fen Bilimleri Dergisi, c. 13, sy. 1, ss. 314–326, 2024, doi: 10.17798/bitlisfen.1401294.
- [13] Lubbad, M. A., Kurtulus, I. L., Karaboga, D., Kilic, K., Basturk, A., Akay, B., ... & Pacal, I. (2024). A Comparative Analysis of Deep Learning-Based Approaches for Classifying Dental Implants Decision Support System. Journal of Imaging Informatics in Medicine, 1-22.
- [14] Kunduracioglu, I., & Pacal, I. (2024). Advancements in deep learning for accurate classification of grape leaves and diagnosis of grape diseases. Journal of Plant Diseases and Protection, 1-20.
- [15] Pacal, I. (2024). A novel Swin transformer approach utilizing residual multi-layer perceptron for diagnosing brain tumors in MRI images. International Journal of Machine Learning and Cybernetics, 1-19.
- [16] Wall Crack Hole Normal Dataset. Available at: <https://kaggle.com/datasets/046eb82640b35c2b06e5a8d6b4cd2c5c277e9ef554d37934c5b3af6ce6e1d347> [Accessed 15.05.2025].



DIYALOG AĞIRLIKLI METİNLERDE KONUŞAN KARAKTER TESPİTİ: BABELSCAPE VE SAVASYBERT NER MODELLERİNİN KARŞILAŞTIRMALI ANALIZI

Tuğçe DENİZ¹ , Pınar ÜNVER¹ , Beytullah TÜTÜNCÜ¹ , Barış ASLAN¹ , Pakize ERDOĞMUŞ^{1,*}

¹ Düzce Üniversitesi, Bilgisayar Mühendisliği Bölümü, Düzce, Türkiye

* Sorumlu Yazar: pakizeerdogmus@duzce.edu.tr

ABSTRACT

Bu çalışma, çok konuşmacılı metin seslendirme (TTS) sistemleri için edebi metinlerdeki diyalogların doğru konuşmacıya atanması sorununu ele almakta ve makine öğrenmesi ile kural tabanlı yaklaşımları birleştiren hibrid bir yöntem önermektedir. Yöntem iki katmandan oluşmaktadır: SavasyBERT ve çok dilli Babelscape modelleri kullanılarak ‘Kişi’ varlıklarının belirlenmesi ve konuşma çizgileri ile tırnak işaretlerine dayalı kural tabanlı diyalog tespiti. “Konuşmacı” kavramı, bu iki katmanın kesişimi olarak tanımlanmıştır. Elde edilen bulgular, Türkçeye özgü SavasyBERT modelinin kurgusal karakterleri daha tutarlı biçimde tespit ettiğini ve daha düşük gürültü ürettiğini göstermektedir. Buna karşılık Babelscape modeli, Türkçe dil özellikleriyle sınırlı uyumu nedeniyle daha fazla hatalı pozitif üretme eğilimi sergilemiştir. Sonuç olarak, önerilen hibrid yaklaşımın SavasyBERT ile birlikte kullanıldığında Türkçe çok konuşmacılı TTS uygulamaları için güvenilir bir karakter tespit altyapısı sunduğu değerlendirilmiştir.

Keywords:

Varlık İsmi Tanıma (NER), Konuşmacı Tespiti, Hibrid Yaklaşım, SavasyBERT, Babelscape, Çok Konuşmacılı Metin Seslendirme

1 GİRİŞ

Metinden konuşmaya (Text-to-Speech, TTS) dönüşüm sistemleri, günümüzde yüksek doğrulukla anlaşılabilir ve akıcı konuşma üretebilen ileri düzey yapılar hâline gelmiştir. Bu ilerleme; dilbilimsel kuramların olgunlaşması, İngilizce’nin akustik-fonetik özelliklerinin ayrıntılı biçimde ortaya konması, insan konuşmasının algısal olarak nasıl işlendiğine ilişkin bulgular, matematiksel konuşma üretim modelleri ile güçlü donanım ve programlama tekniklerinin birleşimi sayesinde mümkün olmuştur. Klatt’ın klasikleşmiş çalışması [1] TTS alanındaki tarihsel gelişimi erken dönem mekanik ve elektronik sentezleyicilerden formant ve artikülasyon temelli yöntemlere kadar sistematik biçimde incelemekte; fonemlerin allofonlara dönüştürülmesi, süre ve temel frekans (F0) kurallarıyla prosodinın modellenmesi, metnin sözdizimsel ve morfolojik analizinin konuşma üretimine entegrasyonu gibi temel bileşenleri ayrıntılı olarak tartışmaktadır.

Güncel konuşma teknolojilerinde, metinden-konuşmaya ve konuşmadan-yazıya (STT) sistemleri giderek daha fazla insan-makine etkileşiminin temel bileşeni hâline gelmiştir. Ancak STT mekanizmalarının ürettiği transkriptler; duraksamalar, yanlış çözümlemeler ve gürültü

kaynaklı hatalar nedeniyle yüksek oranda düzensizlik içerir. Bu durum, konuşma temelli uygulamalarda anlamlı bilgi çıkarımını zorlaştırmakta ve özellikle serbest biçimli girdilerden yapılandırılmış bilgi elde edilmesini kritik bir problem hâline getirmektedir. Bu bağlamda Varlık İsmi Tanıma (Named Entity Recognition, NER), TTS/STT tabanlı sistemlere entegre edilen en önemli doğal dil işleme bileşenlerinden biri olarak öne çıkmaktadır.

Gerçek dünya verilerinin kısıtlı ve yüksek gürültülü olması, büyük dil modellerinin gizlilik ve gecikme sorunları nedeniyle kullanılamaması, uygulamaya özgü hafif NER modellerinin geliştirilmesini zorunlu kılmaktadır. Çalışmada yalnızca 69 adet gerçek, çoğu hatalı transkripsiyon içeren örneğin bulunması, sentetik veri üretimini tek uygulanabilir yaklaşım hâline getirmiştir. Bu doğrultuda SlovakBERT tabanlı bir NER modeli geliştirilmiş ve tamamen sentetik verilerle eğitilerek gerçek test kümesinde %90'ın üzerinde doğruluk elde edilmiştir. Sonuçlar, sentetik veriye dayalı yaklaşımın, TTS/STT tabanlı adres doğrulama ve müşteri etkileşim sistemleri gibi gerçek dünya senaryoları için etkili bir çözüm sunduğunu göstermektedir [2].

Türkçe gibi sondan eklemeli ve morfolojik açıdan zengin dillerde bu problem daha da belirgin hâle gelmektedir. Çok dilli (multilingual) NER modelleri geniş bir dil yelpazesinde çalışabilmek üzere tasarlanmış olsa da, tek bir dilin bağlamsal ve morfolojik derinliğine tam olarak hâkim olamayabilmektedir. Bu durum, özellikle uzun ve diyalog yoğun metinlerde bağlamdan kopuk kişi etiketlerinin üretilmesine ve yüksek oranda hatalı pozitiflerin birikmesine yol açmaktadır. Çok modlu yaklaşımların bu tür sorunları hafifletebildiği, metin ve akustik bilgiyi birleştiren çalışmalarda gösterilmiştir [3].

Bu çalışma, Türkçe edebi metinlerde konuşmacı tespiti görevinde iki farklı NER yaklaşımını karşılaştırmalı olarak incelemektedir: çok dilli bir yapı üzerine kurulu Babelscape modeli ve Türkçeye özgü olarak eğitilmiş SavasyBERT modeli. Babelscape, BabelNet tabanlı çok dilli bir bilgi kaynağına dayanan evrensel bir yaklaşım sunarken [4], SavasyBERT Türkçe dil yapısına özgü verilerle ince ayar yapılmış bir model olarak morfolojik uyum açısından avantaj sağlamaktadır [5].

Çalışmada, makine öğrenmesine dayalı NER çıktıları ile metin içindeki diyalog belirteçlerini kullanan kural tabanlı bir yaklaşım birleştirilerek hibrid bir yöntem önerilmektedir. Bu yaklaşımda, konuşan karakterler yalnızca NER modelleri tarafından tespit edilen kişi varlıkları arasından, diyalog bağlamında yer alan ifadelerle sınırlandırılmaktadır. Böylece, özellikle çok dilli modellerin uzun metinlerde ürettiği bağlamsız ve gürültülü etiketlerin çok konuşmacılı TTS sistemleri üzerindeki olumsuz etkisinin azaltılması hedeflenmektedir.

Bu çalışmanın temel katkısı, Türkçe edebi metinler üzerinde yapılan karşılaştırmalı analiz yoluyla, dile özgü NER modellerinin uzun ve diyalog yoğun metinlerde sağladığı bağlamsal güvenilirliği ortaya koyması ve çok konuşmacılı TTS sistemleri için pratikte kullanılabilir bir konuşmacı tespiti yaklaşımı sunmasıdır.

2 MATERYAL VE METOT

Bu çalışmada, Türkçe edebi metinlerde konuşmacı tespiti problemini incelemek amacıyla, makine öğrenmesine dayalı Varlık İsmi Tanıma modelleri ile kural tabanlı bir diyalog tespit yaklaşımı birleştirilmiştir. Önerilen yöntem, konuşan karakterlerin yüksek kesinlikle belirlenmesini hedefleyen iki aşamalı hibrid bir yapıdan oluşmaktadır.

Çalışmada veri kaynağı olarak, diyalog yoğunluğu yüksek Türkçe edebi metinler kullanılmıştır. Bu metinler, çok konuşmacılı TTS sistemlerinde karşılaşılan gerçek senaryoları yansıtacak şekilde seçilmiştir. Metinler üzerinde herhangi bir ön sadeleştirme yapılmadan, modellerin doğal dil yapısına karşı gösterdiği davranışların gözlemlenmesi amaçlanmıştır.

Konuşmacı tespiti sürecinin ilk aşamasında, metinler üzerinde iki farklı NER modeli çalıştırılmıştır. Bunlardan ilki, çok dilli bir yaklaşıma dayanan Babelscape modelidir. Bu model, geniş dil kapsamı sayesinde farklı dillerde varlık tespiti yapabilmektedir. İkinci model ise

Türkçeye özgü verilerle eğitilmiş SavasyBERT modelidir. SavasyBERT, Türkçenin sondan eklemeli yapısı ve morfolojik özellikleri dikkate alınarak geliştirilmiş olup, özellikle kişi varlıklarının tespitinde bağlamsal uyum sağlamayı hedeflemektedir. Her iki model de metinler üzerinde çalıştırılarak “Kişi” varlığına ait tüm tespitler elde edilmiştir.

İkinci aşamada, metin içerisindeki diyalog cümlelerini belirlemek amacıyla kural tabanlı bir filtreleme uygulanmıştır. Bu filtreleme sürecinde, konuşma çizgileri, tırnak işaretleri ve diyalog yapısını işaret eden biçimsel göstergeler kullanılmıştır. Amaç, anlatıcı metni ile doğrudan konuşma içeren cümlelerin ayrıştırılmasıdır. Bu aşama, konuşmacı tespitinde bağlamın sınırlandırılmasını sağlayarak, NER modellerinin ürettiği bağlamsız kişi etiketlerinin etkisini azaltmayı hedeflemektedir.

Önerilen hibrid yaklaşımda, “konuşan karakter” kavramı, NER modelleri tarafından tespit edilen kişi varlıkları ile kural tabanlı yöntemle belirlenen diyalog cümlelerinin kesişimi olarak tanımlanmıştır. Buna göre, yalnızca diyalog bağlamında yer alan ve NER tarafından kişi olarak etiketlenen varlıklar, potansiyel konuşmacı olarak kabul edilmiştir. Bu yaklaşım sayesinde, özellikle uzun ve diyalog yoğun metinlerde biriken hatalı pozitiflerin sistem üzerindeki olumsuz etkisinin azaltılması amaçlanmıştır.

Elde edilen çıktılar, modellerin uzun metinlerdeki davranışlarını incelemek ve çok konuşmacılı TTS sistemleri açısından pratik kullanılabilirliklerini değerlendirmek amacıyla karşılaştırmalı olarak analiz edilmiştir. Değerlendirme sürecinde, modellerin ürettiği kişi varlıklarının niceliksel dağılımları ve bağlamsal tutarlılıkları temel alınmıştır.

3 BULGULAR VE TARTIŞMA

Önerilen hibrid yaklaşım kapsamında Babelscape ve SavasyBERT NER modellerinin çıktıları, diyalog yoğunluğu yüksek Türkçe edebi metinler üzerinde karşılaştırmalı olarak incelenmiştir. Bulgular, iki modelin kişi varlığı tespitinde niceliksel olarak benzer sonuçlar üretmesine karşın, bağlamsal tutarlılık ve pratik kullanılabilirlik açısından belirgin farklılıklar gösterdiğini ortaya koymaktadır.

Kısa metinler üzerinde yapılan ön değerlendirmelerde, Babelscape modelinin daha yüksek geri çağırma değerlerine ulaştığı gözlemlenmiştir. Bu durum, modelin kişi varlıklarını daha agresif biçimde etiketlediğini ve daha az varlık kaçırdığını göstermektedir. Ancak aynı eğilim, uzun ve diyalog yoğun edebi metinlerde belirgin bir dezavantaja dönüşmektedir. Metin uzunluğu arttıkça, bağlamdan kopuk kişi etiketleri birikmekte ve hatalı pozitif oranı anlamlı ölçüde yükselmektedir.

Uzun metinler üzerinde yapılan analizlerde, Babelscape modelinin ürettiği kişi varlıkları arasında bağlamsal olarak karakter olmayan kelimelerin sıklıkla yer aldığı görülmüştür. Diyalog fiilleri, unvanlar ve metnin doğal akışında yer alan bazı sabit ifadeler, model tarafından kişi varlığı olarak etiketlenmiştir. Bu durum, çok dilli bir modelin Türkçe’nin morfolojik ve bağlamsal özelliklerine sınırlı düzeyde uyum sağlayabildiğini göstermektedir. Niceliksel olarak daha fazla kişi varlığı tespit edilmiş olsa da, bu artış pratik açıdan anlamlı bir kazanım sunmamaktadır.

SavasyBERT modeli ise uzun metinlerde daha dengeli ve bağlama duyarlı bir davranış sergilemiştir. Türkçeye özgü olarak eğitilmiş olması sayesinde, çekim eki almış kişi adlarını ve bağlam içinde karakter olarak kullanılan isimleri daha tutarlı biçimde tespit edebilmiştir. Üretilen kişi listelerinde hatalı pozitiflerin sınırlı düzeyde kaldığı ve karakter olmayan ifadelerin büyük ölçüde elendiği gözlemlenmiştir. Bu durum, SavasyBERT’in uzun edebi metinlerde gürültü birikimini engelleyen daha muhafazakâr bir etiketleme yaklaşımı benimsediğini göstermektedir.

Hibrid yaklaşımın ikinci aşamasında uygulanan kural tabanlı diyalog filtresi, her iki model için de bağlam sınırlandırması sağlamıştır. Ancak bu filtrenin etkisi, SavasyBERT çıktıları üzerinde daha belirgin olmuştur. Babelscape modelinin ürettiği yüksek sayıda bağlamsız kişi etiketi, kural tabanlı filtreleme sonrasında dahi sistem üzerinde ek yük oluşturmaktadır. Buna karşın

SavasyBERT, diyalog bağlamında yer alan ve gerçekten konuşmacı olabilecek varlıkları daha sınırlı ve temiz bir küme hâlinde sunmuştur.

Elde edilen bulgular, çok konuşmacılı TTS sistemleri açısından model seçiminde yalnızca niceliksel performans metriklerine odaklanmanın yeterli olmadığını göstermektedir. Uzun ve diyalog yoğun metinlerde, yüksek geri çağırma değerleri yerine bağlamsal kesinlik ve düşük gürültü oranı daha kritik bir gereksinim hâline gelmektedir. Bu bağlamda SavasyBERT modeli, önerilen hibrid yaklaşım ile birlikte kullanıldığında pratikte daha güvenilir bir konuşmacı tespiti altyapısı sunmaktadır.

Modellerin temel performans özelliklerini karşılaştırmalı olarak incelemek amacıyla, kısa metinlerden oluşan bir veri seti üzerinde standart adlandırılmış varlık tanıma değerlendirme metrikleri hesaplanmıştır. Bu veri seti, kişi varlıklarının açık ve bağlamdan bağımsız biçimde ayırt edilebildiği metinlerden oluşmaktadır. Elde edilen sonuçlar, uzun ve diyalog yoğun edebi metinlerde gözlemlenen model davranışlarını anlamlandırmak için bir referans olarak değerlendirilmiştir. Etiketleme süreci, metin bağlamına hâkim araştırmacılar tarafından manuel olarak gerçekleştirilmiştir.

Bu değerlendirme sonucunda elde edilen kesinlik (precision), geri çağırma (recall) ve F1 puanları Tablo 1’de sunulmaktadır.

Tablo 1. Kısa Metin Veri Seti Üzerinde Model Performansı

Model Adı	F1 Puanı	Precision	Recall
SavasyBERT	0.0784	0.08	0.0769
Babelscape	0.0941	0.065	0.1702

Tabloda görüldüğü üzere, Babelscape modeli kısa metinlerde yüksek geri çağırma değerine sahipken, bu durum kesinlik değerindeki düşüş ile dengelenmektedir. SavasyBERT modeli ise daha dengeli bir precision–recall profili sunmaktadır. Kısa metinlerde gözlemlenen bu davranış, Babelscape’in daha kapsayıcı bir varlık tespit stratejisi izlediğini göstermekte; bu stratejinin uzun ve bağlamsal metinlerde gürültü üretimine yol açmasının temel nedenlerinden biri olarak değerlendirilmektedir.

Elde edilen bulgular, model seçiminde metin uzunluğunun ve uygulama bağlamının önemli bir rol oynadığını göstermektedir. Tablo 1’de sunulan kısa metin sonuçları incelendiğinde, Babelscape modelinin yüksek geri çağırma değerlerinin, düşük kesinlikten kaynaklanan hataları belirli ölçüde dengeleyebildiği görülmektedir. Ancak uzun ve diyalog yoğun edebi metinlerde, Babelscape’in çok sayıda yanlış pozitif üretme eğilimi, veri kümesindeki gürültü oranını artırarak pratik kullanımı sınırlandırmaktadır. Buna karşılık SavasyBERT, daha yüksek kesinlik ile uzun metinlerde daha kontrollü ve güvenilir çıktılar sunmaktadır.

Uzun edebi metin üzerinde elde edilen model çıktıları, kısa metin veri seti için hesaplanan sayısal değerlendirme sonuçlarından farklı olarak, nicel performans ölçütleriyle analiz edilmemiştir. Bunun yerine, modellerin ürettiği kişi, organizasyon ve lokasyon varlıkları hakim araştırmacılar tarafından manuel olarak incelenerek yorumlanmıştır. Bu yaklaşım, kısa metinler üzerinde yapılan ve Tablo 1’de sunulan değerlendirmelerde ortaya çıkan model eğilimlerinin, uzun ve diyalog yoğun bir metin bağlamında nasıl yansıdığını gözlemlemeyi amaçlamaktadır. Bu kapsamda Tablo 2’de, Babelscape ve SavasyBERT modellerinin Felatun Bey ile Rakım Efendi metni [6] üzerindeki adlandırılmış varlık tespit çıktılarının genel bir özeti sunulmaktadır. Tablo, modellerin farklı varlık türlerinde ürettikleri toplam geçiş sayıları ve benzersiz kişi sayıları üzerinden gözlemlenen eğilimleri karşılaştırmalı olarak ortaya koymak amacıyla hazırlanmıştır. Sunulan değerler, mutlak doğruluk iddiası taşımamakta olup, kısa metin değerlendirmelerinde gözlemlenen model davranışlarının uzun edebi metinlerdeki yansımalarını niteliksel olarak değerlendirmek için bir referans niteliği taşımaktadır.

Tablo 2. Felatun Bey ile Rakım Efendi Metni Üzerinde Modellerin Manuel İncelemeye Dayalı Varlık Çıktı Özeti

Model Adı	Toplam Kişi Geçişi	Benzersiz Kişi Sayısı	Toplam Organizasyon Geçişi	Toplam Lokasyon Geçişi
Babelscape	1435	114	3	284
SavasyBERT	1346	61	432	254

SavasyBERT'in düşük gürültü oranı ve yüksek kesinliği, uzun edebi metinlerin karmaşık ve süreklilik gösteren yapısında hataların birikmesini engelleyerek, önerilen hibrit yaklaşım çerçevesinde çok konuşmacılı metinden konuşmaya sistemleri için daha sağlam bir altyapı oluşturmaktadır. Bu durum, çok dilli modellerin geniş veri kapsamına rağmen dile özgü morfolojik ve bağlamsal derinliğin bu tür görevlerde belirleyici olabildiğini ortaya koymaktadır.

Tablo 3. Kısa ve Uzun Metinlerde Model Davranışlarının Karşılaştırması

Kriter	Babelscape (Kısa Metinler)	SavasyBERT (Uzun Metinler)
Öncelik	Daha fazla kişi tespiti	Yanlış kişi üretmeme
Etiketleme Şekli	Daha kapsayıcı etiketleme	Seçici etiketleme
Hatalı Etiket Oranı	Tolere edilebilir	Düşük
Uzun Metin Uyumu	Hata birikir	Yüksek uyum
TTS Açısından Durum	Basit senaryolar için yeterli	Çok konuşmacılı TTS için uygun

4. SONUÇ

Bu çalışmada, Türkçe edebi metinlerde çok konuşmacılı metinden konuşmaya sistemleri için kritik bir problem olan konuşmacı tespiti görevi ele alınmış ve iki farklı NER yaklaşımı karşılaştırmalı olarak incelenmiştir. Çok dilli bir model olan Babelscape ile Türkçeye özgü olarak eğitilmiş SavasyBERT modeli, diyalog yoğunluğu yüksek uzun metinler üzerinde değerlendirilmiştir.

Elde edilen bulgular, kısa metinlerde yüksek geri çağırma değerleri sunabilen çok dilli modellerin, uzun ve bağlama duyarlı edebi metinlerde önemli ölçüde gürültü üretebildiğini göstermektedir. Babelscape modeli, kişi varlığı tespitinde niceliksel olarak daha geniş bir kapsama sahip olsa da, bağlamdan kopuk etiketlerin birikmesi nedeniyle pratik kullanım açısından sınırlı bir performans sergilemiştir. Bu durum, çok konuşmacılı TTS sistemleri için gerekli olan tutarlı ve güvenilir konuşmacı atamasını zorlaştırmaktadır.

Türkçeye özgü SavasyBERT modeli ise uzun metinlerde daha dengeli ve bağlamsal olarak tutarlı sonuçlar üretmiştir. Özellikle kişi varlıklarının tespitinde düşük gürültü oranı ve daha temiz çıktı kümeleri sunması, SavasyBERT'i konuşmacı tespiti görevinde daha uygun bir seçenek hâline getirmiştir. Kural tabanlı diyalog filtresi ile birlikte kullanıldığında, SavasyBERT çıktılarının çok konuşmacılı TTS sistemleri için pratikte daha güvenilir bir altyapı sunduğu gözlemlenmiştir.

Sonuç olarak, bu çalışma, Türkçe gibi morfolojik açıdan zengin dillerde konuşmacı tespiti görevinde model seçiminde yalnızca niceliksel performans metriklerine odaklanmanın yeterli olmadığını ortaya koymaktadır. Dile özgü NER modellerinin, uzun ve diyalog yoğun metinlerde sağladığı bağlamsal kesinlik, çok konuşmacılı TTS sistemlerinin başarısı için belirleyici bir faktördür. Önerilen hibrid yaklaşım, Türkçe edebi metinlerde konuşmacı tespiti için uygulanabilir ve güvenilir bir çözüm sunmaktadır.

Yapay Zekâ Katkı Beyanı

Bu makale, herhangi bir yapay zekâ (AI) aracı kullanılmadan tamamen yazarlar tarafından yazılmış, düzenlenmiş, analiz edilmiş ve hazırlanmıştır.

Bu çalışma, çok konuşmacılı metin seslendirme (TTS) sistemleri için edebi metinlerdeki diyalogların doğru konuşmacıya atanması sorununu ele almakta ve Makine Öğrenmesi ile kural tabanlı mantığı birleştiren bir hibrid yaklaşım önermektedir. Yöntem iki katmandan oluşur: SavasyBERT ve çok dilli Babelscape modelleriyle ‘Kişi’ varlıklarının belirlenmesi, konuşma çizgileri ve tırnak gibi göstergelere dayalı kural tabanlı diyalog tespiti. “Konuşmacı”, bu iki katmanın kesişimi olarak tanımlanmıştır. Bulgular, Türkçeye özgü SavasyBERT modelinin kurgusal karakterleri yüksek doğrulukla tanıdığını ve düşük gürültü ürettiğini göstermiştir. Buna karşın Babelscape, Türkçe dil yapısına uyumsuzluğu nedeniyle yüksek oranda hatalı pozitif üretmiştir. Sonuçlar, önerilen hibrid yaklaşımın SavasyBERT ile birlikte kullanıldığında Türkçe çok konuşmacılı TTS uygulamaları için güvenilir bir karakter tespit altyapısı sağladığını ortaya koymaktadır.

Yazar Katkıları

Bu çalışmada kavramsallaştırma ve yöntem geliştirme Pakize Erdoğan tarafından yürütülmüştür. Deneyel çalışmalar ve veri analizi Tuğçe Deniz, Pınar Ünver, Beytullah Tütüncü ve Barış Aslan tarafından gerçekleştirilmiştir. Makalenin yazımı tüm yazarların katkısı ile tamamlanmıştır. (<https://orcid.org/0009-0009-2865-1394>) (<https://orcid.org/0009-0003-5315-584X>) (<https://orcid.org/0009-0006-5576-9644>) (<https://orcid.org/0009-0000-1599-7876>) (<https://orcid.org/0000-0003-2172-5767>)

KAYNAKLAR

- [1] Klatt, Dennis H. “Review of Text-to-Speech Conversion for English.” The Journal of the Acoustical Society of America, vol. 82, no. 3, 1987, pp. 737–793. <https://doi.org/10.1121/1.395275>
- [2] Lajčínová, Bibiána, Patrik Valábek, and Michal Spišiak. “Named Entity Recognition for Address Extraction in Speech-to-Text Transcriptions Using Synthetic Data.” arXiv, arXiv:2402.05545, 2024.
- [3] Liu, Ruilin, Xuchao Guo, Hongmei Zhu, and Lu Wang. “A Text-Speech Multimodal Chinese Named Entity Recognition Model for Crop Diseases and Pests.” Scientific Reports, vol. 15, no. 1, 2025, article 5429. <https://doi.org/10.1038/s41598-025-05429-9>
- [4] Navigli, Roberto, et al. “Ten Years of BabelNet: A Survey.” Proceedings of the Thirtieth International Joint Conference on Artificial Intelligence (IJCAI), 2021, pp. 4559–4566. <https://doi.org/10.24963/ijcai.2021/625>
- [5] Yıldırım, Savaş. “Fine-Tuning Transformer-Based Encoder for Turkish Language Understanding Tasks.” arXiv, arXiv:2401.17396, 2024.
- [6] Ahmet Mithat Efendi. Felâtun Bey ile Râkım Efendi. Anadolu Üniversitesi Yayınları, 2017 <https://ieeauthorcenter.ieee.org/wp-content/uploads/IEEE-Reference-Guide.pdf>

YOLLARDA KAR VE BUZ KONTROLÜ İÇİN İLETKEN ASFALT KAPLAMALAR

Alev AKILLI EL 

Bitlis Eren Üniversitesi, Teknik Bilimler Meslek Yüksekokulu, İnşaat Bölümü, Bitlis, Türkiye
aakilli@beu.edu.tr

ÖZET

Soğuk iklim bölgelerinde kar ve buz birikimi, yol yüzeylerinde kayma direncini azaltarak trafik güvenliğini ciddi şekilde tehdit eden en önemli çevresel etkenlerden biridir. Geleneksel kar ve buz giderme yöntemleri; mekanik temizleme, manuel müdahale ve kimyasal buz çözücü tuz kullanımı gibi uygulamaları içermektedir. Ancak bu yöntemler hem operasyonel gecikmelere hem de kaplama malzemesinin bozulmasına, ayrıca çevresel kirliliğe yol açmaktadır. Son yıllarda, bu olumsuzlukları ortadan kaldırmak amacıyla geliştirilen iletken kaplama teknolojileri, kar ve buzun etkin bir şekilde eritilmesini sağlayarak yol güvenliğini artıran çevre dostu bir alternatif olarak öne çıkmaktadır. Bu çalışmada, buzlanma ve kar birikiminin yoğun olduğu karayollarında iletken kaplamaların kullanım potansiyeli araştırılmıştır. İletken asfalt betonlarının temel çalışma prensipleri, iletken malzeme türleri (grafit, karbon fiber, çelik tozu vb.), ısıtma mekanizmaları ve enerji verimlilikleri incelenmiştir. Ayrıca literatürdeki güncel araştırmalar değerlendirilerek, farklı iletken dolgu malzemelerinin elektriksel iletkenlik, ısıtma verimi, mekanik dayanım ve çevresel sürdürülebilirlik açısından performansları karşılaştırılmıştır. Elde edilen bulgular, iletken asfalt kaplamaların buzlanmayı önlemede ve kar birikimini azaltmada etkili bir çözüm sunduğunu, aynı zamanda çevreye zarar vermeden uzun dönemli yol güvenliği sağlayabildiğini göstermektedir. Bu kapsamda, iletken kaplama teknolojilerinin kış şartlarında güvenli ve sürdürülebilir ulaşım sistemlerinin geliştirilmesinde önemli bir potansiyele sahip olduğu sonucuna varılmıştır.

Anahtar Kelimeler: İletken asfalt kaplama, Buzlanma önleme, Kar eritme, Yol güvenliği, Sürdürülebilir kaplama teknolojileri.

1 GİRİŞ

Ulaşım sistemleri zaman içerisinde önemli bir evrim süreci geçirmiş ve bu durum kentleşmenin hızla artmasına katkı sağlamıştır. Ulaşım güvenliğinin temini, günümüzde toplumun temel önceliklerinden biri olarak önemini sürdürmektedir. Bu kapsamda, yol güvenliği; yolcular, sürücüler, araç özellikleri, karayolu altyapısı ve çevresel koşullar gibi çok sayıda etmenle yakından ilişkilidir. Özellikle yağmur, buz ve kar gibi doğal iklim koşulları, ciddi yol tehlikeleri oluşturarak frenleme performansının azalmasına, ekonomik kayıplara, yaralanmalara, yol güvenliğinin zayıflamasına ve yol kapasitesinin düşmesine neden olan kazaların başlıca sebepleri arasında yer almaktadır [1].

Yol yüzeyinde biriken kar ve buz tabakaları, kaplamanın kayma direncini önemli ölçüde azaltarak karayolu trafik güvenliğini ciddi biçimde olumsuz etkilemektedir. Bu durum, özellikle

düşük sıcaklıkların uzun süre devam ettiği kış dönemlerinde, sürücü kontrolünün zayıflamasına, frenleme mesafesinin artmasına ve dolayısıyla trafik kazası riskinin yükselmesine neden olmaktadır. Kış aylarında trafik güvenliği ve yol kapasitesinin korunabilmesi için, kaplama yüzeyinde oluşan kar ve buzun zamanında ve etkili biçimde uzaklaştırılması büyük önem taşımaktadır.

Bu amaçla günümüzde manuel kar küreme, mekanik temizleme ve buz çözücü tuz püskürtme gibi geleneksel yöntemler yaygın olarak kullanılmaktadır. Ancak bu yöntemler, hem operasyonel gecikmelere (histerezis etkisi) hem de kaplama yüzeyinin fiziksel bütünlüğünün bozulmasına yol açabilmektedir. Ayrıca, kimyasal tuzların kullanımı nedeniyle kaplama malzemesinin erken yaşlanması, metal korozyonu, bitki örtüsüne zarar verilmesi ve yeraltı suyu kirliliği gibi ciddi çevresel etkiler ortaya çıkmaktadır [2],[3]. Son yıllarda buz çözücü kimyasalların kullanımındaki artış, çevresel sürdürülebilirlik açısından daha büyük zorluklar yaratmakta ve alternatif, çevre dostu çözümlere duyulan ihtiyacı artırmaktadır [4–6].

Bu bağlamda, geleneksel kar ve buz temizleme yöntemlerinin kısıtlarını ortadan kaldırmak amacıyla geliştirilen aktif elektrikli buz ve kar eritme teknolojileri, araştırma dünyasında önemli bir ilgi odağı haline gelmiştir. Gömülü ısıtma kabloları, karbon fiber tabanlı iletken ağlar veya metalik ızgaralarla temsil edilen bu sistemler, enerji verimliliği yüksek, çevreyle uyumlu ve sürdürülebilir çözümler sunmaktadır. Özellikle iletken asfalt beton (ECA) teknolojisi, bu kapsamda öne çıkan yenilikçi bir yaklaşım olarak değerlendirilmektedir. ECA, elektrik enerjisini doğrudan ısı enerjisine dönüştürerek kaplama yüzeyinde homojen ısınma sağlar ve buzlanmayı önleyici etkin bir mekanizma sunar. Bu nedenle, son yıllarda yapılan araştırmalar, iletken asfalt betonların malzeme optimizasyonu, enerji tüketim performansı, uzun dönem dayanıklılığı ve ekonomik uygulanabilirliği gibi konular üzerinde yoğunlaşmıştır [7–9].

İletken asfalt betonu (ECA), yalıtkan özellikteki geleneksel asfalt karışımlarının elektriksel iletkenliğini artırmak amacıyla grafit, iletken elyaf ve iletken agrega gibi malzemelerin karışıma eklenmesiyle elde edilmektedir. Bu yapı sayesinde, asfalt kaplama elektrik enerjisini doğrudan ısı enerjisine dönüştürerek yüzeydeki buz ve karın eritilmesini sağlamaktadır. Ayrıca, iletken asfalt betonları belirgin basınca duyarlı (piezorezistif) ve indüksiyonla ısıtma özelliklerine sahiptir. Bu özellikler, kaplamanın kendi kendini izleme (self-sensing) ve kendi kendini onarma (self-healing) yeteneğini desteklemekte, böylece asfalt karışımının yorulma direncini ve hizmet ömrünü artırmaktadır [10–14].

Arabzadeh ve çalışma arkadaşları, yalnızca karbon fiber içeren tek fazlı ve hem karbon fiber hem de grafit içeren iki fazlı iletken asfalt mastiği geliştirmişlerdir. Bu çalışmada numunelerin hacimsel öz direnci ve ısıtma verimliliği ölçülmüş; ayrıca iletken asfalt betonunun sıcaklık artışı, enerji tüketimi ve kar eritme performansı değerlendirilmiştir [15,16]. Notani ve diğer araştırmacılar, farklı karbon fiber türleri ve uzunluklarının kullanıldığı iletken asfalt betonlarının fiziksel özelliklerini, hacimsel öz direncini ve termal verimliliğini incelemişlerdir [17]. Yuan ve ekibi, iletken asfalt betonunun ısıtma performansını etkileyen faktörleri ayrıntılı biçimde değerlendirmiştir [18]. Rew ve çalışma arkadaşları, kar ve buzun sürücü güvenliği üzerindeki olumsuz etkilerini azaltmak amacıyla grafit içeren iletken asfalt betonlarının kullanımını önermiş; ayrıca iletken tabakanın yerleşim konumu ve kalınlığını optimize etmişlerdir [19]. El-Dieb ve diğerleri, çelik talaşı, karbon tozu ve grafit tozu gibi çeşitli iletken dolgu maddelerinin ince agrega yerine kullanılmasının betonun yol performansı üzerindeki etkilerini araştırmışlardır [20]. Rizvi ve ekibi, karbon nanofiber katkılı iletken asfalt betonları hazırlayarak farklı yük, frekans ve sıcaklık koşullarının piezorezistif tepki üzerindeki etkilerini incelemiştir [21]. Li ve arkadaşları, indüksiyonla onarılabilir asfalt betonları geliştirmek amacıyla asfalt karışımına iletken dolgu maddesi olarak çelik fiber, çelik kumu ve çelik cürufu eklemişlerdir [22]. Benzer şekilde, Liu ve ekibi tarafından yapılan çalışmada, çelik lif katkılı gözenekli asfalt betonunun indüksiyon ısıtması yoluyla kendi kendini onarma oranının artırılabilmesi ve malzemenin yorulma ömrünün önemli ölçüde uzatılabilmesi ortaya konmuştur [23].

Son yıllarda, sürdürülebilir ulaşım sistemlerinin geliştirilmesine yönelik çalışmalar kapsamında enerji verimli, çevre dostu ve uzun ömürlü kaplama çözümlerine olan ilgi artmıştır. Bu bağlamda, elektrik enerjisini doğrudan ısı enerjisine dönüştürebilen iletken asfalt kaplamalar, kar ve buz birikimini önleyerek kış şartlarında yol güvenliğini artıran yenilikçi bir teknoloji olarak öne çıkmaktadır. Ancak bu sistemlerin farklı iletken malzeme türleri, enerji tüketimi, ısıtma verimliliği ve mekanik performans açısından kapsamlı değerlendirmelere ihtiyaç duyduğu görülmektedir. Bu çalışma, buzlanma ve kar birikiminin yoğun olduğu karayollarında iletken kaplamaların kullanım potansiyelini araştırmayı, iletken malzemelerin kaplama performansı üzerindeki etkilerini incelemeyi ve mevcut literatürdeki eksikliklere katkı sağlamayı amaçlamaktadır.

2 İLETKEN KAPLAMA TEKNOLOJİLERİNİN GELİŞİMİ

Son yıllarda teknoloji ve malzeme bilimi alanında kaydedilen ilerlemeler, birçok sektördeki yenilikçi çözümlerin geliştirilmesine olanak sağlamıştır. Bu gelişmeler arasında iletken asfalt beton (ECA, Electrically Conductive Asphalt), yalnızca geleneksel mekanik ve dayanıklılık özellikleriyle sınırlı kalmayıp, aynı zamanda çok işlevli performans özellikleri sunabilmesi nedeniyle inşaat mühendisliği alanında dikkat çeken bir teknoloji olarak öne çıkmaktadır. Geleneksel asfalt karışımları, genellikle iri ve ince agregalar, dolgu maddesi ve bitümden oluşmakta ve 107 ila 109 $\Omega \cdot m$ aralığında değişen özgül direnç değerleriyle elektriksel olarak yalıtkan bir yapı sergilemektedir [24]. Bununla birlikte, bu karışımlara elektriksel iletkenliği artıran dolgu malzemelerinin (örneğin grafit, karbon fiber veya metalik partiküller) entegre edilmesiyle, asfaltın yalıtkan karakteri değişmekte ve malzeme iletken asfalt betonu formuna dönüştürülebilmektedir [25].

Elektriksel olarak iletken asfalt betonu, havaalanları, köprü döşemeleri ve benzeri kritik asfaltlı alanlarda kış bakım sorunlarını azaltmak amacıyla, buzlanmayı önleme veya buz çözme uygulamalarında umut verici bir malzeme olarak değerlendirilmektedir. İletken asfalt betonu (ECA), asfalt betonuna iletken agregalar veya dolgu maddelerin eklenmesiyle üretilebilmektedir. Geleneksel asfalt betonu, bitüm, agregalar ve dolgu maddelerinden oluşmakta olup, agregalar kaplamaya gerekli iskeleti sağlarken, dolgu maddesi bitümle birleşerek agregalar arasında oluşan boşlukları dolduran bir mastik oluşturur [26]. İletken asfalt betonunun üretiminde yaygın bir yöntem, asfalt betonuna elektriksel olarak iletken dolgu maddesinin eklenmesiyle, agregalar sistemi tarafından oluşturulan boşlukları dolduran iletken asfalt mastik üretmektir [27]. Asfalt betonunda dirençli ısıtma yoluyla istenilen miktarda ısı üretilmesinde kritik bir rol oynamaktadır; bu nedenle, ECA'nun direnci ve ısı üretme kapasitesi, agregalar varlığından bağımsız olarak, yani performansını etkileyebilecek diğer katkılar olmadan ayrı bir şekilde incelenmelidir [28].

Tipik olarak, elektriksel olarak iletken asfalt betonu dört ana bileşenden oluşmaktadır: fonksiyonel katkı maddesi, asfalt bağlayıcı, agregalar ve dolgu maddesi (Şekil 1).



Şekil 1. İletken Asfalt Kaplama Yapısı

İletken asfalt betonun hazırlanmasında, uygun hammaddelerin seçimi ve karışım tasarımının doğru biçimde yapılması büyük önem taşımaktadır [29]. İletken asfalt betonu geliştirilirken karşılaşılan temel zorluk, yol performansından ödün vermeden, malzemenin çok işlevli kullanımına uygun biçimde elektriksel iletkenliğinin etkin bir şekilde artırılmasıdır [30].

Önceki çalışmalara göre [31,32], elektriksel olarak iletken asfalt betonu geliştirmek için üç temel strateji bulunmaktadır:

- **İletken asfalt bazlı ECA:** Fonksiyonel katkı maddeleri doğrudan asfalt bağlayıcı ile karıştırılarak geliştirilir.

- **İletken agrega bazlı ECA:** Doğal agregaların yerine iletken agregalar kullanılır.

- **İletken dolgu bazlı ECA:** Mineral dolgu maddelerinin yerine iletken tozlar eklenir.

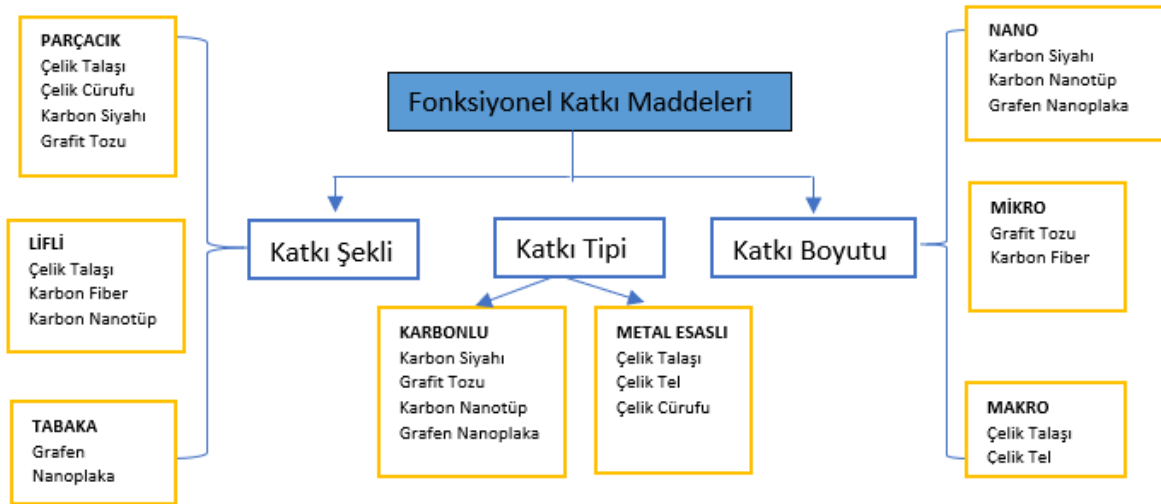
Bu üç ECA türü için hazırlama süreçleri aşağıdaki gibidir:

İletken asfalt bazlı ECAC, kuru ve ıslak karıştırma yöntemleri kullanılarak hazırlanabilir. Lifler ve karbon bazlı nanomalzemeler gibi fonksiyonel katkı maddeleri, ıslak karıştırma yöntemi ile doğrudan asfalt bağlayıcıyla birleştirilir ve ardından agrega ile mineral dolgu maddesi eklenir. Kuru yöntemde ise fonksiyonel katkı maddeleri (ör. çelik elyaf ve karbon elyaf), asfalt bağlayıcı ile bağlanmadan önce agrega ile karıştırılır. Kuru karıştırma yöntemi, asfalt betonundaki liflerin flokülasyonunu azaltarak karıştırma sürecini kolaylaştırabilir. Gerçekte, kuru karıştırma yöntemi laboratuvar ve saha uygulamalarında lif takviyeli asfalt beton üretiminde yaygın olarak kullanılmıştır [33]. Bu pratikliği sayesinde, kuru karıştırma yöntemi ECA üretiminde fonksiyonel katkı maddelerinin karıştırılması için umut verici bir yaklaşım olarak öne çıkmaktadır.

Homojen şekilde dağıtılmış fonksiyonel katkı maddeleri, ECA içerisinde sürekli ve kararlı bir iletken kanal oluşturarak, malzemenin üstün elektriksel iletkenlik ve ısıtma ile kendi kendini iyileştirme kapasitesini ortaya koymasını sağlar [34]. Ayrıca, ECA'ye uygulanan uygun voltaj sayesinde kar ve buzun eritilmesi için gerekli ısı üretilebilir [35]. Asfalt beton yapıların maruz kaldığı gerilim (veya kuvvet), gerinim (veya deformasyon) ve çatlak (veya hasar) durumu, harici yük ile elektriksel sinyal (özgül direnç) arasındaki ilişkiye dayanarak tespit edilebilmektedir [36,37]. Bunun yanı sıra, ECA piezorezistif bir sensör olarak tasarlanabilir ve böylece trafik algılama uygulamalarında, örneğin trafik hacmi izleme ve yol dinamik yükleme değerlendirmeleri için kullanılabilir [38,39].

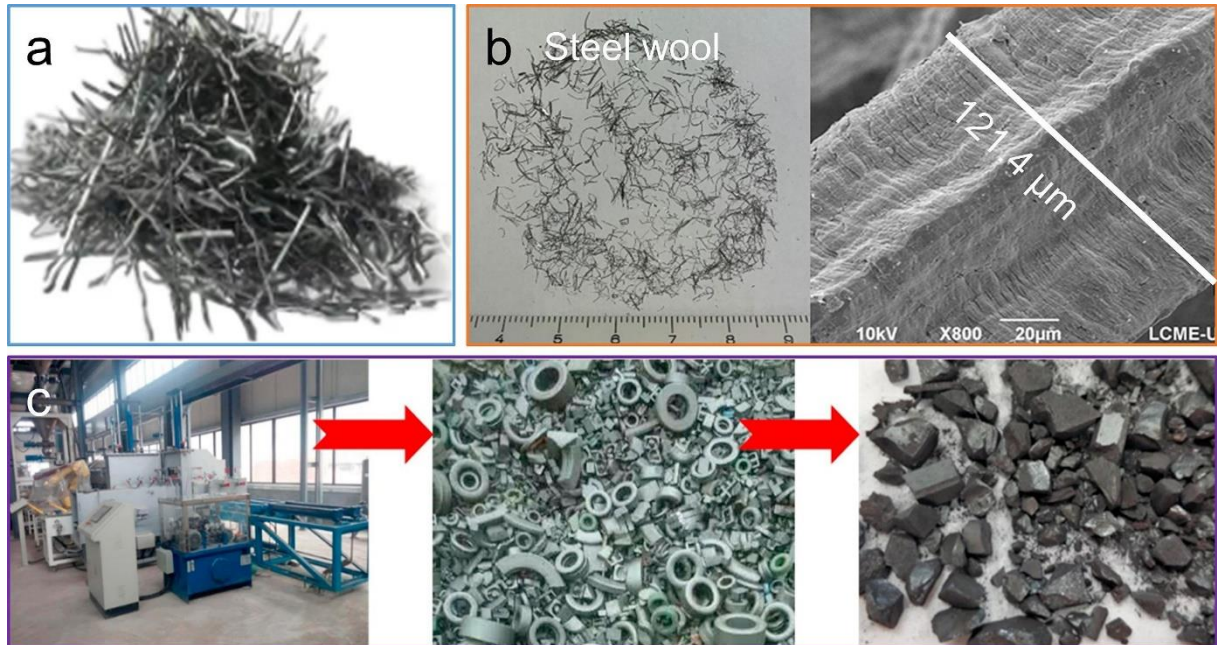
3 İLETKEN MALZEMELERİN PERFORMANS DEĞERLENDİRMESİ

İletken çimento betonu geliştirme sürecine benzer şekilde, ECA'nin geliştirilmesinde temel hedef, asfalt beton matrisi içerisinde etkin bir iletken ağ oluşturmaktır [40,41]. Şekil 2'de özetlendiği üzere, yaygın olarak kullanılan fonksiyonel katkı maddeleri farklı tip, boyut ve şekillerde mevcuttur ve bu çeşitlilik, iletken ağın oluşumunu ve malzemenin elektriksel performansını doğrudan etkilemektedir.



Şekil 2. İletken asfalt kaplamanın geliştirilmesinde kullanılan fonksiyonel katkı maddeleri

Çelik elyaf, çelik yünü ve ferrit gibi metalik esaslı malzemeler, asfalt betonunu elektriksel olarak iletken hale getirebilen düşük maliyetli katkı maddeleri olarak öne çıkmaktadır (Şekil 3). Örneğin, García ve arkadaşları, karıştırılmış çelik yününün ECA'nin iletkenliğini artırarak kendi kendini onarma uygulamalarındaki performansını iyileştirme potansiyelini araştırmıştır. Bununla birlikte, çelik yünü içeren ECA'nin toplu elektriksel direnci, sınırlı boyutları nedeniyle lif uzunluğu veya çapından neredeyse etkilenmemekte ve en düşük değer yalnızca $1 \times 10^4 \Omega \cdot m$ olarak gözlemlenmiştir [42].



Şekil 3. İletken asfalt betonu hazırlamak için kullanılan metal bazlı malzemeler; (a) çelik elyaf, (b) çelik yünü, (c) atık ferritin dönüşümü

Karbon fiber, sıfır boyutlu (0D) karbon nanomalzemeleri (örneğin karbon siyahı ve grafit tozu), bir boyutlu (1D) nanofiberler (örneğin karbon nanotüp) ve iki boyutlu (2D) nanotabakalar (örneğin grafen nanoplaka) gibi karbon bazlı malzemeler, ECA geliştirmek için ideal adaylar olarak

değerlendirilmektedir. Bu malzemeler, neme karşı çözünmezlikleri ve çevresel koşullarda düşük oksidasyon eğilimleri nedeniyle, ECA'de üstün kimyasal kararlılık sağlamak ve uzun süreli performans için uygun özellikler sunmaktadır.

Tüm bu fonksiyonel katkı maddeleri arasında, karbon fiber (CF) öne çıkmaktadır; birkaç santimetre uzunluğa, 10^{-2} – 10^{-4} Ω ·cm aralığında öz dirence, 300 GPa Young modülüne ve 200–3500 MPa çekme dayanımına sahiptir [43]. Karbon fiber, asfalt beton ile yüksek düzeyde uyum gösterdiğinden, CF bazlı ECA'nın hem yapısal hem de elektriksel açıdan istenen özellikleri sergilemesini sağlar ve bu da malzemeyi hem yapısal hem işlevsel olarak arzu edilen bir seçenek haline getirir. CF bazlı ECA, asfalt betonun yorulma ömrünü ve termal çatlamaya karşı direncini artırmanın yanı sıra, yüksek elektriksel iletkenlik elde edebilir ve kendi kendini iyileştirme, kendi kendini ısıtma ile kendi kendini algılama yeteneklerini gösterebilir [44–47]. ECA'da en yüksek elektriksel iletkenliğin sağlanabilmesi için, sızma eşiği dikkate alınarak karbon fiber dozajı optimize edilmelidir.

Tek boyutlu (1D) karbon nanofiber olarak karbon nanotüp (CNT), tek katmanlı grafenden oluşan tüp yapısına sahiptir ve yaklaşık 10^{-2} Ω ·cm'lik üstün elektriksel iletkenlik ile 200 GPa çekme dayanımına sahiptir [48,49]. Bu özellikleri nedeniyle, ECA'nın elektriksel direncini düşürmek için son derece uygun bir aday olarak değerlendirilmektedir [50,51]. CNT, çok işlevli performans ve mükemmel takviye etkisi sunması nedeniyle çekici bir fonksiyonel katkı maddesi olarak öne çıkmaktadır. Bununla birlikte, CNT bazlı asfalt ECA'nın performansı büyük ölçüde matris içindeki dağılım kalitesine bağlıdır [52]. Bu nedenle, karıştırılmış CNT'nin beton içinde homojen şekilde dağılmasını sağlamak üzere daha fazla araştırma yapılması gerekmektedir.

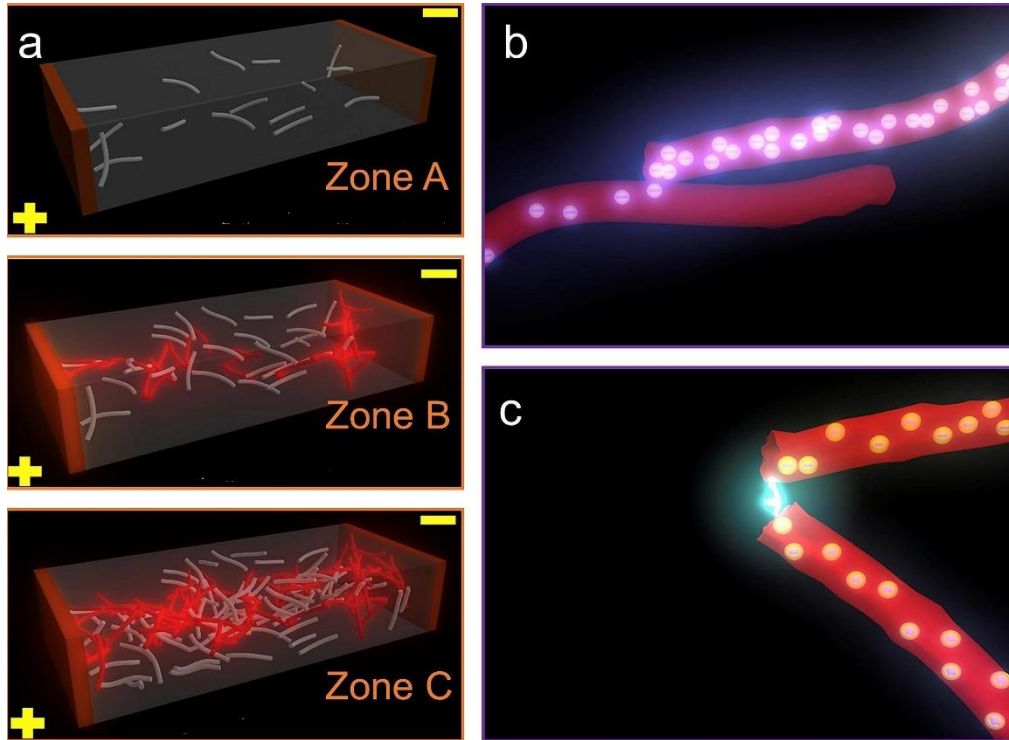
GNP (Grafen Nanoplaka), grafen yığınlarından oluşan iki boyutlu (2D) bir nanotabakadır [53,54] ve olağanüstü mekanik dayanımı ile üstün elektriksel özellikleri ile bilinmektedir [55]. CNT'ye kıyasla daha yüksek elektriksel hareketliliğe sahip olması, GNP'yi ECA geliştirmek için ideal bir aday haline getirmektedir [56]. Tıpkı CF ile bağlantılı sıfır boyutlu iletken nanoparçacıklar kullanılarak ECA'nın öz direncinin önemli ölçüde azaltılması gibi, CF bağlantılı GNP kullanımıyla da ECA'nın öz direnci belirgin şekilde düşürülebilir. Örneğin, Arabzadeh ve arkadaşları, kış koşullarında buz çözme ve buzlanmayı önleme amaçlı ECA üretmiş ve bunu, %5 hacim GNP ile birleştirilmiş %0–2,5 hacim CF içeren modifiye asfalt mastik kullanarak başarmıştır [57]. Karbon, doğada en bol bulunan elementlerden biri olup, karbon bazlı malzemeler endüstriyel ölçekte yaygın olarak kullanılmaktadır; bu durum, çok işlevli ECA geliştirmek için önemli bir fırsat sunmaktadır.

Genel olarak, ECA'nın iletkenliğini artırmada metalik malzemelerin potansiyeli, karbon bazlı malzemelere kıyasla daha sınırlıdır [58]. Metalik malzemeler, ECA'nın elektriksel direncini yalnızca yaklaşık 100 Ω ·m seviyesine kadar düşürebilmekte, bu da bazı pratik uygulamaların gereksinimlerini karşılamak için yetersiz kalmaktadır [59]. Ayrıca, metalik malzemelerin uzun süreli kullanım sırasında paslanma ve aşınma eğilimi göstermesi, ECA'nın performansını olumsuz yönde etkileyebilmektedir [60]. Buna karşın, karbon bazlı malzemeler neme karşı çözünmez olmaları ve çevresel koşullarda düşük oksidasyon eğilimi göstermeleri nedeniyle ECA geliştirmede daha uygun adaylar olarak öne çıkmaktadır [61]. Bu özellikleri, karbon bazlı katkıların ECA içerisinde yüksek kimyasal kararlılık sergilemesini sağlamaktadır. Ayrıca, bu malzemeler, betonun elektriksel ve termal iletkenliğini iyileştirmede metalik katkılara kıyasla daha etkin bir performans sunmaktadır. Özellikle karbon fiber (CF), yüksek en-boy oranı sayesinde izole işlevsel katkı partikülleri arasında bağlantılar kurarak, CF ve karbon bazlı nanomalzemelerin birlikte kullanılmasıyla ECA içerisinde hiyerarşik bir iletken ağı oluşumunu destekler. Bu sinerjik etki, ECA'nın genel iletkenlik performansında önemli bir artışa yol açmaktadır.

3.1 Buzlanmayı Önleme ve Buz Çözme Uygulamaları İçin İletken Asfalt Beton

Tipik olarak, fonksiyonel katkı maddeleri asfalt ve mineral dolgu malzemesi ile karıştırılarak, agregre sistemindeki hava boşluklarını doldurabilen iletken bir asfalt mastiği elde edilir; bu yapı, iletken asfalt esaslı ECA olarak tanımlanmaktadır [61]. Bu yöntem, kaplamanın kendi kendini iyileştirme kapasitesine ulaşması açısından umut verici bir yaklaşım olup, özellikle asfalt kaplamaların buzlanmayı önleme ve buz çözme uygulamalarında kullanılma potansiyeline sahiptir [62,63]. Son yıllarda yapılan çalışmalar, doğal agregalar yerine çelik cürufu kullanımının, ısıtma elemanı işlevi görebilen iletken agregre bazlı ECA üretimi için alternatif ve verimli bir yöntem olabileceğini ortaya koymuştur.

Elektriksel olarak iletken asfalt betonundaki (ECA) elektron iletim mekanizması, karışıma eklenen fonksiyonel katkı maddelerinin içsel iletkenliği, temas direnci ve elektron tünelleme etkisine bağlı olarak gerçekleşmektedir [5], [60], [170]. İstatistiksel sızma teorisine göre [171], ECA'nın iletkenliği ile karışıma katılan fonksiyonel katkı maddesinin miktarı arasında bir ilişki kurulabilir ve bu ilişki aracılığıyla optimum katkı miktarı belirlenebilir. Şekil 4a'da gösterildiği üzere, fonksiyonel katkı maddesinin hacmi sızma eşiğinin altında kaldığında (Bölge A), sürekli bir iletken ağ oluşamaz ve bu durumda ECA'nın özdirenci, katkı oranının artmasıyla kademeli olarak azalma eğilimi gösterir. Katkı miktarının sızma eşiğine ulaşmasıyla birlikte (Bölge B), bitişik katkı parçacıkları doğrudan temas ederek kararlı iletken yollar oluşturur; bu da ECA'nın özdirencinde birkaç büyüklük mertebesinde bir azalma meydana getirir. Katkı dozajı sızma eşiğini aştığında ise (Bölge C), özdirençte yalnızca küçük dalgalanmalar gözlenir. Sonuç olarak, asfalt betonundaki fonksiyonel katkı maddelerinin sızma eşiği değerinin doğru biçimde belirlenmesi, ECA'nın elektriksel özelliklerinin optimize edilmesi açısından kritik bir parametredir. Bu nedenle, ECA'nın geliştirilmesi sürecinde uygun katkı miktarının belirlenmesinde söz konusu teori temel alınmalıdır.

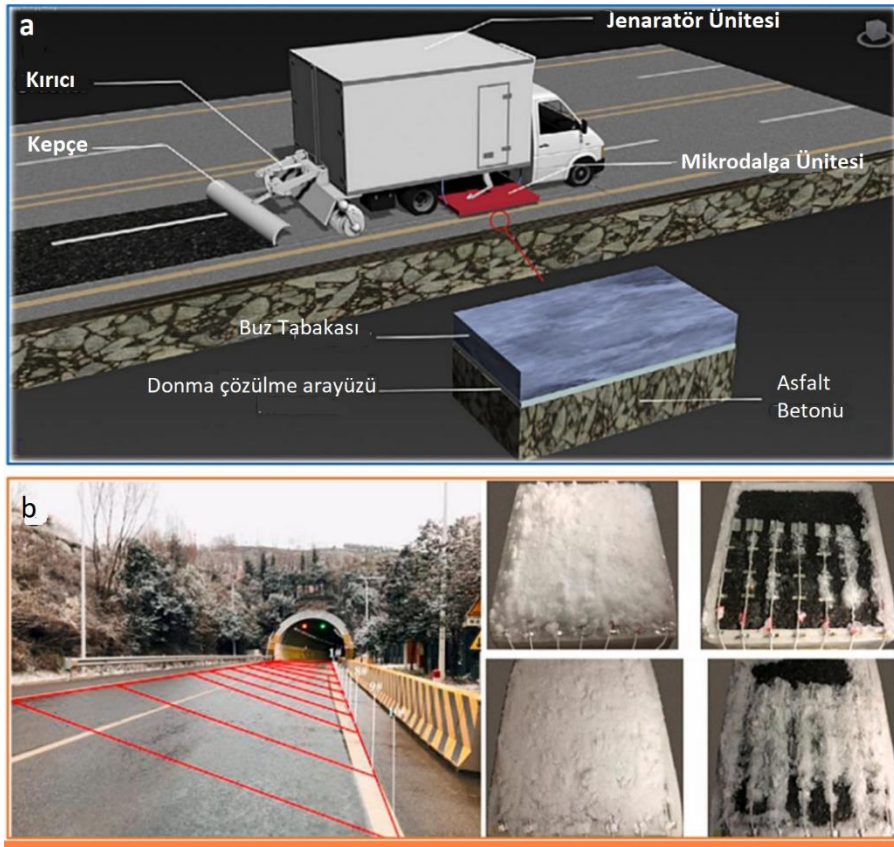


Şekil 4. (a) Özdirenç ve dolgu konsantrasyonu arasındaki ilişki; (Bölge A) Yalıtılmış faz, (Bölge B) Geçiş fazı, (Bölge C) aşırı iletken dolgu; iletken asfalt betonundaki elektron iletim mekanizmaları (b) temas direnci, (c) elektron tünelleme

3.2 Buzlanmayı önleme ve kar eritme uygulamaları için iletken asfalt betonunu ile ilgili yapılan çalışmalar

Kış mevsiminde kar ve buz birikimi, asfalt kaplamalarda ciddi ekonomik kayıplara, güvenlik risklerine ve hatta ölümcül kazalara yol açabilmektedir [64]. Geleneksel kar ve buz temizleme yöntemleri ile çeşitli ısıtma sistemleri uzun yıllardır kullanılmakla birlikte, bu yöntemlerin çevre kirliliğine yol açması ve yapısal donatı üzerinde erozyon etkisi yaratması gibi dezavantajlar, kaplama mühendisliğindeki uygulama alanlarını önemli ölçüde sınırlamaktadır. Kış koşullarında yol bakımını otomatikleştirmek amacıyla yapılan çalışmalar, dirençli veya mikrodalga ısıtma yöntemleriyle kar ve buzun etkin biçimde eritilebileceğini göstermiştir. Bu bağlamda, elektriksel olarak iletken asfalt beton (ECA), kar ve buz eritme amacıyla kaplamalarda, köprü tabliyelerinde, otoyol yüzeylerinde ve havaalanı pistlerinde potansiyel bir ısıtma elemanı olarak değerlendirilmektedir.

Örneğin, Arabzadeh ve arkadaşları, karbon fiber takviyeli ECA (CF-ECA) kaplaması geliştirmiş ve %1 oranında CF içeren ECA levhalarının sıcaklığının 25 dakika içerisinde 23 °C arttığını, ancak geleneksel asfalt kaplamalara kıyasla yaklaşık %50 daha yüksek bir inşaat maliyeti gerektirdiğini bildirmiştir [16]. Benzer şekilde, Gao ve arkadaşları, mikrodalga ile buz çözme amacıyla ECA karışımında hacimce %40–60 oranında çelik cürufu kullanmış ve bu uygulamanın, kaynak erişilebilirliği, maliyet ve çevresel etkiler açısından değerlendirildiğinde, kış koşullarında yol güvenliğini artırmada etkili bir çözüm sunduğunu belirtmiştir (Şekil 5a) [65]. Jiao ve arkadaşları ise ısı transfer verimliliğini artırmak amacıyla ECA'ye çelik cürufu eklemiş ve elektrik-termal sistemlere kıyasla kar eritme verimliliğinin %25–38 oranında iyileştiğini, ayrıca elde edilen ECA'nın yol performans parametrelerinin teknik şartname gereksinimlerini karşıladığını tespit etmiştir (Şekil 5b)[66]



Şekil 5. İletken asfalt beton ve asfalt kaplamanın buzlanmayı önlem ve kar eritmedeki uygulaması (a) mikrodalga yöntemi ile buz çözmek için iletken asfalt betonunda çelik cüruf kullanımı, (b) tünel çıkışı ve -3 °C'de ısıtma işlemi sırasında kar tabakasının değişimi

Sonuç olarak, gelecekteki arařtırmaların, ECA karıřımlarında kullanılan fonksiyonel agregaların hacim oranını artırmaya odaklanması önerilmektedir. Bu yaklařım, buzlanmayı önleme ve kar eritme uygulamaları için ECA'nın ısı üretim ve ısı transfer kapasitesinin önemli ölçüde geliştirilmesine katkı sağlayabilir.

4 SONUÇLAR

Bu çalışmada, elektriksel olarak iletken asfalt beton (ECA) ile ilgili literatürdeki güncel arařtırmalar incelenmiř ve farklı katkı maddeleri, tasarım stratejileri ile ECA'nın performans potansiyeli deęerlendirilmiřtir. Özellikle iletken asfalt bazlı, iletken agregası bazlı ve iletken dolgu bazlı ECA türlerinin termal, elektriksel ve yapısal özellikleri karşılařtırılmıř; kar ve buz eritme, kendi kendini iyileřtirme ve piezorezistif algılama gibi çok iřlevli uygulama potansiyelleri tartıřılmıřtır. Bu sonuçlar, ECA'nın kiř kořullarında yol güvenlięi ve kaplama performansını artırmadaki rolünü daha iyi anlamak ve gelecekteki arařtırmalar için yol gösterici ilkeler sunmak amacıyla özetlenmektedir.

Yaklařık yirmi yıllık arařtırma ve geliştirme faaliyetlerine raęmen, elektriksel olarak iletken asfalt betonun (ECA) kompozisyon tasarımı, performans optimizasyonu ve saha uygulamaları hâlen arařtırılmakta olup, bu alandaki geliştirme ve uygulanabilirlięin artırılması için ilave çabalar gerekmektedir.

Geleneksel asfalt betonuna fonksiyonel katkı maddelerinin ilavesi, malzemenin termal ve elektriksel iletkenlięini artırarak ısıl iyileřtirme kapasitesini geliřtirebilir. Çeřitli katkı maddeleri arasında, karbon fiber (CF), köprüleme etkisini güçlendirme ve ECA içerisinde iletken aęların oluřumunu kolaylařtırma aęısından, karbon bazlı nanomalzemelere kıyasla daha yüksek bir etkililik sergilemektedir. Bununla birlikte, CF ile karbon bazlı nanomalzemelerin birlikte kullanılması, ECA içinde hiyerarřik iletken yolların oluřturulması aęısından ideal bir strateji olarak deęerlendirilebilir.

İletken dolgu bazlı ECA'nın ısıtma ve kendi kendini iyileřtirme kapasitesi, dolgu maddesinin sınırlı hacim oranı nedeniyle, iletken asfalt bazlı veya iletken agregası bazlı ECA'ya kıyasla görece daha düşüktür. ECA'nın yol mühendislięinde indüklenen ısıtma ve iyileřtirme performansını artırmak amacıyla, gelecekteki çalışmaların ek deneysel deęerlendirmeler, sayısal modelleme ve saha uygulamaları üzerine odaklanması gerekmektedir. Bu çalışmalar, ECA'nın etkili ısıtma ve iyileřtirme uygulamalarındaki temel mekanizmalarının daha iyi anlařılmasını sağlayacak ve malzemenin tasarım ile performansının optimize edilmesine katkı sunacaktır.

İletken agregası bazlı ECA, yüksek verimlilięi ve ısı kaynaklarının homojen daęılımı nedeniyle asfalt kaplamalarda kar ve buz eritme uygulamaları için özellikle önerilmektedir. Isıtılmalı bir ECA kaplama sisteminin performansı, voltaj veya mikrodalgası radyasyon ayarları kullanılarak hedeflenen sıcaklıęa optimize edilebilir; bu da verimli ve stabil bir ısı üretim performansı sağlar. Kar ve buz eritme sırasında asfalt kaplamanın kendi kendini onarma kapasitesini artırmak amacıyla, buz eridikten sonra ek bir ısıtma iřleminin uygulanması tavsiye edilmektedir.

Sonuç olarak, elektriksel olarak iletken asfalt beton (ECA), kiř kořullarında kar ve buz yönetimi, yol güvenlięinin artırılması ve asfalt kaplamaların kendi kendini iyileřtirme yeteneęinin geliřtirilmesi aęısından önemli bir potansiyele sahiptir. Literatürdeki çalışmalar, farklı katkı maddeleri ve tasarım stratejilerinin ECA'nın elektriksel, termal ve mekanik performansını önemli ölçüde etkiledięini göstermektedir. Özellikle karbon fiber ve karbon bazlı nanomalzemelerin birlikte kullanımı, hiyerarřik iletken aęların oluřturulmasını sağlayarak çok iřlevli performansı optimize etmektedir. Gelecekteki arařtırmalar, ECA'nın saha uygulamalarını ve uzun dönemli performansını deęerlendirmeye, uygun katkı maddesi oranlarını ve tasarım parametrelerini optimize etmeye odaklanmalıdır; bu da malzemenin pratik uygulamalarda güvenli, verimli ve sürdürülebilir bir çözüm olarak kullanılmasını destekleyecektir.

Çıkar Çatışması Beyanı (Conflict of Interest Statement)

Yazar, bu makalenin yayınlanmasıyla ilgili herhangi bir çıkar çatışmasının bulunmadığını beyan eder.

Araştırma ve Yayın Etiği Beyanı (Statement of Research and Publication Ethics)

Bu çalışma, araştırma ve yayın etiği ilkelerine uygun olarak hazırlanmıştır.

Yapay Zekâ (AI) Katkı Beyanı (Artificial Intelligence (AI) Contribution Statement)

Bu makale, herhangi bir yapay zekâ (AI) aracı kullanılmadan tamamen yazarlar tarafından yazılmış, düzenlenmiş, analiz edilmiş ve hazırlanmıştır. Tüm içerik, metin, veri analizi ve şekiller yalnızca yazarlar tarafından üretilmiştir.

Yazar Katkıları (Contributions of the Authors)

Yazar, çalışmanın kavramsallaştırılması, metodolojisi, veri toplanması, resmi analizi, bulguların yorumlanması ve makalenin hazırlanması dahil olmak üzere tüm aşamalarında tek başına görev almıştır.

KAYNAKLAR

- [1] Zhao HM, Wang SG, Wu ZM, Che GJ. Concrete slab installed with carbon fiber heating wire for bridge deck deicing. J Transp Eng 2010;136. [https://doi.org/10.1061/\(ASCE\)TE.1943-5436.0000117](https://doi.org/10.1061/(ASCE)TE.1943-5436.0000117).
- [2] Chen Q, Wang C, Sun X, Cao Y, Guo T, Chen J. Evaluation and prediction for effect of conductive gussasphalt mixture on corrosion of steel bridge deck. Constr Build Mater 2019;228. <https://doi.org/10.1016/j.conbuildmat.2019.116837>.
- [3] Wang C, Yang X, Li Q, Guo T, Jiang T. Preparation and performance of conductive gussasphalt concrete. Transp A Transp Sci 2019;15. <https://doi.org/10.1080/23249935.2018.1449913>.
- [4] Xu H, Wang D, Tan Y, Zhou J, Oeser M. Investigation of design alternatives for hydronic snow melting pavement systems in China. J Clean Prod 2018;170. <https://doi.org/10.1016/j.jclepro.2017.09.262>.
- [5] Sassani A, Arabzadeh A, Ceylan H, Kim S, Sadati SMS, Gopalakrishnan K, et al. Carbon fiber-based electrically conductive concrete for salt-free deicing of pavements. J Clean Prod 2018;203. <https://doi.org/10.1016/j.jclepro.2018.08.315>.
- [6] Aghazadeh N, Nojavan M, Mogaddam AA. Effects of road-deicing salt (NaCl) and saline water on water quality in the Urmia area, northwest of Iran. Arab J Geosci 2012;5. <https://doi.org/10.1007/s12517-010-0210-6>.
- [7] Cao Y, Sha A, Liu Z, Li J, Jiang W. Energy output of piezoelectric transducers and pavements under simulated traffic load. J Clean Prod 2021;279. <https://doi.org/10.1016/j.jclepro.2020.123508>.
- [8] Wang S, Wang C, Gao Z, Cao H. Design and performance of a cantilever piezoelectric power generation device for real-time road safety warnings. Appl Energy 2020;276. <https://doi.org/10.1016/j.apenergy.2020.115512>.
- [9] Liu Q, García Á, Schlangen E, Ven M Van De. Induction healing of asphalt mastic and porous asphalt concrete. Constr Build Mater 2011;25. <https://doi.org/10.1016/j.conbuildmat.2011.04.016>.
- [10] Sun Y, Wu S, Liu Q, Hu J, Yuan Y, Ye Q. Snow and ice melting properties of self-healing asphalt mixtures with induction heating and microwave heating. Appl Therm Eng 2018;129. <https://doi.org/10.1016/j.applthermaleng.2017.10.050>.
- [11] Sun X, Qin X, Liu Z, Yin Y, Zou C, Jiang S. New preparation method of bitumen samples for UV aging behavior investigation. Constr Build Mater 2020;233. <https://doi.org/10.1016/j.conbuildmat.2019.117278>.
- [12] Wang C, Chen Q, Guo T, Li Q. Environmental effects and enhancement mechanism of graphene/tourmaline composites. J Clean Prod 2020;262. <https://doi.org/10.1016/j.jclepro.2020.121313>.
- [13] Chen Q, Wang C, Qiao Z, Guo T. Graphene/tourmaline composites as a filler of hot mix asphalt mixture: Preparation and properties. Constr Build Mater 2020;239. <https://doi.org/10.1016/j.conbuildmat.2019.117859>.
- [14] Wan J, Wu S, Xiao Y, Fang M, Song W, Pan P, et al. Enhanced ice and snow melting efficiency of steel slag based ultra-thin friction courses with steel fiber. J Clean Prod 2019;236. <https://doi.org/10.1016/j.jclepro.2019.117613>.

- [15] Arabzadeh A, Ceylan H, Kim S, Sassani A, Gopalakrishnan K, Mina M. Electrically-conductive asphalt mastic: Temperature dependence and heating efficiency. *Mater Des* 2018;157. <https://doi.org/10.1016/j.matdes.2018.07.059>.
- [16] Arabzadeh A, Notani MA, Kazemiyan Zadeh A, Nahvi A, Sassani A, Ceylan H. Electrically conductive asphalt concrete: An alternative for automating the winter maintenance operations of transportation infrastructure. *Compos Part B Eng* 2019;173. <https://doi.org/10.1016/j.compositesb.2019.106985>.
- [17] Notani MA, Arabzadeh A, Ceylan H, Kim S, Gopalakrishnan K. Effect of Carbon-Fiber Properties on Volumetrics and Ohmic Heating of Electrically Conductive Asphalt Concrete. *J Mater Civ Eng* 2019;31. [https://doi.org/10.1061/\(asce\)mt.1943-5533.0002868](https://doi.org/10.1061/(asce)mt.1943-5533.0002868).
- [18] Yuan Y, Xu H, Zhang Y. Experimental study on warming performance of conductive asphalt concrete. *Huazhong Keji Daxue Xuebao (Ziran Kexue Ban)/Journal Huazhong Univ Sci Technol (Natural Sci Ed)* 2014;42. <https://doi.org/10.13245/j.hust.141026>.
- [19] Rew Y, Shi X, Choi K, Park P. Structural Design and Lifecycle Assessment of Heated Pavement Using Conductive Asphalt. *J Infrastruct Syst* 2018;24. [https://doi.org/10.1061/\(asce\)is.1943-555x.0000440](https://doi.org/10.1061/(asce)is.1943-555x.0000440).
- [20] El-Dieb AS, El-Ghareeb MA, Abdel-Rahman MAH, Nasr ESA. Multifunctional electrically conductive concrete using different fillers. *J Build Eng* 2018;15. <https://doi.org/10.1016/j.jobbe.2017.10.012>.
- [21] Rizvi HR, Khattak MJ, Madani M, Khattab A. Piezoresistive response of conductive Hot Mix Asphalt mixtures modified with carbon nanofibers. *Constr Build Mater* 2016;106. <https://doi.org/10.1016/j.conbuildmat.2015.12.187>.
- [22] Li H, Yu J, Liu Q, Li Y, Wu Y, Xu H. Induction Heating and Healing Behaviors of Asphalt Concretes Doped with Different Conductive Additives. *Adv Mater Sci Eng* 2019;2019. <https://doi.org/10.1155/2019/2190627>.
- [23] Liu Z, Yang X, Wang Y, Luo S. Engineering properties and microwave heating induced ice-melting performance of asphalt mixture with activated carbon powder filler. *Constr Build Mater* 2019;197. <https://doi.org/10.1016/j.conbuildmat.2018.11.094>.
- [24] Wu S, Pan P, Chen M, Zhang Y. Analysis of Characteristics of Electrically Conductive Asphalt Concrete Prepared by Multiplex Conductive Materials. *J Mater Civ Eng* 2013;25. [https://doi.org/10.1061/\(asce\)mt.1943-5533.0000565](https://doi.org/10.1061/(asce)mt.1943-5533.0000565).
- [25] Chen F, Balieu R. A state-of-the-art review of intrinsic and enhanced electrical properties of asphalt materials: Theories, analyses and applications. *Mater Des* 2020;195. <https://doi.org/10.1016/j.matdes.2020.109067>.
- [26] Bressi S, Dumont AG, Partl MN. An advanced methodology for the mix design optimization of hot mix asphalt. *Mater Des* 2016;98. <https://doi.org/10.1016/j.matdes.2016.03.003>.
- [27] Wu S, Mo L, Shui Z, Chen Z. Investigation of the conductivity of asphalt concrete containing conductive fillers. *Carbon N Y* 2005;43. <https://doi.org/10.1016/j.carbon.2004.12.033>.
- [28] Bozorgzad A, Kazemi SF, Moghadas Nejad F. Evaporation-induced moisture damage of asphalt mixtures: Microscale model and laboratory validation. *Constr Build Mater* 2018;171. <https://doi.org/10.1016/j.conbuildmat.2018.03.171>.
- [29] Gwon S, Kim H, Shin M. Self-heating characteristics of electrically conductive cement composites with carbon black and carbon fiber. *Cem Concr Compos* 2023;137. <https://doi.org/10.1016/j.cemconcomp.2023.104942>.
- [30] Wang YY, Tan YQ, Liu K, Xu HN. Preparation and electrical properties of conductive asphalt concretes containing graphene and carbon fibers. *Constr Build Mater* 2022;318. <https://doi.org/10.1016/j.conbuildmat.2021.125875>.
- [31] Lou B, Sha A, Barbieri DM, Liu Z, Zhang F, Jiang W. Improved microwave heating uniformity and self-healing properties of steel slag asphalt containing ferrite filler. *Mater Struct Constr* 2021;54. <https://doi.org/10.1617/s11527-020-01577-7>.
- [32] Zhu X, Ye F, Cai Y, Birgisson B, Lee K. Self-healing properties of ferrite-filled open-graded friction course (OGFC) asphalt mixture after moisture damage. *J Clean Prod* 2019;232. <https://doi.org/10.1016/j.jclepro.2019.05.353>.
- [33] Jiang Q, Liu W, Wu S. Analysis on factors affecting moisture stability of steel slag asphalt concrete using grey correlation method. *J Clean Prod* 2023;397. <https://doi.org/10.1016/j.jclepro.2023.136490>.
- [34] Li C, Wu S, Chen Z, Tao G, Xiao Y. Improved microwave heating and healing properties of bitumen by using nanometer microwave-absorbers. *Constr Build Mater* 2018;189. <https://doi.org/10.1016/j.conbuildmat.2018.09.050>.

- [35] Chen J, Ma X, Wang H, Xie P, Huang W. Experimental study on anti-icing and deicing performance of polyurethane concrete as road surface layer. *Constr Build Mater* 2018;161. <https://doi.org/10.1016/j.conbuildmat.2017.11.170>.
- [36] Birgin HB, García-Macías E, D'Alessandro A, Ubertini F. Self-powered weigh-in-motion system combining vibration energy harvesting and self-sensing composite pavements. *Constr Build Mater* 2023;369. <https://doi.org/10.1016/j.conbuildmat.2023.130538>.
- [37] Chung DDL. First review of capacitance-based self-sensing in structural materials. *Sensors Actuators A Phys* 2023;354. <https://doi.org/10.1016/j.sna.2023.114270>.
- [38] Gulisano F, Buasiri T, Apaza FRA, Cwirzen A, Gallego J. Piezoresistive behavior of electric arc furnace slag and graphene nanoplatelets asphalt mixtures for self-sensing pavements. *Autom Constr* 2022;142. <https://doi.org/10.1016/j.autcon.2022.104534>.
- [39] Liu L, Zhang X, Xu L, Zhang H, Liu Z. Investigation on the piezoresistive response of carbon fiber-graphite modified asphalt mixtures. *Constr Build Mater* 2021;301. <https://doi.org/10.1016/j.conbuildmat.2021.124140>.
- [40] Kim GM, Nam IW, Yang B, Yoon HN, Lee HK, Park S. Carbon nanotube (CNT) incorporated cementitious composites for functional construction materials: The state of the art. *Compos Struct* 2019;227. <https://doi.org/10.1016/j.compstruct.2019.111244>.
- [41] Jahanbakhsh H, Karimi MM, Jahangiri B, Nejad FM. Induction heating and healing of carbon black modified asphalt concrete under microwave radiation. *Constr Build Mater* 2018;174. <https://doi.org/10.1016/j.conbuildmat.2018.04.002>.
- [42] García Á, Schlangen E, van de Ven M, Liu Q. Electrical conductivity of asphalt mortar containing conductive fibers and fillers. *Constr Build Mater* 2009;23. <https://doi.org/10.1016/j.conbuildmat.2009.06.014>.
- [43] Dharmasiri B, Randall JD, Stanfield MK, Ying Y, Andersson GG, Nepal D, et al. Using surface grafted poly(acrylamide) to simultaneously enhance the tensile strength, tensile modulus, and interfacial adhesion of carbon fibres in epoxy composites. *Carbon N Y* 2022;186. <https://doi.org/10.1016/j.carbon.2021.10.046>.
- [44] Kim HK, Park IS, Lee HK. Improved piezoresistive sensitivity and stability of CNT/cement mortar composites with low water-binder ratio. *Compos Struct* 2014;116. <https://doi.org/10.1016/j.compstruct.2014.06.007>.
- [45] Konsta-Gdoutos MS, Aza CA. Self sensing carbon nanotube (CNT) and nanofiber (CNF) cementitious composites for real time damage assessment in smart structures. *Cem Concr Compos* 2014;53. <https://doi.org/10.1016/j.cemconcomp.2014.07.003>.
- [46] Lee SJ, You I, Kim S, Shin HO, Yoo DY. Self-sensing capacity of ultra-high-performance fiber-reinforced concrete containing conductive powders in tension. *Cem Concr Compos* 2022;125. <https://doi.org/10.1016/j.cemconcomp.2021.104331>.
- [47] Zhu Y, Fan X, Suo L, Luo C, Gao T, Wang C. Electrospun FeS₂@Carbon fiber electrode as a high energy density cathode for rechargeable lithium batteries. *ACS Nano* 2016;10. <https://doi.org/10.1021/acs.nano.5b07081>.
- [48] Ghahremani P, Mostafatabar AH, Bahlakeh G, Ramezanzadeh B. Rational design of a novel multi-functional carbon-based nano-carrier based on multi-walled-CNT-oxide/polydopamine/chitosan for epoxy composite with robust pH-sensitive active anti-corrosion properties. *Carbon N Y* 2022;189. <https://doi.org/10.1016/j.carbon.2021.11.067>.
- [49] Ouyang Y, Qiu L, Zhang X, Feng Y. Modulating heat transport inside CNT assemblies: multi-level optimization and structural synergy. *Carbon N Y* 2023;205. <https://doi.org/10.1016/j.carbon.2023.01.041>.
- [50] Ruoff RS, Lee KH, Lee SH. Synthesis of diamond-like carbon nanofiber films. *ACS Nano* 2020;14. <https://doi.org/10.1021/acs.nano.0c05810>.
- [51] Zhu J, Zhang Q, Zhao Y, Zhang R, Liu L, Yu J. Robust N-doping porous carbon nanofiber membranes with inter-fiber cross-linked structures for supercapacitors. *Carbon N Y* 2023;202. <https://doi.org/10.1016/j.carbon.2022.11.021>.
- [52] Lu D, Shi X, Zhong J. Understanding the role of unzipped carbon nanotubes in cement pastes. *Cem Concr Compos* 2022;126. <https://doi.org/10.1016/j.cemconcomp.2021.104366>.
- [53] Marchesini S, Turner P, Paton KR, Reed BP, Brennan B, Koziol K, et al. Gas physisorption measurements as a quality control tool for the properties of graphene/graphite powders. *Carbon N Y* 2020;167. <https://doi.org/10.1016/j.carbon.2020.05.083>.

- [54] Myapati S, Sellathurai A, Kontopoulou M, Docoslis A, Barz DPJ. High concentration graphene nanoplatelet dispersions in water stabilized by graphene oxide. *Carbon N Y* 2021;174. <https://doi.org/10.1016/j.carbon.2020.12.068>.
- [55] Young KT, Smith C, Krentz TM, Hitchcock DA, Vogel EM. Graphene synthesized by chemical vapor deposition as a hydrogen isotope permeation barrier. *Carbon N Y* 2021;176. <https://doi.org/10.1016/j.carbon.2021.01.127>.
- [56] Budde H, Coca-López N, Shi X, Ciesielski R, Lombardo A, Yoon D, et al. Raman Radiation Patterns of Graphene. *ACS Nano* 2016;10. <https://doi.org/10.1021/acsnano.5b06631>.
- [57] Arabzadeh A, Sassani A, Ceylan H, Kim S, Gopalakrishnan K, Taylor PC. Comparison between cement paste and asphalt mastic modified by carbonaceous materials: Electrical and thermal properties. *Constr Build Mater* 2019;213. <https://doi.org/10.1016/j.conbuildmat.2019.04.060>.
- [58] Wu W, Jiang W, Yuan D, Lu R, Shan J, Xiao J, et al. A review of asphalt-filler interaction: Mechanisms, evaluation methods, and influencing factors. *Constr Build Mater* 2021;299. <https://doi.org/10.1016/j.conbuildmat.2021.124279>.
- [59] Franesqui MA, Yepes J, García-González C. Top-down cracking self-healing of asphalt pavements with steel filler from industrial waste applying microwaves. *Constr Build Mater* 2017;149. <https://doi.org/10.1016/j.conbuildmat.2017.05.161>.
- [60] Baowen L, Aimin S, Yupeng L, Wentong W, Zhuangzhuang L, Wei J, et al. Effect of metallic-waste aggregates on microwave self-healing performances of asphalt mixtures. *Constr Build Mater* 2020;246. <https://doi.org/10.1016/j.conbuildmat.2020.118510>.
- [61] Lu D, Shi X, Zhong J. Interfacial bonding between graphene oxide coated carbon nanotube fiber and cement paste matrix. *Cem Concr Compos* 2022;134. <https://doi.org/10.1016/j.cemconcomp.2022.104802>.
- [62] Liu J, Wang Z, Li M, Wang X, Wang Z, Zhang T. Microwave heating uniformity, road performance and internal void characteristics of steel slag asphalt mixtures. *Constr Build Mater* 2022;353. <https://doi.org/10.1016/j.conbuildmat.2022.129155>.
- [63] Jiao W, Sha A, Liu Z, Li W, Jiang W, Qin W, et al. Study on thermal properties of steel slag asphalt concrete for snow-melting pavement. *J Clean Prod* 2020;277. <https://doi.org/10.1016/j.jclepro.2020.123574>.
- [64] Li H, Zhang Q, Xiao H. The Self-Heating Carbon Nanofiber Polymer Composite and its Applications in Deicing and Snow Thawing of Pavement. *Innov. Adv. Multifunct. Nanocomposites Civ. Struct. Eng.*, 2016. <https://doi.org/10.1016/B978-1-78242-326-3.00011-7>.
- [65] Gao J, Sha A, Wang Z, Tong Z, Liu Z. Utilization of steel slag as aggregate in asphalt mixtures for microwave deicing. *J Clean Prod* 2017;152. <https://doi.org/10.1016/j.jclepro.2017.03.113>.
- [66] Jiao W, Sha A, Liu Z, Jiang W, Hu L, Qin W. Analytic investigations of snow melting efficiency and temperature field of thermal conductive asphalt concrete combined with electrical-thermal system. *J Clean Prod* 2023;399. <https://doi.org/10.1016/j.jclepro.2023.136622>.



RESNET-50 BASED CNN MODEL FOR GRAPE LEAF IMAGE CLASSIFICATION IN MATLAB

Seda YETKİN YESİL ^{1*} , Olcay PALTA ¹

^{1*} Bitlis Eren University, Vocational School of Technical Sciences, Department of Electronics and Automation, Bitlis, Turkey

* Corresponding Author: syetkin@beu.edu.tr

ABSTRACT

The primary aim of this study is to investigate the effectiveness of a Convolutional Neural Network (CNN) architecture, specifically ResNet-50, in accurately classifying grapevine leaves belonging to five different species (Ak, Ala Idris, Buzgulu, Dimnit, and Nazli). Thanks to its capacity to extract rich and detailed features from images, the ResNet-50 architecture enables the high-accuracy differentiation of leaf species that are morphologically very similar. To this end, a comprehensive dataset comprising a total of 500 grapevine leaf images, representing the five species, was created. Each species is represented by 100 images, all of which were captured under similar lighting and environmental conditions to enhance data consistency and minimize noise. Prior to model training, various preprocessing steps were applied to the dataset. The ResNet-50-based CNN model was implemented in MATLAB, and both training and validation were conducted through custom MATLAB scripts. In the experimental setup, the dataset was divided into training (70%) and test (30%) subsets. Additionally, due to the limited amount of data, a 5-fold cross-validation technique was employed. The average results from this cross-validation process indicated that the model achieved an accuracy of 75.40%.

Keywords: Convolutional neural network, grape leaf, Resnet-50, image, classification

1 INTRODUCTION

Viticulture is one of the significant branches of agriculture in our country. Its importance is reinforced by the fact that it serves as a source of livelihood for many farmers and that grapes can be utilized in various forms. In Turkey, grapes harvested from vines are processed for multiple purposes, including drying, winemaking, and fresh consumption. Similarly, grapevine leaves hold an important place in traditional Turkish cuisine. One of the dishes symbolizing the classical Ottoman cuisine, sarma, is prepared using vine leaves. Moreover, the economic value of the leaves of certain grape varieties has been observed to exceed that of the grapes themselves. For instance, in 2023, 1,500 tons of vine leaves were exported from the Manisa region, generating approximately 500,000 USD in revenue, despite incurring no production costs.

Not all vine leaf varieties are suitable for culinary use. Leaves selected for consumption are generally preferred to be as hairless, thin, and finely veined as possible. Additionally, varieties that are seedless and impart a slightly tart taste on the palate tend to be favored.

Today, the agricultural sector is increasingly benefiting from technologies incorporating artificial intelligence. Numerous approaches have been proposed in the literature for the identification of plant species. In systems where leaf features serve as distinguishing characteristics, deep learning models known for their high accuracy are commonly preferred. For example, Ghosh and colleagues employed the Swedish Leaf dataset [2], the FLAVIA dataset [3], and the Leafsnap dataset [4], utilizing two approaches: CNN + Support Vector Machine (SVM) and CNN + k-Nearest Neighbors (kNN).

Li et al. [5] conducted a study in which they designed a series of processing procedures combining U-Net and VGG-19 networks, developed using grape leaves as samples, to acquire plant leaf images via agricultural drones and to enable regional segmentation and disease detection in leaf clusters over large areas. Koklu et al. [6] conducted a classification of grapevine leaf images using a state-of-the-art CNN model, specifically a fine-tuned MobileNetV2. Liu et al. [7] proposed a novel recognition approach based on convolutional neural networks (CNN) for the diagnosis of six common grape leaf diseases: anthracnose, brown spot, mites, black rot, downy mildew, and leaf blight. First, a dataset of 107,366 grape leaf images was generated using 4,023 images collected in the field and 3,646 images obtained from public datasets, with the help of image enhancement techniques. Subsequently, the Inception architecture was applied to improve multidimensional feature extraction performance, and the model's performance was compared with GoogLeNet and ResNet34.

In the study by Islam and colleagues, the aim was to diagnose diseases and identify potential treatments using images of grape and strawberry leaves through deep learning methods. Nowadays, researchers can develop highly accurate and efficient systems for object detection and recognition using deep learning techniques. In this research, a dataset was trained using a Convolutional Neural Network (CNN) model [8]. In the food industry, classifying vine leaves based on quality is critically important because the leaves are visually difficult to distinguish. Since the vine leaves used in canned products prepared for export exhibit significant variety, accurately classifying the large number of leaf types presents a considerable challenge. In this study, an original method is proposed to automatically identify the types of vine leaves, addressing the problem and providing a practical solution for efficient classification.

2 MATERIAL AND METHOD

In this section, the methodology followed in conducting the research, the data collection process, the techniques employed, and the criteria used for evaluating the results are systematically explained.

2.1 Bibliometric Analysis

With the rapid advancement of artificial intelligence technologies, research on the visual classification of plant leaves has experienced substantial growth in recent years. The increasing adoption of deep learning architectures and advanced image processing techniques has significantly enhanced the robustness, accuracy, and scalability of plant classification systems, thereby expanding their range of practical applications. In this study, a comprehensive bibliometric analysis was performed on publications indexed in the Web of Science and Scopus databases between 2023 and 2024, with the objective of systematically identifying and evaluating current research trends in the domain of plant classification. The results of the conducted bibliometric analysis are illustrated in Figure 1.

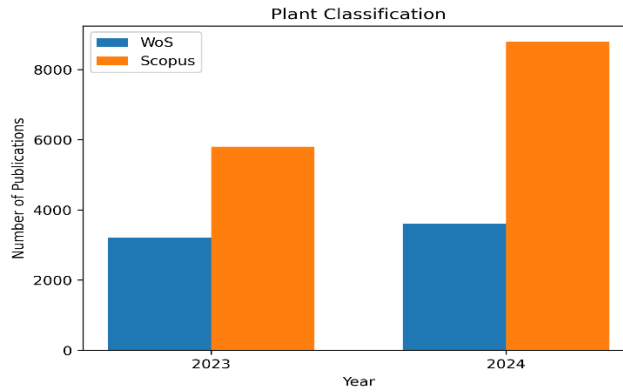


Figure 1.Yearly distribution of plant classification publications in Scopus and Web of Science

As presented in Figure 1, the number of publications related to the keyword ‘plant image classification’ indexed in the Web of Science database increased from approximately 3,100 in 2023 to 3,600 in 2024. Additionally, the number of publications related to the keyword ‘plant image classification’ indexed in the Scopus database increased from approximately 5,720 in 2023 to 8,800 in 2024. The obtained findings indicate that the number of publications has increased over the years in both the Web of Science and Scopus databases.

2.2 Grape Leaf Dataset

Grapevine leaves are also harvested once a year as a by-product. The types of grapevine leaves are important in terms of price and taste. In this study, as shown in Figure 2, a deep learning–based classification was performed using images of grapevine leaves. For this purpose, the effectiveness of a Convolutional Neural Network (CNN) based on the ResNet-50 architecture was investigated for the accurate classification of grapevine leaves belonging to five different varieties, namely Ak, Ala Idris, Buzgulu, Dimnit, and Nazli.

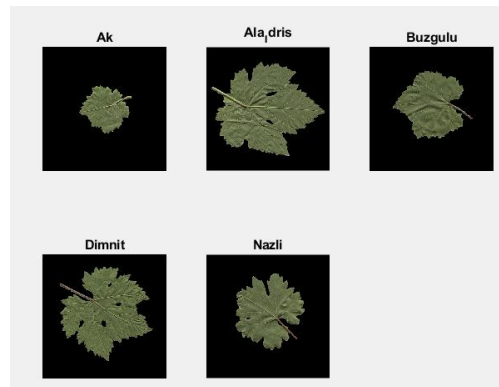


Figure 2. Five different grapevine leaf varieties

The image size of the dataset was set to $511 \times 511 \times 3$ in order to satisfy the input layer dimensional requirements of the pre-designed convolutional neural network. This resizing ensures that all input images are compatible with the network architecture, allowing for proper feature extraction and consistent performance during the training and classification processes. The dataset, consisting of 100 images for each grapevine leaf species and a total of 500 images, is accessible via the relevant <https://www.muratkoklu.com/datasets/> link. Comprehensive information regarding the specific types of image data used in this study is presented in Table 1. The table includes five grape leaf species—Ak, Ala İdris, Büzgülü, Dimnit, and Nazlı—and provides details on the number of images per category, their respective resolutions, as well as the distribution of training and test data.

Table 1. Grapevine Leaf Imaging Dataset

Category	Leaf Type	Number	Image Size	ResNet-50 input size	Training Number	Testing Number
Training: Testing (70 %: 30 %)	Ak	250	511x511x3	224x224x3	175	75
	Ala Idris	250	511x511x3	224x224x3	175	75
	Buzgulu	250	511x511x3	224x224x3	175	75
	Dimnit	250	511x511x3	224x224x3	175	75
	Nazli	250	511x511x3	224x224x3	175	75

2.3 Structure and Working Principles of CNN

Convolutional Neural Networks are one of the multilayer architectures developed for the analysis and recognition of two-dimensional image data. A Convolutional Neural Network (CNN) is a deep learning technique frequently applied in image analysis, accepting pictures as input [9]. It contains four layers: an input layer, a convolution layer, a pooling layer, and a flattening layer, as shown in Figure 3.

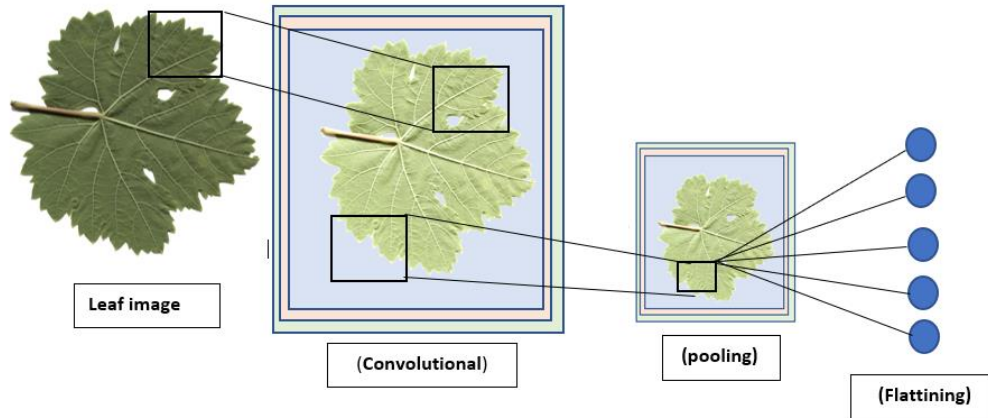


Figure 3. Architecture of the CNN model for grapevine leaves

In this study, instead of developing a new deep learning architecture, ResNet-50, one of the widely used pre-trained CNN models, was employed for the classification of grapevine leaves according to their species. Numerous CNN models with different structural designs have been proposed, each with its own advantages and limitations. The main advantage of ResNet-50 used in this study is that it provides high accuracy in very deep networks while preventing the vanishing gradient problem, and it offers flexible usage through transfer learning.

Not all layers within a CNN are suitable for image feature extraction; only certain layers can be used for this purpose. The initial layers are not suitable for feature extraction as they capture basic image features. Logically, it is preferred to extract features from one of the deeper layers of the network using the activation method. We consider the activation values of the layer just before the final classification layer to be more appropriate. For example, in Google-Net this layer is called

'loss3-classifier' in ResNet-50 it is 'fc1000,' and in AlexNet it is 'fc8' [10]. In this study, feature extraction was performed using the fc1000 layer of the ResNet-50 architecture.

2.3.1 Convolutional layer

The convolutional layer is a fundamental component of a CNN. Here, feature maps are extracted by performing a convolution operation between the input tensor X and small learnable filters (kernels). As shown in Figure 4, feature extraction from a 5×5 image is performed using a 3×3 filter [11].

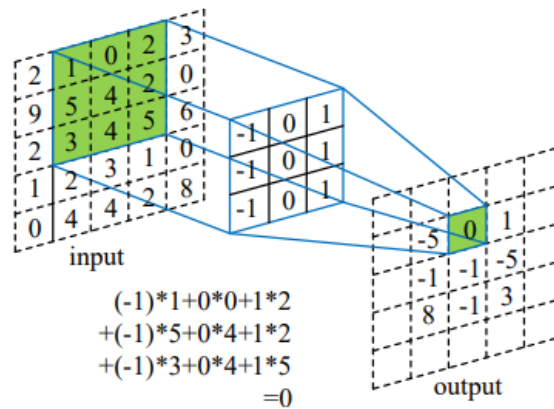


Figure 4. Convolutional layer of CNN

As shown in Figure 4, starting from the top-left corner to the bottom-right, each 3×3 matrix is passed through the filter to extract a feature.

The filter weights of the first convolutional layer in the grape leaf CNN model are visualized and presented in Figure 5.

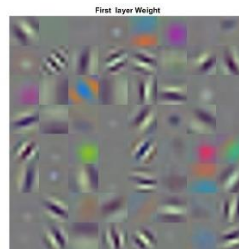


Figure 5. first convolutional layer in CNN

2.3.2 Pooling layer and Flatting layer

This layer is used to reduce the size of the feature map, thereby decreasing both the number of parameters and the computational cost. The most commonly used types of pooling layers are max pooling and average pooling. Max pooling involves selecting the highest value within a given region. An example of a pooling layer is shown in Figure 6.

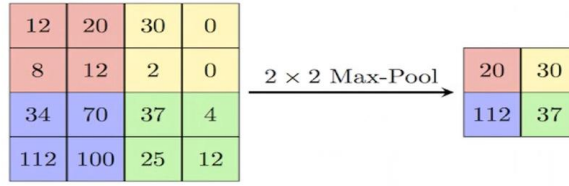


Figure 6. Max pooling layer in a CNN

This layer is the final layer in a CNN, where all neurons are fully connected. It transforms the obtained feature map into a one-dimensional vector to produce outputs, such as category classification (flattening).

2.3.3 Resnet 50

Residual Networks (ResNet) constitute a class of deep learning architectures engineered to mitigate the vanishing gradient problem that often arises in very deep neural networks. ResNet-50, a 50-layer variant renowned for its efficiency, is among the most widely adopted models. Its design enables exceptional performance in image recognition tasks, establishing it as a foundational framework in modern deep learning research. The ResNet-50 architecture is illustrated in Figure 6.

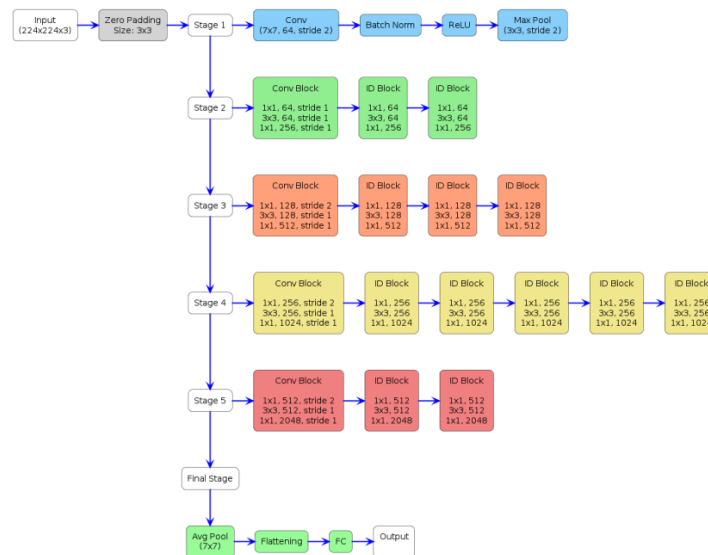


Figure 7. ResNet50 architecture diagram [12]

The CNN model was implemented in MATLAB. The computer used for building the model was equipped with a 13th Gen Intel® Core™ i7-13700H (2.40 GHz) processor and 16 GB of RAM.

The K-Fold Cross-Validation method divides the dataset into “k” equal parts, using each part as the validation set in turn. This ensures that every data point is used at least once for validation, allowing for a more accurate assessment of the model’s overall performance.

The confusion matrix shown in Figure 8, obtained from the 5-fold cross-validation, illustrates the model’s classification performance across all classes. The Nazli class achieved the highest recognition rate at 87%, followed by the Ak class at 83%, indicating strong performance for these categories. In contrast, the Dimnit class had the lowest accuracy at 56%, showing that the model struggled most with this class. The Büzgülü (68%) and Ala İdris (74%) classes showed moderate accuracy, with notable misclassifications occurring primarily between these classes and the Dimnit class.

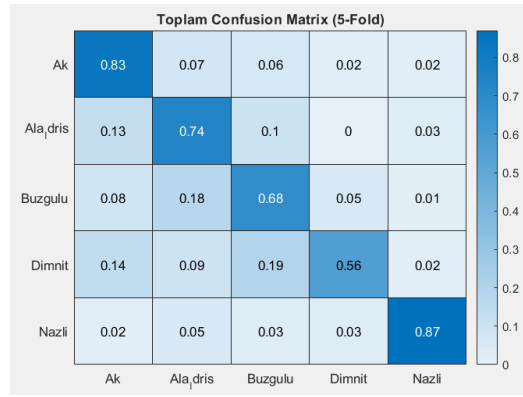


Figure 8. Confusion matrix of 5-fold cross-validation

3 RESULTS AND DISCUSSIONS

➤ The ResNet-50-based Convolutional Neural Network (CNN) demonstrated a generally strong capability in classifying five grapevine leaf varieties (Ak, Ala Idris, Buzgulu, Dimnit, and Nazli) that exhibit very similar morphological characteristics. Owing to its deep architecture, the model was able to extract discriminative features related to leaf shape, texture, and vein patterns, enabling effective differentiation among visually similar classes.

➤ To ensure a reliable evaluation under limited data conditions, a 5-fold cross-validation strategy was employed. The experimental results yielded an average classification accuracy of 75.40%, indicating that the proposed deep learning approach maintains a satisfactory level of generalization performance despite the relatively small dataset size.

➤ Class-wise performance analysis revealed that the Nazli (87%) and Ak (83%) grape leaf varieties achieved the highest recognition rates. This suggests that these leaf types possess more distinctive visual features, allowing the CNN model to learn and identify their characteristics more effectively compared to other classes.

➤ The Dimnit variety exhibited the lowest classification accuracy (56%), primarily due to its strong visual similarity to the Buzgulu and Ala Idris varieties. The confusion matrix analysis showed that most misclassifications occurred among these classes, highlighting the challenges faced by the model in distinguishing subtle morphological differences between closely related grapevine leaf types.

➤ Overall, the findings demonstrate that the ResNet-50 architecture implemented in the MATLAB environment provides a practical and extendable solution for automatic grapevine leaf classification. The study also indicates that incorporating larger and more diverse datasets, applying data augmentation techniques, or comparing multiple deep learning architectures could further improve classification accuracy, making the proposed approach highly promising for applications in viticulture and the food processing industry.

In future studies, the classification performance can be further improved by expanding the dataset with a larger number of grapevine leaf images captured under varying environmental conditions and by applying advanced data augmentation techniques to increase data diversity. Additionally, the effectiveness of different deep learning architectures such as EfficientNet, DenseNet, or Vision Transformers can be comparatively evaluated alongside ResNet-50. Integrating hybrid models that combine deep features with traditional machine learning classifiers and exploring real-time implementation for field or industrial applications may also contribute to the development of more robust and scalable grapevine leaf classification systems.

Conflict of Interest Statement

The authors declare that they have no conflicts of interest

Statement of Research and Publication Ethics

This study has been prepared in accordance with the principles of research and publication ethics.

Artificial Intelligence (AI) Contribution Statement

This article has been entirely written, edited, analyzed, and prepared by the authors without the use of any artificial intelligence (AI) tools. All content, text, data analysis, and figures have been solely produced by the authors

Contributions of the Authors

Seda Yetkin Yesil carried out the analysis of the CNN model in MATLAB and the literature review, while Olcay Palta contributed to the interpretation and writing of the manuscript.

REFERENCES

- [1] S. Ghosh, A. Singh, N. Z. Jhanjhi, M. Masud, and S. Aljahdali, "SVM and KNN Based CNN Architectures for Plant Classification," *Computers, Materials & Continua*, vol. 71, no. 3, 2022.
- [2] O. Söderkvist, Computer vision classification of leaves from Swedish trees, M.Sc. thesis, Linköping Univ., Sweden, 2001.
- [3] FLAVIA Leaf Image Dataset. SourceForge, 2007. Available: <https://sourceforge.net/projects/flavia>
- [4] N. Kumar et al., "Leafsnap: A computer vision system for automatic plant species identification," pp. 502-516, 2012.
- [5] W. Li, X. Yu, C. Chen, and Q. Gong, "Identification and localization of grape diseased leaf images captured by UAV based on CNN," *Computers and Electronics in Agriculture*, vol. 214, p. 108277, 2023.
- [6] M. Koklu, M. F. Unlarsen, I. A. Ozkan, M. F. Aslan, and K. Sabanci, "A CNN-SVM study based on selected deep features for grapevine leaves classification," *Measurement*, vol. 188, p. 110425, 2022.
- [7] B. Liu, Z. Ding, L. Tian, D. He, S. Li, and H. Wang, "Grape leaf disease identification using improved deep convolutional neural networks," *Frontiers in Plant Science*, vol. 11, p. 1082, 2020.
- [8] M. Tariqul Islam and A. N. Tusher, "Automatic detection of Grape, Potato and Strawberry Leaf Diseases using CNN and image processing," in *Data Engineering for Smart Systems: Proceedings of SSIC 2021*, Singapore: Springer Singapore, 2021, pp. 213-224.
- [9] J. Ludwig, "Image Convolution," Portland State University, pp. 1–8, 2013.
- [10] Y. Peng, S. Zhao, and J. Liu, "Fused-deep-features based grape leaf disease diagnosis," *Agronomy*, vol. 11, no. 11, p. 2234, 2021.
- [11] Y. Zhou, "Research on the construction and sustainable development of online teaching model for universities based on deep learning," *Applied Mathematics and Nonlinear Sciences*, vol. 9, no. 1, Jan. 2024, doi: 10.2478/amns.2023.2.00142.
- [12] S. Ram, S. Vinoth, R. N. Gopalakrishnan, A. A. Balakumar, L. Kalinathan, and T. A. Velankanni, "Leveraging diverse CNN architectures for medical image captioning: DenseNet-121, MobileNetV2, and ResNet-50 in ImageCLEF 2024," *Conference and Labs of the Evaluation Forum*, 2024.

4 A MACHINE LEARNING AND CLUSTERING-BASED FRAMEWORK FOR ASSESSING ENVIRONMENTAL EFFECTS IN THE TEXTILE INDUSTRY

İsmail ÇALIKUŞU^{1,*} , Kadir HALTAŞ² 

¹ Nevşehir Hacı Bektaş Veli University, Department of Electronics and Automation, Nevşehir, Türkiye

² Nevşehir Hacı Bektaş Veli University, Department of Computer Technologies, Nevşehir, Türkiye

*Corresponding Author: ismailcalikusu@nevsehir.edu.tr

ABSTRACT

The objective of this study is to comprehensively assess the environmental impacts of the textile and ready-to-wear clothing industry and to establish a machine learning-based multivariate framework for predicting the Air Quality Index (AQI). In this context, 21 years of monthly data obtained from the city of Surat in India were utilized. Eight different machine learning models were evaluated to predict the AQI using the aforementioned data: Long Short-Term Memory (LSTM), Linear Regression, Ridge, Lasso, Support Vector Regression–Radial Basis Function (SVR-RBF), K-Nearest Neighbor (KNN), Decision Tree, and Gradient Boosting. The analysis results showed that LSTM achieved the best performance ($R^2 = 0.2932$, $MAE = 22.87$) due to its sensitivity to patterns that change over time, while the Gradient Boosting model was the second most successful model. In contrast, the SVR-RBF, KNN, and Decision Tree models showed lower accuracy. Principal Component Analysis (PCA) was applied for dimension reduction to examine seasonal pollution trends, followed by the Density-Based Clustering in Noise-Affected Applications (DBSCAN) method. The clustering resulted in five clusters and one noise segment. Cluster 3, in particular, stood out with consistently high pollution levels (AQI = 241) despite low variance. This study demonstrates that there is a non-linear relationship between production volume and pollution, and that industrial modernization has the potential to reduce environmental damage. Overall, the findings reveal that machine learning models are effective tools for environmental monitoring, risk classification, and developing data-driven sustainability strategies.

Keywords:

Machine Learning, Air Quality Prediction (AQI), Environmental Impacts, Principal Component Analysis (PCA), Clustering (DBSCAN)

1 INTRODUCTION

The textile and apparel industry is a sector that makes significant contributions to global economic development. At the same time, it stands out as one of the industries with serious environmental impacts. The high consumption of energy and water during raw material production, yarn and fabric manufacturing, dyeing, finishing processes, and throughout the product lifecycle alongside the widespread use of toxic chemicals and high carbon emissions makes this sector one of the most environmentally problematic industries in terms of sustainability [1-3]. Moreover, wastewater discharge, particulate matter emissions, and the intensive use of chemicals are key risk factors that increase environmental health problems, especially in developing countries [4, 5].

In the literature, the primary methods used to evaluate the environmental impacts of the textile sector include Life Cycle Assessment (LCA), Product Carbon Footprint (PCF), and

Ecological Footprint (EF) [1, 2, 6]. While these approaches make it possible to systematically assess the direct and indirect environmental impacts of production processes, they are limited in modeling temporal environmental changes, dynamic relationships between production volume and environmental effects, and regional disparities [7-9].

In recent years, the inclusion of artificial intelligence (AI) and machine learning (ML) approaches in environmental monitoring and analysis has opened new research opportunities. These technologies are increasingly being used for pattern discovery in large datasets, prediction of environmental indicators, and modeling the relationship between production and pollution [10-13]. In particular, methods such as LSTM, Random Forest (RF), Support Vector Machines (SVM), and Artificial Neural Networks (ANN) have been successfully applied in areas such as energy consumption prediction, optimization of textile dyeing processes, texture analysis, and the reduction of production losses [13-15].

However, a review of the existing literature reveals that studies utilizing machine learning and clustering algorithms for the direct modeling of environmental impacts are quite limited. In clustering-based research, the focus has largely been on topics such as quality control, production classification, or typologies of corporate sustainability trends; however, issues such as environmental monitoring, identification of high-risk periods, or classification of regional environmental performance are often neglected [16, 17]. Despite the strong potential of algorithms like DBSCAN and K-Means in identifying density-based anomalies in environmental monitoring scenarios, their application in the textile sector remains relatively underexplored [10, 16].

Furthermore, many studies on environmental sustainability in the textile industry focus on broader perspectives such as firm-based Environmental, Social, and Governance (ESG) practices [18], digital transformation and circular economy [19, 20], waste management [14], water footprint and toxic emission calculations [6, 8, 21], or green export strategies [22]. However, very few of these studies offer an integrated approach that predicts concrete outcomes such as air quality using long-term, multivariate environmental data while also clustering observations based on temporal variability.

This study aims to assess the environmental impacts of textile production using a comprehensive dataset comprising 21 years of monthly observations from the city of Surat in the state of Gujarat, India. Eight different machine learning algorithms were employed to predict environmental pollutants, particularly the AQI, and the accuracy and error rates of these models were comparatively analyzed. Additionally, DBSCAN clustering was applied on the PCA-reduced feature space to identify periods with similar environmental behavior patterns, and the relationships between production and emissions across clusters were examined.

In this regard, the study provides not only predictive modeling but also offers original contributions in terms of data segmentation, environmental risk classification, and the design of data-driven sustainability strategies. By integrating advanced data analytics and artificial intelligence techniques, this research proposes a novel environmental assessment framework that can contribute to the transformation of the textile sector in the context of sustainability.

2 MATERIALS AND METHODS

This section outlines the methodological framework adopted in the study. It includes a detailed description of the dataset, preprocessing techniques, applied machine learning models, clustering analysis, evaluation metrics, and implementation environment. The aim is to ensure reproducibility and transparency in experimental procedures.

2.1 Dataset

In this study, a multivariate time series dataset was used to evaluate the environmental impacts of the textile industry operating in Surat, a city in the state of Gujarat, India. The dataset was obtained from the publicly available study titled “*Surat Textile Pollution Dataset*” on the Kaggle platform (<https://www.kaggle.com/datasets/riasingh11/surat-textile-pollution>). The data is licensed under the World Bank Dataset Terms of Use and is intended solely for research and educational purposes.

The dataset comprises 252 monthly observations from January 2004 to December 2024. During this period, systematic measurements were collected regarding both production activities and environmental pollution indicators. The dataset includes industry-specific variables such as textile output (MT/month), water usage (ML/day), electricity consumption (GWh), and the number of active textile units. Environmental impact indicators include the AQI, particulate matter (PM_{2.5}), nitrogen oxides (NO_x), sulfur dioxide (SO₂), carbon monoxide (CO) levels, wastewater discharge, biochemical oxygen demand (BOD) in water, and total industrial emissions.

2.2 Data Preprocessing

In this study, all data were scaled to the [0, 1] range using the Min–Max normalization method to ensure comparability. Since the dataset contained no missing values, no imputation was required. For predictive time-series modeling with the LSTM algorithm, the data were redesigned to include observations from the previous three months. For other regression-based predictive models, the data were randomly split into 80% training and 20% test sets.

2.3 Machine Learning Models

To predict AQI values, this study employed and comparatively evaluated eight different machine learning and deep learning-based regression algorithms. Each model captures the relationship between AQI and input variables differently, reflecting unique advantages and limitations based on the nature of the data.

Linear Regression is a classical approach that assumes a linear relationship between AQI and independent variables. It is widely used in literature due to its simplicity and high interpretability, especially when linear relationships are present. However, it is often inadequate for modeling nonlinear relationships frequently observed in environmental data [23].

Ridge Regression is a generalized version of linear regression that incorporates an L2 norm penalty to regularize model coefficients and prevent overfitting. It is especially effective in datasets with multicollinearity, producing more stable and reliable predictions. By shrinking coefficients, it reduces variance while still allowing all variables to contribute to the model [24].

Lasso Regression applies an L1 norm penalty, driving some coefficients to zero. This enables automatic variable selection, enhancing interpretability and generalization capacity by removing irrelevant or weakly correlated features in AQI prediction [25].

SVR, developed within the support vector machine framework, is effective in modeling nonlinear relationships. In this study, the SVR model was configured with an RBF kernel, enabling the modeling of complex, nonlinear patterns in high-dimensional feature space. However, the need for careful hyperparameter tuning and high computational cost makes SVR challenging for large datasets [26].

KNN is a non-parametric method that predicts new observations based on proximity to neighboring points in the data space. It performs well in clustered data scenarios but is sensitive to noise and outliers and suffers from performance loss in high-dimensional datasets [27].

Decision Tree Regressor partitions the dataset based on decision rules and provides constant predictions at each leaf node. While it offers high interpretability, the model tends to overfit the training data unless the tree depth and splitting criteria are carefully controlled [28].

GB Regressor is a powerful ensemble learning method that combines weak learners (typically decision trees) sequentially to minimize errors. Each iteration corrects the residuals of the previous model [29]. It effectively models nonlinear and complex patterns, though training time is longer and hyperparameter tuning is critical.

Finally, the LSTM network was used for time series processing. LSTM differs from traditional recurrent neural networks in its ability to learn long-term dependencies. With its embedded memory, it can retain past environmental information, allowing it to model AQI trends over time effectively [30]. It is especially advantageous for predicting AQI based on time-dependent relationships with meteorological variables such as temperature, humidity, and pressure. However, training LSTM models requires high computational power and careful configuration to avoid overfitting.

Each of these eight models relies on different theoretical foundations and analytical strategies, and comparing their AQI prediction performance constitutes one of the primary goals of this study.

2.4 Clustering and Segmentation Analysis

Beyond predictive modeling, a DBSCAN was applied to examine the seasonal variation of environmental impacts and identify periods with similar environmental conditions. Prior to this analysis, all numerical variables were scaled, and PCA was applied to reduce the dimensionality to two features. DBSCAN forms clusters based on the density of data points within a specified radius and marks low-density, anomalous observations as outliers. The clustering results revealed meaningful environmental segments, such as periods with high production and low AQI levels (indicating sustainable conditions), or periods with high emissions and pollutants accompanied by lower productivity. Summary statistics across these clusters allowed for a clearer understanding of the temporal intensity of environmental risks and the impact of industrial activity.

2.5 Model Evaluation Metrics

Model performances were compared using three main evaluation metrics. The R^2 score indicates the proportion of variance in the target variable explained by the model. MAE calculates the average absolute differences between predicted and actual values. Root Mean Square Error (RMSE), by taking the square root of the average squared errors, provides a more sensitive assessment of larger errors. These metrics were used to evaluate and compare all models and determine the most suitable one.

2.6 Implementation Environment

All analyses were conducted using Python 3.11 programming language. Open-source libraries such as pandas, numpy, matplotlib, seaborn, and scikit-learn were used for data processing and analysis. The LSTM model was trained using the TensorFlow (Keras) library. DBSCAN clustering and PCA were performed using the scikit-learn framework. In addition to statistical performance, factors such as computational time, resource usage, and practical applicability were also considered in model evaluation.

3 RESULTS

This section presents the results of the applied machine learning techniques and clustering analysis. The aim is to evaluate how well different models predict AQI and to identify patterns in environmental conditions over time. The findings are discussed in detail through performance metrics, visualizations, and statistical comparisons.

3.1 Performance Comparison of Machine Learning Models in AQI Prediction

In this study, eight different machine learning models were compared to evaluate the environmental impacts of textile production and to predict the AQI. These models include LSTM, Linear Regression, Ridge Regression, Lasso Regression, SVR (RBF), KNN Regressor, Decision Tree, and GB algorithms. The models were evaluated using accuracy and error metrics, and the findings are presented through tables and visualizations (Table 1).

Table 1. Performance Comparison of Machine Learning Models

Model	R ² Score	MAE	RMSE
LSTM	0.2932	22.8743	29.3120
Linear Regression	0.2859	22.8387	29.4637
Ridge Regression	0.2859	22.8387	29.4637
Lasso Regression	0.2859	22.8448	29.4639
SVR (RBF)	0.1054	25.6751	32.9770
KNN Regressor	0.1011	25.7770	33.0572
Decision Tree	-0.0052	27.2720	34.9564
Gradient Boosting	0.2926	22.8752	29.3247

As shown in Figure 1, the highest R² score was achieved by the LSTM model, with a value of 0.2932. The GB model also demonstrated high accuracy with a similar R² score of 0.2926. Linear-based models Linear Regression, Ridge Regression, and Lasso Regression performed comparably, each achieving an R² score around 0.2859. In contrast, models such as SVR (0.1054) and KNN (0.1011) yielded significantly lower R² scores. The Decision Tree model produced a negative R² score of -0.0052, indicating inadequate predictive accuracy.

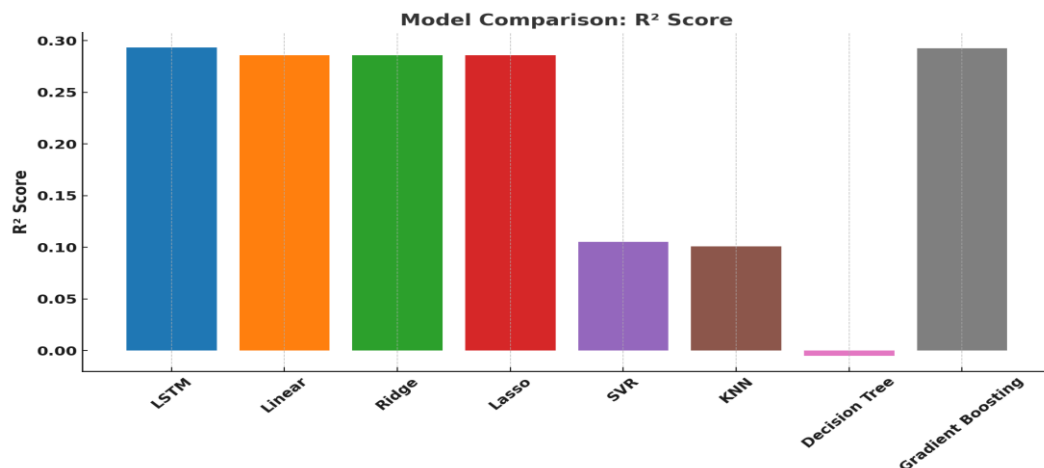


Figure 1. Comparison of R² scores of the models

One of the error metrics, MAE, is presented in Figure 2. The lowest MAE was obtained from the LSTM model with a value of 22.8743, followed closely by the GB model with 22.8752. The linear models also produced values close to these two; the MAE values for the Linear, Ridge, and Lasso Regression models were 22.8387 and 22.8448, respectively. In contrast, a noticeable increase in error was observed in the SVR, KNN, and Decision Tree models.

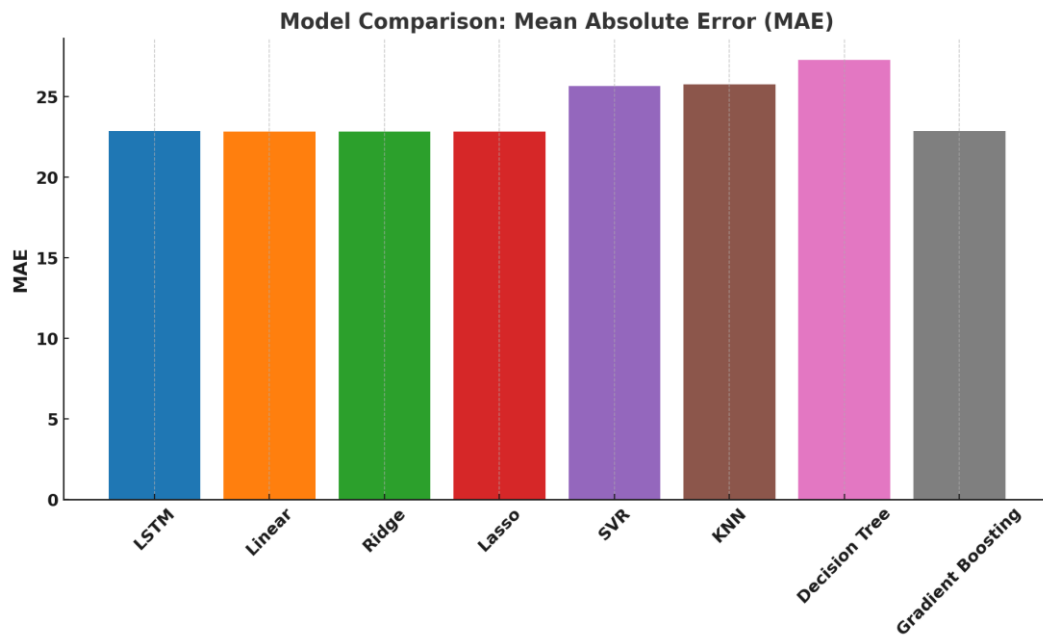


Figure 2. Mean Absolute Error (MAE) values of the models.

The RMSE comparison shown in Figure 3 reveals the models' tendencies toward large errors. The LSTM (29.312) and Gradient Boosting (29.3247) models again demonstrated the lowest values in this metric. In contrast, the linear models showed RMSE values around 29.46. However, the prediction errors were significantly higher in the SVR (32.977), KNN (33.0572), and Decision Tree (34.9564) models.

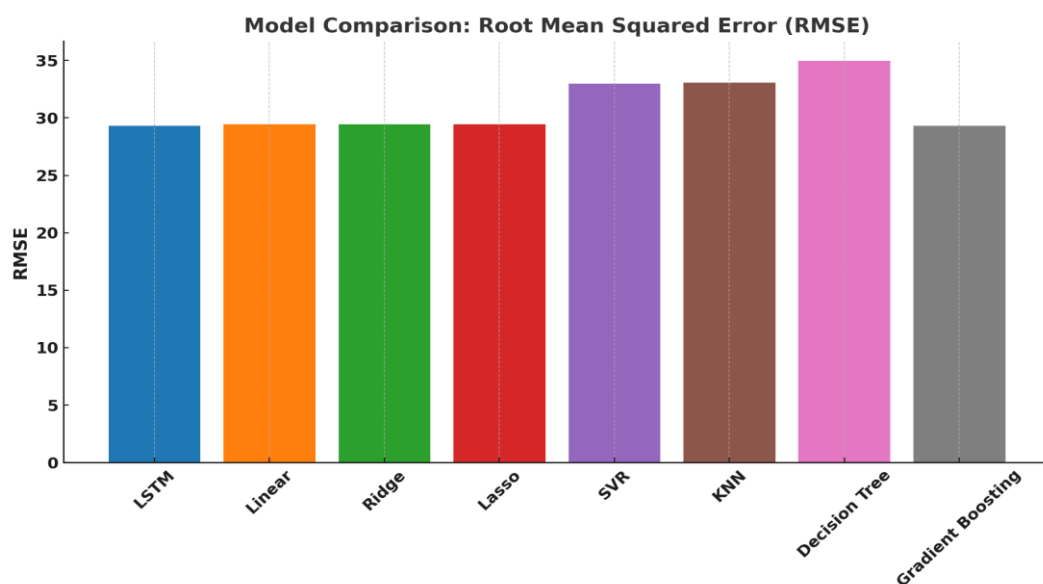


Figure 3. Root Mean Square Error (RMSE) values of the models

The relationship between the predicted and actual AQI values was also visualized using line graphs to provide a clearer assessment of each model's performance. For example, the LSTM model's predicted and actual curves showed strong alignment in most instances, while the Decision Tree model exhibited noticeable deviations. This visual pattern is consistent with the RMSE and MAE results presented earlier.

Overall, the LSTM model, which is sensitive to time-dependent data structures, emerged as the most successful approach in terms of both accuracy and error metrics for AQI prediction. The Gradient Boosting model also demonstrated strong performance. While traditional linear models yielded balanced results, models such as SVR, KNN, and Decision Tree were not suitable for this specific dataset. Therefore, it is recommended to use more advanced models capable of capturing complex and temporal relationships in environmental data.

In the process of predicting AQI through machine learning models, it is essential to consider not only the performance of the models but also the seasonal and temporal patterns inherent in the dataset. For this reason, the next step of the study focuses on the temporal segmentation of environmental impacts. The DBSCAN clustering analysis presented below offers a holistic view of the data by grouping time periods based on similar environmental conditions.

3.2 Environmental Segmentation: DBSCAN Clustering Findings

To group the environmental impacts of textile production on a temporal basis, the DBSCAN clustering analysis revealed five distinct clusters and one "noise" group. The observations labeled as Cluster -1, defined as noise, exhibit environmental characteristics that significantly deviate from the other clusters. The resulting clusters provide clearer insights into how the textile sector influences production volume, resource usage, and air and water quality.

The noise cluster (Cluster -1) is characterized by an average AQI of 181, industrial emissions of 4,229 tons/month, and elevated levels of CO and BOD. These months likely represent periods marked by unusual industrial activities or environmental crises. On the other hand, Cluster 2 stands out as the segment with the highest textile production volume (approximately 70,000 MT/month), while showing only a moderate increase in AQI levels (average 196). This indicates that high production volume does not necessarily correspond to proportionally high pollution levels, suggesting that modernization or effective treatment systems may be in place.

The most notable cluster is Cluster 3, representing the periods with the highest air pollution, with an average AQI value of 241. This segment also shows elevated concentrations of other pollutants such as SO₂, CO, and BOD. The low variance within this cluster indicates that the pollution is not temporary but rather reflects a persistent environmental condition. Table 2 below summarizes the mean and standard deviation values for each segment identified through the DBSCAN clustering analysis.

Table 2. Descriptive Statistics of Clusters Identified via DBSCAN.

Cluster	-1	0	1	2	3
Textile Out. Mean	58832.59	53225.60	47795.52	70055.19	62005.35
Textile Out. Std	9986.36	8304.64	6321.65	6111.93	3289.75
Units Mean	1796.72	1594.59	1546.42	2050.24	1875.58
Units Std	285.43	259.44	111.59	173.73	108.97
Elec. Cons. Mean	113.86	101.59	97.84	145.69	136.46
Elec. Cons. Std	26.14	20.39	11.46	17.44	14.68
Water Use Mean	230.50	210.48	202.64	247.98	236.30
Water Use Std	35.81	30.28	9.27	11.75	19.86
Wastewater Mean	198.11	178.44	172.47	213.03	205.97
Wastewater Std	32.59	29.14	12.79	13.47	14.26
PM2.5 Mean	93.81	81.87	77.88	100.03	99.87
PM2.5 Std	17.14	12.71	6.03	6.50	6.08
NOx Mean	69.29	60.81	58.31	77.89	71.92
NOx Std	12.61	10.09	8.20	7.15	4.31
SO2 Mean	29.43	25.53	27.99	32.32	30.91
SO2 Std	7.32	6.31	4.28	5.04	6.23
CO Mean	1.87	1.49	1.85	2.01	2.33
CO Std	0.62	0.37	0.24	0.32	0.20
BOD Mean	19.31	17.74	16.52	22.69	22.56
BOD Std	4.11	3.27	2.74	2.35	2.34
AQI Mean	181.68	163.17	165.12	196.45	241.49
AQI Std	46.22	34.69	11.36	21.10	14.45
Emissions Mean	4229.98	3820.07	2941.76	4657.69	4225.12
Emissions Std	1297.25	740.27	319.19	414.92	682.38

4 DISCUSSION AND CONCLUSIONS

This study makes significant contributions to literature by analyzing the environmental impacts of the textile and apparel industry through both predictive modeling and clustering-based segmentation using machine learning algorithms. The findings demonstrate how critical it is to evaluate the effects of industrial activity on air quality using a multivariate approach, particularly for informing environmental decision-making processes.

4.1 Evaluation of Prediction Performance

Regarding the performance of machine learning models in AQI prediction, the LSTM model, with its ability to learn time-dependent patterns, achieved the highest R^2 score (0.2932) and the lowest MAE (22.8743) among all tested algorithms. This result highlights that air quality data contains temporal components that cannot be adequately represented by traditional linear models. The effectiveness of time-series-based deep learning models like LSTM in environmental monitoring and air quality forecasting has also been emphasized in recent literature [12, 13, 15].

The GB algorithm also demonstrated a high level of accuracy, offering a strong alternative especially for modeling complex and nonlinear relationships. Its success in applications such as pollution forecasting, energy consumption modeling, and production optimization has been well

documented [14, 31]. On the other hand, the low R^2 scores and high error metrics of models like SVR, KNN, and Decision Tree indicate that these models failed to capture the underlying patterns in the dataset. This aligns with previous studies, which suggest that such algorithms tend to underperform in high-dimensional and noisy datasets [10, 11]. In particular, the negative R^2 value of the Decision Tree model illustrates its tendency to overfit and its limited generalization capability. These findings underscore that in complex, time-varying systems like environmental data analysis, model selection must consider not only theoretical framework but also the nature of the data [9].

4.2 Persistent Pollution and Temporal Segmentation via DBSCAN Clustering

In the second stage of the study, DBSCAN clustering analysis allowed for the classification of environmental parameters based on temporal patterns. The identified clusters showed meaningful distinctions not only in AQI levels but also in the distribution of pollutants such as CO, SO₂, and BOD, as well as their relationship with production inputs. This is consistent with previous findings supporting the applicability of DBSCAN to time-sensitive and anomaly-prone environmental data [10, 16].

Cluster 3 represents the periods with the highest levels of pollution, with an average AQI of 241. The low variance within this cluster suggests that this is not a temporary but rather a persistent environmental issue. The high levels of SO₂ and CO in this segment likely reflect the impact of fossil fuel usage, inefficient energy systems, and inadequate flue gas treatment infrastructure [5, 7]. In contrast, Cluster 2 despite its high production volume exhibited relatively lower AQI values, indicating the potential influence of modernization investments, energy efficiency practices, or advanced environmental control systems. This finding reveals that increased production capacity does not necessarily result in higher pollution levels and that technological advancements can weaken this correlation [8, 19, 20]

4.3 Comparison with Literature and Contributions

In existing literature, the environmental impacts of the textile sector are often assessed using approaches such as LCA, PCF, or ESG-based sustainability frameworks [1, 2, 18, 20]. However, these methods are typically process-focused and cannot directly model temporal variability or dynamic production–pollution relationships. By integrating predictive machine learning algorithms with density-based clustering methods for temporal risk classification, this study provides a novel contribution to overcome these limitations.

Additionally, DBSCAN's ability to detect noise-labeled observations offers an advantage in identifying environmental anomalies compared to other clustering techniques. This enables the classification of unusual production conditions, crisis periods, or atypical environmental behaviors—areas often overlooked in the literature [10, 16]. Therefore, the framework proposed in this study serves as a practical example for both sectoral decision support systems and data-driven environmental management approaches.

4.4 Policy and Sustainability Implications

The findings of this study clearly highlight the potential of AI-based modeling approaches in forecasting and monitoring environmental impacts in the textile sector. In particular, the strong performance of advanced algorithms such as LSTM and GB in time-series datasets shows that these models can play an active role in environmental forecasting processes. This suggests that the dynamic nature of environmental indicators can be more effectively analyzed through advanced machine learning techniques rather than traditional statistical methods [13-15].

Furthermore, the density-based clustering approach using DBSCAN has proven more effective than traditional algorithms such as K-Means in identifying anomalies and forming variance-sensitive temporal segments. Most environmental assessments in the textile sector still

rely on frameworks like LCA, PCF, or sustainability reporting [1, 2], and data mining or machine learning-based studies remain relatively limited [7, 19, 20].

By integrating both predictive and clustering methods, this study not only explains environmental outcomes but also presents a framework for developing decision-support strategies based on these results. Modeling the causal and time-dependent relationships between production inputs and air quality outputs offers a crucial contribution to sectoral policymaking. While most studies focus on corporate ESG practices [18], water footprints [8], waste management [14], or circular economy strategies [20], this study uniquely contributes to the literature through its application-driven analysis of production-volume-based environmental monitoring and risk classification.

In conclusion, this machine learning-based approach provides an exemplary methodology for developing data-driven sustainability management practices in environmentally intensive sectors like textiles and significantly fills a gap in the current academic literature.

5 CONCLUSION

This study presents a comprehensive framework for evaluating the environmental impacts of the textile and apparel industry using machine learning and clustering-based segmentation. Among the eight models tested for AQI prediction, the Long Short-Term Memory (LSTM) algorithm demonstrated superior performance due to its ability to capture temporal dependencies, followed closely by Gradient Boosting. Simpler models such as SVR, KNN, and Decision Tree failed to adequately model the nonlinear and time-sensitive nature of environmental data.

Clustering analysis via DBSCAN effectively segmented production periods based on environmental patterns, identifying high-risk clusters such as Cluster 3, which exhibited persistently high pollution levels. Notably, the findings revealed that high production volume does not always correlate with increased pollution, suggesting that modernization and environmental control systems can mitigate adverse impacts.

The study highlights the potential of AI-based approaches for real-time environmental monitoring, risk classification, and sustainability planning. Future research should incorporate additional variables—such as meteorological data, regional policies, and production technologies—and integrate clustering results with GIS to develop spatial risk maps. Furthermore, multi-criteria decision-support systems that include water footprint, carbon intensity, and energy efficiency could significantly advance sustainable textile production. These insights offer valuable contributions to both academic literature and industry practices.

5.1 Artificial Intelligence (AI) Contribution Statement

This manuscript was written and revised entirely by the authors. No artificial intelligence (AI) tools were used for data analysis, statistical processing, result interpretation, or the development of the scientific content of the study. However, AI-based language tools were used solely to assist in improving the academic writing style and to correct minor grammatical issues. All scientific ideas, analyses, interpretations, results, and conclusions presented in this article are exclusively the work of the authors.

REFERENCES

- [1] S. Moazzem, E. Crossin, F. Daver, and L. Wang, "Environmental impact of apparel supply chain and textile products," *Environment, Development and Sustainability*, vol. 24, no. 8, pp. 9757-9775, 2022.
- [2] S. S. Muthu, *Assessing the environmental impact of textiles and the clothing supply chain*. Woodhead publishing, 2020.

- [3] S. Roos, *Advancing life cycle assessment of textile products to include textile chemicals. Inventory data and toxicity impact assessment*. Chalmers Tekniska Hogskola (Sweden), 2017.
- [4] P. Kumari, S. J. Singh, and N. M. Rose, "Eco-textiles: for sustainable development," *International Journal of Scientific & Engineering Research*, vol. 4, no. 4, pp. 1379-1390, 2013.
- [5] T. L. Lewis, X. Zeng, V. Sanchez, and J. Fan, "Environmental evaluation of fabric dyeing and water use for a global apparel manufacturer," *AATCC Journal of Research*, vol. 4, no. 1, pp. 1-13, 2017.
- [6] S. Roos, R. Arvidsson, and C. Jönsson, "Calculating the toxicity footprint of Swedish clothing consumption," in *8th International Conference on Life Cycle Management*, 3-6 September, Luxembourg, 2017.
- [7] C. Gomes, I. Pires, L. Monteiro, T. M. Lima, and P. D. Gaspar, "Empowering eco-friendly choices: An environmental impact assessment decision support system for textiles and clothing," *Applied Sciences*, vol. 14, no. 2, p. 659, 2024.
- [8] D. Mikucioniene *et al.*, "Understanding and addressing the water footprint in the textile sector: a review," *AUTEX Research Journal*, vol. 24, no. 1, p. 20240004, 2024.
- [9] S. Sharpe, M. Retamal, and M. C. Martinez-Fernandez, *Assessing the impact: Environmental impact assessment in the textile and garment sector in Bangladesh, Cambodia, Indonesia and Viet Nam* (no. 51). ILO Working Paper, 2022.
- [10] R. Feng, X. Xu, Z.-T. Yu, and Q. Lin, "A machine-learning assisted multi-cluster assessment for decarbonization in the chemical fiber industry toward net-zero: A case study in a Chinese province," *Journal of Cleaner Production*, vol. 425, p. 138965, 2023.
- [11] C. Satinet and F. Fouss, "A supervised machine learning classification framework for clothing products' sustainability," *Sustainability*, vol. 14, no. 3, p. 1334, 2022.
- [12] M. Seçkin, A. Ç. Seçkin, P. Demircioglu, and I. Bogrekci, "FabricNET: a microscopic image dataset of woven fabrics for predicting texture and weaving parameters through machine learning," *Sustainability*, vol. 15, no. 21, p. 15197, 2023.
- [13] K. Yilmaz, İ. Ö. Aksu, M. Göçken, and T. Demirdelen, "Sustainable textile manufacturing with revolutionizing textile dyeing: Deep learning-based, for energy efficiency and environmental-impact reduction, pioneering green practices for a sustainable future," *Sustainability*, vol. 16, no. 18, p. 8152, 2024.
- [14] C. Atik, A. Kut, D. Birant, and S. Birol, "Prediction of cloth waste using machine learning methods in the textile industry," in *2022 9th International Conference on Electrical and Electronics Engineering (ICEEE)*, 2022: IEEE, pp. 165-169.
- [15] S. Ghosh, S. Dan, and P. Tarafder, "Machine learning-enabled multiscale modeling platform for damage sensing digital twin in piezoelectric composite structures," *Scientific Reports*, vol. 15, no. 1, p. 6631, 2025.
- [16] S. M. Alam, "Application of k-means clustering to enhance the quality control and the impact of the productivity in the apparel industries," *Journal homepage: www. ijrpr. com ISSN*, vol. 2582, p. 7421, 2022.
- [17] P. Yildirim, D. Birant, and T. Alpyildiz, "Data mining and machine learning in textile industry," *Wiley Interdisciplinary Reviews: Data Mining and Knowledge Discovery*, vol. 8, no. 1, p. e1228, 2018.
- [18] A. Magotra, M. R. I. Rana, F. S. Shishir, and S. Shomaji, "Data-Driven Insights into Sustainability: An Artificial Intelligence (AI) Powered Analysis of ESG Practices in the Textile and Apparel Industry," in *International Textile and Apparel Association Annual Conference Proceedings*, 2025, vol. 81, no. 1: Iowa State University Digital Press.
- [19] A. Kanwal, M. A. Nazeer, and S. Rasul, "Digitalization in the textile sector for circularity," in *Circularity in textiles*: Springer, 2023, pp. 213-231.

- [20] F. Rubik *et al.*, "Textiles on the Path to Sustainability and Circularity—Results of Application Tests in the Business-to-Business Sector," *Sustainability*, vol. 16, no. 14, p. 5954, 2024.
- [21] Y. Guo *et al.*, "Comprehensive assessment of the chemical footprint of yarn dyed fabric," *AATCC Journal of Research*, vol. 9, no. 3, pp. 127-133, 2022.
- [22] C. Nosirova, "Sustainable Textile Exports: Real-time Decision Making through Information Extraction for Green Strategy Optimization," in *Proceedings of the 7th International Conference on Future Networks and Distributed Systems*, 2023, pp. 443-447.
- [23] G. James, D. Witten, T. Hastie, R. Tibshirani, and J. Taylor, "Linear regression," in *An introduction to statistical learning: With applications in python*: Springer, 2023, pp. 69-134.
- [24] G. C. McDonald, "Ridge regression," *Wiley Interdisciplinary Reviews: Computational Statistics*, vol. 1, no. 1, pp. 93-100, 2009.
- [25] J. Ranstam and J. A. Cook, "LASSO regression," *Journal of British Surgery*, vol. 105, no. 10, pp. 1348-1348, 2018.
- [26] M. Awad and R. Khanna, "Support vector regression," in *Efficient learning machines: Theories, concepts, and applications for engineers and system designers*: Springer, 2015, pp. 67-80.
- [27] A. Sumayli, "Development of advanced machine learning models for optimization of methyl ester biofuel production from papaya oil: Gaussian process regression (GPR), multilayer perceptron (MLP), and K-nearest neighbor (KNN) regression models," *Arabian Journal of Chemistry*, vol. 16, no. 7, p. 104833, 2023.
- [28] A. Gupta, A. Bansal, and K. Roy, "Solar energy prediction using decision tree regressor," in *2021 5th International Conference on Intelligent Computing and Control Systems (ICICCS)*, 2021: IEEE, pp. 489-495.
- [29] L. W. Rizkallah, "Enhancing the performance of gradient boosting trees on regression problems," *Journal of big data*, vol. 12, no. 1, p. 35, 2025.
- [30] H. Alizadegan, B. Rashidi Malki, A. Radmehr, H. Karimi, and M. A. Ilani, "Comparative study of long short-term memory (LSTM), bidirectional LSTM, and traditional machine learning approaches for energy consumption prediction," *Energy Exploration & Exploitation*, vol. 43, no. 1, pp. 281-301, 2025.
- [31] M. W. Younis *et al.*, "Exploring the Influence of Tropical Cyclones on Regional Air Quality Using Multimodal Deep Learning Techniques," *Sensors*, vol. 24, no. 21, p. 6983, 2024.